Structural characterization and evaluation of the bio-adhesive strength and temperature effects on latex extracted from the candelabra tree

By

Alpheus Madiba

39342891

A dissertation submitted in partial fulfillment of the requirements for

Masters in Engineering

Engineering: Mechanical.

Department of Mechanical, Bioresources and Biomedical Engineering

in the School of Engineering and the Built Environment

in the College of Science, Engineering and Technology

at the

University of South Africa

©Unisa



Supervisor: Prof. H. M. NGWANGWA

Supervisor: Dr. R. T. TEBETA

Submission Date: August 2026

DEDICATIONS

TO MY WIFE

MY KIDS (DAUGHTER AND SON)

MY FATHER

MY LATE MOTHER

MY MOTHER-IN-LAW

ACKNOWLEDGMENTS

Firstly, I thank the Lord for embracing me with bravery, persistence, and perseverance to accomplish this Master Dissertation work.

The success of this work is based on the people stated below, to whom I want to say thank you for your contribution.

Dr H. M. Ngwangwa: my supervisor, for your patience, support, and for believing in me always. Thank you for your technical support, expertise, guidance, and most of all for putting enough pressure on me to ensure my work is completed.

Mr. R. T. Tebeta: my supervisor, thank you for your passionate support, technical support & expertise, and lastly for always being willing to motivate and go the extra mile.

I also want to express my appreciation to everyone who contributed to my work.

To God be the glory! Thank you, Lord, for this achievement. My victory is a reflection of Your love and grace.

Thank you to everyone

The following papers resulted from this Dissertation work, and supporting documents are listed in Appendix H

Professor. H.M. Ngwangwa, Professor. D.M. Madyira and Mr. R.T. Tebeta 'Rheological analysis of bio-adhesive material from candelabra tree' ICMIMT 2025

Professor. H.M. Ngwangwa, Professor. D.M. Madyira and Mr. R.T. Tebeta 'Characterization properties of bio-adhesive material from candelabra tree' SEMC 2025

Professor. H.M. Ngwangwa, Professor. D.M. Madyira and Mr. R.T. Tebeta 'Investigating material properties of bio-adhesive extracted from candelabra tree' ISASEM 2026

ABSTRACT

Adhesives are used in applications where substrates are bonded together under variable applied loads. Adhesive materials are in demand across many industries, including packaging, automobiles, aviation, aerospace engineering, and construction. Rather than using solvent-based synthetic adhesives, this paper focuses on biodegradable bio-adhesives extracted from plant-based sources that bond to paper substrates.

The aim of the research paper was to develop methods to extract latex from plant-based materials, process latex to produce a bio-adhesive material, bond surfaces of different substrates, and examine the influence of temperature on this bio-adhesive material. To assess the mechanical properties of bio-adhesive materials, T-peel and single-lap shear tests were conducted. Thermal analysis was performed via differential scanning calorimetry (DSC), thermogravimetric analysis (TGA), and rheological testing.

Latex extraction involves using a laboratory blender to process candelabra tree branches into small pieces, resulting in white sap. This material is refined through a filtration process to remove impurities. Purified latex is cured at room temperature, where it changes from a liquid to a solid state. By applying heat at varying temperatures of 100^0C, 110^0C, 120^0C, 130^0C, 140^0C, and 150^0C, this latex is transformed into a bio-adhesive material.

Thermal analysis and bio-adhesive properties were investigated under varying temperature limitations and under chemically controlled conditions using TGA, DSC, and rheological testing methods. The testing conditions remained constant, guaranteeing the steadiness and dependability of the data measured. The TGA-DSC testing method ensured that weight changes were correlated with thermal events and improved material stability assessments. Rheological measurements investigated the association between shear rate and shear stress of bio-adhesive material in a state of laminar flow. It also investigated other factors that cause material distortion.

Mechanical properties were evaluated via T-peel and single-lap shear examinations to investigate bio-adhesive shear strength in paper-to-paper specimens. Using tensile testing equipment, a single lap-shear test was conducted to examine bio-adhesive mechanical effects. The T-Peel test was conducted using a U-Stretch Mechanical Test System. For both mechanical tests, a steady application of force to the two peel arms at opposite ends was used to obtain analytical data under varying temperature parameters of the processed bio-adhesive material. In the experimental method, only processed latex was used, whereas in the thermal analysis method, both unprocessed and processed latex were used.

TGA results indicated that 130^0C is the temperature at which the bio-adhesive material achieves higher oxidation, with 1,12% weight loss at a furnace temperature of 320^0C. Unprocessed latex materials require a higher oxidation temperature than treated bio-adhesive materials. DSC results indicated that the 140^0C bio-adhesive material performed better than other bio-adhesive materials. The maximum heat flow value of this bio-adhesive at 200^0C is 1,2 W/g. Rheometer results showed that the 100^0C-processed material is the most robust, with a high storage modulus of 39 Pa and a peak of 124 Pa.

Single-lap shear test results showed that the material processed at 110°C produced the highest signal-to-noise ratio of 24,69 and the highest average elastic modulus of 17,333 MPa, indicating superior stiffness, strength, and rigidity. T-peel test results showed that higher-temperature-processed bio-adhesive materials could achieve higher peeling forces than materials processed at a lower temperature. In this case 130^0C is a material with a much higher average peeling strength of 529,22 N/m.

Thermal results indicated that bio-adhesives can maintain thermal stability while undergoing multiple decay stages. Unprocessed latex materials require more energy to break down and have higher oxidation temperatures than treated bio-adhesive materials. The elastic properties of bio-adhesive materials are improved when processed at low temperatures. According to the results, bio-adhesive materials processed at low temperatures exhibit a steady recovery rate, whereas those processed at high temperatures show a rapid recovery rate. According to mechanical results, the bio-adhesive exhibits elastic deformation properties as indicated by graphical linear behaviour and enhanced peeling strength as processing temperature increases. This provides further validation that at higher temperatures, processed bio-adhesive materials with greater UTS and lower Elastic Modulus can endure significant stresses, strains, and applied forces without breaking or losing their bond.

This investigation and material characterization will help in understanding the mechanical and thermal properties and performance of this novel bio-adhesive material. These data will guide the foundation for processing raw latex materials, and characterize the bio-adhesive behaviour linked to changes in processing temperature. The major contribution will be to environmental impact because bio-adhesive materials are biodegradable. Moreover, the life cycle assessment compares its environmental footprint with that of conventional synthetic adhesives, highlighting improvements in recyclability and reduced toxic emissions.

TABLE OF CONTENTS

ACKNOWLEDGMENTS ii
ABSTRACT iii
TABLE OF CONTENTS v
LIST OF FIGURES ix
LIST OF TABLES xiii
LIST OF ABBREVIATIONS xiv
NOMENCLATURE xvi
CHAPTER ONE 1
1. INTRODUCTION 1
1.1 Statement of the problem 2
1.2 Research aims 3
1.3 Research objectives 3
1.4 Research questions 3
1.5 Justification of the study 3
1.6 Research design and methodology 4
1.6.1 Literature review 4
1.7 Bio-adhesive development, characterization and experimental methods 4
1.8 Limitations of this study 5
1.9 Delimitations of this study 5
1.10 Structure of the dissertation 6
CHAPTER TWO 7
2. LITERATURE REVIEW 7
2.1 Overview 7
2.2 Adhesive 7
2.3 Synthetic adhesive 9
2.4 Hot-melt adhesives 9
2.5 Solvent-based adhesives 11
2.6 Water-based adhesives 12
2.7 Cellulose-based adhesives 13
2.8 Starch-based adhesives 15
2.9 Lignin-based adhesives 17
2.10 Protein-based adhesives 18
2.11 Recently developed bio-based adhesives and their performance 20

2.12 Biodegradable adhesives 22
2.13 Significance of biodegradable adhesives 23
2.14 Toxicity in biodegradable adhesives 23
2.15 Mechanical adhesive bonding 25
2.16 Latex and adhesive curing 27
2.17 Effect of temperature 29
2.18 Surface preparation 31
2.19 Mechanical properties of adhesives 32
2.19.1 Tensile test (adhesives in direct tensile loading mode) 32
2.19.2 T-Peel test adhesives 34
2.19.3 Single-lap shear test 37
2.20 Thermal testing of bio-adhesive 39
2.20.1 Thermogravimetric analysis (TGA) 39
2.20.2 Differential scanning calorimetry (DSC) 41
2.20.3 Rheology 44
2.21 Summary 48
CHAPTER THREE 49
3. MATERIALS AND METHODS 49
3.1 Harvesting and processing latex to produce a bio-adhesive 49
3.1.1 Harvesting candelabra tree branches 49
3.1.2 Extracting latex from candelabra tree branches 50
3.1.3 Equipment and methods used to produce bio-adhesive from latex 51
3.2 Thermogravimetric analysis (TGA) 54
3.2.1 Aim of performing TGA characterization 54
3.2.2 TGA methods and materials used 54
3.2.3 Preparation of TGA specimens 55
3.2.4 TGA testing method and procedure 56
3.3 Differential scanning calorimetry (DSC) 58
3.3.1 Aim of performing DSC characterization 58
3.3.2 DSC methods and material used 59
3.3.3 DSC specimen preparation process 59
3.3.4 DSC testing method and procedure 60
3.4 Rheology 63
3.4.1 Aim of performing rheology characterization 63
3.4.2 Rheology methods and materials used 63
3.4.3 Rheological specimen preparation process 64

3.4.4 Rheology testing method and procedure 65
3.5 Experimental approach 67
3.6 Single lap-shear test 67
3.6.1 The aim of performing a single-lap shear test 67
3.6.2 Single-lap shear test material and methods used 68
3.6.3 Single lap-shear testing method 68
3.6.4 Single lap-shear test testing procedure 71
3.7 T-Peel test 72
3.7.1 The aim of performing the T-Peel test 72
3.7.2 T-Peel test methods and materials used 73
3.7.3 T-Peel testing method 74
3.7.4 T-Peel testing Procedure 76
3.8 Summary 77
CHAPTER FOUR 79
4. RESULTS AND DISCUSSIONS 79
4.1 Overview 79
4.2 Thermal analysis results 79
4.3 Thermogravimetric analysis (TGA) 79
4.3.1 Temperature against TGA mass percentage of bio-adhesive at varying temperatures limitations 79
4.3.2 TGA derivative weight percent against temperature curve of bio-adhesive processed at different temperature parameters 83
4.4 Differential scanning calorimetry (DSC) 87
4.4.1 Heat Flow (normalized) (W/g) verses Temperature (^{0}C) curve (first stage at Ramp 10^{0}C /min to 200^{0}C 87
4.5 Rheological analysis 92
4.5.1 Rheology, complex viscosity versus angular viscosity curve for bio-adhesive at different temperature parameters 93
4.5.2 Rheology, loss modulus versus shear stress in percentage curve for bio-adhesive at different temperature parameters 94
4.5.3 Rheology, storage modulus versus shear stress in percentage curve for bio-adhesive at different temperature parameters 96
4.6 Experimental results 99
4.7 Single-lap-shear tests 99
4.8 T-Peel test 104
CHAPTER FIVE 109
5. CONCLUSION AND RECOMMENDATIONS 109

5.1 Experimental study 109
5.1.1 The effect of processing temperature on elastic modulus investigated via single-lap shear test 109
5.1.2 The effect of processing temperature on peeling strength is investigated through T-Peel test results 110
5.2 Summary of mechanical investigations findings 110
5.3 Thermal analysis investigations 110
5.3.1 The effect of processing temperature on percentage weight loss and percentage weight derivative of processed bio-adhesive material investigated through TGA 111
5.3.2 The effect of processing temperature on bio-adhesive's percentage weight loss and percentage weight derivative of processed bio-adhesive material investigated through DSC 111
5.3.3 The effects of processing temperature on viscosity investigated through rheological analysis 112
5.3.4 The effects of processing temperature on loss modulus investigated through rheological analysis 112
5.3.5 The effects of processing temperature on storage modulus investigated through rheological analysis 113
5.4 Summary of thermal investigation findings 113
6. RECOMMENDATIONS FOR UPCOMING RESEARCH WORK 114
7. REFERENCES 115
8. APPENDICES 127
8.1 Appendix A: Determining Elastic Modulus using Stress-Strain Curve 127
8.2 Appendix B: Single-lap shear test force versus strain curve 132
8.3 Appendix C: Single-Lap Shear Test: Signal-to-Noise Ratio calculations for Level 1 to Level 6 133
8.4 Appendix D: T-Peel Test Force versus Time curve (Test 1, 100^0C to 150^0C) 134
8.5 Appendix E: T-Peel Test Displacement Versus Time curve (Test 1, 100^0C to 150^0C) 137
8.6 Appendix F: T-Peel Test, Maximum Peel Strength for test 1, test 2, and test 3 140
8.7 Appendix G: T-Peel Test: Signal-to-Noise Ratio calculations for Level 1 to Level 6 140
8.8 Appendix H: Conference Paper Submitted & Presented 141

LIST OF FIGURES

Chapter 1 Figures

Figure 1. 1 Flow diagram for steps followed to process latex into a bio-adhesive material and conduct thermal and mechanical testing methods (self-developed) ---------- 5

Chapter 2 Figures

Figure 2. 1 Polyol as an additive in the polyurethane synthesis process ---------- 8
Figure 2. 2 Risk of hydrolysis of diphenylmethane diisocyanate in solventless adhesives to aromatic amines ---------- 13
Figure 2. 3 Starch-based wood adhesive shear strength influenced by SDS ---------- 16
Figure 2. 4 Measurements of wood substrates' tensile shear strength ---------- 19
Figure 2. 5 Schematic representation of the life cycle thinking approach for bio-based adhesive ---------- 22
Figure 2. 6 Adhesive & substrate ---------- 25
Figure 2. 7 Surface adhesion mechanism ---------- 25
Figure 2. 8 (a) Drying process of latex (b) representation of the drying front for a latex dispersion ---------- 28
Figure 2. 9 Before and after aging test stress-deformation curves ---------- 28
Figure 2. 10 Araldite 2014 samples cured at room temperature and examined in tension --- 29
Figure 2. 11 Amorphous (a) and semicrystalline (b) polymers and their approximate relations between temperature, molecular weight, and physical state ---------- 29
Figure 2. 12 Relationship between volume and temperature when a glass-forming polymer crystallizes. Melting point T_m and glass transition temperature T_g are temperatures for uncrystallized materials ---------- 30
Figure 2. 13 (a) and (b) (multiple attachment points) show the highest adhesion strength, while (d) (least attachment points) shows the lowest (e) examples of good and (f) examples of poor wetting by adhesives ---------- 31
Figure 2. 14 Characteristic stress-strain curve of an elastic material ---------- 33
Figure 2. 15 Typical apparatus of a tensile tester ---------- 34
Figure 2. 16 Different types of peel tests. (a) 90^0 Peel, (b) 180^0 Peel, (c) general layout, (d) T-Peel, and (e) climbing drum ---------- 35
Figure 2. 17 A typical load curve of the peel ---------- 36
Figure 2. 18 Single-lap and double-lap shear specimens ---------- 38
Figure 2. 19 Single-lap shear stress / strain characterization curve ---------- 38
Figure 2. 20 TGA measuring equipment ---------- 40
Figure 2. 21 Characteristic thermogravimetric curve ---------- 41
Figure 2. 22 Heat-flow diagram DSC measurement unit ---------- 43
Figure 2. 23 T_g, T_c, and T_m transitioning phases. Exothermic and endothermic processes from DSC measurement ---------- 44
Figure 2. 24 Two-plate rheometer operational diagram ---------- 45
Figure 2. 25 Graph showing association among storage modulus (G′), Loss modulus (G ″), and complex shear modulus (G*) ---------- 47
Figure 2. 26 Viscoelastic materials range of $0° < \delta < 90°$ ---------- 47

Chapter 3 Figures

Figure 3. 1 Candelabra tree branches (self-developed) ---------- 50
Figure 3. 2 Harvesting of milky latex (a); branches cut into smaller sections (b); outer greener sections removed (c) with inner section of the branch (self-developed)---------- 50
Figure 3. 3 Harvesting of milky latex: (a) inner section of the branches placed inside a non-food blender (b) extracted latex in a liquid form (self-developed) ---------- 51
Figure 3. 4 Milky sticky material in a solid state (self-developed)---------- 52
Figure 3. 5 Processing of latex (a) samples weighed and ready for processing (b) weighing process using a scale (self-developed)---------- 52
Figure 3. 6 Flow diagram for steps followed to harvest, process latex into bio-adhesive material, and experimental testing methods (self-developed)---------- 53
Figure 3. 7 (a) Ceramic pan and bio-adhesive sample weight (b) ceramic pan on scale (self-developed) ---------- 55
Figure 3. 8 TGA (a) Ceramic pan (b and c) 25-position autosampler (d) gas purging pipeline (self-developed)---------- 56
Figure 3. 9 TA TGA 5500 measuring equipment (a) 25-position autosampler (b) TGA display, and control screen (c) evolved gas exhaust (d) monitor (e) computer hardware (self-developed)---------- 56
Figure 3. 10 Flow diagram and steps followed to execute TGA thermal analysis testing methods (self-developed)---------- 58
Figure 3. 11 DSC (a) pan and lid on the scale: (b) press device (self-developed) ---------- 60
Figure 3. 12 DSC mounting panel (self-developed)---------- 60
Figure 3. 13 TA DSC 2500 (a) monitor (b) hardware (c) DSC display unit (d) sample mounting panel (e) sample feeder (f) DSC software system (g) refrigeration cooling system (self-developed)---------- 61
Figure 3. 14 Flow diagram and steps followed to execute DSC thermal analysis testing methods (self-developed)---------- 62
Figure 3. 15 Anton Paar rheometer (a) rheometer control screen (b) bio-adhesive specimen placed on rheometer parallel plates (self-developed)---------- 64
Figure 3. 16 Anton Paar rheometer operating environment (a) in an open position (b) in a closed position (self-developed)---------- 65
Figure 3. 17 Flow diagram and steps followed to execute rheometer thermal analysis testing methods (self-developed)---------- 66
Figure 3. 18 (a) Instron 8801 tensile testing machine (b) paper sample tested on tensile machine (self-developed)---------- 69
Figure 3. 19 Single shear lap joint parameters (self-developed)---------- 69
Figure 3. 20: Paper specimen for single-lap Joint (self-developed)---------- 70
Figure 3. 21 Flow diagram and steps followed to execute single lap-shear testing methods (self-developed)---------- 72
Figure 3. 22 T-Peel Test Illustration (self-developed) ---------- 74
Figure 3. 23: (A) T-Peel test specimen parameters (B) paper specimen for T-Peel test (self-developed) ---------- 74
Figure 3. 24 (a) Cell-scale U-Stretch mechanical test system (b) paper-to-paper specimen on T-Peel clamps (self-developed)---------- 75
Figure 3. 25 Flow diagram and steps followed to execute T-Peel testing methods (self-developed) ---------- 77

Chapter 4 Figures

Figure 4. 1 TGA Percentage weight against temperature curve indicating varying processing temperatures of bio-adhesive materials ---------- 80
Figure 4. 2 TGA Percentage weight against temperature curve showing points A & B of five bio-adhesive materials prepared at varying temperatures (100^0C, 110^0C, 120^0C, 130^0C & 140^0C) ---------- 81
Figure 4. 3 TGA Percentage weight against temperature curve for unprocessed latex -------- 82
Figure 4. 4 TGA Percentage weight versus temperature curve of bio-adhesive prepared at 150^0C ---------- 82
Figure 4. 5 TGA Derivative weight against temperature curve indicating varying processing temperatures of bio-adhesive materials ---------- 83
Figure 4. 6 TGA Derivative weight percent against temperature curve showing a detailed section between points C & D for processed & unprocessed bio-adhesive material ------ 84
Figure 4. 7 TGA derivative weight percent against temperature curve showing a detailed section between point F for bio-adhesive material ---------- 85
Figure 4. 8 TGA derivative weight percent against temperature curve showing a detailed section between point E for the bio-adhesive material ---------- 86
Figure 4. 9 DSC heat flow (normalized) (W/g) versus temperature (^{0}C) curve for bio-adhesive processed at 100^0C, 110^0C, 120^0C and 130^0C ---------- 88
Figure 4. 10 DSC heat flow (normalized) (W/g) versus temperature (0C) curve for bio-adhesive processed at 100^0C, 110^0C, 120^0C and 130^0C (ramp 10^0C /min to 200^0C) ----- 89
Figure 4. 11 DSC heat flow (normalized) (W/g) versus temperature (0C) curve for bio-adhesive processed at 140^0C ---------- 90
Figure 4. 12 DSC heat flow (normalized) (W/g) versus temperature (^{0}C) curve for bio-adhesive processed at 150^0C ---------- 90
Figure 4. 13 DSC heat flow (normalized) (W/g) versus temperature (^{0}C) curve for unprocessed latex ---------- 91
Figure 4. 14 Rheology: complex viscosity versus angular viscosity curve for bio-adhesive at different temperature parameters ---------- 93
Figure 4. 15 Rheology: loss modulus versus shear stress in percentage curve for bio-adhesive at different temperature parameters ---------- 95
Figure 4. 16 Rheology: storage modulus versus shear stress in percentage curve for bio-adhesive at different temperature parameters ---------- 97
Figure 4. 17 Rheology: analysis, storage modulus versus shear stress in percentage curve for bio-adhesive at different temperature parameters (110^0C, 130^0C, 140^0C and 150^0C) ---- 98
Figure 4. 18 Stress-strain curve for paper-to-paper specimens joined by process bio-adhesive (Test 1) ---------- 100
Figure 4. 19 UTS and varying elastic modulus of processed bio-adhesive materials processed at 100^0C, 110^0C, 120^0C, 130^0C, 140^0C & 150^0C ---------- 101
Figure 4. 20 UTS and modulus of elasticity of processed bio-adhesive materials processed at 100^0C, 110^0C, 120^0C, 130^0C, 140^0C & 150^0C ---------- 102
Figure 4. 21 T-Peel test force versus time curve (Test 1 at 100^0C, 110^0C, 120^0C, 130^0C, 140^0C and 150^0C) ---------- 105
Figure 4. 22 T-Peel test peel displacement versus time curve (Test 1 at 100^0C, 110^0C, 120^0C, 130^0C, 140^0C and 150^0C) ---------- 106

Figure 4. 23 T-Peel test: average peel strength versus bio-adhesive processing temperature ---------- 108

Chapter 7 Figures

Figure 7. 1 Test 1: Finding the elastic modulus using the stress-strain curve (a) 100^0C (b) 110^0C ---------- 127
Figure 7. 2 Test 1: Finding the elastic modulus using the stress-strain curve (a) 120^0C (b) 130^0C ---------- 127
Figure 7. 3 Test 1: Finding the elastic modulus using the stress-strain curve (a) 140^0C (b) 150^0C ---------- 128
Figure 7. 4 Test 2: Finding the elastic modulus using the stress-strain curve (a) 100^0C (b) 110^0C ---------- 128
Figure 7. 5 Test 2: Finding the elastic Modulus using the stress-strain curve (a) 120^0C (b) 130^0C ---------- 129
Figure 7. 6 Test 2: Finding the elastic Modulus using the stress-strain curve (a) 140^0C (b) 150^0C ---------- 129
Figure 7. 7 Test 3: Finding the elastic modulus using the stress-strain curve (a) 100^0C (b) 110^0C ---------- 130
Figure 7. 8 Test 3: Finding the elastic Modulus using the stress-strain curve (a) 120^0C (b) 130^0C ---------- 130
Figure 7. 9 Test 3: Finding the elastic Modulus using the stress-strain curve (a) 140^0C (b) 150^0C ---------- 131
Figure 7. 10 Force versus strain curve for paper-to-paper specimens joined by process bio-adhesive (Test 1) ---------- 132
Figure 7. 11 Force versus strain curve for paper-to-paper specimens joined by process bio-adhesive (Test 2) ---------- 132
Figure 7. 12 Force versus strain curve for paper-to-paper specimens joined by process bio-adhesive (Test 3) ---------- 133
Figure 7. 13 T-Peel test force versus time curve (Test 1 at 100^0C) ---------- 134
Figure 7. 14 T-Peel test force versus time curve (Test 1 at 110^0C) ---------- 134
Figure 7. 15 T-Peel test force versus time curve (Test 1 at 120^0C) ---------- 135
Figure 7. 16 T-Peel test force versus time curve (Test 1 at 130^0C) ---------- 135
Figure 7. 17 T-Peel test force versus time curve (Test 1 at 140^0C) ---------- 136
Figure 7. 18 T-Peel test force versus time curve (Test 1 at 150^0C) ---------- 136
Figure 7. 19 T-Peel test peel displacement versus time curve (Test 1 at 100^0C) ---------- 137
Figure 7. 20 T-Peel test peel displacement versus time curve (Test 1 at 110^0C) ---------- 137
Figure 7. 21 T-Peel test peel displacement versus time curve (Test 1 at 120^0C) ---------- 138
Figure 7. 22 T-Peel test peel displacement versus time curve (Test 1 at 130^0C) ---------- 138
Figure 7. 23 T-Peel test peel displacement versus time curve (Test 1 at 140^0C). ---------- 139
Figure 7. 24 T-Peel test peel displacement versus time curve (Test 1 at 150^0C) ---------- 139
Figure 7. 25 Conference paper certificate. Presented at ICMIMT and to be published by Springer Nature ---------- 141
Figure 7. 26 Proof of conference paper submission. Presented at Structural Engineering Mechanical and Computation (SEMC) ---------- 141
Figure 7. 27 Proof of conference paper submission. Submitted to the International Symposium on Advances in Structural Engineering Mechanics (ISASEM) ---------- 142

LIST OF TABLES

Chapter 1 Tables

Table 1. 1 Literature review method and approach (self-developed) ---------- 4

Chapter 2 Tables

Table 2. 1 Adhesion system theories ---------- 26
Table 2. 2 Purpose and output of TGA analysis ---------- 40
Table 2. 3 Purpose and output of DSC analysis ---------- 41
Table 2. 4 Sample rheological parameters with the conversion factors ---------- 46
Table 2. 5 Configuration and applications of rheometer measuring equipment ---------- 46

Chapter 3 Tables

Table 3. 1 Latex processing temperature parameters (self-developed) ---------- 53
Table 3. 2 Specimen arrangements for TGA analysis (self-developed) ---------- 57
Table 3. 3 Specimen arrangements for DSC analysis (self-developed) ---------- 62
Table 3. 4 Sample arrangements for rheology analysis (self-developed) ---------- 66
Table 3. 5 Single-lap shear test paper-to-paper specimen dimensions (self-developed) ------ 68
Table 3. 6 Experimental design – Taguchi's method (self-developed) ---------- 71
Table 3. 7 T-Peel test paper-to-paper specimen dimensions (self-developed) ---------- 73
Table 3. 8 Experimental design – Taguchi's method (self-developed) ---------- 76

Chapter 4 Tables

Table 4. 1 TGA thermal stages for both processed bio-adhesives and unprocessed latex material ---------- 86
Table 4. 2 DSC thermal stages for processed bio-adhesives ---------- 92
Table 4. 3 Rheology: complex viscosity versus angular viscosity performance parameters-- 94
Table 4. 4 Rheology: loss modulus versus % shear stress performance parameters ---------- 96
Table 4. 5 Rheology: loss modulus versus % shear stress performance parameters ---------- 98
Table 4. 6 Single-lap shear test elastic modulus and ultimate tensile strength for Test 1, Test 2 & Test 3 ---------- 100
Table 4. 7 Single-lap shear: average maximum force (F) and strain (mm) ---------- 103
Table 4. 8 Single-lap shear test: signal-to-noise ratio (S/N) ---------- 104
Table 4. 9 T-Peel test: average peel force and peel displacement for Test 1, Test 2 & Test 3 ---------- 106
Table 4. 10 T-Peel test: signal-to-noise ratio (S/N) ---------- 107

Chapter 7 Tables

Table 7. 3 T-Peel test: maximum peel force and maximum peel displacement for Test 1, Test 2 & Test 3 ---------- 140
Table 7. 4 T-Peel test: maximum peel strength for Test 1, Test 2, and Test 3 ---------- 140

LIST OF ABBREVIATIONS

ADP	Ammonium Dihydrogen Phosphate
AEL	Acetonitrile Extracted Lignin
ASTM	American Society for Testing
B-O	Boronic Ester
BS EN	British Standard, European Norm
C-O bonds	Carbon-Oxygen polar covalent bonds
CSIR	Council for Science and Industrial Research
DACs	Dialdehyde Cellulose
DIN	Deutsches Institut für Normung
DSC	Differential scanning calorimetry
D1, D2 & D3	Durability Classes
FTIS	Fourier-transform infrared spectroscopy
g	grams
G_P	Bending Energy
GHG	Greenhouse Gas
HM	Hot Melt
HOD	Hydro-Ddeoxygenated
ICMIMT	International Conference on Mechanical and Intelligent Manufacturing Technologies
ISO	International Standards Organization
K	Kilo
K30	Polyvinylpyrrolidone
L	Displacement
LISP	Lignin-Isolated Soy Protein
LVE	Linear Viscoelastic Region
m	minute
MA	Maleic Anhydride
MCR	Modular Compact Rheometer
MFT	Minimum film-forming temperature

mg	milligrams
ml	milliliters
mm	millimetres
MOE	Modulus of Elasticity
MUF	Melamine-Urea-Formaldehyde
MSPI	Maleic Soy Protein Isolate
N	Newton
NMR	Nuclear Magnetic Resonance
N_2	Molecular Nitrogen
nm	nanometres
OD	Oxidation Degrees
OEM	Original Equipment Manufacturer
Pa	Pascal
PAEL	Phenol-Acetonitrile Extracted Lignin
PEI	Poly-Ethylenimine
PF	Phenol–Formaldehyde
P-F	petroleum-derived
PPE	Personal Protective Equipment
SAHPRA	South African Health Products Regulatory Authority
SDS	Sodium Dodecyl Sulphate
SEM	Scanning Electron Microscopy
SEMC	Structural Engineering, Mechanics and Computation
SPI	Soy Protein Isolate
TA	Thermal Analysis
TMSC	Trimethylsilyl Cellulose
UF	Urea-Formaldehyde
UTS	Ultimate Tensile Strength
VOCs	Volatile Organic Compounds
WD	Weight Derivative
WG	Wheat Gluten

NOMENCLATURE

Symbol	Description	Unit
A	Area	Mm^2
b	surface width	mm
DW%	Derivative Weight Percentage	%
E	Elastic Modulus	MPa
E_{max}	Maximum Elastic Modulus	MPa
E_{min}	Minimum Elastic Modulus	MPa
E_y	Young's modulus	GPa
F	Force	N
GE	Sum of energy and energy dissipation	KJ
G_P	Bending Energy	KJ
G'	Storage Modulus	MPa
G"	Loss Modulus	MPa
G*	Complex Modulus	MPa
G	Adhesive Energy Input	J
H	Height	mm
ΔH	Change in Enthalpy	kJ mol^{-1}
M	Toque	Nm
n	Number of observations on the product	-
P	Peel Strength	N/m
Q	Heat Flow	W/g
R_{th}	Thermal resistance	°C/W
S/N	Signal-to-Noise Ratio	-
t	Time	s
T	Temperature	^0C
T_C	Crystallization Temperature	^0C
T_g	Glass Transition Temperature	^0C
T_m	Melting Temperature	^0C
T_o	Onset Temperature	^0C
T_p	Derivative Peak Temperature	^0C
T_R	Reference temperature	^0C
UTS	Ultimate Tensile Stress	MPa
W	Weber	Wb
W%	Weight Percentage loss	%
v	Poisson's ratio	-
WD%	Percentage Weight Derivatives	%
y	Respective Character	-
α	Thermal Expansion Coefficient	$°C^{-1}$
Wa	Work of Adhesion	J/m^2
Wc	Work of Cohesion	J/m^2
Ψ_{plast}	Plastic Deformation	%

$\Psi_{v/e}$	Viscoelastic Loss	MPa
Ψ^{bend}	Bending	Nm
Φ	Heat Flow Rate	J g^{-1} s^{-1}
Φ_S	Specimen Heat Flux	W/m²
Φ_R	Reference Heat Flux	W/m²
ΔT	Change in Temperature	^0C
Symbol	**Description**	**Unit**
σ	Shear Stress	MPa
Δx	Change in Distance	mm
γ	Shear Strain	MPa
δ	Phase Angle	degrees (°)
σ_{max}	Peak Shear Stress	MPa
γ_o	Peak Shear Strain	MPa
σ_{ya}	Yield strength	MPa
σ_r	Tensile strength	MPa
ε_f	Failure Strain	%
η^*	Complex Viscosity	Pa. s
ω	Angular Frequency	Rad/s
y	Respective character	-

CHAPTER ONE

1. INTRODUCTION

Adhesive materials have been used since the earliest eras of human evolution. This was demonstrated recently by the discovery of a tar-hafted flint tool dating back several eras [1, 2, 3]. The tool retains adhesive that, with advanced analysis, was identified as equivalent to birch-tar adhesives derived from birch tree bark [4]. This finding indicates that some of the original sources of adhesives were plant, animal, and mineral, and shows how adhesive materials have evolved.

Conventional adhesives mainly rely on petroleum-based resins like urea-formaldehyde (UF), phenol-formaldehyde (PF), melamine-formaldehyde (MF), polyurethane, and epoxy, valued for their strength, quick curing, durability, and processability [5]. However, environmental concerns, fossil-fuel depletion, formaldehyde emissions, and reliance on non-renewables have increased interest in bio-based adhesives from renewable sources such as lignin, starch, soy protein, tannins, cellulose, sugars, and plant oils [6, 7]. These offer sustainable alternatives that can lower dependence on petroleum and emissions, but their performance needs enhancement for broader industrial use.

The primary challenge in replacing synthetic adhesives with bio-based alternatives is balancing environmental sustainability with adhesive performance. Although many bio-based adhesives have good dry bonding strength, they often exhibit poor water resistance, lower wet strength, inconsistent mechanical performance, longer curing times, and limited durability. These limitations are especially important because moisture exposure can cause adhesive bonds to swell and weaken, leading to bond failure. The natural variability of biological raw materials can also affect formulation consistency and processing. Major developments in the utilization of adhesives focus on engineering applications, mainly in the packaging, automotive, aircraft & construction industries [2]. Synthetic adhesives generally provide more reliable mechanical and moisture resistance, but some systems raise environmental and health concerns, particularly those associated with formaldehyde emissions and petroleum-derived components [8, 9]. Therefore, the key research challenge is to develop a bio-based adhesive that combines high dry bonding strength, good moisture resistance, durability, minimal Volatile organic compound (VOCs) emissions, and reasonable curing time.

Several recent studies have sought to address these challenges through chemical modification, crosslinking, and hybrid bio-based formulations. A study of a lignin-based, formaldehyde-free thermoset containing 75% by weight of biomass [10], which achieved a promising particleboard bond strength of 1.42 MPa. Although the adhesive had high biomass content and good bonding performance, it still relied on a commercial crosslinker at 25% by weight, so it was not a completely bio-based material. The study evaluating lignin-isolated soy protein (LISP) adhesives using techno-economic and life-cycle analyses [11] is particularly useful for highlighting the economic and environmental challenges, but its focus was on techno-economic and life-cycle analyses rather than on developing a higher-performance adhesive. Chemically

modified lignin was developed [12] to create a bio-adhesive with better water resistance, a key weakness of conventional bio-adhesives. Using sucrose and ammonium dihydrogen phosphate (ADP), it achieved a modulus of elasticity (MOE) of up to 4910 MPa. However, it still needed a high curing temperature of 200°C in hot pressing. Development of fully bio-based adhesive systems from epoxidized plant oils and bio-derived crosslinking agents [13], demonstrates the feasibility of renewable thermoset adhesives. Although promising, plant-oil-based systems still require optimization of bond strength, curing conditions, moisture resistance, and industrial processing.

Collectively, these studies demonstrate that researchers have successfully improved the bonding strength, renewable content, recyclability, and environmental profile of bio-based adhesives. However, their limitations consistently occur in areas such as long-term durability, low-energy processing, high renewable content, curing energy, formulation complexity, and comprehensive comparison with commercial synthetic adhesives.

The purpose of this research is to develop and evaluate an improved bio-based adhesive that overcomes the limitations of existing bio-adhesives, particularly in durability, processing efficiency, and curing, while achieving better bonding performance.

This will be achieved by harnessing a latex extracted from the candelabra tree by mechanical means. This latex will be processed using cooking techniques at varying temperature parameters to produce a bio-adhesive material. This type of latex has been proven to have adhesive properties, as it is sticky and can bond two substrates together [14]. Minimal investigative research has been done on the bio-adhesive properties of this type of latex, as well as on the applications of this type of latex [15].

Analyzing and understanding the structure and mechanical properties of this material through thermal and experimental methods. Thermal properties are measured via TGA, rheological analysis, and DSC. Mechanical property examinations are carried out using a single-lap shear test performed on tensile testing equipment and a T-peel test conducted on a U-Stretch Mechanical Test System. The samples for the single-lap shear and T-peel tests are paper-to-paper substrates joined by a processed bio-adhesive material.

1.1 Statement of the problem

Recent studies have shown that bio-based adhesives can achieve strong bonding while reducing reliance on petroleum-based and formaldehyde-containing adhesives. However, significant limitations remain, including low reactivity, structural variability, durability, and the need for chemical modification. Other bio-based formulations have shown good dry and wet bonding performance, but their effectiveness is often demonstrated under controlled laboratory conditions, leaving uncertainty about long-term aging, repeated moisture exposure, processing efficiency, and industrial application. Even highly successful systems, such as hot-melt adhesives, require further assessment of their performance under broader service and manufacturing conditions. Therefore, the major research gap is the lack of a bio-based adhesive that simultaneously combines high dry bonding strength, long-term durability, 100% renewable content, and low processing energy.

It's important to address this requirement by developing a 100% naturally sourced bio-adhesive and optimizing its formulation by systematically varying the processing temperature. Therefore, systematically varying the processing temperature can identify the optimal condition that balances bond strength, mechanical, and thermal properties. This approach could improve the practical applicability of a naturally sourced adhesive and provide a more sustainable alternative to conventional synthetic adhesives.

1.2 Research aims

To develop a naturally sourced bio-adhesive and investigate the effect of processing temperature on its bonding performance by conducting thermal and mechanical experimental assessments.

1.3 Research objectives

- To develop methods of extracting latex from a candelabra tree.
- To develop methods of processing extracted latex to produce plant-based bio-adhesive.
- To determine the impact of temperature when processing and developing bio-adhesive through different temperature parameters. These are unprocessed latex and processed bio-adhesive at 100^0C, 110^0C, 120^0C, 130^0C, 140^0C and 150^0C.
- Undertake a mechanical testing approach through T-peel and single-lap shear tests to understand bio-adhesive mechanical properties.
- Undertake a thermal testing approach through TGA, DSC & Rheological testing to understand bio-adhesive thermal properties.

1.4 Research questions

The following questions can be asked based on the research objectives:

- What practical techniques can be used to extract latex from the candelabra tree?
- What practical techniques can be used to process extracted latex into bio-adhesive materials?
- How will heat influence the mechanical and thermal properties of bio-adhesive materials?
- What are the techniques that can be used to assess and understand bio-adhesive mechanical and thermal properties?

1.5 Justification of the study

This research in bio-adhesives is important due to their low carbon footprint and their potential impact on reducing manufacturing's environmental footprint by replacing petroleum-derived chemicals with renewable biological and biodegradable resources. It forms a basis for studying the processing parameters, mechanical and thermal properties of bio-based adhesive materials, as well as identifying suitable performance behavior influenced by varying processing temperatures. In this study, various processing parameters will be evaluated to determine their impact on bio-adhesive bond strength, durability, and degradation rate. The study will also help

to come up with recommendations for the most effective and efficient processing methods to extract latex and produce compatible bio-adhesive material.

1.6 Research design and methodology

Latex from the candelabra tree, developed into a bio-adhesive, has minimal readily available research information. To identify methods of extracting latex, the processing techniques, and the testing methods applied to this bio-adhesive material, a relevant literature review must be conducted.

1.6.1 Literature review

Conduct an in-depth and extensive review of existing work and literature that is available to help in understanding the following:

Table 1. 1 Literature review method and approach (self-developed)

Description	Questions
Understanding Latex and bio-adhesives.	Understand different synthetic adhesives and their environmental impact. Research on previous work that has been undertaken on bio-adhesive material. Understand chemical reactions at different stages of transition. Understand the impact of curing on adhesive strength. What analytical equipment is currently being used, and how do the results compare to theoretical literature available?
Latex toxicity composition.	How does this affect humans? What can be done to make this latex safe for human handling?
Temperature effects on latex.	How does temperature affect the structural integrity of latex and adhesive materials? Understanding glass transition temperature (T_g) & melting temperature (T_m). What is the effect of temperature during the curing process? Why will varying temperatures affect the structure of latex?
Processing techniques for developing bio-adhesive materials.	What methods are being used to process and develop bio-adhesive materials?
Testing methods to determine adhesive properties.	What are the most common mechanical and thermal testing methods used to determine bio-adhesive properties? What mechanical and thermal testing methods are most appropriate for this type of bio-adhesive material? Why are these mechanical and thermal testing methods suitable for bio-adhesive materials?

1.7 Bio-adhesive development, characterization and experimental methods

Figure 1.1 is a schematic representation of the process to be followed, and this will outline the key steps to elaborate in this sequence. Harvesting the candelabra tree branches, extracting

latex, processing latex at different temperatures to produce bio-adhesive, conducting mechanical and thermal testing, and analyzing and interpreting data obtained from these testing methods. This schematic representation is pivotal in structuring this paper and ensuring that the methodology is presented in a clear and organized manner.

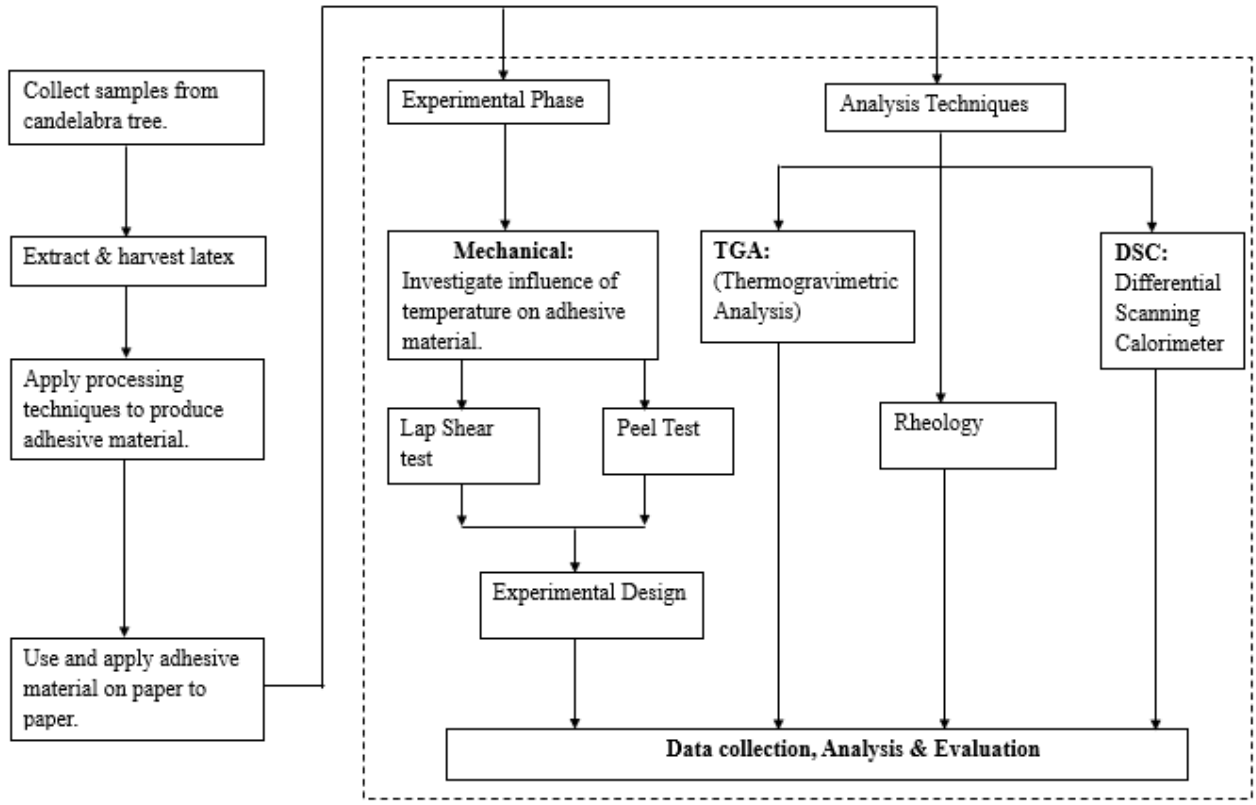


Figure 1. 1 Flow diagram for steps followed to process latex into a bio-adhesive material and conduct thermal and mechanical testing methods (self-developed)

1.8 Limitations of this study

Because of the novelty of this study, there is limited prior research on the characterization and mechanical investigations of bio-adhesive materials. This created challenges in identifying and finding relevant research that had been completed, and in understanding the research methodology and approaches undertaken previously.

To address this, a broader approach to sourcing research and investigations from previously undertaken work was expanded to include natural plant-based, animal-derived, and natural additive adhesive materials. Using this approach, the previous research and investigative methods could be linked and applied to this study.

1.9 Delimitations of this study

This study will investigate the effects of temperature on the processing of bio-adhesive materials at temperatures of 100^0C, 110^0C, 120^0C, 130^0C, 140^0C, and 150^0C.

This study only investigates the mechanical properties of bio-adhesive materials applied to paper-to-paper specimens. Bio-adhesive mechanical properties will be investigated experimentally using a single-lap shear and T-peel test. The investigations of Mechanical properties are restricted to bio-adhesive materials processed at 100^0C, 110^0C, 120^0C, 130^0C, 140^0C, and 150^0C.

Thermal characterization and analysis will be undertaken using TGA, DSC, and rheological testing methods. Thermal analysis and investigations are restricted to unprocessed latex and bio-adhesive materials processed at 100^0C, 110^0C, 120^0C, 130^0C, 140^0C, and 150^0C parameters.

1.10 Structure of the dissertation

In accordance with University of South Africa guidelines, the thesis is submitted in an essay format. To achieve the research objectives, the following steps were followed and undertaken.

Chapter 1 focused on an overview of the problem statement, research objectives, research questions, the research design and methods to be followed, and the anticipated outcomes of the study. It provided a foundation for grasping the significance and scope of the research, outlining steps necessary to achieve the aims and address the problem statement effectively.

In Chapter 2, literature review topics relevant to the subject under investigation are discussed. Among the topics covered are the material properties of adhesives, the material properties of synthetic adhesives, the biodegradable life cycle of bio-adhesives, latex toxicity, and the curing properties of adhesives. The effect of temperature on latex materials and the resulting transition phases, namely the glass-transition temperature (T_g), melting temperature (T_m), and crystallization temperature (T_C). Identifying standard testing methods used for the mechanical properties and thermal characterization of bio-adhesives.

Chapter 3 discusses the harvesting, extraction, and processing of latex to produce bio-adhesive materials. Discusses the experimental design and setup procedure implemented through thermal and mechanical testing methods and collects data on the temperature effects of bio-adhesive materials.

Chapter 4 presents preliminary results on the mechanical and thermal performance of the bio-adhesive specimen. The thermal bio-adhesive specimen results discussed are for Thermogravimetric Analysis (TGA), Differential Scanning Calorimetry (DSC), and Rheological analysis. The mechanical results discussed are for the single-lap shear test and the T-peel test.

Chapter 5 presents the conclusions drawn from this work.

Chapter 6 presents the corresponding recommendations for future research work.

CHAPTER TWO

2. LITERATURE REVIEW

2.1 Overview

In the preceding chapter, the topic was presented, along with the problem statement, the goals, and the importance of the study. This chapter presents a literature review of the introductory topic, focusing on previous research comparable to the topic in this paper. This chapter will include the collection and study of relevant information on the topic to gain a clear understanding of how experimental methods and characterization studies can be conducted. Aside from improving current investigative work, it's important to know what happened in past investigations, as it will improve the results of future investigations. Thus, literature reviews are crucial to this type of study.

2.2 Adhesive

Most synthetic adhesives are polymers originating from non-recyclable petroleum feedstocks. Petroleum is a non-renewable resource, and once extracted and used, it cannot be replaced on a human timescale, making it a finite resource that must be managed carefully.

This means that once the reserves are depleted, it cannot be replenished, and alternative energy sources will need to be developed. Additionally, the extraction and use of petroleum contribute to environmental issues, including climate change and pollution, further emphasizing the need for sustainable resource management. Therefore, it is crucial to invest in renewable energy technologies and reduce our dependence on petroleum.

One of the emissions produced from the process of producing adhesive material from non-renewable petroleum feedstocks are many volatile organic compounds (VOCs) that might be harmful to humans and contribute to air pollution [16]. Furthermore, because it’s not biodegradable, these can persist in the environment, contributing to waste and potentially harming the environment.

The latest research indicates a 10,2% increase in VOC emissions in Asia, China, and Sub-Saharan Africa from the year 2000 to 2019 [17]. There have been several problems identified with synthetic adhesive materials in recent years. These include VOC-emitting gases, namely toluene, benzene, xylene, and formaldehyde. VOCs negatively impact the environment because of their contribution to air pollution, which might lead to health-related adverse effects.

Occupational exposure to VOCs has been linked to an increased likelihood of respiratory diseases, whereas heart diseases and neurological disorders are associated with long-term exposure. As stated by the US Environmental Protection Agency, VOCs are known and probable human carcinogens through different exposure routes [18].

The increase in mass production of synthetic adhesive materials and their potential impact on the environment has led to a greater need for regulations such as Euro norm EN 314 class 1. These regulations have been introduced to promote the development of renewable bio-adhesive

materials that have lower VOC emissions [19]. As a result of their contribution to photochemical smog, VOCs are subject to more restrictions.

The adverse effects of VOC emissions have prompted a growing number of researchers to explore alternatives, such as bio-based adhesives made from plant-based materials. This is supported by a significant upsurge in the number of publications over the last few years, and the use of natural resources reduces the need for fossil fuels because they are biodegradable and have a minimal negative environmental impact [20].

Bio-Adhesives with low VOC emissions are also becoming possible due to advances and accelerated initiatives in adopting green chemistry. This is driven by the rising demand for consistent, maintainable, and eco-friendly substitutes to customary synthetic adhesives. Environmental responsibility is becoming increasingly important to industries and consumers, and renewable bio-adhesives can play a significant role in reducing reliance on nonrenewable resources.

Recent advances have been reported [21], in the field of polymer mixtures and composites made from renewable resources. These advances highlight the potential of renewable resource-based polymer blends to replace conventional petroleum-derived materials. By utilizing polyols derived from biomass, researchers aim to enhance the mechanical and thermal properties of elastomers while maintaining sustainability and decreasing environmental effects. Polyols are multi-hydroxylated alcohols, as shown in Figure 2.1, which are used as an additive in the polyurethane synthesis process [22].

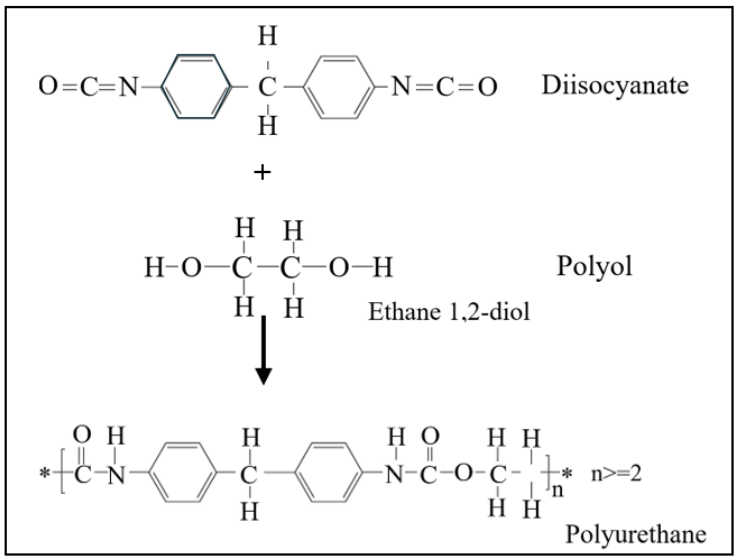


Figure 2. 1 Polyol as an additive in the polyurethane synthesis process [22]

According to a study conducted by Gandini and Belgacem, polyols can be produced by oxy-propylation of plant-based or animal biomass deposits [23]. This process involves the reaction of biomass with propylene oxide in the presence of a catalyst, followed by the creation of polyols. These polyols can then be used in the production of polyurethane foams, adhesives, and other materials, presenting a sustainable option to petroleum-based polyols.

Having said that, the objective of this study is to create a bio-adhesive material with biodegradable properties that are not harmful to the environment and do not produce VOCs, which could have long-term negative health impacts when handled by people. The goal is to further explore the mechanical and thermal properties of this bio-adhesive material through experimental & laboratory analysis.

2.3 Synthetic adhesive

Polymer-based adhesives are made from hydrocarbons extracted from crude oil and are processed into various adhesive formulations [24]. These adhesives can be categorized as water-based, solvent-based, responsive, or hot-melt (HM) adhesives, depending on how they are dried or solidified.

Because synthetic adhesives are easy to apply and set quickly, they are ideal for high-speed application requirements. Additionally, these are versatile adhesives, bonding well with various materials such as plastics, metals, and wood, which enhances their utility across industries. These adhesives provide strong bonding properties, making them widely used in industries like construction, automotive, and packaging [25]. However, their reliance on petroleum raises environmental and sustainability concerns.

2.4 Hot-melt adhesives

Compared to solvent and water-based adhesives, hot-melt (HM) adhesives have fewer VOC emissions, are 100% solid, and can be applied quickly, with faster setting times and ease of application. Once heated, the thermoplastic material becomes a viscous liquid that can be applied to surfaces [25]. Upon cooling, it solidifies, forming a strong bond. This process allows hot-melt adhesives to be used in numerous applications, including packaging, woodworking, and automotive assembly, due to their efficiency and strength.

There is a relationship between the open and set time and the solidification mechanism. The period through which the adhesive continues to retain its bonding properties after application is referred to as open time, while set time is the duration needed for it to fully solidify and achieve its bonding strength. These factors are critical to determining the adhesive's suitability for specific applications and to ensuring optimal performance in various industrial processes.

This HM adhesive material is available in granules, powders, slats, blocks, foils, and ribbons. The HM adhesive becomes a liquid when activated by thermal or solvent methods, forming a molten solid. This process ensures strong adhesion and is particularly effective for applications requiring rapid assembly or where solvent fumes need to be minimized.

These are designed for easy handling and application, depending on the necessity of the task. The versatility of these forms allows hot melt adhesives to cater to diverse industrial needs, ensuring efficient bonding solutions across various sectors.

Additionally, the absence of carrier fluid in HM adhesives enhances their environmental profile by reducing emissions and waste. This makes them particularly advantageous when compared to other synthetic adhesive materials.

However, even with the absence of carrier fluid, the formulation and composition of HM is explained in [26] as a typical formulation that contains a base polymer (polyolefins), a Tackifier (liphatic hydrocarbons), and a wax or plasticizer (paraffins), which control melt viscosity.

Polyolefins are characterized by their high chemical resistance, durability, and flexibility. These are known for being recyclable, making them an environmentally friendly option.

Plasticizers are additives that increase the flexibility, workability, and pliability of polymers. They reduce the melt viscosity of the polymer, allowing it to flow more easily during processing. This results in softer, more flexible materials, which can be used in a variety of applications.

Tackifiers are crucial in formulations because of their augmented bonding properties of the polymer base. By increasing tack, these ensure the material adheres effectively to surfaces, which is essential for applications like adhesives and sealants. This improved adhesion allows for better performance and improved bonding.

According to [27], Tackifiers, polyolefins & plasticizers are petroleum-based additives that are not biodegradable, making their final disposal significantly hazardous to the environment. They contribute to pollution and the accumulation of non-degradable waste in landfills. These materials persist in the environment for comprehensive periods, contributing to persistent ecological damage. Moreover, their production and disposal release greenhouse gases, exacerbating climate change and environmental degradation.

Recently, significant efforts have been made to ensure that all adhesive components are replaced with biodegradable or renewable alternatives. This initiative was undertaken to ensure environmental requirements could be met without compromising performance. The most recent alternative was a synthetic biodegradable thermoplastic combined with natural polymers.

Soy proteins have shown promise in enhancing the adhesive properties of synthetic biodegradable thermoplastics [28, 29]. By leveraging their natural adhesive capabilities, researchers aim to develop stronger, more sustainable materials for a variety of applications. This approach could significantly reduce reliance on non-renewable resources while addressing environmental concerns.

However, according to [30], most bioplastics have different hydrophilic characteristics from soybean proteins, and these are incompatible, resulting in partially haphazard mixtures. This incompatibility can lead to poor mechanical properties and reduced functionality in bioplastic-based products.

As a result, the largest challenge is to enhance compatibility between both mechanisms by moderating or adding compatibilizing agents. This can involve altering the chemical structure of bioplastics to make them more hydrophilic, which can act as intermediaries to bridge the differences between the two materials. The aim of this approach is to enhance the overall stability and performance of bioplastic-based products.

To address this issue, researchers are exploring methods to modify bioplastic surface chemistry or use compatibilizers to enhance their interaction with soybean proteins. The study conducted

by [27], has shown that natural materials, like pine rosin, can replace the non-renewable bioplastic in HM adhesives to improve their strength.

However, the research work is still in its early phases but shows promising potential for creating more sustainable and effective adhesives. By incorporating natural materials, researchers aim to develop alternatives that are stronger and more durable but also environmentally friendly. This aligns with the growing demand for greener solutions in industrial applications.

2.5 Solvent-based adhesives

Solvents are essential to most chemical transformations and manipulations, both in the laboratory and on an industrial scale. These also provide a medium for heat transfer and help separate components in a reaction mixture. Without solvents, many chemical processes would be inefficient or even impossible to perform.

Dispersion adhesives and solvent-based adhesives may be polyvinyl acetate-based, polyurethane, acrylates, or natural or artificial rubber [31]. This chemical reaction process requires solvents to keep reagents together, and these are widely used in purification techniques like recrystallization, liquid-liquid extraction, and chromatography [32].

When investigating crystalline formation of solvents, many recrystallization methods have been used, including cooling and anti-solvents. These methods involve dissolving the solute in a solvent at high temperature and then allowing it to cool, causing the solute to recrystallize in a purer form [33]. Anti-solvent methods use a second solvent to reduce the solubility of the compound, promoting crystallization.

However, it is not surprising, as further elaborated by [34], and [35], that the rate at which the anti-solvent is added directly influences the rate at which supersaturation is generated in crystallization, thus affecting the crystal dimensions and formation.

This is because the degree of supersaturation determines how quickly nuclei form and grow, which influences crystal size distribution and morphology. Consequently, precise control of anti-solvent addition is crucial for attaining the preferred crystal properties and safeguarding consistent product quality. These processes are cost-effective with high yields and energy efficiency, compared with liquid-liquid extraction and chromatography.

In analytical chemistry, solvent extraction remains the most widely used method. It is typical for the two phases to be immiscible, with one phase being rich in organic solvents and the other being mostly water. Chemical processes can be adversely affected by this separation. There can be two clearly different phases of a solution of some liquid-liquid organic solvents and water when inorganic material is present. This technique is essential for isolating and purifying substances, making it a cornerstone in various industries.

This classical extraction method, however, has some serious shortcomings that limit its popularity. This is further stated in [36], which notes that this process is inefficient because partition equilibrium often requires specialized equipment and an extended period to complete. It involves handling large parts of toxic, carbon-based solvents, which pose significant health and environmental risks. Moreover, the process often requires specialized equipment and

extensive time to achieve partition equilibrium, making it less efficient than modern extraction techniques.

This is also contended by [37] that due to some obvious shortcomings, these two extraction processes are still very limited. These limitations include challenges in scalability, compatibility with certain sample types, and the need for precise control over experimental conditions. As a result, further research is required to address these issues and unlock the full potential of these innovative extraction methods.

2.6 Water-based adhesives

One of the major disadvantages of water-based adhesives is that removing depleted molecular-mass components is necessary, posing toxic risks. This is because these ingredients can migrate from the adhesive to the substrate area, posing potential health risks. In the absence of sufficient molecular weight of the reactive adhesive, adhesive cohesion shows very limited resistance to mechanical stress.

To address this, manufacturers often use alternative formulations or processing methods to ensure safety while maintaining adhesive performance [38]. For example, to overcome this limitation, researchers have investigated incorporating nanoparticles into water-based adhesives to further strengthen the bond and enhance resistance to environmental stresses, ensuring long-term durability in demanding applications.

These approaches aim to enhance adhesion properties by ensuring the required molecular weight is achieved during the holding storage period, thereby significantly improving cohesive strength and allowing the adhesion strength to withstand greater mechanical stress. This transition is critical to ensuring durability and performance, particularly in high-stress or high-strain environments.

However, there is an essential limitation of water-based adhesion since most substrates are less permeable to water. Water molecules can gradually reach the substrate-adhesive interface, which reduces bonding strength and accelerates debonding [39]. To overcome this challenge [40] illustrated that polymerizing emulsions can produce water-based resins with a variety of physicochemical properties. In this process, colloids and polymers in aqueous stages are dispersed by an emulsifier to create oil-in-water mixtures. The emulsifier stabilizes the interface between the two phases, preventing coalescence. This method is widely used in a variety of applications to create stable emulsions with desired properties, such as uniformity and a long shelf life.

There is a percentage of monomeric aromatic isocyanates, particularly in solventless adhesives, such as diphenylmethane diisocyanate. These monomers are commonly used in polyurethane adhesives due to their strong bonding properties and durability [38].

With all this said regarding water-based adhesives, harmful exhaust gases and minerals such as aromatic isocyanates can migrate into substrates and the environment. This is due to unreacted aromatic isocyanates remaining in the adhesive, which hydrolyze to form volatile amines. This

migration can pose serious health risks, as aromatic amines are known to be carcinogenic and toxic, as shown in Figure 2.2.

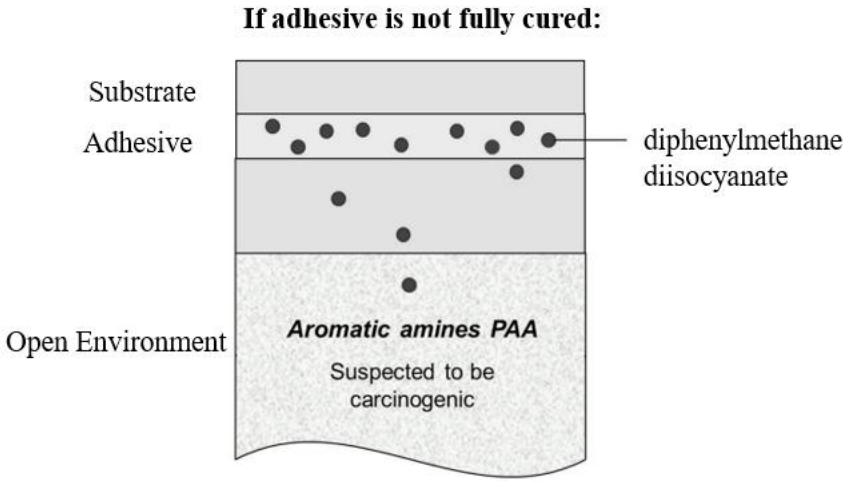


Figure 2. 2 Risk of hydrolysis of diphenylmethane diisocyanate in solventless adhesives to aromatic amines [38]

Further investigative work is still required to examine the full reaction of isocyanate migration in water-based adhesive material to ensure a clean process and prevent toxic and contamination risks.

2.7 Cellulose-based adhesives

A cellulose adhesive is a glue or binder made from natural polymer cellulose. These can be formulated as simple pastes, like methylcellulose glue. They have been developed into high-performance materials for uses ranging from everyday packaging to advanced electronics and medical equipment. For better strength and water resistance, chemical modifications can enhance the bonding mechanism, often involving chemical or hydrogen bonding.

The first adhesive based on cellulose was trimethylsilyl cellulose (TMSC). Almost 70 years ago, according to [41], this well-known cellulose derivative was introduced.

The findings of this investigation [41] are based on prior work and investigations, in which several studies regarding the treatment of cellulose with organosilicon halides for water repellence have already been done. Based on this prior investigation, the surface reaction was attributed to moisture or hydroxyl groups in cellulose in one case. However, it was not possible to measure or analyze the amount of product formed.

According to [41] a study that was conducted to investigate the reaction between organosilanes and cellulose. A relatively stable compound was formed when halo-silanes reacted with cellulose and pyridine. In the presence of pyridine, cellulose was combined with different silyl chlorides to produce TMSC. His experimental work involved the use of commercially graded TMSC and acetoxy silanes, which were analyzed via silylation of cellulose in a Parr bomb in collaboration with gravimetric analysis.

The gravimetric procedure allowed for precise measurement of weight changes, providing insights into the efficiency of the newly formed compound. This approach ensured accurate characterization of the chemical modifications achieved during the experiment.

The results from [41] have demonstrated that TMSC can be obtained in a controlled manner with varying degrees of substitution. However, it has lower solubility in certain carbon-based solvents, such as a toluene-ethanol (80/20) mixture. By reacting with cellulose, TMSC and other chloro- and acetoxy silanes yield products that, by gain and the presence of silicon substances, indicate a complete replacement of up to 2,75 per glucose unit.

The difference in mass of a specimen of trimethylsilyl cellulose over a certain duration shows that it is steady in a dry atmosphere. However, when the temperature is increased, or moisture is in the air, it decomposes. Based on this data, cellulose compounds with substituted silanes are formed. Because cellulose is hydrophilic and insoluble in organic solvents and water, it is often overlooked as an adhesive component.

This was a significant milestone in the initial development of adhesives and was achieved with this invention. By using pyridine as a catalyst, cellulose is combined and reacted with different organo-chloro silanes to develop an adhesive.

Based on this initial research and results, over the years there has been a meaningful upsurge in investigative work on cellulose-based adhesives, with a keen interest in improving properties like poor water resistance.

The latest research by [42] was to study diverse dialdehyde cellulose (DACs) to evaluate their potential for developing a bio-based adhesive with improved water resistance. By introducing two aldehyde groups, cellulose is not only less crystalline but also more soluble in hot water. This increased solubility allows for easier chemical modification and processing. The reduction in crystallinity also enhances its compatibility with other biodegradable materials and compounds.

It was possible [42] to obtain various oxidation degrees (DOs) for DAC adhesive formulations by using various reaction conditions. These reaction conditions, including temperature, time, and various reagents, were used to arrange DACs with different degrees of oxidation (DOs). Then, further experimental work was conducted via tensile and shear strength measurements to examine the adhesion performance of the developed DAC adhesives.

The results obtained [42] proved that under dry conditions, DOs and DACs absorption in their aqueous solutions played a crucial role in adhesion. This is because the concentration of DOs and DACs directly affects adhesive properties by influencing molecular interactions at the interface. As DAC-DOs increased, the shear strength of DAC adhesive intensified, but as DOs increased, the strength decreased. Similarly, the bonding strength of DAC solution intensified with higher concentrations. The largest dry adhesion strength was gauged to be 9,53 MPa on wood samples.

The results suggest that DAC is a feasible and promising bio-adhesive material. However, further research is still needed to improve and optimize the formulation and enhance the water resistance of DAC adhesives.

2.8 Starch-based adhesives

Despite their similarity, starch and cellulose have dissimilar linkages amid anhydro-glucose units. As opposed to starch, which has two types of molecules, amylase and amylopectin, cellulose has three types of molecules, forming a ribbon-like pattern [43].

As a result of this conformational difference, starch is less crystalline than cellulose but can be easily soluble.

Several studies have shown that when starch is joined with vinyl monomers, the result is a promising substitute for petrochemical-based adhesives. These exhibit comparable performance to traditional petroleum-based adhesives in terms of bonding strength and durability.

Previous studies [44] elaborated that an adhesive based on starch was prepared using ammonium persulfate as an oxidizing chemical compound and acting as a polymerization initiator to splice together vinyl acetate onto starch. However, despite this, starch-based adhesives showed weak mobility and storage steadiness, possibly because of starch retrogradation, which led to depleted adhesive performance.

The extension of this study was further pursued [45], and through research work, which looked at ways to enhance the performance of adhesives based on starch, utilizing sodium dodecyl sulphate (SDS). An organo-sulphate with a nonpolar 12-carbon chain connected to a sulphate group, SDS is a widely used anionic surfactant. The principal function of this substance is to act as a surfactant, lowering water surface tension.

To confirm the positive effects of SDS, the flexibility and storage stability of the starch-based adhesive [45], an investigative and analytical study was carried out through experimental and characterization work. This was executed using wood specimen samples that were tested for their shear strength, and characterization was conducted via scanning electron microscopy (SEM) and differential scanning calorimetry (DSC).

The results indicated that with the addition of 0,5 to 2% SDS [45], the adhesive's shear strength was slightly reduced, possibly due to SDS micelles formed during polymerization that are soluble. Due to the accumulation of micelles, a feeble coating formed at the adhesion and substrate interfaces. This weak layer formation compromised and adversely affected adhesion strength, as the micelles disrupt the cohesive network necessary for strong bonding. While adhesives with 0,5–2% SDS still had a higher fusing capacity for wood-based composites, these were not significantly less strong than adhesives without SDS, as illustrated in Figure 2.3.

According to SEM results, starch-based adhesives without SDS showed non-uniform holes on their surfaces, suggesting particle accumulation. Conversely, adhesives containing 1,5% SDS exhibited relatively uniform holes. An indication of effective mobility and storage stability is well-dispersed latex particles. Amylose-SDS complexes or SDS adsorption of starch molecules might cause charged latex particles. This hinders the accumulation of latex particles in the starch-based adhesive.

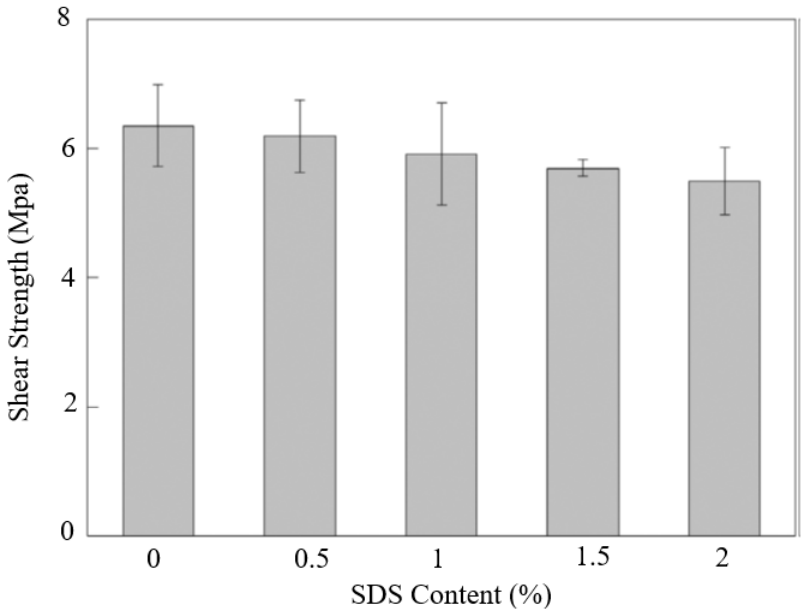


Figure 2. 3 Starch-based wood adhesive shear strength influenced by SDS [45]

With increasing storage time, DSC indicates that the enthalpy change (Δ*H*) during the thermal transition increases in adhesive materials with and without 1,5% SDS. However, even after 25 days of storage, adhesives without SDS have a much higher ΔH of 5,61 ΔH (J/g) than 1,5% SDS adhesives with a value of 1,26 H (J/g).

Based on these observations, SDS appears to inhibit starch retrogradation in adhesives. It is also possible that this factor contributes to the high storage stability of SDS adhesives. By forming amylose-SDS complexes, SDS may also prevent amylose-induced retrogradation. The suitable storing steadiness of the adhesive with SDS may also be due to retrogradation in the adhesive.

The most recent work and study carried out [46], whereby a starch-based adhesive is synthesized by adding cross-linking compounds such as gelatinization. To further evaluate its water resistance, a thermosetting starch-based adhesive was prepared, and specimens were tested at temperatures ranging from 63^0C to 98^0C. This was done to assess the durability of this starch-based adhesive material in moist, high-temperature environments.

Adhesive material morphology might change under the said conditions, and to determine this, crosslink density, enlargement ratio, and particle dimensions were tested. To investigate emulsion and cured film structure and chemical reaction mechanisms [46], the use of measuring instruments, namely thermogravimetric analysis (TGA), was employed for characterization. Mechanical properties were determined through shear strength tests, and the specimen was wood-to-wood.

The results show that crosslinking can increase the thermal stability of the main section to a certain degree [46]. However, heating can speed up the crosslinking preservation process. The shear strength of the adhesive exceeded 0,7 MPa. By crosslinking starch, high-performance starch-based adhesives can be produced.

The introduction of a polymerization initiator led to reduced flexibility and poor storage stability. Further supplementation of SDS resulted in a reduction of the adhesive's shear

strength. Lastly, recent crosslinking of starch-based adhesives promises high-performance adhesives.

However, most of the research work conducted relied on enhancing the functioning of organic starch-based adhesives with additives such as SDS and cross-linking compounds. Even though some of the added compounds might still come from natural resources, this paper aims to utilize a single biodegradable natural resource. This can be an alternative to petroleum-based adhesive materials.

2.9 Lignin-based adhesives

The third most significant constituent of wood's dry mass is lignin, found in its cell walls. Lignocellulose binds cellulose and hemicellulose together, acts as an adhesive material within wood cell walls, and renders material properties such as strength and rigidity [47]. Because of its phenolic nature, lignin is an attractive substitute for adhesives since it is the natural glue in plant materials.

Lignin can be obtained from a wide range of recyclable biomasses, comprising softwood, hardwood, sugarcane, and bagasse. A large amount of lignin is found in softwoods, which are the most used material [47].

In this study [48] the use of lignin extracted from acetonitrile as a substitute for formaldehyde in conventional phenol-formaldehyde adhesives was investigated. As a raw material, acetonitrile-extracted lignin (AEL) was used, along with phenol and polyvinylpyrrolidone (K30), as a biocompatible agent, to produce a formaldehyde-unrestricted lignin-based adhesive.

Acetonitrile-extracted lignin (AEL), with a natural structure that enables hydrogen bonding, makes it suitable for adhesive preparation. AEL is chosen to react with phenol to form phenolated AEL (PAEL), and PAEL is mixed with K30 aqueous solution to form a formaldehyde-unrestricted adhesive. For mechanical properties, a shear strength experimental approach was used.

The results obtained [48] Indicate the optimal process at 80°C with a reaction time of 3 hours. In addition, it indicated a 10% concentration of K30 at a mole ratio of lignin-to-K30 of 1;0,4. The adhesive shear strength can reach 1,70 MPa. The adhesive also shows water-resistant strength, which is a very important factor in increasing its applications.

Other work completed by [49], and [50], whereby the research results showed that lignin-containing adhesives have low adhesion strength because nominal lignin has a high molecular weight and low crosslinking ability under alkaline circumstances. Replacing petroleum-based compounds with lignin increased viscosity and decreased flowability. Due to this, adhesion strength is decreased, and curing conditions are more severe.

Further studies [51] meant to address these challenges was the preparation of totally lignin-based adhesives. As part of this two-step strategy, nominal lignin is hydro-deoxygenated (HOD), followed by an acid-mediated reaction process, which involves adding a hydroxymethyl group to organic compounds. When organic compounds are reacted with hydrogen, HDO removes oxygen from these compounds.

In addition to reducing lignin's molecular weight, HDO can improve water resistance by breaking down carbon-oxygen (C-O) polar covalent bonds. This was a promising adhesive with stronger adhesion strength under both dry and wet circumstances.

The research work in [48] and [51], which provided promising results with an adhesive material with stronger adhesion properties. However, the process used is a combination of more than one phase that is dependent on a chemically enhanced reaction process, which is interdependent with other components such as PAEL and a K30 ratio to form a formaldehyde-free adhesive. There is still further risk of formaldehyde emission even at the lowest level.

The objective in this paper is to extract and produce a novel biodegradable adhesive that is obtained from natural resources, which, in this case, is latex from the candelabra tree, and the process to develop this bio-adhesive with no chemical modifications involved.

2.10 Protein-based adhesives

During the 1930s and 1960s, soy-protein adhesives were extensively utilized in applications such as wood composite production [52]. Compared with other synthetic phenol–formaldehyde (PF) or urea–formaldehyde resins, soy protein-based adhesives exhibit inferior water resistance properties. Currently, soy protein-based adhesives have been substituted by synthetic adhesives. However, soy protein is a promising renewable material for producing bio-friendly adhesive materials.

The latest approach [53] of developing a stronger and water-resistant adhesive based on soy protein. To form maleic anhydride (MA)-grafted SPI (MSPI), soy protein isolate (SPI) was primarily customized with maleic anhydride (MA) through amide linkages and ester linkages. Then, the last stage was the combination of MSPI and poly-ethylenimine (PEI) to form MSPI–PEI. In this study, the effect of temperature was investigated, and the formulation or processing approach was developed.

The study [53] further showed that MSPI adhesive material had a lower lap-shear strength. However, adding PEI to MSPIs dramatically improved their adhesive properties. Shear strength was highest with adhesive 20 Wt% PEI. Lap Shear strength and water resistance were not affected by varying temperature within 120°C –160°C. Another study [54] that was conducted to evaluate the adhesive bonding properties of SPI and wheat gluten (WG). A combination of tensile shear strength capacities, optical microscopy, atomic force microscopy, and adhesion dimensions at the nanoscale was conducted. However, this paper focused only on the lap shear test.

Figure 2.4 elaborates on measurements of wood substrates' tensile shear strength. In Accordance with European Standard EN 204, the horizontal lines at 10, 8, and 2 MPa show the limitations of mechanical strength classes D1, D2, and D3 [54].

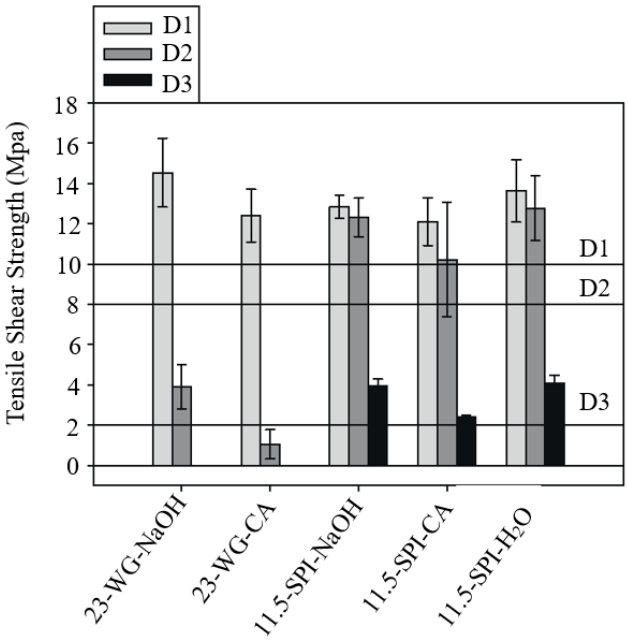


Figure 2. 4 Measurements of wood substrates' tensile shear strength [54]

Investigating the water resistance and joint strength of wood substrates fused with SPI or WG using tensile shear strength capacity [54]. Consistent with the results, WG is inferior to SPI, particularly regarding water resistance in acidic and alkaline environments, as shown in Figure 2.4. SPI-bonded substrates pass all durability tests (D1–D3) irrespective of dissolving agent, whereas WG-fused substrates pass only toughness class D1 (≥10 MPa).

Furthermore, the tensile shear strength and atomic force microscopy capacities are similar. This shows that fusing properties translate satisfactorily through covering regimes from the macro- to the nanoscale.

Most recent research work completed [55], was the study inspired and base on recyclable SPI. In this study, SPI/BP@mica was invented by co-assembling mica and SPI via dynamic catechol-derived boronic ester (B-O) interfacial fusing of boron and nitrogen (B-O). This further promoted composite functional modification, and the proposed design strategy can provide guidance for the construction of durable, recyclable protein-based materials.

The results obtained [55] showed a relatively low shear strength, and neat SPI adhesive had a dry shear strength of 1,31 MPa and a wet shear strength of 0,54 MPa. The weak wet shear strength was caused by the weak water resistance of SPI adhesive. There is a small increase in the wet and dry shear strength of SPI/Mica adhesives, reaching 1,57 MPa and 0,68 MPa, respectively. With the addition of BP@mica, SPI-based adhesives' wet and dry shear strength recovered significantly, reaching the greatest wet and dry shear strength of SPI/BP@mica of 2,39 and 1,05 MPa, respectively.

However, the excess addition of BP@mica leads to a reduction in mechanical properties and a brittle adhesive layer due to restricted molecular chain mobility occurring from the increase in compound density.

The research work and results obtained [53, 54, 55] are quite significant for the study of protein-based adhesives, and the results were quite positive. However, there is still more research and investigative work required to address the challenges of poor water resistance, curing rate, and low bonding performance when compared to other bio-adhesive materials [56].

This is because soybean protein adhesives are easily eroded by water, and these tend to have weaker water resistance, depleted fusing performance, and a slow curing rate. Protein molecules are thermally denatured and dehydrated during curing. A mechanical locking load and hydrogen bonds among polar groups are produced by entanglement of protein molecules after curing [56].

As a result, soybean protein's molecular weight is relatively high, and the intermolecular friction rises because of the interaction of side chain groups. Furthermore, the raw material contains high levels of polysaccharides, resulting in a high viscosity.

2.11 Recently developed bio-based adhesives and their performance

Bio-based adhesives are attracting interest as alternatives to petroleum-based adhesives due to concerns about fossil fuels, formaldehyde emissions, and environmental impact. Recent studies show that lignin, soy protein, sucrose, and Xylan can be modified to produce adhesives with competitive bonding performance. Adhesive performance depends on functional-group reactivity, crosslinking, network formation, viscosity, wetting, and curing temperature. Hydrophilic carbohydrate- and protein-based materials can absorb moisture and plasticize, whereas lignin exhibits structural heterogeneity and lower reactivity.

Recent studies demonstrate considerable progress but also reveal a common structure–processing–performance trade-off. Development of a fully bio-based soy-protein or citric-acid adhesive achieved dry, cold-water, and hot-water shear strengths of 1,65 MPa, 1,99 MPa, and 1,58 MPa, respectively, demonstrating that chemical modification can significantly improve the hydrothermal performance of protein-based adhesives [57]. However, optimal performance required 180^0C for 5 minutes, indicating relatively demanding curing conditions. The development of a formaldehyde-free sucrose/ADP adhesive with promising dry and boiling-water performance [12], but its processing required hot pressing at approximately 200^0C, raising questions about curing energy and process efficiency. Lignin-based systems have similarly benefited from chemical modification, but recent reviews identify low reactivity, structural heterogeneity, limited durability and water resistance, and the cost of modification as ongoing barriers.

A recent study focused on the development of an all-bio lignin adhesive using oxidized sucrose as a multi-aldehyde. Oxidation of sucrose introduced aldehyde groups that reacted with sodium lignosulfonate, forming a dense network [58]. Fourier-transform infrared spectroscopy (FTIR), nuclear magnetic resonance (NMR), and X-ray photoelectron spectroscopy (XPS) confirmed this. The adhesive achieved a shear strength of 1,04 MPa, increasing to 1,42 MPa after hot water and to 1,03 MPa after boiling for 3 hours. These results indicate that reactive groups enhance hydrothermal stability. However, chemical steps such as sucrose oxidation add complexity. The optimal hot-pressing temperature of 200^0C raises concerns about energy use. Overall, chemical

functionality and crosslink density are vital for water resistance, but improving these properties at lower temperatures remains challenging.

In contrast, a recent study demonstrated the potential for exceptionally high performance with Xylan, reporting approximately 30 MPa of lap-shear strength and excellent reusability [59]. However, the system is a specialized hot-melt adhesive, and its long-term environmental durability, processing energy, and broader industrial applicability require further investigation.

When the four studies are considered collectively, an important pattern emerges. None of the successful bio-based systems relies solely on untreated natural material. Soy protein was chemically modified with citric acid, sucrose was converted using ADP or oxidation strategies, lignin was functionalized via a bio-aldehyde route, and lastly, xylan was engineered into a high-performance hot-melt system. This indicates that the central scientific challenge is not merely the selection of a renewable raw material but the controlled manipulation of its molecular structure and processing behavior.

A second important observation is the recurring importance of thermal processing. This achieved optimal performance at 180^0C and demonstrated strong hydrothermal stability in a modified soy-protein system [57].

While the two studies [12, 58] used approximately 200^0C processing conditions, this suggests that temperature influences molecular mobility, reaction kinetics, crosslinking, and the formation of the final adhesive network. Additionally, a functional formaldehyde-free sucrose adhesive was demonstrated. Furthermore [58] showed that lignin reactivity can be enhanced through bio-derived chemistry, and this demonstrated [59] exceptionally high-performance Xylan-based adhesion. However, higher temperature should not automatically be interpreted as better performance. Insufficient temperature can result in incomplete curing and inadequate cohesive strength, whereas excessive temperature may increase energy consumption and potentially promote thermal degradation of the adhesive.

The studies also show that dry bond strength alone is insufficient to assess adhesive performance. All incorporated water-related testing demonstrates [12, 57, 58], and that an adhesive's ability to maintain mechanical integrity after water exposure is a critical performance indicator. Consequently, a more rigorous assessment should consider dry strength, wet strength, strength retention, water absorption, and, ideally, repeated wet–dry exposure.

Overall, the literature indicates that the next stage of bio-adhesive research should shift from simply maximizing bond strength to optimizing the relationship among material chemistry, processing temperature, and final adhesive performance. This provides a strong rationale for systematically investigating processing temperature in a naturally sourced adhesive. The proposed research can therefore determine whether a lower or intermediate processing temperature can provide an appropriate balance among dry bonding strength, durability, and processing energy. Future studies can further extend to a direct comparison of bio-adhesives with a conventional synthetic adhesive under standardized testing conditions, including water resistance. However, further interrogation reveals that the remaining problem is not simply adhesive strength. The central challenge is achieving an optimal combination of bond strength,

wet-state performance, durability, curing temperature, energy efficiency, formulation simplicity, and industrial reproducibility.

In my view, the strongest point of the existing studies is that they have largely demonstrated that bio-based adhesives can work. The remaining question is under what processing conditions they can perform optimally and efficiently. That distinction clarifies the technical research gap in this paper. Consequently, this can lead to a meaningful contribution by systematically varying processing temperature and determining its effect on the bio-adhesive's structure–processing–property relationship. This would allow not merely for identifying the strongest bio-adhesive, but also for determining the optimum processing condition that provides the best overall balance among mechanical performance, thermal performance, and processing efficiency.

2.12 Biodegradable adhesives

Biodegradable adhesives are typically made from natural materials such as starch, cellulose, or protein, which can easily be broken down by microorganisms in the environment, as elaborated in Figure 2.5 [12] and providing the full environmental impact life Cycle for bio-based adhesives. This creates an environmentally friendly alternative to traditional adhesives, which persist in the environment for a long time. Additionally, these can be produced from renewable resources, making them a more sustainable alternative to conventional adhesives.

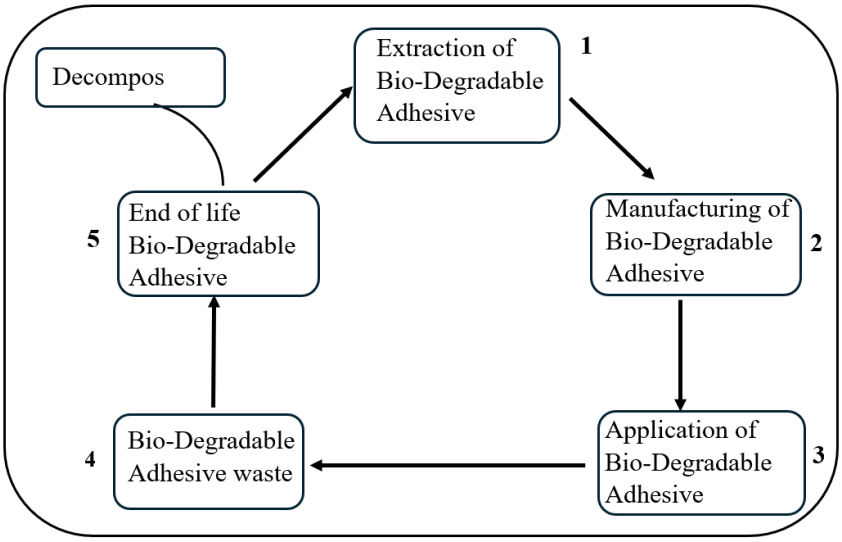


Figure 2. 5 Schematic representation of the life cycle thinking approach for bio-based adhesive [60]

Biodegradation occurs across almost all types of material, with the difference being the period in which this degradation occurs. Biodegradation rates depend on a material's composition and surrounding circumstances, such as temperature, moisture, and microbial activity. For example, natural materials like starch degrade faster than synthetic polymers, which may require specific conditions or longer periods to break down completely [61].

By choosing biodegradable adhesives, industries can significantly lower their environmental footprint, contribute to a healthier planet, and promote and drive the need for formaldehyde (VOC)-free resources. Researchers have also made remarkable advances due to the need for products made from recyclable, sustainable bases, typically biopolymers. In what follows is an

overview of some of the major achievements in adhesives produced from cellulose, lignin, starch, and proteins.

2.13 Significance of biodegradable adhesives

The use of biodegradable bio-adhesives reduces toxic volatile organic compound (VOC) emissions, optimizes the recycling of electronic waste, and significantly reduces the carbon footprint of structural materials. Modern engineering practices and applications can achieve robust material bonding without creating long-term microplastic waste or end-of-life disposal issues, and this can be achieved by replacing petroleum-based resins with natural polymers [62].

Furthermore, their low greenhouse gas (GHG) emissions can lead to the cultivation of renewable plant feedstocks such as starch, lignin, or soy that can trap carbon dioxide. As a result, the cradle-to-grave carbon footprint is significantly reduced compared to fossil-fuel-based systems, such as synthetic adhesives.

The adaptability and flexibility of these bio-adhesive materials make them ideal for biomedical, packaging, furniture, construction, aviation, and automotive applications. The gradual increase in demand is also motivated by the lower costs of raw materials, the vast abundance of renewable materials, and their derivatives, which have also drawn much interest in industrial production [63].

Previous researchers have demonstrated the benefits of bio-based adhesives as sustainable alternatives to synthetic resins in a variety of studies [64]. Researchers focused on improving water resistance, shelf life, bonding strength, lifecycle assessment, and end-of-life scenarios while maintaining environmental benefits. Assessing moisture resistance and aging under real-life conditions to validate durability, as well as optimizing cost and processing compatibility.

The development of bio-adhesives has revolutionized scientific research by providing biocompatible, wet-tolerant, and dynamic bonding solutions that overcome the limitations of synthetic adhesives. Through their research, structural engineering principles have been shifted toward biomimicry, advancing fields like biomedical engineering and environmental science significantly [65].

Several alternative systems have also been investigated, but none of them have been commercialized. If this problem can be solved cost-effectively, it can provide an outlet for abundant, low-cost, relatively consistent bio-adhesive usage. Furthermore, bio-based materials could form cross-linked networks and adhere to a variety of surfaces, which enhances their properties [50].

Therefore, from the viewpoint of environmental and economic sustainability, the use of bio-adhesive materials could be considered as a viable alternative.

2.14 Toxicity in biodegradable adhesives

Latex toxicity may cause inflammation of the eyes, nose, throat, and lungs. Contact can be made through inhalation of discharged fumes, and direct skin contact can cause a reaction. [66, 67].

The effect of this toxic element is not visible to the human eye, but it can have long-term effects such as lung inflammation. The reason for the lack of visibility is that these are small particles ranging from 1 to 100 nanometres (nm) in size. Therefore, these are called nanoparticles [68], and examples of natural nanoparticles are airborne nanocrystals, metal oxides, hydroxides, and anthropogenic [69].

Molecular and atomic nanoscience is being developed to investigate and manipulate substances on a nanoscale. This field aims to understand and control the conduct of substances at the atomic and molecular levels. By doing so, academics can invent novel materials with unique properties, develop advanced technologies, and improve existing processes in areas such as medicine, electronics, and energy production [70].

Nanotechnology is the utilization of nanoscience to create nanomaterials and nanoparticles with structural components between 1 and 100 nanometres. Nanomaterials and nanoparticles have unique properties that differ from those of larger-scale materials, such as increased strength, enhanced reactivity, and improved electrical conductivity. These characteristics make them valuable in various scientific fields, where they can be used to develop advanced technologies and solutions.

A wide range of physico-chemical characteristics can be observed when nanoparticles are used in biological systems. In the life cycle of nanomaterials and nanoparticles, some potential hazards have been identified [71, 72]. The behavior of nanoparticles in biological systems depends on their size, shape, surface charge, and composition. These factors influence how they interact with cells, tissues, and organs. Understanding these interactions is crucial for predicting toxicity and ensuring the safe design of nanoparticles for various applications.

In vitro and in vivo assays are the most common laboratory tests used by toxicologists. In vitro assays are conducted outside a living organism, typically in a controlled environment such as a petri dish or test tube, to study the effects of substances on cells or biological molecules. In vitro laboratory testing procedures are managed with the endorsement of regulatory bodies, namely SAHPRA (South African Health Products Regulatory Authority) [73].

In vivo assays, on the other hand, are performed within a living organism, providing insights into how a substance behaves in a complex biological system [68].

Furthermore, toxicologists conduct toxicity tests and assays to determine whether nanoparticles can cause toxic effects in the environment, on humans, and on animals [70]. These tests are crucial for assessing potential risks associated with new materials, ensuring that these are safe for use in various applications. Toxicologists also evaluate the dose-response relationship to determine safe exposure levels and identify any long-term effects that may arise from repeated exposure.

Based on previous research and existing toxicity assessment standards, these standards are designed to test chemical toxicity. However, nanoparticles have other characteristics that can cause interference with the use and results of a traditional toxicity assay. These require special attention due to their unique particle sizes compared with those of normal chemical compounds.

Correct characterization of nanoparticles, which accounts for size, surface area, chemistry, porosity, and solubility, will ensure accurate categorization of their physicochemical properties and biological effects.

This will ensure greater reliability and more accurate results. This approach will help researchers and regulators better understand how nanoparticles interact with biological systems, ensuring that safety assessments are both comprehensive and accurate. By addressing the unique properties of nanoparticles, more effective methods can be developed for evaluating their potential risks and benefits [69, 74]. However, the work in this paper does not include an experimental or characterization approach to investigating the toxicity level of bio-adhesive material. Future research could incorporate experimental studies to validate these predictions and comprehensively assess toxicity levels. This would ensure the material's safety and efficacy for practical applications.

2.15 Mechanical adhesive bonding

In this paper, the composite material used as a substrate is paper-on-paper, with a biodegradable material utilized to create an adhesive joint. The joint that occurs between the substrate surface and adhesive material is called an adhesion procedure, as shown in Figure 2.6.

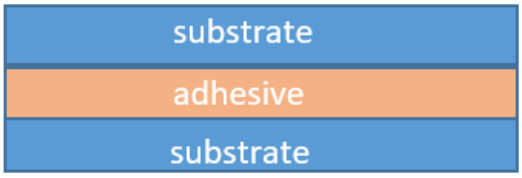


Figure 2. 6 Adhesive & substrate [75]

The working mechanism of an adhesive is that, in liquid form, it diffuses into pores and irregularities of a metal surface and hardens, creating a physical interlock with the substrate, increasing the area of contact. This is shown in Figure 2.7. This is a process defined as mechanical adhesion [75]. This causes an interfacial force that binds the adherends. Interfacial forces are only one factor that determines the mechanical strength of a system, but properties at the interface, as well as properties in the bulk phases, are also important.

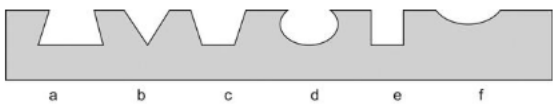


Figure 2. 7 Surface adhesion mechanism [76]

Bonding is possibly caused by an arrangement of different mechanisms. The degree to which all mechanisms contribute may vary depending on the adhesive system used. The mechanism of adhesive bonding has recently been the subject of several theories, as demonstrated in Table 2.1.

Table 2. 1 Adhesion system theories [76]

Traditional	Recent	Scale of Action
Mechanical Interlocking	Mechanical Interlocking	Microscopic
Electrostatic	Electrostatic	Microscopic
Diffusion	Diffusion	Molecular
Surface Reaction	Wettability	Molecular
	Chemical Bonding	Atomic
	Weak boundary layer	Molecular

Mechanical bonds are defined at all scales, not just at the molecular level. As atom groups become large enough to permit entanglements in space, mechanical bonds emerge in chemistry as an emergent type of bond. These are formed between groups of atoms, or molecular entities, which we will call component parts, rather than chemical bonds between atoms [77].

In macrocosms, mechanical adhesion is defined as a form-fitting connection. It creates a mechanical anchor between two components by filling all pores, cracks, and surfaces.

Part of the bond properties should moreover be tough over the course of its lifespan, which might be many years. The shear strength of a structural bond should be greater than 7 MPa, and it should be resistant to aging [78].

It has been demonstrated that an adhesive penetrates the unevenness of the exterior surfaces of two adherends and can fuse them together. The "mechanical interlocking" between the adhesive and the adherends contributes to adhesive joint strength. There is a consensus that adhesives form sturdier joints on porous or abrasive surfaces than those joined on smooth ones [79].

It is important to note, however, that this viewpoint does not apply universally, as effective adhesion can be achieved on smooth surfaces. After roughening the adhesive surfaces, adhesion could be enhanced because of mechanical interlocking, tidy surface creation, extremely responsive surface formation, and an upsurge in contact exterior area [80].

The strength of adhesives is believed to increase with differences in the surface's physical and chemical properties. It can be debated whether mechanical interlocking produces a stronger bond or whether a rise in the contact surface of adhesive increases other mechanisms [81].

The mechanical adhesion of a system is defined as a form-fitting connection that affects the macroscopic level. When the low-viscosity adhesive hardens, it seals in the holes, cracks, and hollows in the surface, creating a mechanical anchor between two components [82].

In general, pores are classified based on micromechanical and microchemical adhesion. Pore dimensions less than 0,1 mm are involved in micromechanical adhesion [83].

The mechanical properties of components are intensely influenced by the current orientations of the material. With differences in molecular and filling orientations, molecular chains can diffuse across the interface once sufficient contact has been established between the layers through wetting. If the layers are compatible and mobile enough, this can be achieved.

Diffusion, however, enhances interfacial strength through closer contact between chains, allowing attraction (such as dispersive forces), entanglement, and crystallization in short ranges. Eventually, the interface disappears as penetration proceeds.

As with auto-adhesion, diffusion and strength build up at the border between different materials. It is further thought that there is little chain entanglement, and the cohesive strength among chains linked to the surface and those that are nearby is weak. It is possible for the near-surface regions to fill in over time if the surface energetics are right, and nearby chains entangle, enlarging the cohesive strength [84].

Mechanical bonding can be affected by external factors, such as curing, which alters the material's chemical structure and influences bond strength. Proper curing ensures that the material achieves its intended properties, while inadequate curing can lead to weak bonds, reduced performance, and potential failure.

2.16 Latex and adhesive curing

Because of their thermoset polymer structure, adhesives have properties that vary not only with the testing surroundings but also with their thermal and environmental histories. A thorough understanding of adhesives as materials is necessary before test procedures can be designed for adhesive joints. In the context of accelerated testing, this is especially pertinent.

For the test to be valid, it must replicate the conditions that would exist during a real adhesive application. After prolonged exposure to the adhesive, it must be maintained under the same conditions found in the field. As a thermoset adhesive cures and contains water, its glass transition temperature (T_g) differs [85].

The rate of curing and plasticization also affects other mechanical properties. It is difficult to compare the results of a newly formed joint with those of an aged joint. In addition to changes in the substrate-adhesive interface, the mechanical performance of the adhesive can also change, affecting the interface loading during testing.

The least film-forming temperature (MFT) is used as a gauge of the deformability of the adhesive particles throughout the drying process, and this is connected to the glass transition temperature (T_g) of latex [86]. Latex curing occurs in several stages, as indicated in Figure 2.8 (a). During the evaporation of liquid substances, latex particles become more concentrated. After evaporation, the load as part of the drying process surpasses the modulus of the particles, where particle deformation occurs, leading to mechanically inferior particles.

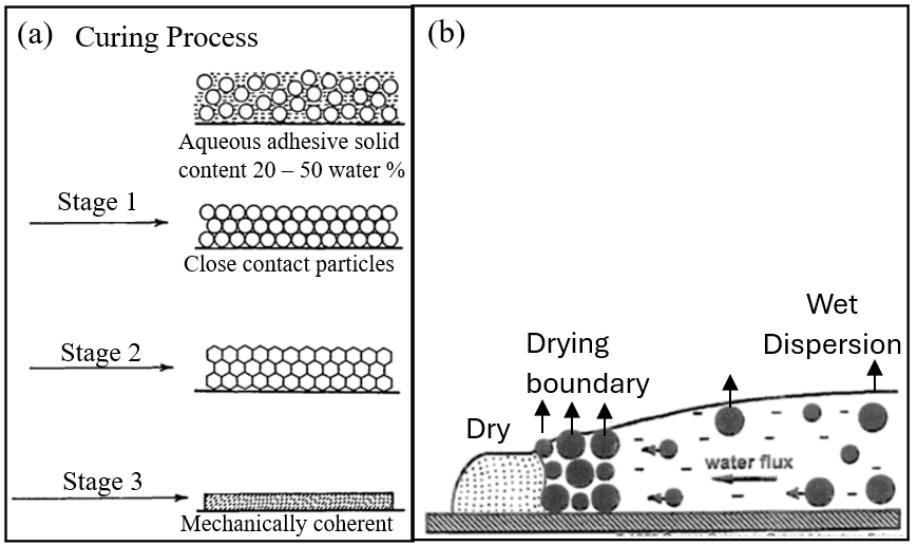


Figure 2. 8 (a) Drying process of latex (b) representation of the drying front for a latex dispersion [86]

The last phase then leads to polymer diffusion that happens across the solid-liquid particle boundaries to provide more entanglement that strengthens latex properties. Drying starts at the edge of the wet latex, where a modulation zone forms to separate the clear, dry region from the wet area, as in Figure 2.8(b). In most cases, drying occurs uniformly at the same rate.

Aging, as shown in Figure 2.9, also plays a critical role in influencing the curing process. In water vapor environments, this can cause plasticization of adhesives and lead to lower storage modulus (G') and stress, while the plastic contribution to the total deformation is increased.

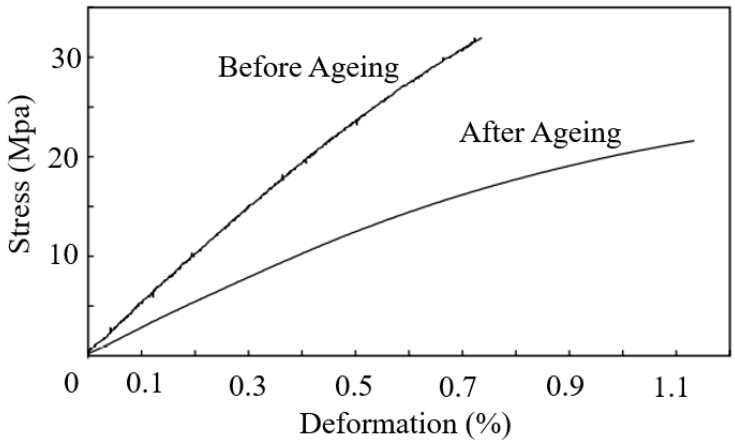


Figure 2. 9 Before and after aging test stress-deformation curves [85]

The adaptation factor reaches a plateau-like state when adhesive characterization diffusion is controlled and slowed down when the temperature increases. The entire maturation process takes 28 days at room temperature [87, 85], and this is also illustrated in Figure 2.10.

Positive mechanical properties are found from latex atoms with a T_g beyond room temperature, whereas in some cases, to enhance these properties, a filler such as bio-based Organic fillers can be added to the adhesive material and will act as a unit to lower the modulus of the adhesive

particles so that these can deform after drying [88]. Bio-based Organic fillers also promote polymer diffusion and increase the T_g of the latex beyond room temperature.

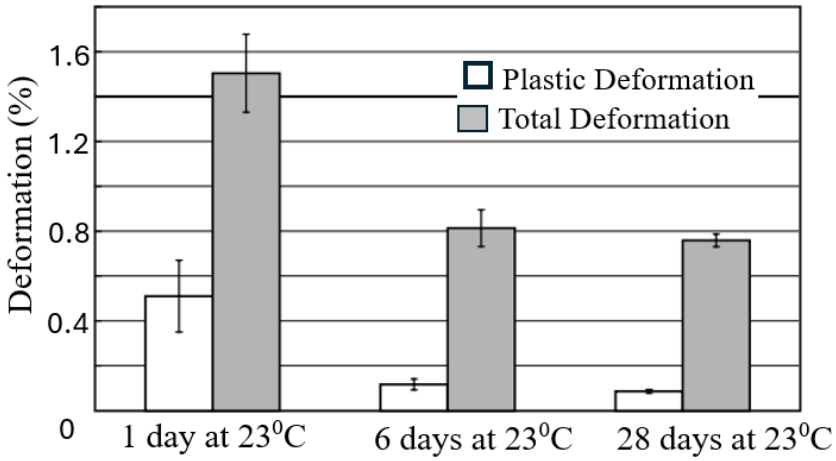


Figure 2. 10 Araldite 2014 samples cured at room temperature and examined in tension [85]

2.17 Effect of temperature

It is imperative to note that crystallizable polymers melt at varying temperatures and do not crystallize wholly, particularly when their molecular mass is high, as indicated in Figure 2.11. Due to the presence of amorphous chains, most crystallizable polymers are classified as semicrystalline [89].

Extracted latex processed at different temperatures, such as high and low, reacts differently under these conditions. At high temperatures, the latex may undergo faster polymerization, resulting in a denser and more uniform material. Conversely, at low temperatures, the reaction slows down, potentially leading to a less cohesive structure with altered physical properties. These differences highlight the importance of temperature control in latex processing. According to Figure 2.11, there are three clearly defined sections, and in this case, the temperature range was between -50^{0}C to 150^{0}C [90, 91].

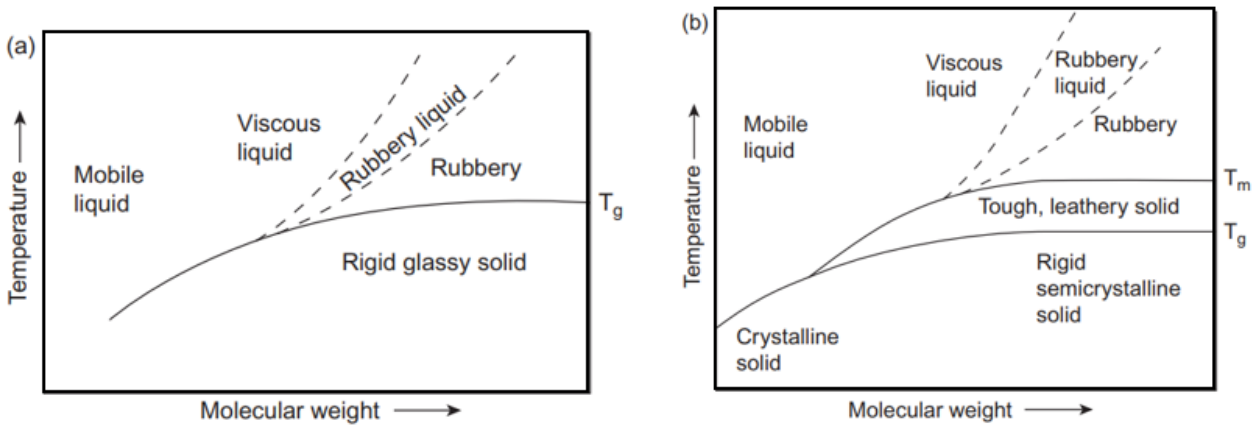


Figure 2. 11 Amorphous (a) and semicrystalline (b) polymers and their approximate relations between temperature, molecular weight, and physical state [89]

The glass transition region (T_g) occurs under conditions where changes in temperature and pressure cause amorphous materials to transition between a rigid, brittle "glassy" state and a soft, viscous liquid state. There is a high value of storage Modulus that is almost not proportional to the change in temperature.

In addition, it is shown that Tg occurs when the loss modulus G" is at a maximum value. This stage is a form of a deteriorating or slowing down phase of the thermal expansion coefficient, as shown in Figure (α) [91]. The loss modulus (G") provides insight into the material's capability to dissipate energy, and its peak indicates the transition to a more rigid structure. This phenomenon highlights the complex interplay between temperature and material properties in the glass region.

The transition state follows when the latex material changes from a glassy state to a high-temperature stage. The high-temperature stage is known as the melting stage (T_m), and in this case, it is the adhesive material. The conditions of the adhesive are more of a rubbery state with high elasticity material properties, and this indicates lower values of G'.

The importance of T_m is typically the temperature at which the greatest melting crystallites disappear, as shown in Figure 2.12. Depending on the sample's thermal history, crystallites that melt at higher temperatures have more ideal properties.

By using slow crystallization processes, more time is given to structural differences required to fit macromolecular segments into suitable crystal patterns. The T_m and melting span are determined using thermal testing methods such as differential scanning calorimetry (DSC).

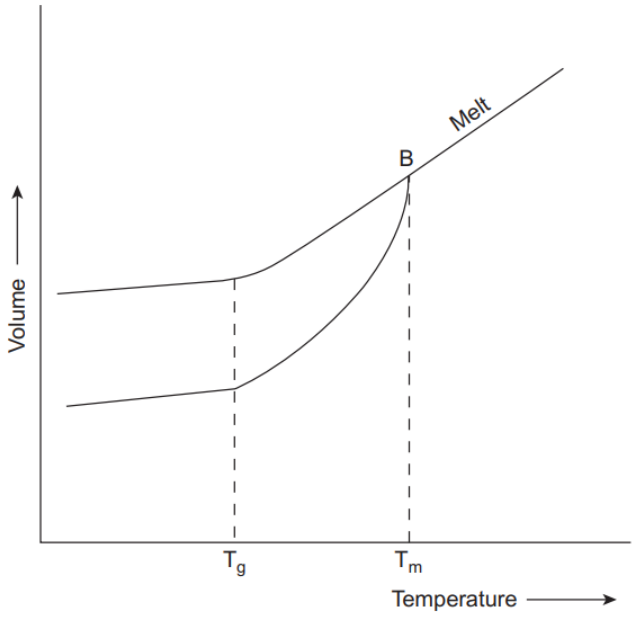


Figure 2. 12 Relationship between volume and temperature when a glass-forming polymer crystallizes. Melting point T_m and glass transition temperature T_g are temperatures for uncrystallized materials [89]

A key factor in the molecular and physical structure of latex, as well as its mechanical properties, is temperature, as colder temperatures make this material more brittle in its glassy state. It has characteristics such as rubbery, elastic, and viscoelastic properties when heated. All

these factors affect the extraction, storage, processing, and testing of latex materials. In addition, these have an impact on the adhesive mechanical properties tested via lap-shear and peel tests.

To enhance adhesive bond strength, surface preparation is critical. Surface preparation eliminates contaminants such as dust, oil, or moisture that could weaken the bond. This step also enhances the ability of the adhesive to spread evenly, improving contact and maximizing joint strength.

2.18 Surface preparation

Different surface applications include surface roughness, micro-profiles, surfaces with low levels of water-soluble molecules, and other surfaces attracted to water. Surface roughness plays a crucial role in how materials interact with their environments. It can affect properties such as the adhesion mechanism and influence product performance and longevity. Additionally, surface roughness impacts material wettability, which is critical in adhesive applications.

Lubricant wettability may also be required depending on the surface. Lubricant wettability ensures proper distribution of the lubricant across the surface, reducing friction and wear. Surfaces with low water-soluble molecules may require specific lubricants to prevent degradation, while water-attracting surfaces might need hydrophilic coatings to enhance performance in humid or wet conditions [92].

To improve adhesion strength to substrates like paper, wood, and plastic, surfaces must be prepared. Surface preparation consists of removing loose material from the substrate exterior layer. This enables the application of adhesive materials to a substrate surface to form a bond. Plastic materials increase polarity to enhance wettability. [87]

Surface roughness and wettability are by far the most effective factors for durable, strong adhesive bonding between substrates. In most cases, a glass finish or a smoother surface tends to result in poor adhesive bonding, as further elaborated in Figure 2.13. Applying liquid to an adherend will remove air from its surface, increasing the effective contact area.

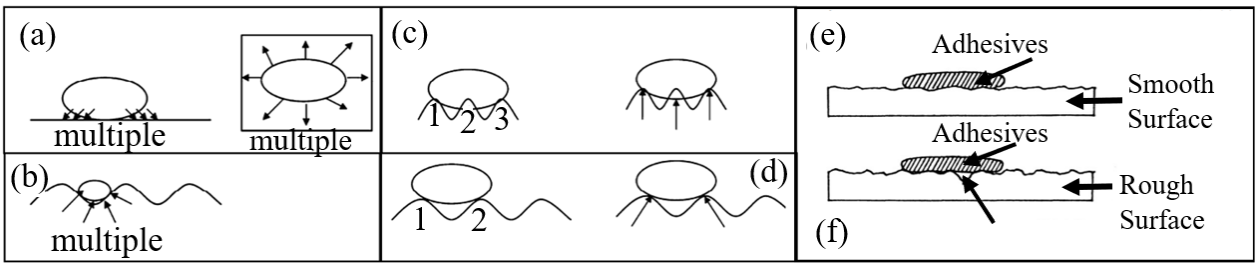


Figure 2. 13 (a) and (b) (multiple attachment points) show the highest adhesion strength, while (d) (least attachment points) shows the lowest (e) examples of good and (f) examples of poor wetting by adhesives [87, 93]

A strong or weak adhesive bond will largely depend on the surface preparation. Moreover, these two factors suggest that the adhesive material is also affected by outside factors that can affect the experimental results.

2.19 Mechanical properties of adhesives

In terms of experimental testing methods, peel, tensile, and shear tests are the three most used. These tests are utilized to assess materials' mechanical properties, like strength, adhesion, and deformation under stress. Each method focuses on a specific type of force, and peel tests assess adhesion, tensile tests measure the resistance of the material being pulled apart, and shear tests evaluate its ability to withstand sliding forces [94].

It is possible to gauge the required load to tear, disrupt, and delaminate the surface at a point where two substrates are joined together by any adhesion material using various direct adhesion measurement methods [95]. The results are influenced by external factors such as temperature, moisture, and the adhesive material's thickness. However, despite these drawbacks, destructive testing remains a valuable tool for understanding material failure mechanisms [94].

The testing of adhesives has been formalized and standardized in several ways. ASTM (American Society for Testing and Materials) and ISO (International Organization for Standardization) have accumulated the most comprehensive environmental reports around the world [96].

Throughout the world, ASTM committees and related agencies have designed and published standard test methods and reports. The results of tests can be compared between laboratories because of this.

There are a variety of ASTM standards for evaluating adhesives, but this section focuses on the mechanical properties of adhesive joints. Breakage mechanics classifies adhesive strength examinations into three customary classes, namely, shear tests, peel tests, and tensile tests.

An overview of the three categories will be provided.

2.19.1 Tensile test (adhesives in direct tensile loading mode)

Specimens are tested for operational load limits by tensile testing. This experimental approach can verify properties like fundamental tensile strength, yield strength, and extension by applying regulated tensile load to samples until reaching a state of fracture. Material safety and performance standards are ensured by these tests [97].

It is possible to describe the behavior of a tensile sample in terms of elastic and plastic responses. Pulling on the sample initially results in elastic elongation. Plastic strain occurs when a sample undergoes permanent deformation due to increasing stress. Using a stress-strain curve, one can determine when reversible elastic strain exceeds permanent plastic deformation.

Stresses that cause significant plastic deformation (usually 0,2% strain) are called yield strengths. As indicated in Figure 2.14, the stress and strain can be characterized by Young's modulus, or the modulus of elasticity. During yielding, there is significant dislocation retraction within the adhesion area. This method is known as destructive testing, as the test specimen is permanently deformed and often fractured during testing.

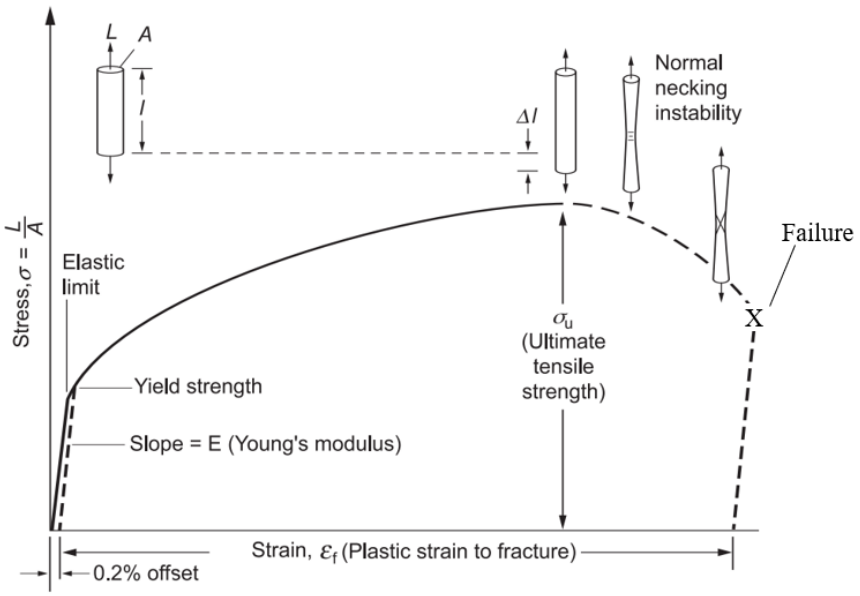


Figure 2. 14 Characteristic stress-strain curve of an elastic material [98, 99]

This stress-strain path, as indicated in Figure 2.14, has four distinct stages, the first of which is uniform deformation and background strain accumulation. Secondly, material instability indicates a loss of load-bearing capacity. Finally, there is transition deformation, which is the normal shear mode, followed by accumulation of damage resulting in a fracture surface.

In this paper, the testing method is based on ASTM D1002, ASTM D3163 & ISO 4587, in which specimens are paper-to-paper substrates joined together by bio-adhesive material.

The results from these methods report the magnitude of load at which breakdown occurs, divided by the sectional area of the adhesives. Additionally, results of tensile applied force influence the cross-sectional area, which means an increase in adhesive area might result in higher tensile strength. This relationship between adhesive area and tensile strength highlights the importance of optimizing the adhesive's cross-sectional area to achieve desired mechanical properties. However, increasing the area must be balanced with other components, like material compatibility and application constraints, to ensure overall performance and reliability [100].

In this testing method, the specimen is clamped on both ends and pulled apart at constant speed, as shown in Figure 2.15, which illustrates the typical apparatus of a tensile tester. The specimen's reaction force is measured and plotted against displacement at various points along its length. This data is used to analyze the specimen's behavior under load and determine its mechanical properties, like stiffness, strength, and deformation characteristics. The resulting graph provides insights into the material's performance and possible failure points.

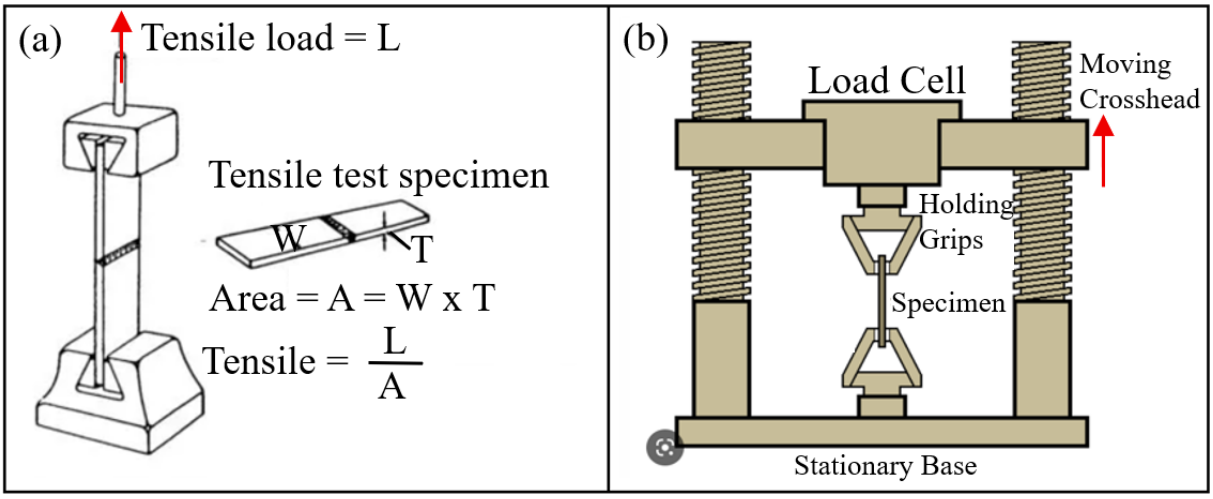


Figure 2. 15 Typical apparatus of a tensile tester [101]

The data obtained from a tensile tester can be converted into a stress-strain curve. This indicates the stress the specimen can withstand under a specific amount of strain. This illustration of information helps in evaluating and analyzing adhesives' mechanical properties and material strength [102].

The tensile test measures a material's strength by pulling it apart until it breaks. This provides data on the ultimate tensile strength, elongation, and modulus. In contrast, the T-peel test assesses the strength of adhesive between two fused materials by measuring the load needed to peel them apart. Both tests are essential for assessing material properties, but with a focus on different aspects of mechanical behavior.

2.19.2 T-Peel test adhesives

The objective of the peel test is to measure the peel strength of paper-to-paper specimens. Peel strength is a critical property that indicates a material's adhesive strength between two surfaces. The test involves applying a force to peel apart two bonded materials and measuring the ultimate peel force required.

There are numerous kinds of peel tests, including the fixed-arm peel test and the T-Peel. The fixed-arm peel test involves securing one end of the test specimen, whereas the other end is tugged at a steady speed to measure peel strength, as shown in Figure 2.16 (a).

The T-peel test involves securing the test specimen in a T-shaped configuration, where the two arms of the "T" are pulled apart at a constant rate.

This examination is commonly utilized to measure the adhesive strength of bonded materials, such as laminates or tapes, by measuring the force required to separate them, as shown in Figure 2.16 (d). Because of the type of specimen suitable to be tested in T-Peel, it is ideal for the paper-to-paper specimen in this paper to be tested using a T-Peel experimental approach.

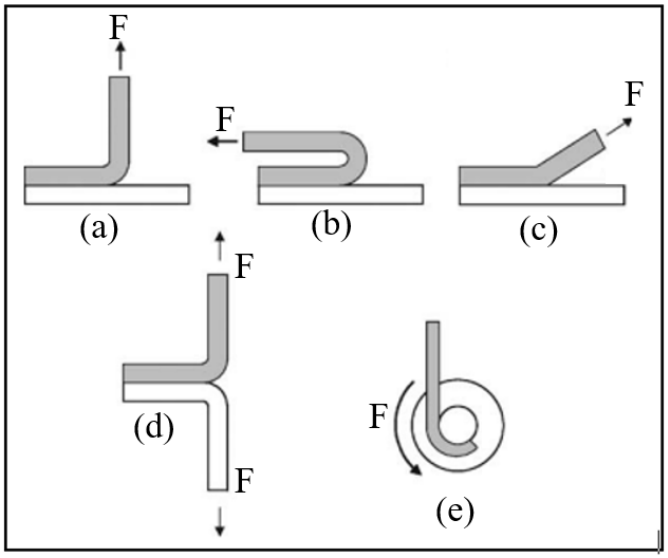


Figure 2. 16 Different types of peel tests. (a) 90^0 Peel, (b) 180^0 Peel, (c) general layout, (d) T-Peel, and (e) climbing drum [94]

The tests are different, but they also have similarities in the aim of converting measured peel strength into interfacial fracture work. The tests also differ in their configurations. Despite these differences, both methods aim to quantify the energy required to overcome adhesion, providing valuable insights into material bonding performance [103].

In this paper, a substrate joined with adhesive material is used, and this experimental test will determine and gauge the load per unit width of the paper-to-paper specimen. Peel strength is the total energy per unit area. This includes energy for the fracture or any other separation. Peel strength will also include the dissipation of local plastic yielding in the adhesive, and this is considered a material parameter [104].

In a T-peel test simulation, a thin flexible substrate is pulled apart from another substrate at a 90^0 angle and a specific rate until it delaminates. Once a significant amount of crack extension occurs, this test will reach a steady state. To determine and characterize adhesive bond strength, peel strength is used to separate the top adhesive from the substrate.

Under most T-peel test conditions, only a fraction of the total tearing energy is due to fracture toughness, with the remainder attributable to tensile and bending deformations in the substrates. Testing parameters, such as speed, temperature, and peeling force, can be adjusted depending on the purpose of the investigation or test [105].

It has been shown previously that the measured peel strength is affected by peel angle and the adhesive's viscoelastic properties. In addition, the peel force rate and the adhesion properties of the adhesive material. Other factors that may influence the T-peel test are temperature and environmental conditions [104].

The purpose of this examination was to verify peel strength, tearing load, and breakage mechanism as shown in Figure 2.17. A typical force-displacement curve shows a load upsurge at the commencement and the greatest load at the end. Furthermore, there is a plateau area where

the sample is peeled. The load needed to peel the joint between the two substrates is called a peel force [106].

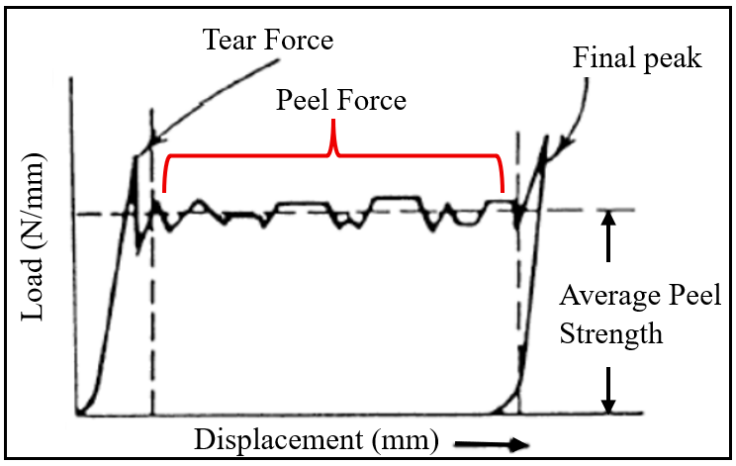


Figure 2. 17 A typical load curve of the peel [104]

Another alternative for determining peel force is to use calculations based on the following equations. These equations are derived from principles of material mechanics and adhesive properties. Consider factors such as adhesive thickness, surface area, and the applied force. By inputting these variables, the peel force can be estimated with reasonable accuracy, making this method a valuable tool in adhesive testing and material analysis. The energy balance approach:

$$P = F/b \qquad 2.1$$

$$P = \frac{F}{b} = \mathrm{Wa} + \Psi\,\mathrm{plast} + \Psi\,\mathrm{v/e} + \Psi\,\mathrm{bend} \qquad 2.2$$

Where:

P is peel strength

F is measured peel load

Wa is work of adhesion

Wc is work of cohesion

Ψ_{plast} is plastic deformation

$\Psi_{v/e}$ is viscoelastic loss

Ψ^{bend} is bending

Like the peel energy P in equation 2.1, the GE can be stated as the sum of energy and energy dissipation terms:

$$GE = P(1 - Cos\omega) \geq G_C \qquad 2.3$$

Where GE is the sum of energy and energy dissipation.

$$GE = W_a + \Psi \qquad 2.4$$

To objectively determine the adhesive breakage durability, this can be verified when an alteration is created for the plastic bending energy (G_P) that is related to the peel arm [107]. This correction ensures that the measured toughness accurately reflects the material's resistance to crack propagation, rather than being influenced by energy dissipated through plastic deformation. By accounting for plastic bending energy, more precise and reliable data for analyzing adhesive performance can be obtained.

2.19.3 Single-lap shear test

The shear strength of a material is measured by shear tests. When exposed to forces, these tests provide insight into the material's resistance to deformation. The results of these tests are critical for understanding a material's capability to withstand shear forces, and these forces are common in structural and mechanical applications.

If a force is applied to two surfaces, two parts of the surface or two different surfaces will slide past each other, causing shear stress. Shear stress can lead to deformation or failure if the material cannot withstand the applied force. Understanding shear strength is vital to understanding an adhesive material's deformation strength [108].

Testing is executed utilizing a standard tension mechanical test, a tensile tester in this case, with a proper pair of self-positioning grips to hold the specimen. There are two types of testing mechanisms that can be conducted to assess adhesive material shear strength, and these are the double and single-lap shear tests as demonstrated in Figure 2.18 (a and b).

In the double-lap shear test, as indicated in Figure 2.18 (b), specimens are reinforced in the middle and forces are applied at two points, resulting in two shear planes. These tests are appropriate for rods, bolts, and materials where a solitary shear might induce a bending load. The double-lap shear test is particularly useful for applications involving structural components, as it provides a more accurate representation of real-world stress distribution. Using two shear planes minimizes the influence of bending forces, providing clearer knowledge of the adhesive's performance.

A single-lap shear test is demonstrated in Figure 2.18 (a), consisting of two rectangular substrates. Joined together by an adhesive layer. Substrates are pulled apart at a steady rate, and the load required to separate them is gauged [109]. This is a commonly used shear test to assess lighter application materials, and it is suitable to be used in this paper as the specimen is a paper-to-paper specimen joined together by a bio-adhesive material.

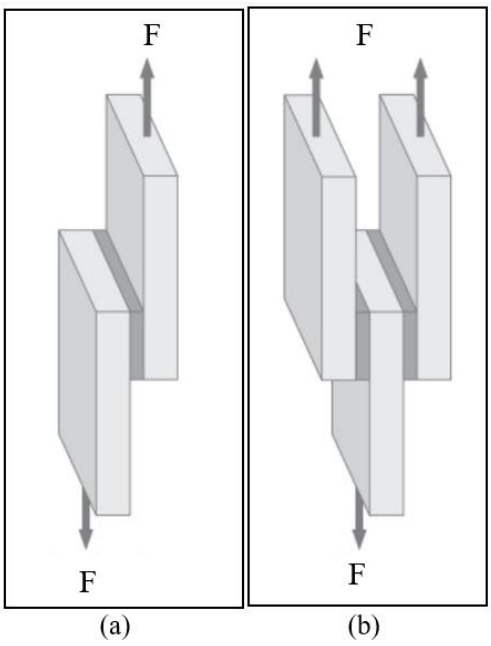


Figure 2. 18 Single-lap and double-lap shear specimens [110, 111]

Determining the resistance of bonded systems to tensile shear stresses provides a reliable indicator of bond strength. Test results are often used to evaluate adhesive performance under different conditions, like varying temperatures or environmental factors. This experimental method helps identify potential weaknesses in adhesive joints and optimizes adhesive selection for specific applications. The single-lap shear test is conducted in accordance with BS EN 1465 (74). The data received from the single-lap shear test are illustrated in Figure 2.19 and can be analyzed and interpreted.

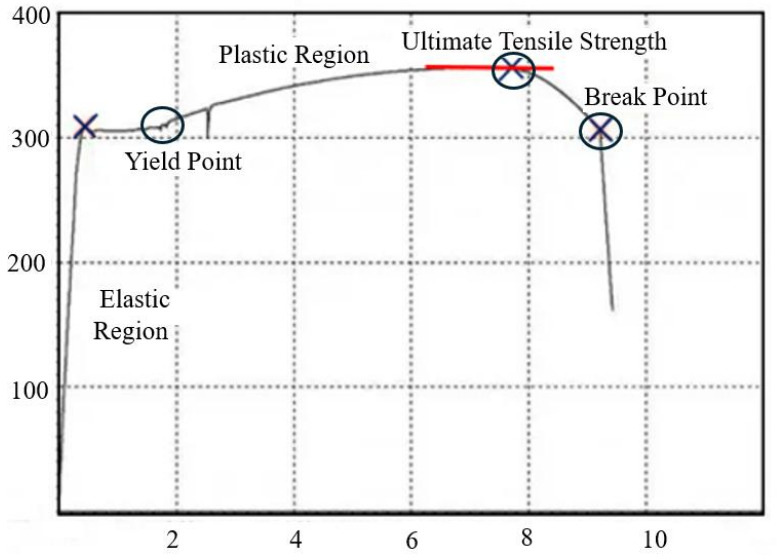


Figure 2. 19 Single-lap shear stress / strain characterization curve [112]

Testing begins in the elastic region and continues until the material reaches its yield point, where it transitions from elastic behavior to plastic deformation. During this phase, the material experiences permanent alterations in shape as stress increases, marking the onset of irreversible structural alterations.

Ultimate tensile strength is the greatest stress a material can endure before it fractures. This occurs when the material transitions from plastic deformation to complete failure. At this stage, the material can no longer sustain additional stress and breaks apart, marking the loss of its structural integrity, as shown in Figure 2.19.

2.20 Thermal testing of bio-adhesive

Thermal analysis involves studying how bio-adhesives respond to changes in temperature, such as heating or cooling. This analysis assists in comprehending thermal durability, phase transitions, and decomposition performance of bio-adhesives. It is crucial for determining the material's behavior in various applications, ensuring reliability and safety in biomedical or industrial uses [113]. By understanding their thermal properties, researchers can optimize bio-adhesive formulations to withstand specific temperature ranges, ensuring long-term stability and effectiveness.

2.20.1 Thermogravimetric analysis (TGA)

Thermogravimetric analysis (TGA), also called Thermogravimetric analysis, is a process in which the specimen weight is measured when there is a change in temperature over a certain period [114]. TGA is mainly utilized to investigate any process that will result in a bio-adhesive material losing any unstable gases during the testing procedure. Most of the adhesives will behave differently and produce different thermal stability results when undergoing the change in temperature. Hence, TGA operational properties such as a wide temperature range and the ability to detect material decomposition provide an accurate way to differentiate and analyze this material [115].

This method of analysis is unique as it makes it possible to collect accurate changes in material data that can be logged as decay, dryness, and oxidation of a specimen [116]. The results are a characteristic thermogravimetric curve derived from the percentage mass loss over a change in temperature. This data is important in the research field, as it enables quantitative investigation of bio-adhesive materials.

The TGA entails a temperature program, an accurate equilibrium scale that is joined to the specimen pan inside the furnace, and a thermocouple. The balance scale measures the sample mass inside the furnace as elaborated in Figure 2.20, and the thermocouple is used to observe specimen temperature. During the testing procedure, nitrogen (N_2) gas is fed from the purge side of the furnace, and then, after the reaction, the exhaust gas exits through the evolved gas exit.

This gas passes through the sample at a specific flow rate, time, and temperature to enable analysis of the adhesive. This process occurs under enclosed furnace environmental conditions. The analysis is conducted in an inert-specimen purge-gas environment. The process in which a specimen is heated under inert conditions. This is the process in which the chemical decay of the natural specimen is heated in a furnace without oxygen or other gases that can react with it, and this process is known as Pyrolysis. The pyrolysis process occurs inside the TGA furnace and provides ideal conditions for investigating mass change and thermal stability [117].

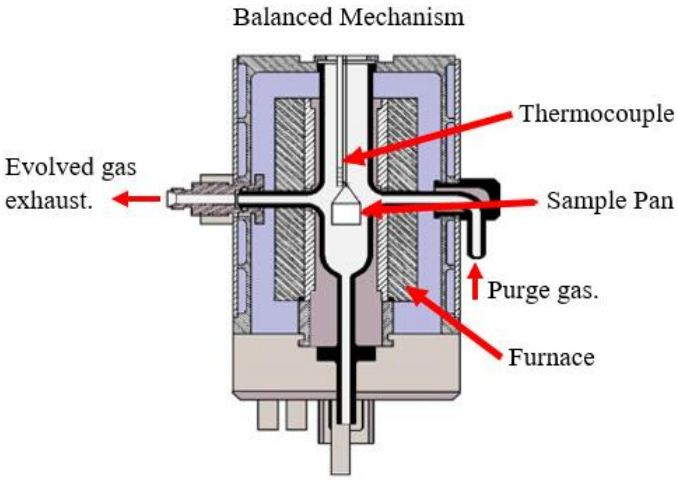


Figure 2. 20 TGA measuring equipment [116]

The limitation of using TGA is that it's not able to pick up phase transitions, polymorphous changes, or any other reactions where mass is unchanged. However, when used in combination with DSC measuring equipment, both results can be used to quantify and complement the overall results [118].

The main purpose of TGA, as stated in Table 2.2, is to detect and record changes in sample weight over time under a fixed temperature range. This procedure can comprise heating, refrigeration, steady temperature points, or a combination thereof. Most polymeric materials, including adhesive materials, will exhibit melting-point behavior before reaching the decay stage. TGA is mostly utilized to investigate, identify, and classify the thermal durability of these materials. This is important because of the novelty of the material used in this paper, and it will provide much-needed feedback for recording and investigating the mass loss over different temperature ranges.

Table 2. 2 Purpose and output of TGA analysis [119]

Feature	Thermogravimetric Analysis
What does it detect?	Weight change of the sample
Main Function	Quantify volatiles, determine composition, and assess thermal stability
Answer to the key question	At what temperature does this material begin to break down?
Results output	TGA curve. Percentage weight loss versus temperature increases

In this case, the investigation focuses on the heating process and, through it, a characteristic thermogravimetric curve can be derived and plotted solely to analyze adhesive material loss over time.

The graph in Figure 2.21 indicates two curves, where the red curve is the mass loss curve, and the blue curve is the derivative mass percentage (%) curve. From this curve, it can be observed that there are clear thermal processes occurring, namely the onset Temperature (T_o) as shown

at position X, as well as the 1st derivative peak temperature (T_p), which is at position 2. These details will help with understanding and analyzing the results in the upcoming chapters of this paper.

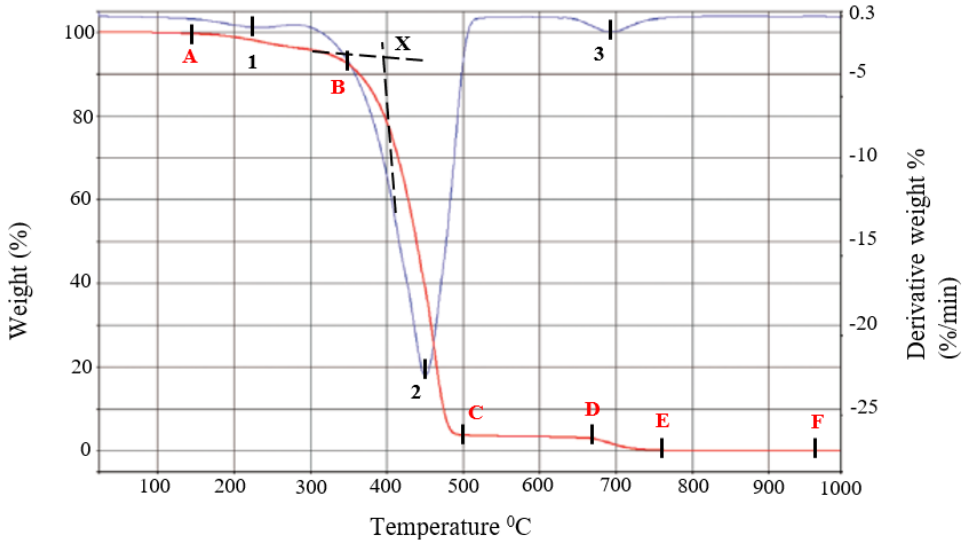


Figure 2. 21 Characteristic thermogravimetric curve [118]

2.20.2 Differential scanning calorimetry (DSC)

Differential scanning calorimetry (DSC) is a method broadly utilized for investigating, analyzing, and understanding the physical properties of materials and the development of new materials, which in this case are non-developed adhesive materials [120, 121]. DSC is one of the most used tools in the research field, as shown in Table 2.3, and can provide a wide range of answers to fundamental questions such as evaluating material performance, comparing materials, and testing the compatibility of new products and materials.

Table 2. 3 Purpose and output of DSC analysis [119]

Feature	Differential scanning calorimetry (DSC)
What does it detect?	Energy and heat flow.
Main Function	Recognizes phase transitions such as melting, crystallization, and glass transitions.
Answer to the key question	What is the melting point of this material, and how much energy does it require?
Results output	Temperature-dependent heat flow events are shown in a graph.

The technique used is thermal analysis, whereby the temperature of the main specimen and that of the reference are kept at almost the same rate and measured. The results provided are the differences in the amount of heat required to increase both the specimen and reference temperatures.

The calorimeter evaluates the energy received or released by the specimen undergoing a

specified temperature path; during this period, chemical changes occur that are linked to heat created and heat utilized. This exercise produces a signal in the form of heat flow that is then evaluated and assessed by the DSC equipment [120]. The trait of application is that the evaluated data are directly comparable to the heat flow rate (J g^{-1} s^{-1}) (Φ), and this makes it possible for the period in which change takes place to be studied and built on the time (t) dependence against the heat flow curve Φ (t) [122].

DSC is designed in a way that there is a linear increase in temperature for the specimen holder when measured against time [123]. To get accurate results when studying different polymers, the material for the reference sample must have a clearly stated heat capacity span of maximum and minimum scanning or experimental temperatures. It should also have stable properties with minimal to no changes observed during the entire duration of the temperature scan or experiment [124]. The reference samples used in the test conducted in this paper are an empty aluminum pan, and the samples enclosed in specimen pans are also made of aluminum and have the same weight as that of the reference pan [124].

There are quite a few different DSC being used for different applications. However, for our process requirement, the DSC *Heat Flux* (TA DSC 2500) equipment is utilized. Referring to Figure 2.22, which shows heat moving from the specimen pan and the reference pan, which are located symmetrically towards the middle, and thereafter going through the disk, which is situated in the furnace chamber. The movement of heat from the sample resembles the changes in the movement to the specimen chamber and to the reference.

A point to note is that the heat moving to the specimen pan and the reference pan is similar, and when the specimen pan is empty, the temperature change, ΔT, will then be zero. When modulation occurs in the specimen pan, a disparity signal is produced.

According to Fourier's law, the DSC signal (Φ) is calculated by [120] which is the change in the specimen heat flow rate and that of the reference. DSC signal is measured in W (Weber).

$$\Phi = \Phi_S - \Phi_R = \frac{(T_S - T_R)}{R_{th}} = \frac{\Delta T}{R_{th}} \qquad 2.5$$

The referred equation 2.5, where Φ_S is the specimen heat flux, Φ_R is the reference heat flux, T_S is the specimen temperature, T_R is the reference temperature, R_{th} is the thermal resistance of the sensors, and ΔT is the change in temperature.

DSC equipment, as shown in Figure 2.22, is ideal for investigating thermal transitions in polymeric materials. T_c is the crystallization temperature, T_m is the melting temperature, and T_g is the glass transition temperature [121]. With this process, it will be possible to determine if the material's configuration undergoes all or some of the transition phases (e.g., T_m points, T_g, and T_c). Since the material used in this paper is new and undeveloped, the use of DSC will help establish baseline parameters for its composition and transitional phases.

However, there are mainly two types of material, namely semicrystalline and amorphous, and semicrystalline materials will undergo all transitional phases (T_m, T_c, and T_g), whereas amorphous materials will only undergo the T_g transitional phase [125].

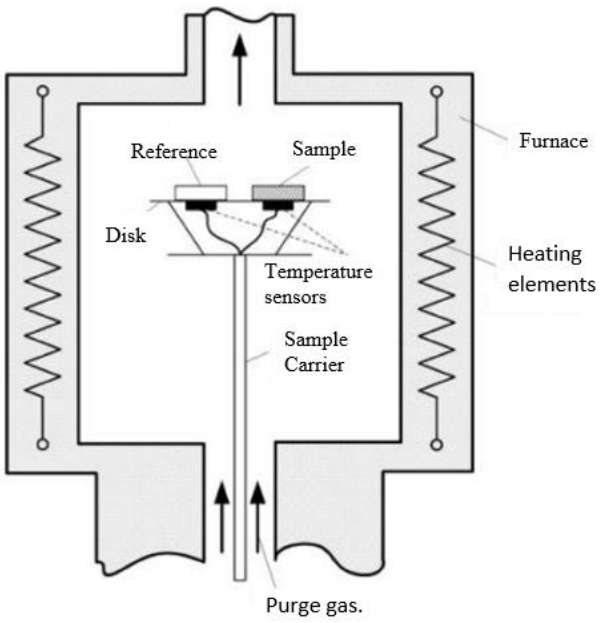


Figure 2. 22 Heat-flow diagram DSC measurement unit [120]

T_g occurs during the DSC scan of a solid material as the temperature increases, and this transition is indicated on the logged DSC baseline signal as a peak or a change in the baseline, as shown in Figure 2.23 [126]. The only change in material composition during this phase is that it dissolves from a solid to a liquid state, and this means that there will be more heat transfer to the specimen to a similar degree as that of the reference. This process is known as a solid-to-liquid endothermic phase transition, as the specimen is receiving heat, as shown in Figure 2.23 [126]. T_c occurs when, upon continuing the scanning process, less heat is needed to increase the specimen temperature, and, through this process, the molecules tend to move freely to rearrange into what is known as a crystalline structure. The process of materials changing to crystalline is also known as an exothermic process, as shown in Figure 2.23 [126].

Further increase in temperature will result in the specimen reaching T_m [126, 127]. Hence, this process indicates how the DSC can be utilized to investigate different transitional phases of material.

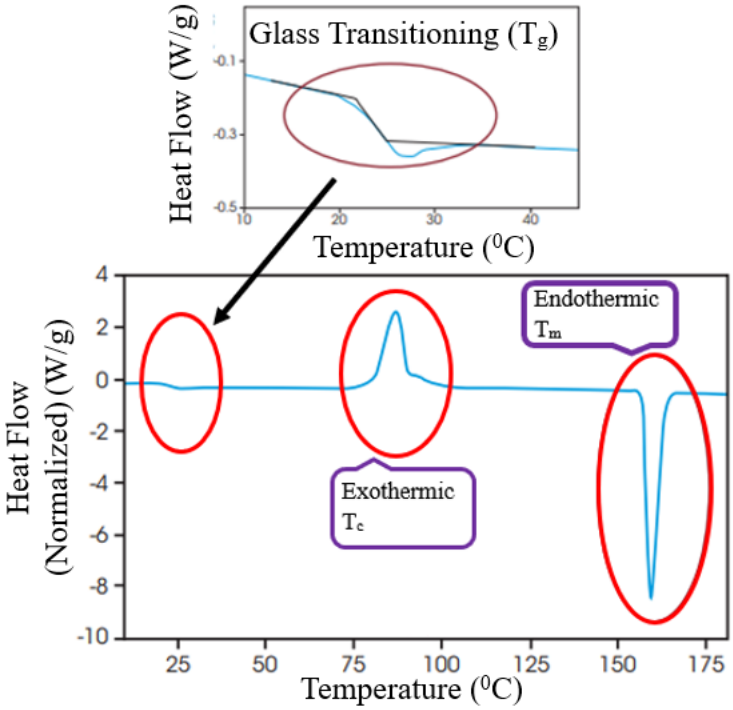


Figure 2. 23 T_g, T_c, and T_m transitioning phases. Exothermic and endothermic processes from DSC measurement [126]

2.20.3 Rheology

Rheology is a process of investigation undertaken to determine a material's performance and response when subjected to applied forces and stresses. The investigation is based on the relation between rates of stress-strain interaction and the resultant material distortion being measured [128].

Rheological performance of material can be categorized into three different states, namely viscous, elastic solid, and viscoelastic [129]. Viscous material is mainly in a liquid state whereby enhanced energy is dissipated in the form of heat during the rheological process and testing. Elastic materials are in a solid state with the potential to regain or go back to the original state and shape after undergoing a deformation process.

Viscoelastic materials are positioned somewhere in the middle, as these are made up of material possessing both perfect elastic (solid) and viscous (liquid) properties. These can also be classified as viscoelastic solid or viscoelastic liquid materials. Viscoelastic performance can be demonstrated in many ways, however, the Kelvin–Voigt model is one that simply shows the classification of elastic material. When a constant force or stress is continuously applied, this material will gradually move closer to a finite state of distortion and be able to recover to its initial form or length when this load or stress is removed [130].

The Maxwell model subsequently illustrates the classification of viscous processes under steady displacement, where the applied internal stress of the material transitions in relation to time, and when this force or stress is removed, the material refrains from returning to its initial form or length [130].

To investigate and describe the viscoelastic performance of the processed bio-adhesive material with the aim of understanding the structure that is still contained and not destroyed during the testing process, in this instance, a rotational rheometer is used [131] [132]. The most common rheometer used for viscoelastic material is a two-plate shear rheometer. This rheometer operates by using a specimen crammed between two plates shown in Figure 2.24, whereby the bottom plate is temperature-controlled and stationary, whereas the plate above can move upwards or downwards as well as rotate during the application process.

Then, operation is such that the upper plate moves to a lower position, applying force and sandwiching the sample, while the upper plate will move uninterruptedly in a single direction, resulting in a shear measurement being recorded [133].

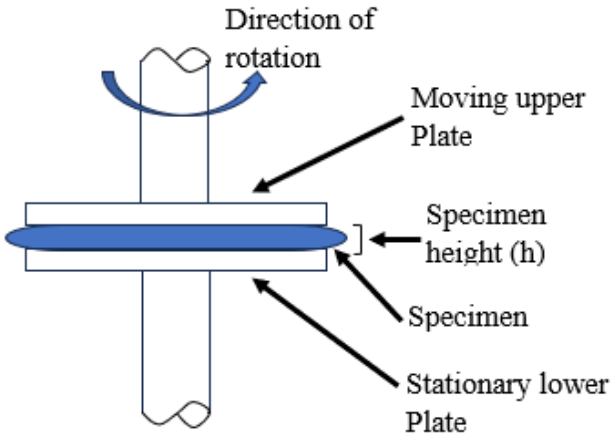


Figure 2. 24 Two-plate rheometer operational diagram [133]

The force from outside is represented by a shear stress (σ), which is equal to the load (F) applied to a unit area (A), as shown by Equation 2.6.

$$\sigma = \frac{F}{A} \qquad 2.6$$

The lower layer stays parallel to the given height (h), known as the gap, and stays constant, while the upper layer moves to a given distance (Δx) in response to this force (F). This configuration of plates is known as parallel plating, as shown in Figure 2.24. Equation 2.7 might be utilized to ascertain the shear strain (γ), or the displacement gradient across the sample, as shown below.

$$\gamma = \frac{\Delta x}{h} \qquad 2.7$$

Furthermore, the rheometer measures torque, deflection angle, and speed, while these values are used with correct conversion factors (shown in Table 2.4) to provide the data required to determine rheological parameters like the storage modulus (G') or loss modulus (G''). When distortion energy is stored, it is described by G', and when it is lost due to internal friction during flow, it is characterized by G".

Table 2. 4 Sample rheological parameters with the conversion factors [132]

Measurement Values	Conversion factors	Rheological parameters
Torque *M* [Nm]	C_{SS}-factor	Shear stress τ [Pa]
Deflection angle φ [μrad]	C_{SD}-factor	Deformation γ [%]
Speed n [min-1]	C_{SR}-factor	Shear rate γ [s-1]

The process adhesive material used in this paper can be categorized as a viscoelastic material because its physical state is solid when cured and changes to a liquid state when processed at a temperature range from 80^0C and above. This type of material behavior classifies the processed adhesive as being in the region anywhere between that of solids and liquids [133]. The reason for choosing and using the parallel plate rheometer is because of its capability to investigate and analyze the adhesive material characterized as a soft solid material, and this is elaborated in Table 2.5 showing equipment compatibility in relation to different materials.

Rheological measurement is the investigation of the association between shear rate and shear stress of any material experiencing a state of laminar flow and other factors that can cause material distortion, whereas in this case the analysis is conducted using parallel plates and the specimen being processed is bio-adhesive material.

Table 2. 5 Configuration and applications of rheometer measuring equipment [134]

Rheology geometry	Applicable for this type of material
Concentric Cylinder	Coatings, beverages, slurries. Starch pasting.
Cone and Plate	Low-viscosity fluids. Viscosity standards, sparse materials. Polymer melts in steady shear
Parallel Plate	Adhesives, polymer melts. Hydrogels. Asphalt, curing of thermosetting materials. Foods Cosmetics.
Torsion Rectangular	Thermoplastic solids. Thermoset solids

The rheometer measurements are obtained by rotating the top plate at a specific speed while the bottom plate is stationary, and from this process, maximum shear strain and shear stress are measured, while the rheometer's internal programming system is utilized to determine the complex modulus (G*) and phase angle (δ), as referred to in Figure 2.25.

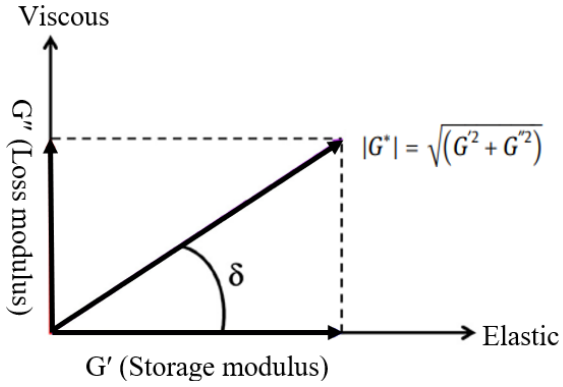


Figure 2. 25 Graph showing association among storage modulus (G′), Loss modulus (G ″), and complex shear modulus (G*) [134]

A rheometer is a machine used to measure and verify a sample's rheological properties such as phase angle and the complex shear modulus. The complex shear modulus of a viscoelastic material under load conditions is described by the ratio of peak shear stress (σ_{max}) to peak shear strain (γ_o) proportion shown in equations 2.6 and 2.7, while the phase angle indicates the intervals on how the adhesive specimen behaves under load. The use of a vector diagram derived from the phase difference can be utilized to verify the values of G′ and G″, as demonstrated in Figure 2.25.

The phase angle tends to be larger for viscoelastic materials showing more viscous properties, and when the phase angle value is towards zero degrees, then the viscoelastic material will have elastic properties. This viscoelastic material characteristic is indicated in Figure 2.26, where the phase angle ranges from 0^0 to 90^0, that is, $0° < \delta < 90°$.

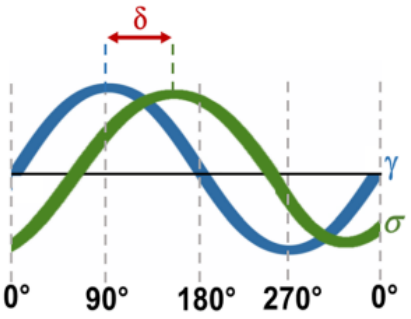


Figure 2. 26 Viscoelastic materials range of $0° < \delta < 90°$ [128]

$$G^* = \frac{\sigma_{max}}{\gamma_o} \qquad 2.8$$

The material character of flow reaction is, however, time-dependent, resulting in relaxation and creep material classification.

The conditions under which a viscoelastic material undergoes steady stress, longer distortion and strain over a short period of time yield the phenomenon known as Creep or cold flow.

The other condition whereby a viscoelastic material undergoes a process whereby the required stress deteriorates over a period to maintain the initial structure, shape, or strain of the material under constant deformation is also known as relaxation.

2.21 Summary

The relevant issues involved in the development and testing of adhesive materials were discussed in Chapter 2. Additionally, this chapter examined the influence of temperature on mechanical properties of bio-adhesive materials. A description of the standard tensile, single-lap shear, and T-Peel tests was also provided, demonstrating the expected outcomes and the classification of mechanical properties. A description of the standard TGA, DSC, and Rheology tests was also provided. This demonstrated the expected results and the classification of thermal properties of bio-adhesives. Chapter 2 was helpful in understanding the mechanical and thermal behavior of bio-adhesives.

Using Chapter 2 as a guide, Chapter 3 provides the research methodology.

CHAPTER THREE

3. MATERIALS AND METHODS

In this section, the experimental processes conducted are explained in detail. Each of these procedures is carefully selected to satisfy the identified goals of this research paper. The procedures range from harvesting latex from the candelabra tree up to the analysis and interpretation of the test results. During latex harvesting, a non-food blender was used as a shredder to cut and process the inner section of the plant until latex was produced, which was then collected into a container. The collected latex has been processed at different temperatures between 100 degrees Celsius (^{0}C) up to 150 ^{0}C. Thereafter, thermal and mechanical tests were executed on the latex to assess its properties and potential as an adhesive.

3.1 Harvesting and processing latex to produce a bio-adhesive

This section explains the methods and processes utilized to create bio-adhesive material. The process starts with harvesting candelabra tree branches from the Limpopo region, where the plant grows well due to the high-temperature environment. The second stage is the extraction of latex from the candelabra tree branches. This was executed by using a blender as a shredder to produce fine, stable latex from candelabra tree branches. The latex produced was liquid and solidified after 24 hours of curing. This was processed at this temperature parameters 100 ^{0}C, 110 ^{0}C, 120 ^{0}C, 130 ^{0}C, 140 ^{0}C and 150 ^{0}C to produce and bio-adhesive. In this section, the steps for harvesting candelabra tree branches, extracting latex, and processing latex to produce a bio-adhesive are explained in detail.

3.1.1 Harvesting candelabra tree branches

The equipment used to harvest candelabra tree branches was a stainless-steel knife. Used to cut the tree branches, along with safety gloves to prevent toxic exposure, personal protective equipment (PPE), a stepladder to climb and reach tree branches, and a mobile chiller to maintain tree branches at a cooler temperature.

The method followed for harvesting candelabra tree branches started with wearing PPE and gloves to ensure safety and prevent exposure to toxic elements from the tree branches. Position the ladder such that it is supported on the top section of the candelabra tree. Using the ladder to reach branches, use the knife to cut enough tree branches. Collect the tree branches as indicated in Figure 3.1 and store them in a mobile chiller to maintain a cooler temperature. Transport the branches to the laboratory and store them in a refrigerator set to about 10°C. The tree branches are now ready to be used in the next stage, which is the extraction of latex.



Figure 3. 1 Candelabra tree branches (self-developed)

3.1.2 Extracting latex from candelabra tree branches

The following equipment listed below was used to extract latex from candelabra tree branches.

- Stainless-steel knife.
- Ceramic plate.
- Non-food processing blender with built-in shredder.
- Glass beaker.
- Clothing material used as a sieve.
- Filter funnel.
- Laboratory rubber gloves.

The process followed for extracting latex from candelabra tree branches is shown in Figure 3.2 (a). Before starting the extraction process, rubber gloves were worn to ensure safety and prevent exposure to toxic elements. To prevent contamination and the introduction of foreign objects, all processing equipment was cleaned with isopropanol. The process started with placing a tree branch as shown in Figure 3.2 (a) on the ceramic plate. A stainless-steel knife was used to cut these branches into smaller sections of about 20 millimeters (mm), as illustrated in Figure 3.2 (a).



Figure 3. 2 Harvesting of milky latex (a); branches cut into smaller sections (b); outer greener sections removed (c) with inner section of the branch (self-developed)

The greener sections of the branches are removed by cutting the edges with a stainless-steel knife, as shown in Figure 3.2(b). After removing the edges, Figure 3.2 (c) shows only the inner section, which is white in colour as it contains latex material.

As illustrated in Figure 3.3 (a), the white inner section is placed inside the non-food blender with a built-in shredder. The blender was used to cut the white inner sections into smaller and finer material to produce stable latex sludge. The latex sludge is now poured from the blender into glass beaker number one. The clothing material is placed on top of the filter funnel, which is then placed on top of the glass beaker number two. Filtration now starts, which is a process of separating an insoluble solid from a liquid material. Through filtration, liquid latex is filtered from the clothing material via the funnel into glass beaker number two. This process can take about two to four hours to complete.

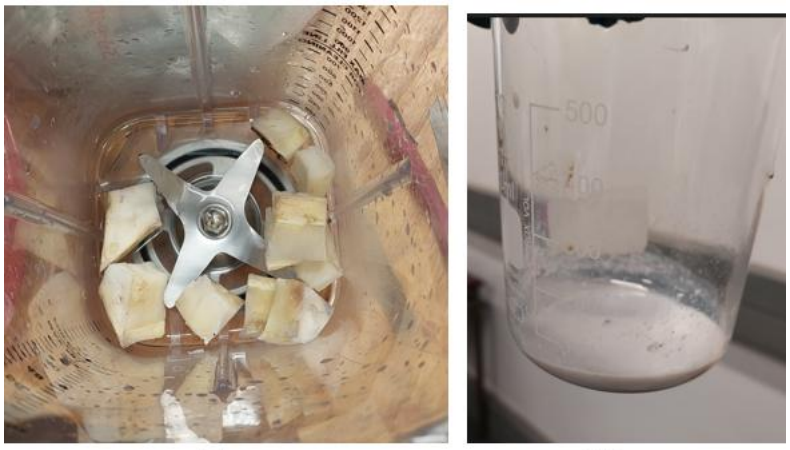


Figure 3. 3 Harvesting of milky latex: (a) inner section of the branches placed inside a non-food blender (b) extracted latex in a liquid form (self-developed)

The remaining insoluble material that remains on the clothing material is disposed of, as it will not form part of the experimental process in this paper. When the filtration process is completed, glass beaker number two will contain a white liquid sap material, which is called latex, as shown in Figure 3.3 (b). The extracted latex is now ready to be processed at different temperatures to produce a bio-adhesive, as detailed in the next section.

3.1.3 Equipment and methods used to produce bio-adhesive from latex

The extracted latex material was left to cure, where it changed from a liquid to a solid structure after 24 hours. This process is very critical, as it enables coagulation formation, which is a result of reactions of latex carbohydrates when exposed to bacterial contamination, and this can result in the carbohydrates changing into fatty acids.

Coagulation can compromise the material's adhesive properties, making it unsuitable for its intended use. To prevent this, the curing process is carefully monitored to maintain the latex in an optimal state. Proper curing ensures a stable and reliable adhesive, free from structural defects [135, 136].

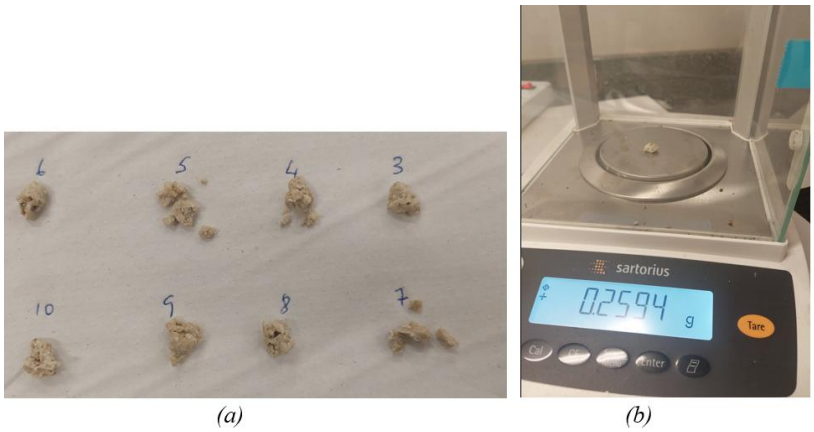
Latex was used without any additives or enhancing substances that might change its properties, structure, and characterization performance. Solid latex was divided into smaller pieces of similar weight as shown in Figure 3.4. This section provides details of the equipment used and the processing methods employed to produce a bio-adhesive from latex.



Figure 3. 4 Milky sticky material in a solid state (self-developed)

The following equipment was used in producing bio-adhesives: a glass beaker for storing sludge and latex, a stainless-steel knife for cutting cured latex, and a stainless-steel spatula. A portable laboratory stove was used to process latex into bio-adhesive material at varying temperatures, along with a weighing scale and a calibrated infrared thermometer.

The processing methods followed in producing bio-adhesive started with a curing process in which liquid latex was kept in a well-ventilated area at a monitored, controlled constant temperature to facilitate uniform drying and prevent any potential defects in the final solid structure. Cut the cured solid latex into smaller pieces as shown in Figure 3.5 (a), using a stainless-steel knife. Use the scale to weigh solid latex to an average weight of 0,25 grams (g), as illustrated in Figure 3.5 (b). This is to ensure consistency later in the application of this material on the specimen that will be used for testing purposes.



(a) (b)

Figure 3. 5 Processing of latex (a) samples weighed and ready for processing (b) weighing process using a scale (self-developed)

The 0,25 g samples were placed in the beaker, which was placed on the stove, with the heat gradually increased from 0^0C to 50^0C in 10^0C increments until the desired temperature was

reached. Referring to Table 3.1, the processing temperature parameters differed for each 0,25 g of solid latex.

At a specific processing temperature in accordance with Table 3.1, the solid latex material is now transformed into bio-adhesive material, which is brownish in colour and a thick liquid material. The produced bio-adhesive material is now ready to be applied to join two substrate materials, which in this case are paper-to-paper specimens.

Table 3. 1 Latex processing temperature parameters (self-developed)

Temperature (^{0}C)	Adhesive Material	Adhesive Weight (g)	Application
100	Neat Latex	0,25	Paper
110	Neat Latex	0,25	Paper
120	Neat Latex	0,25	Paper
130	Neat Latex	0,25	Paper
140	Neat Latex	0,25	Paper
150	Neat Latex	0,25	Paper

The stages undertaken in this section are shown in Figure 3.6. These started with harvesting candelabra tree branches, extraction of latex, the process of curing latex, and processing latex material using heat at varying temperatures of 100^{0}C, 110^{0}C, 120^{0}C, 130^{0}C, 140^{0}C and 150^{0}C. The process of transforming latex is now complete, with the produced bio-adhesive in liquid form ready to be applied and joined to the paper-to-paper specimen for further mechanical investigation, which is covered in the next sections.

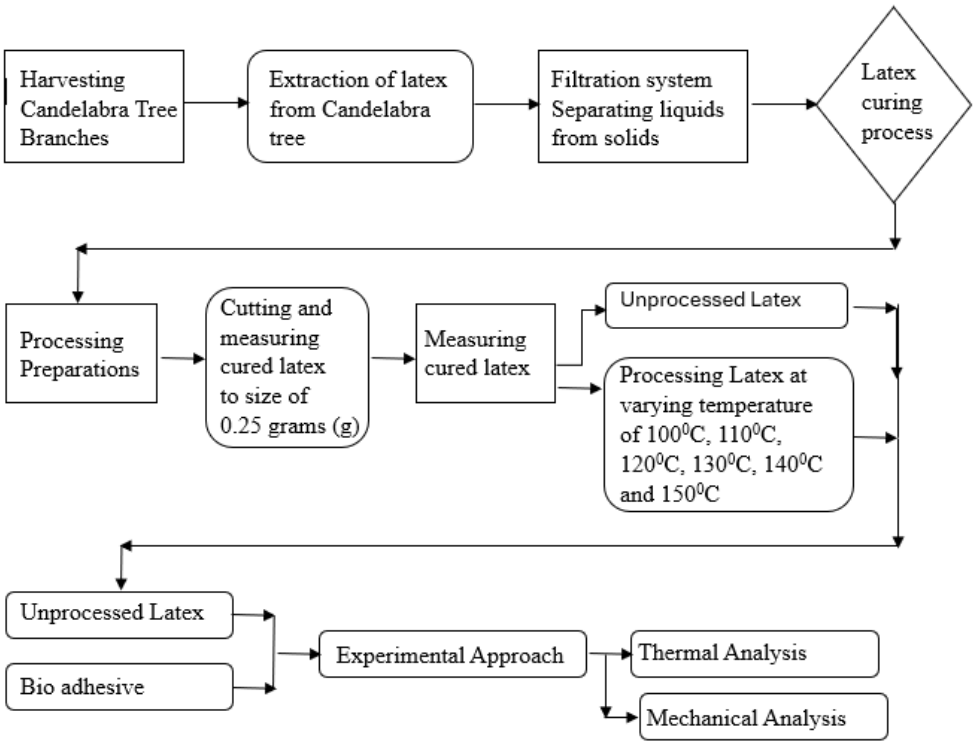


Figure 3. 6 Flow diagram for steps followed to harvest, process latex into bio-adhesive material, and experimental testing methods (self-developed)

The liquid bio-adhesive will transform into a solid state when left for a period of 24 hours to cure. In this form, the bio-adhesive can be analyzed further through thermal testing, and characterization work is covered in the next sections.

3.2 Thermogravimetric analysis (TGA)

This section explains the systems and processes utilized to conduct a thermal test using thermogravimetric analysis (TGA) for investigating, analyzing, and understanding the physical properties of processed bio-adhesive. The technique used is thermal analysis, in which specimen mass is measured over time as the specimen undergoes a temperature change and loses unstable gases during testing.

This method of analysis is unique as it makes it possible to collect accurate changes in material data that can be logged as decay, dryness, and oxidation of a specimen [116]. The results are a characteristic thermogravimetric curve derived from the percentage mass loss versus temperature. This data is important in this paper because it makes it possible to quantitatively investigate bio-adhesive thermal properties.

3.2.1 Aim of performing TGA characterization

The main purpose of TGA is to detect and record changes in sample weight over time under a fixed temperature span, and this procedure can comprise heating at steady temperature set points. Most polymeric materials, including bio-adhesive materials, exhibit melting point properties before reaching the decay stage, and TGA is primarily used to investigate, identify, and classify thermal stability. This is important because of the novelty of the material used in this paper, and it will provide much-needed feedback for recording and investigating mass loss over varying temperature spans.

This investigation focuses on the heating process, during which a characteristic thermogravimetric curve can be derived and plotted to analyze the mass loss of the bio-adhesive material over time. In this paper, the objective of conducting this thermal analysis is to understand the properties and bio-adhesive behavior of samples processed at temperatures of 100^0C, 110^0C, 120^0C, 130^0C, 140°C, and 150^0C.

3.2.2 TGA methods and materials used

This section provides full details of the equipment used to prepare the bio-adhesive samples tested via the TGA measuring machinery. The equipment used to conduct this thermal characterization process is a TA TGA 5500.

The material used for conducting TGA testing is bio-adhesives extracted from candelabra trees and processed at different temperatures. The specimen ceramic pan with hooks is used for loading and carrying the specimen during testing. A knife was used to cut bio-adhesive material to the required size. Tweezers were used to handle and move bio-adhesive material from position A to B. A scale was used to weigh the bio-adhesive material.

3.2.3 Preparation of TGA specimens

All the preparation and testing were done at the Council for Scientific and Industrial Research (CSIR). Preparation sequences were followed, including weighing and sample preparation.

The bio-adhesive material has already been processed in accordance with the required temperature parameters, which are 100^0C, 110^0C, 120^0C, 130^0C, 140^0C and 150^0C.

At ultra-high temperatures, ceramic pans as shown in Figure 3.7 (b) are used for holding, in this case, bio-adhesive specimens while tracking weight changes. The design operating temperature range for the ceramic pans is -120^0C to 1200^0C [126]. They are also capable of withstanding operating pressure and other factors during the analysis phase. Ceramic Pans were purchased from TA Instruments, which is the original equipment manufacturer (OEM) of DSC equipment.

The steps followed to prepare the TGA bio-adhesive specimen, as illustrated in Figure 3.7(a), began with weighing the ceramic pan. The average weight recorded was 344 mg. A scale was reset to zero with the ceramic pan still on it, so that the pan's weight could be ignored. For the sample specimen, place the bio-adhesive sample on the ceramic pan and reweigh both the sample and the ceramic pan. This gave a weight of 9 mg, as shown in Figure 3.7 (a), which represents only the weight of the bio-adhesive specimen. Note that samples that are bigger in size (more than 50 mg) might not yield accurate results. This is because these might result in poor mass transfer, and an isothermal state is not ensured due to a slower heat rate inside the bio-adhesive specimen.

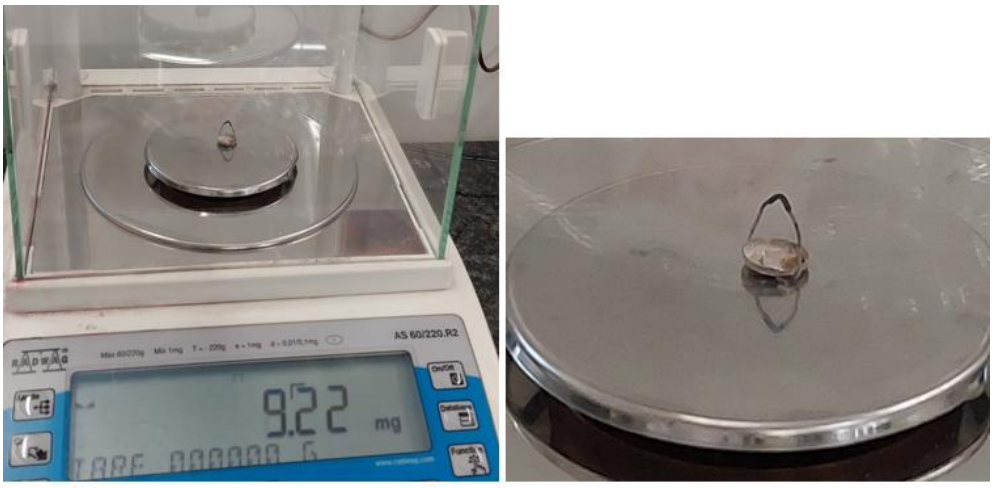


Figure 3. 7 (a) Ceramic pan and bio-adhesive sample weight (b) ceramic pan on scale (self-developed)

Before loading the bio-adhesive specimen onto the TGA autosampler panel, remove both bio-adhesive samples and the ceramic pan from the scale. Then remove the bio-adhesive specimen from the scale using a pair of tweezers and place it onto the TGA 25-position autosampler, as shown in Figure 3.8 (a and b). Record your samples and specimen numbers on the TGA panel against the bio-adhesive processing temperature. This is to ensure that the TGA results obtained are correctly linked to the bio-adhesive sample and the processing temperature.

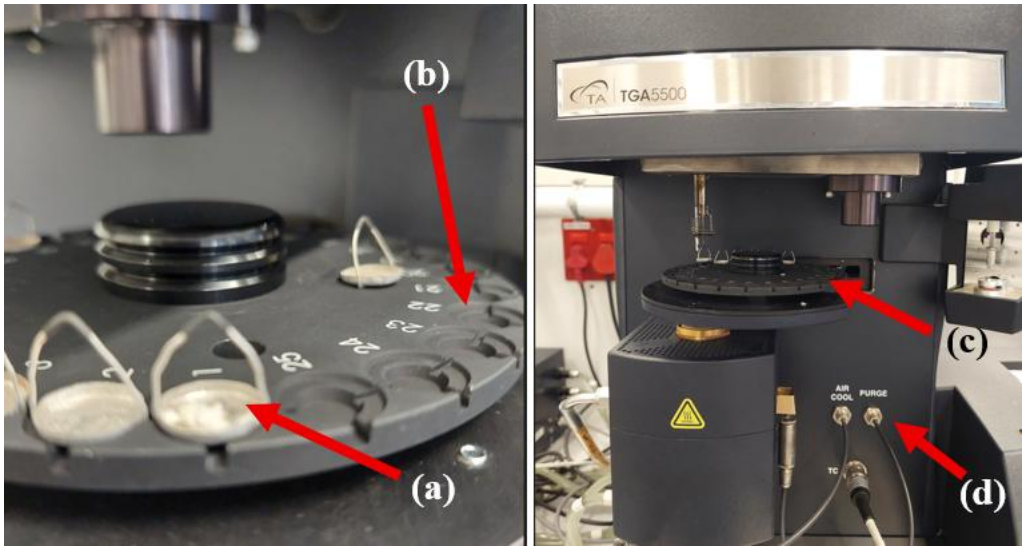


Figure 3. 8 TGA (a) Ceramic pan (b and c) 25-position autosampler (d) gas purging pipeline (self-developed)

The sample specimen is ready to be tested on the TGA instrument. The samples are prepared in a similar manner for all temperature parameters, which are 100^0C, 110^0C, 120^0C, 130^0C, 140^0C, and 150^0C.

3.2.4 TGA testing method and procedure

The section explains the settings and procedures that were used when conducting TGA measurements and characterization of processed bio-adhesives. The bio-adhesive specimen prepared as illustrated in the previous section is now ready to be loaded onto the TGA autosampler panel, as shown in Figure 3.8 (a). Testing of this specimen was conducted in a credible laboratory environment at CSIR, and thermal analysis of the bio-adhesive was executed using TA TGA 5500 measuring equipment, as shown in Figure 3.9, which was equipped with all required software and hardware to complete this exercise.

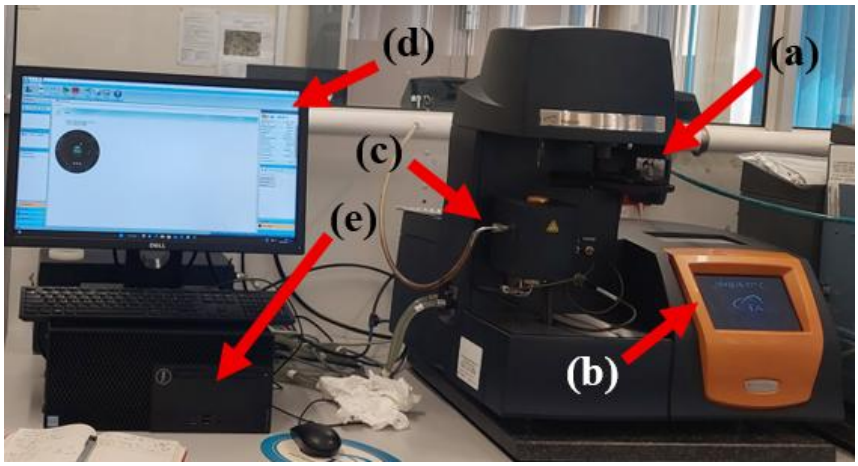


Figure 3. 9 TA TGA 5500 measuring equipment (a) 25-position autosampler (b) TGA display, and control screen (c) evolved gas exhaust (d) monitor (e) computer hardware (self-developed)

Throughout the TGA testing period, the following settings and procedures were followed and maintained. TGA temperature range was maintained for all specimens from -0^0C to 1000^0C at

a heating rate of 10^0C/minute under inert conditions, where nitrogen gas flowed through the environment at 50 ml/minute. High-performance ceramic pan specifications were kept the same for all the tests done on samples and the reference specimen. All tested specimens were placed in the ceramic pan, and all tests were conducted using the 25-position autosampler to ensure consistent results.

Two samples per processing temperature were tested and analyzed, as illustrated in Table 3.2. There were 14 processed bio-adhesive specimens weighing 9 mg that were utilized to conduct thermal analysis through TGA. For each temperature parameter, two specimens were tested, simply to have a backup in case the first test was spoiled for some reason.

Table 3. 2 Specimen arrangements for TGA analysis (self-developed)

Sample Number	Sample position mounting Panel	Processing Temperature (^{0}C)	Weight (mg)
1	1	100	9
2	2	100	9
3	3	110	9
4	4	110	9
5	5	120	9
6	6	120	9
7	7	130	9
8	8	130	9
9	9	140	9
10	10	140	9
11	11	150	9
12	12	150	9
13	13	Unprocessed Latex	9
14	14	Unprocessed Latex	9

As moisture and other gaseous compounds are released during bio-adhesive material decomposition, TGA measures moisture content and examines the relationship between weight loss and the decomposition of the bio-adhesive material. Compound composition can be determined by measuring bio-adhesive percentages. Predict stability and lifespan based on degradation rates. The TGA provides an answer to the question of the temperature at which bio-adhesive materials break down, which will aid in understanding the rate at which this material breaks down.

The flow diagram in Figure 3.10 demonstrates the key processes followed to conduct a TGA thermal analysis testing method, and these stages start with specimen weighing, positioning of the specimen on the TGA autosampler, loading and setting operational parameters, operating TGA equipment to start the thermal analysis process, and TGA results and data recordings being made available for analysis.

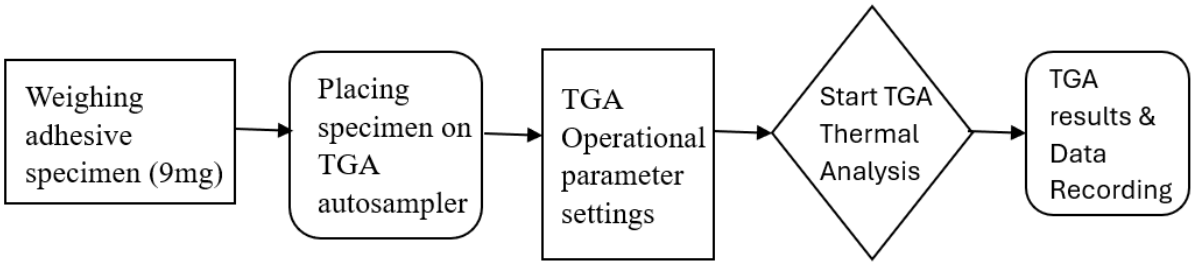


Figure 3. 10 Flow diagram and steps followed to execute TGA thermal analysis testing methods (self-developed)

However, TGA focuses on understanding the bio-adhesive material's weight-loss patterns, which is also a limitation, as this thermal analysis does not provide data on bio-adhesive energy and heat flow, and does not account for the bio-adhesive behavior under varying environmental conditions. This limitation necessitates the use of complementary techniques, in this case differential scanning calorimetry (DSC), which is explained in the subsequent section, and this provides a comprehensive understanding of bio-adhesive's toughness and performance.

3.3 Differential scanning calorimetry (DSC)

This section describes the methods and processes for conducting a thermal test using differential scanning calorimetry (DSC) to investigate, analyze, and understand the physical properties of processed bio-adhesive. The technique used is thermal analysis, whereby the temperature of the specimen (in this case, the bio-adhesive) and the reference are maintained and measured at almost the same rate. The results provided are differences in the quantity of heat required to raise both the reference temperature and the sample temperature. The goal of conducting thermal analysis is to understand the properties and bio-adhesive behavior that have been processed at different temperature parameters of 100 ^{0}C, 110 ^{0}C, 120 ^{0}C, 130 ^{0}C, 140 ^{0}C and 150 ^{0}C.

3.3.1 Aim of performing DSC characterization

The DSC is ideal for investigating polymeric materials and understanding their thermal transition processes. These changing phases are known as glass transition temperature (T_g), melting temperature (T_m), and crystallization temperature (T_c) [121]. These temperatures are crucial for understanding the material's behavior under different conditions, such as storage, processing, and usage. T_c indicates when the polymer begins to form an ordered structure, T_m marks the point where it transitions to a liquid state, and T_g reflects the polymer's flexibility and stiffness.

This process will help us understand the bio-adhesive material from the candelabra tree by determining whether the configuration of the bio-adhesive undergoes all or some of the transition phases (i.e., T_m, Tg, and T_c). Because the material used in this paper is still novel and undeveloped, this process of using the DSC will provide an understanding of setting the base parameters for this bio-adhesive composition and transitional phases.

3.3.2 DSC methods and material used

This section provides full details of the equipment used to prepare the bio-adhesive samples tested via the DSC measuring machinery. The equipment used to conduct this thermal characterization process is a TA DSC 2500.

The equipment used for conducting DSC testing was used to process bio-adhesives from candelabra trees at different temperature parameters. Specimen aluminum pans and lids were used to store and protect bio-adhesive material during testing. The reference aluminum pans and lids and the press device were used to seal them. A knife was used to cut bio-adhesive material to the required size, and tweezers were used to handle and move bio-adhesive material from position A to B. The scale that was used to weigh bio-adhesive material.

3.3.3 DSC specimen preparation process

The section also explains the settings and procedure used when conducting DSC measurements and characterization of processed bio-adhesives. All the preparation and testing were done at the Council for Scientific and Industrial Research (CSIR). Preparation sequences were followed, and this included weighing, sample preparation, and joining sample pans. Preparation of bio-adhesive material samples has already been processed in accordance with the required temperature parameters, which are 100^0C, 110^0C, 120^0C, 130^0C, 140^0C, and 150^0C.

Not much preparation was required, as the pans met the processing requirements; only the weight of the pan was recorded using the scale. Aluminum Pans were bought from TA Instruments, which is the original equipment manufacturer (OEM) of DSC equipment.

Steps that were followed to prepare the sample and reference specimen are illustrated in Figure 3.11 (a); the scale was used to weigh the aluminum pan and lids shown in Figure 3.11 (b). The average weight recorded was 16,8 g. The scale is reset to zero while an aluminum pan and lid are placed on it to allow the weight of the pan and lid to be reset to zero grams. For the sample specimen, place the bio-adhesive sample on the aluminum pan and reweigh the sample, aluminum pan, and lid. This provides a weight of 0,57 milligrams (mg), which is the weight of the bio-adhesive specimen. Note that only the sample specimen has a bio-adhesive sample placed inside its pan and lid, while the reference specimen does not have a bio-adhesive sample placed inside its lid, as shown in Figure 3.11 (a).

The preparation process further continues with closing the pan and lid of the sample specimen, as elaborated in Figure 3.11 (b). followed by the removal of both bio-adhesive samples, the aluminum pan, and the lid from the scale. Place the aluminum pan with the bio-adhesive sample inside on the press device. Lower the press device Figure 3.11 (b) to assemble and seal both the aluminum pan and lid with the bio-adhesive sample inside.



Figure 3. 11 DSC (a) pan and lid on the scale; (b) press device (self-developed)

Remove the sample from the press device using a pair of tweezers and place it onto the DSC mounting panel as shown in Figure 3.12. Record your samples and specimen numbers on the DSC panel against the bio-adhesive processed temperature. This is to ensure that the DSC results obtained are correctly linked to the bio-adhesive sample and the processing temperature. This is critical to the analysis and interpretation of results that are obtained from DSC testing methods. The sample specimen is ready to be tested on the DSC instrument. The samples are prepared in a similar manner for all temperature parameters, which are 100^0C, 110^0C, 120^0C, 130^0C, 140^0C, and 150^0C.

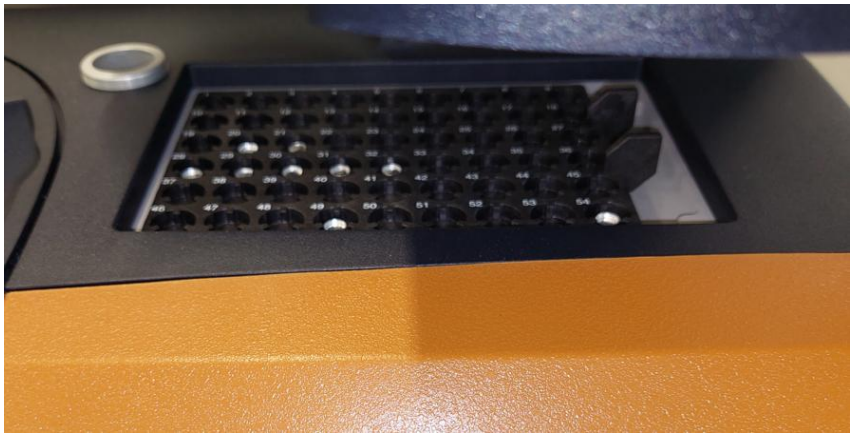


Figure 3. 12 DSC mounting panel (self-developed)

3.3.4 DSC testing method and procedure

The sample and reference specimen prepared as illustrated in the previous section are now ready to be loaded onto the DSC mounting panel as illustrated in Figure 3.13 (e). The testing of this specimen was conducted in a credible laboratory environment at CSIR, and thermal analysis of the bio-adhesive was executed using TA DSC 2500 measuring equipment as shown in Figure 3.13, which was equipped with all required software and hardware to complete this exercise.

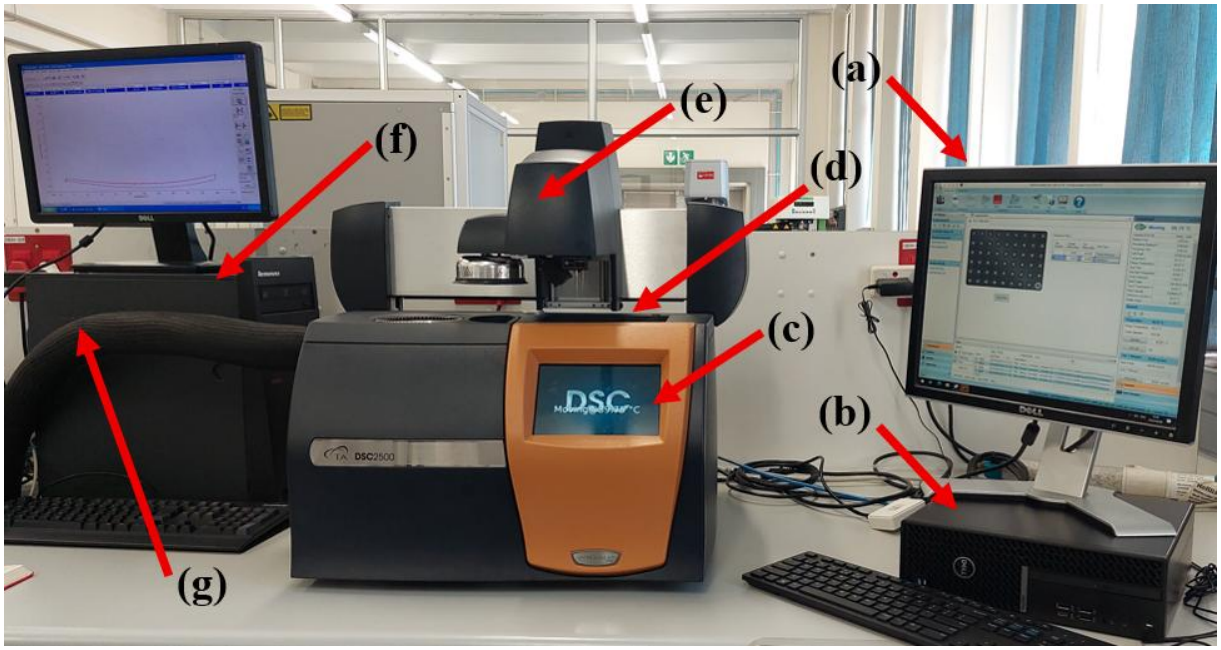


Figure 3. 13 TA DSC 2500 (a) monitor (b) hardware (c) DSC display unit (d) sample mounting panel (e) sample feeder (f) DSC software system (g) refrigeration cooling system (self-developed)

Throughout the DSC testing period, the following settings and procedures were maintained. DSC temperature range was maintained for all specimens from -100^{0}C to 200^{0}C at a heating rate of 10^{0}C/minute and through a dry nitrogen gas flow environment at 50 ml/minute. All activities were carried out under a contained and safe DSC molecular nitrogen (N_2) purge-protected environment. The operating temperature range for these aluminum pans and lids is -120^{0}C to 600^{0}C [126]. These are also capable of withstanding operating pressure and other factors during the analysis phase. High-performance aluminum caps and lids specifications were kept the same for all the sample and reference specimens. All the specimens that have been tested were placed inside the aluminum pan, tightly sealed with a lid to ensure consistent results.

Two samples per processing temperature were tested and analyzed, as illustrated in Table 3.3. There were 14 processed bio-adhesive specimens weighing 0,57 mg that were utilized to conduct thermal analysis through DSC. For each temperature parameter, two specimens were tested, simply to have a backup in case the first test was spoiled for some reason.

Table 3. 3 Specimen arrangements for DSC analysis (self-developed)

Sample Number	Sample position mounting Panel	Processing Temperature (^{0}C)	Weight (mg)
1	1	100	0,57
2	2	100	0,57
3	3	110	0,57
4	4	110	0,57
5	5	120	0,57
6	6	120	0,57
7	7	130	0,57
8	8	130	0,57
9	9	140	0,57
10	10	140	0,57
11	11	150	0,57
12	12	150	0,57
13	13	Unprocessed Latex	0,57
14	14	Unprocessed Latex	0,57

The flow diagram in Figure 3.14 demonstrates the key processes followed to conduct a DSC thermal analysis testing method, and these stages start with specimen weighing, sealing of specimen lids and pans, positioning of the specimen on the DSC mounting panel, loading and setting operational parameters, operating DSC equipment to start the thermal analysis process, and DSC results and data recordings being made available for analysis.

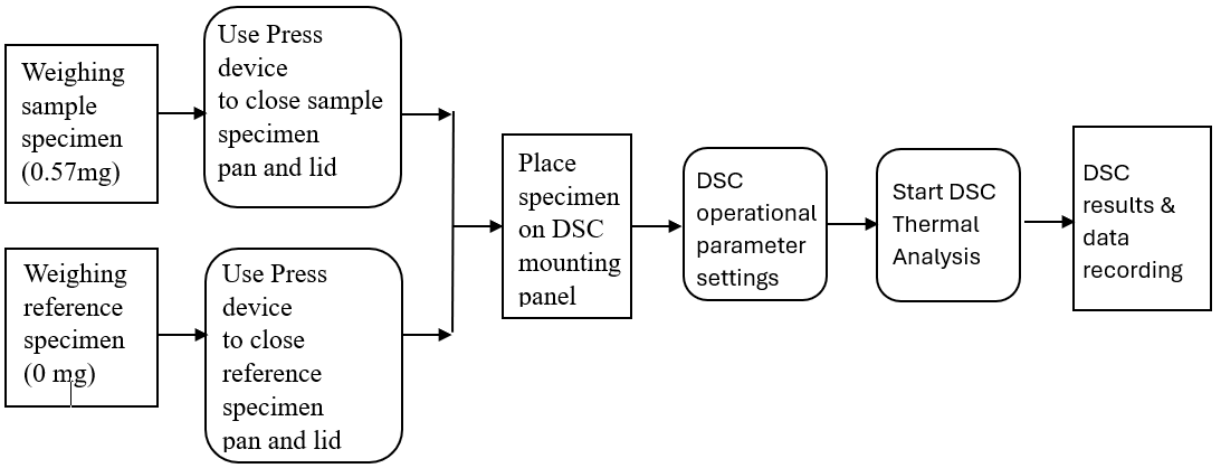


Figure 3. 14 Flow diagram and steps followed to execute DSC thermal analysis testing methods (self-developed)

The previous sections, which are TGA and DSC analysis, mainly focus on the characterization of material behavior. TGA focuses on material decomposition, and DSC focuses on investigating and understanding the thermal transition processes of bio-adhesive materials, namely the changing phases, which are glass transition temperature (T_g), melting temperature (T_m), and crystallization temperature (T_c).

The next section focuses on understanding the performance of bio-adhesive materials through rheological analysis. Rheology is used to describe and assess the deformation and flow behavior of bio-adhesive materials. Rheology normally accounts for the behavior of liquids by understanding the relationship between stress and strain. This is conducted through measurements of a minimal number of functions that are required to connect stress with strain rates or the rates of change of strain.

3.4 Rheology

This section explains the systems and processes utilized to conduct a rheological test for investigating, analyzing, and understanding the material performance and reaction when subjected to applied forces and stresses. The method of investigation is based on the relationship between rates of stress-strain interaction and the resultant material distortion being measured. This section provides details on rheological methods and the performance of bio-adhesives that, through this process, can be categorized into three different states, namely viscous, elastic solid, and viscoelastic.

3.4.1 Aim of performing rheology characterization

Rheological measurement is the investigation of the association between shear rate and shear stress of any material experiencing a state of laminar flow and other factors that can cause material distortion [137]. Hence, in this case, the analysis is conducted using parallel plates, and the specimen is processed with bio-adhesive material. The bio-adhesive material is subjected to controlled shear forces while measuring its flow behavior and viscosity under specific conditions.

During this process, the maximum shear strain and shear stress are measured, while the complex modulus and phase angle are calculated using the rheometer's internal programming system. The complex modulus provides information about the material's overall stiffness, while the phase angle indicates the degree of energy dissipation during deformation.

These parameters are essential for evaluating a bio-adhesive's suitability for specific applications. This highlights its ability to withstand mechanical stresses and maintain its functionality over time. This method provides critical insights into bio-adhesive material performance and provides quantitative data that can be analyzed to classify and understand how the bio-adhesive behaves under different conditions.

3.4.2 Rheology methods and materials used

This section provides full details of the equipment used to prepare the bio-adhesive samples tested with rheological measuring equipment. The equipment used for this thermal characterization process is the Anton Paar CTD 450 Modular compact MCR302 model.

The equipment used to conduct Rheological testing was bio-adhesives extracted from candelabra trees, which were processed at different temperatures. A knife was used to cut the bio-adhesive material to the required size, and tweezers were used to handle and move the bio-adhesive material from position A to B. The scale used to weigh the bio-adhesive material.

3.4.3 Rheological specimen preparation process

The section explains the settings and procedures used in conducting rheological measurements and characterizing processed bio-adhesives. The preparation process and preparation sequences were followed, and this included weighing, sample preparation, and setting of parallel plates. All the tests were executed in a credible laboratory environment at CSIR. Analysis of bio-adhesive material processed from candelabra tree was executed using an Anton Paar Rheometer CTD 450 Modular compact MCR302 model.

Preparation of bio-adhesive material samples was performed on bio-adhesive that had already been processed at the required temperature parameters, which are 100^0C, 110^0C, 120^0C, 130^0C, 140^0C, and 150^0C.

Preparation of Rheology testing equipment included rheology equipment, parallel plates, and the combustion chamber, which were cleaned with isopropanol to prevent contamination or prevent any introduction of foreign material. The Anton Paar Rheometer was used to test the bio-adhesive specimens, and this equipment has 25mm diameter parallel plates and two built-in combustion chamber molds used for housing the specimen during the testing process.

The process started with the pre-heating of the parallel plates as shown in Figure 3.15 (b), which is a prerequisite stage before starting the specimen test. This ensures the plates reach the required temperature evenly, avoiding inconsistent test results. Once the desired temperature is achieved, specimen testing can begin. The testing temperature for the 25mm plates is set in the range of 34°C and 46°C on the rheometer control screen, as shown in Figure 3.15 (a).



(a) (b)

Figure 3. 15 Anton Paar rheometer (a) rheometer control screen (b) bio-adhesive specimen placed on rheometer parallel plates (self-developed)

The steps followed to prepare the bio-adhesive specimen started with using a knife to cut the bio-adhesive material to the required size. The scale was used to weigh the bio-adhesive material to an average weight of 6 g. A pair of tweezers was used to handle and move the bio-adhesive material from the storage box position to the rheology parallel plates. A specimen of bio-adhesive material, as shown in Figure 3.15 (b), was placed between the two plates. The temperature of the specimen is kept constant at normal room temperature, and the weight is kept

constant at 6 g to maintain consistency of the results during the testing process. Adjust the two parallel plates so that there is about a 2 mm distance between the two plates.

Remove excess bio-adhesive material from the sides of the test plates using a knife tool. Adjust both test plates again so that the testing gap is 0,5 mm. Close and lock the two chamber housing plates with the specimen inside, and this is illustrated in Figure 3.16 (a and b).

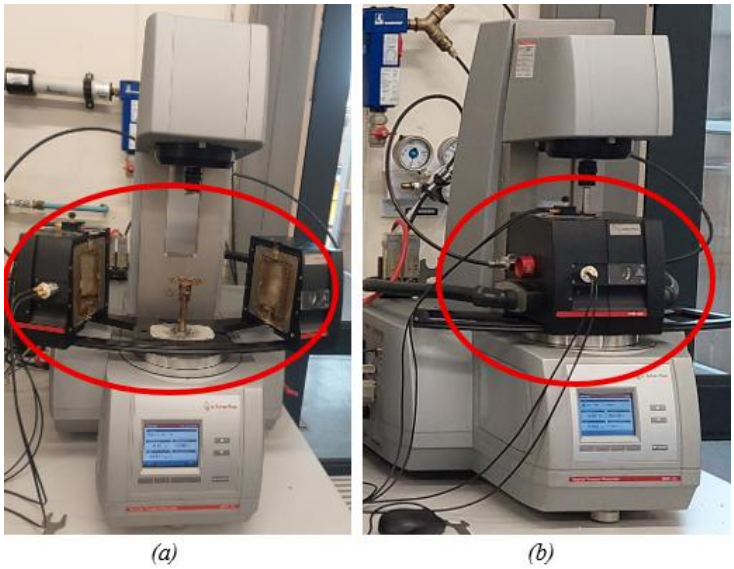


Figure 3. 16 Anton Paar rheometer operating environment (a) in an open position (b) in a closed position (self-developed)

The testing process can now be started. The environmental chamber parameters can now be set to the testing temperature while providing room for the specimen to steadily adjust to the testing temperature, and this can be done over a 10-minute period. The rheometer automatically conducts the test with the following operational parameters and results. The plate at the top rotates at an oscillatory speed of 10 radians per second. During this time, the rheometer measures the full operational shear strain and stress. When the testing process is completed, the rheometer analytical software automatically finds the influence of applied shear stress and how it influences the storage modulus (G") and loss modulus (G'). Results derived from this testing procedure are G' against the percentage shear stress, G" against the percentage shear stress, and, lastly, complex viscosity against angular viscosity curves. These results can now be interpreted with the goal of understanding this bio-adhesive material performance.

3.4.4 Rheology testing method and procedure

Throughout the Rheology testing period, the following settings and procedures were followed. The rheology temperature range was maintained for all specimens from 30^0C to 250^0C with an initial applied Force (F) range of 1 newton (N) to 1 kilonewton (KN), and an oscillating frequency of 10 radians per second. A heating rate of 10^0C/minute was maintained through a dry nitrogen gas flow environment at 50 ml/minute.

All activities were carried out in a contained, safe, rheometer-molecular-nitrogen (N_2) purge-protected environment. The operating temperature range for the parallel plates and the combustion chamber is -120^0C to 1200^0C, these are also capable of withstanding operating

pressure and other factors during the analysis phase. High-performance parallel plates were consistently used for all tests executed on all bio-adhesive samples. All the specimens that have been tested were maintained at room temperature to guarantee consistency of the results. The G' tolerance span of divergence was derived by analytical software in accordance with the ASTM D7175 and DIN 51810-2 standards.

Two samples per processing temperature were tested and analyzed, as illustrated in Table 3.4. There were 14 processed bio-adhesive specimens weighing 6 g that were utilized to conduct thermal analysis through rheometer testing equipment. For each temperature parameter, two specimens were tested, simply to have a backup specimen in case the first test was spoiled for some reason.

Table 3. 4 Sample arrangements for rheology analysis (self-developed)

Sample Number	Sample position of sample on mounting Panel	Processing Temperature (^{0}C)	Weight (g)
1	1	100	6
2	2	100	6
3	3	110	6
4	4	110	6
5	5	120	6
6	6	120	6
7	7	130	6
8	8	130	6
9	9	140	6
10	10	140	6
11	11	150	6
12	12	150	6
13	13	Unprocessed Latex	6
14	14	Unprocessed Latex	6

The flow diagram in Figure 3.17 demonstrates the key processes followed to conduct a Rheological thermal analysis testing method, and these stages start with specimen weighing, placing the bio-adhesive specimen on the two parallel plates, adjusting the parallel plates to a 2mm gap, loading and setting operational parameters, operating rheometer testing equipment to start the thermal analysis process, rheometer results and data recordings being made available for analysis.

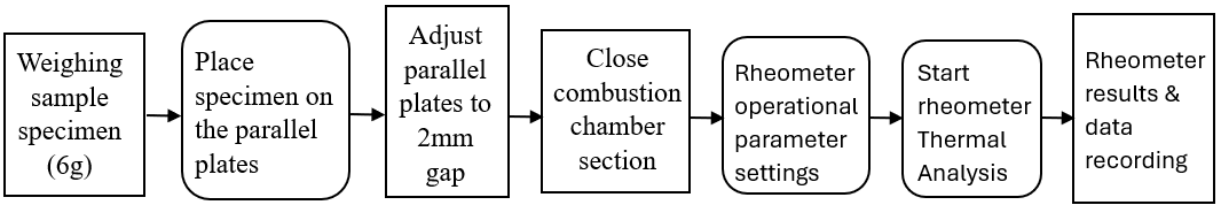


Figure 3. 17 Flow diagram and steps followed to execute rheometer thermal analysis testing methods (self-developed)

The previous sections, which covered TGA, DSC, and Rheology analyses, focused on understanding bio-adhesive properties by conducting thermal testing. This aims to understand the decomposition, degradation, and performance properties of bio-adhesives. To increase our understanding of bio-adhesives, it is essential to execute experimental investigations that will provide the mechanical properties of these materials. These studies will focus on evaluating the strength of bio-adhesives under various conditions. This is discussed in detail in the next sections.

3.5 Experimental approach

In this section, the mechanical properties and the effect of temperature on this bio-adhesive are investigated through the collection of primary data undertaken by laboratory experiments, namely T-peel tests and single-lap shear tests.

The investigation conducted in this paper is a quantitative experimental approach to evaluate bio-adhesive performance under varying conditions. This approach and research work focus on understanding the underlying principles and mechanisms through data interpretation and experimental analysis.

Single-lap shear tests measure the ability of bio-adhesive to endure shear stress, while T-peel tests assess its resistance to peeling forces. The quantitative data obtained can then be analyzed to provide critical insight into the bio-adhesive's mechanical properties.

The experimental approach for this paper is applicable to the single-lap shear test and T-peel test. The experimental design system, the Taguchi method, is used because it is most effective in applications that require numerical and statistical analysis. The bio-adhesive material was applied only to paper-to-paper substrates for the single-lap shear test and T-peel test.

3.6 Single lap-shear test

This section explains the systems and processes utilized to conduct a mechanical test using the single lap-shear test for investigating, analyzing, and understanding bio-adhesive material’s mechanical performance. In a single-lap shear test, two overlapping substrates are bonded and pulled in opposite directions by a universal testing machine. In response to this tensile load, the bonding line is subjected to shear stresses until failure occurs.

3.6.1 The aim of performing a single-lap shear test

By exposing bio-adhesives to elevated temperatures, the effect on shear strength is investigated and evaluated in relation to the processed bio-adhesive material. In this section, the objective is to elaborate on the experimental methods used to investigate the shear strength of the processed bio-adhesive and how it is affected by a change in processing temperature.

These methods include applying controlled shear forces to test specimens under varying temperature conditions, measuring the resulting bio-adhesive failure stress, and analyzing the data to determine the maximum shear strength.

The single lap-shear test experimental approach is executed using a tensile test machine (Instron 8801). This was chosen because the expected results from a tensile testing machine are mechanical properties, namely Young's modulus E_y (GPa), Yield strength σ_{ya} (MPa), tensile strength σ_r (MPa), and failure strain ε_f (%) [138]. From these outcomes, it's likely that a stress-strain curve can be created to investigate differences in the bio-adhesive's shear strength. The ultimate tensile strength and maximum tensile strain can be found using the stress-strain curve.

3.6.2 Single-lap shear test material and methods used

This section provides full details of the methods and equipment used to prepare the bio-adhesive specimen, which was tested on a tensile testing machine to conduct a single-lap shear test. The equipment used to conduct this mechanical test process was an Instron 8801 tensile testing machine.

Table 3. 5 Single-lap shear test paper-to-paper specimen dimensions (self-developed)

Description	Operating Parameters (mm)
Shape	Rectangular
Length	185
Width	25
Thickness	0,5
Fixture separation	6
Separation length	185
Adhesive applied Area: Length	15
Adhesive applied Area: Width	25

A knife was used to cut the bio-adhesive material to the required size, and a scale was used to weigh it, yielding an average of 0,25 g. The material used for single-lap shear testing is a bio-adhesive extracted from candelabra trees and processed at different temperatures. In this case, the processed bio-adhesive material is applied to a paper-to-paper specimen while it is in a hot liquid state.

A knife was also used to cut the paper substrates to size for use as paper-to-paper substrates bonded together with a bio-adhesive material. The dimensions of these paper-to-paper substrates are provided in Table 3.5.

3.6.3 Single lap-shear testing method

The single lap-shear test is a prevalent technique for explaining bio-adhesive joint strength and behavior, due to its simple design. It is made up of two rectangular plates, as referred to in Figure 3.18, or substrates, joined by bio-adhesive material [108].

During the experimental process, the tensile testing speed is kept constant. The operating environment was maintained consistently throughout the experiments, conducted under mechanical workshop conditions. To make the testing instrument easy to operate, this tensile testing machine has a robust structure, a load cell, grips, and a crosshead assembly as shown in Figure 3.18. This design ensures precise handling of the paper-to-paper specimen. The crosshead assembly allows for smooth adjustment of the test space while the load cell accurately measures the applied load.



Figure 3. 18 (a) Instron 8801 tensile testing machine (b) paper sample tested on tensile machine (self-developed)

For this experimental approach, the dimensions of the rectangular substrates, shape, and size were maintained and kept constant throughout this experiment to ensure that other factors that might affect the results are eliminated. The bio-adhesive material used was a naturally processed bio-adhesive sourced from candelabra trees, and the material used in this experiment was paper-to-paper, as shown in Figure 3.18 and Figure 3.19.

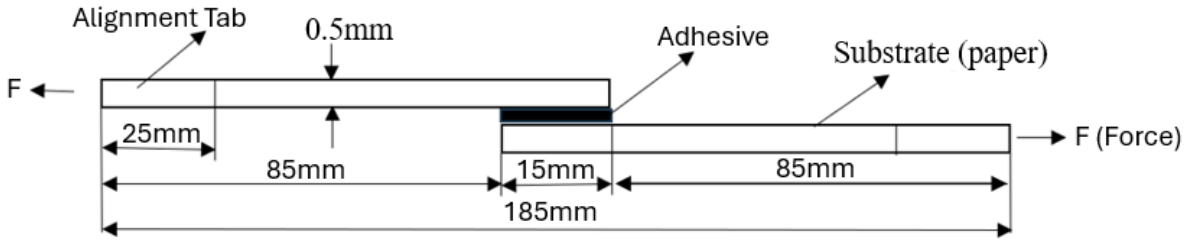


Figure 3. 19 Single shear lap joint parameters (self-developed)

The two paper-to-paper substrates shown in Figures 3.19 and 3.20 were joined by bio-adhesive material, and constant pressure was applied by hand. The specimen was left to cure for 24 hours, and thereafter any bio-adhesive overlap was removed before the experimental process began.

The sample testing was carried out on a tensile machine using the ASTM D1002 and ISO 4587 standards for single-lap shear tests. The load cell utilized in the tensile machine had a 100 N capacity and a steady crosshead speed of 6 mm/min. In a tensile test, the specimen is pulled to

its breaking point during the examination. Measurements are made of the Load (F) applied to the specimen and its extension (ΔL) to discover the ultimate tensile strength of the bio-adhesive material. Data collected from the tensile machine provided results for the single-lap shear test and made it feasible to plot a stress (σ) strain (ε) curve, which will provide the material's mechanical properties.



Figure 3. 20: Paper specimen for single-lap Joint (self-developed)

The stress-strain curves show the different stages the specimen goes through during the tensile lap shear test, with the maximum point being the ultimate tensile strength.

This will be the point at which maximum bio-adhesive strength is measured. The stress-strain curve also highlights the material's elastic and plastic deformation regions, providing insights into bio-adhesive mechanical properties. From the stress-strain curve, yield strength and modulus of elasticity are critical characteristics that can be determined.

Because the stress-strain curve is nonlinear, Young's modulus (E_y) cannot be found directly from the curve. Instead, the modulus is typically determined by analyzing the linear portion of the stress-strain curve, which characterizes the elastic deformation region. This linear relationship allows for the calculation of Young's modulus as the gradient of the stress-strain curve in this region.

The process for determining Young's modulus (E_y) can be further carried out using the following calculation method.

$$\sigma = \frac{F}{A} \quad 3.1$$

$$\varepsilon = \frac{\Delta L}{L} \quad 3.2$$

$$Ey = \frac{\sigma_2 - \sigma_1}{\varepsilon_2 - \varepsilon_1} \quad 3.3$$

$$G = \frac{E}{2(1+\nu)} \quad 3.4$$

$$\nu = \frac{E}{2G - 1} \quad 3.5$$

3.6.4 Single lap-shear test testing procedure

For this experimental approach, the procedure consists of five runs conducted at each temperature parameter. The approach and assumptions were that, from the five experimental runs, an average of 3 runs per temperature parameter would yield positive results, as elaborated in Table 3.6. In this case, an application of a Taguchi experimental matrix L_{18} of 6 levels with 18 experimental runs was designed to influence the strength and confidence of the results [108]. Data collected will be analyzed using a statistical test and the normal distribution curve, as this is mostly applicable in the science field for most variables with numerical data.

Table 3. 6 Experimental design – Taguchi's method (self-developed)

Sample Number	Number of experimental runs	Temperature (^{0}C)	Adhesive Weight (g)
1	3	100	0,25
2	3	110	0,25
3	3	120	0,25
4	3	130	0,25
5	3	140	0,25
6	3	150	0,25

The flow diagram in Figure 3.21 demonstrates the key processes involved in conducting a single-lap shear test, starting with the development of paper substrates 1 and 2 and the use of a bio-adhesive material in a liquid state to join them. Mounting and clamping the specimen on the tensile testing machine and setting tensile tester operating parameters. Operating the tensile test machine to start the single lap-shear testing process, with single lap-shear results and data recordings being made available for analysis.

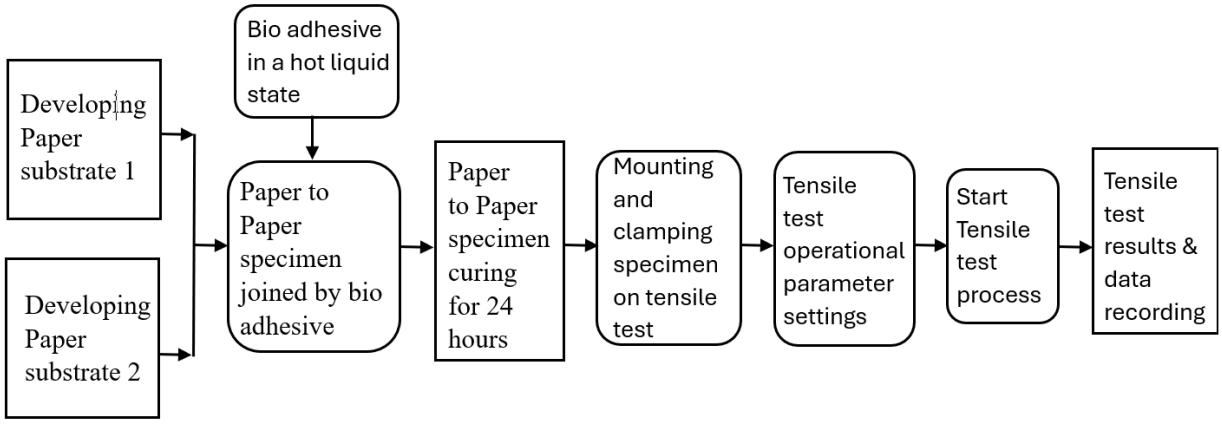


Figure 3. 21 Flow diagram and steps followed to execute single lap-shear testing methods (self-developed)

This single-lap shear test was performed using tensile machines calibrated in accordance with the Original Equipment Manufacturer (OEM) specifications and requirements. Normal paper samples without any adhesive bonding material applied. The parameters of these samples were measured to verify compliance with the following standards: ASTM D1002, ASTM D3163, and ISO 4587.

Data obtained from the single-lap shear test are critical and will be examined to determine bio-adhesive mechanical properties in the next chapter. The next section is still a continuation of conducting mechanical integrity tests, which are undertaken through the T-Peel test.

3.7 T-Peel test

This section explains the systems and processes utilized to conduct a mechanical test using the T-peel test for investigating, analyzing, and understanding bio-adhesive material's mechanical performance. The T-peel test is primarily used to gauge the bio-adhesive strength between two substrates and is well-suited to testing thin substrate materials, in this case a 0,5 mm thick paper substrate. Peel strength is an important property of bio-adhesive material that forms the basis for determining the reliability and durability of these bio-adhesive materials.

3.7.1 The aim of performing the T-Peel test

The T-Peel test is a technique utilized to determine the adhesion strength between two substrates joined by a bio-adhesive material. This testing method has been proven to be the most standard method in determining bio-adhesive peel strength, for assessing peeling behavior and giving insightful information about their bio-adhesion qualities and mechanical attributes [94]. Peeling force is a very crucial, essential measure for determining characteristics of material adhesion, and this is the load required to separate the bio-adhesive film from the two substrates.

In this section, the objective of the experiment is to determine the bio-adhesive's mechanical properties using a T-Peel test and to investigate how the bio-adhesive is affected by changes in processing temperature.

The T-Peel testing method will be conducted using a U-Stretch Mechanical Test System. This testing machine can conduct this experiment because of its range of settings and the load cell

limit. This is ideal because the bio-adhesive material is not ductile, and the paper substrate material is also not rigid.

3.7.2 T-Peel test methods and materials used

This section provides full details of the methods and equipment used to prepare the bio-adhesive specimen, which was tested on a T-Peel testing machine to conduct mechanical investigation and analysis. The equipment used to conduct this mechanical test process was the U-Stretch Mechanical Test System.

Table 3. 7 T-Peel test paper-to-paper specimen dimensions (self-developed)

Description	Operating Parameters (mm)
Shape	Rectangular
Length	100
Width	15
Thickness	0,5
Fixture separation	6
Separation length	100
Adhesive applied Area: Length	15
Adhesive applied Area: Width	10

A knife was used to cut to size paper substrates that will be used as paper-to-paper substrates that are bonded together by bio-adhesive material. The dimensions of these paper-to-paper substrates are provided in Table 3.7 and Figure 3.22, which show the complete assembled specimens.

A knife was further used to cut the bio-adhesive material to the required size, and the scale was used to weigh out an average of 0,25 g of this material. The material used for T-peel testing is a bio-adhesive extracted from candelabra trees and processed at different temperatures. In this case, the processed bio-adhesive material is applied to a paper-to-paper specimen while it is in a hot liquid state.

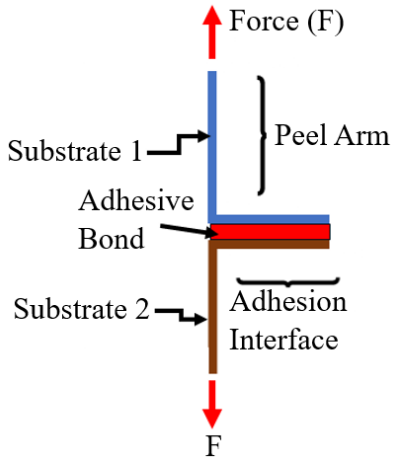


Figure 3. 22 T-Peel Test Illustration (self-developed)

During this process, the pulling force is recorded in newtons (N), and peel bio-adhesive strength is recorded as the peel load divided by the width of the specimens (F/m), which is the strength required to cause the bio-adhesive material to fracture per unit length. From this experiment, raw data on force and displacement in meters (m) are recorded and used to plot and produce the graph. From this graph, it is possible to find the minimum and maximum average peel force. Bio-adhesive energy can also be calculated from the force-displacement graph as the average bio-adhesive peel strength per area of adhesion interface (F/m^2 or Pa).

3.7.3 T-Peel testing method

Figure 3.23 (A) illustrates a peel test in which both materials are pulled at the same time and at the same speed. The two substrates are clamped by jaws at both ends and pulled in opposite vertical directions to induce the debonding process of the bio-adhesive material. The substrate's dimensions and area of bio-adhesive application were always kept constant throughout the experimental process, as shown in Figure 3.23 (A). The material used in this experiment was paper-to-paper, as shown in Figure 3.23 (B). The material used was a naturally processed bio-adhesive sourced from the candelabra tree, which in this case was in a hot liquid state.

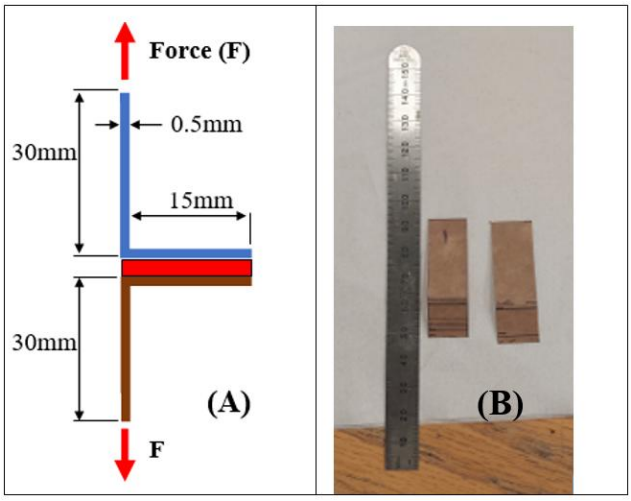


Figure 3. 23: (A) T-Peel test specimen parameters: (B) paper specimen for T-Peel test (self-developed)

The two substrates were joined with a bio-adhesive material as illustrated in Figure 3.23 (B), and constant pressure was applied by hand. The specimen was left to cure for 24 hours, and thereafter the overlapping bio-adhesive was removed before the experimental process started.

The sample testing was carried out on a U-Stretch Mechanical Test System illustrated in Figure 3.24 (a), using ASTM 1876 – 08 Peel resistance of adhesive standards for adhesive peel test. The candelabra bio-adhesive material used in this experiment is a perfect match for this type of mechanical testing apparatus, which leads the industry in precision biomaterial test systems [139]. The load used in the Mechanical testing system had a capacity of 100 N and a steady crosshead speed of 6 mm/min.

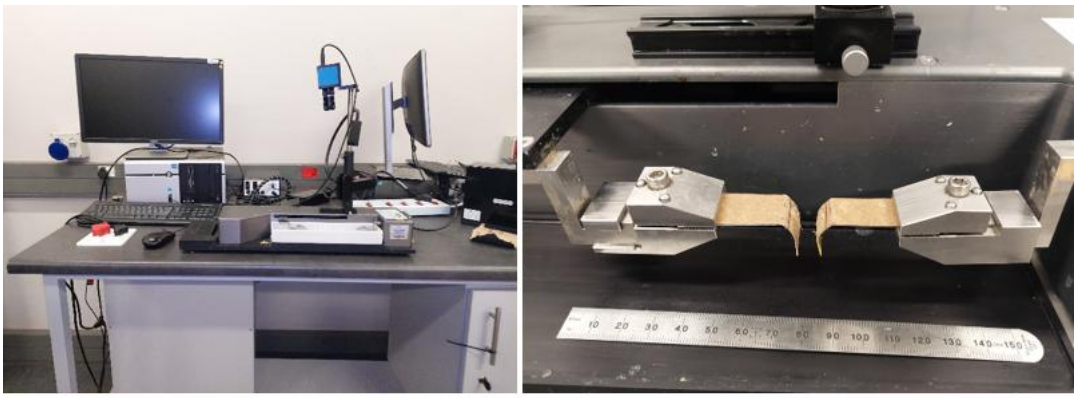


Figure 3. 24 (a) Cell-scale U-Stretch mechanical test system (b) paper-to-paper specimen on T-Peel clamps (self-developed)

Peeling occurs when a load is applied perpendicularly to the surface, as demonstrated in Figure 3.24 (b). This pulls the two substrates in opposite directions, resulting in debonding of the bio-adhesives from these substrates. The debonding process occurs because of bio-adhesive failure and proceeds in several stages.

The initial loading stage is the process of gradually applying force to the specimen until the interface area begins to delaminate, which may be due to the onset of small cracks starting to occur. The initiating stage is when the peel force reduces slightly after delamination. This is because of an increase in cracks, which reduces effective load transfer.

Average peel force, also known as the evaluation region, is the process in which a stabilized force is applied over a section of the displacement area, and toward the end a small peak occurs, which is the maximum peel force for this process. This is the load required to detach two joined substrates, measured during the test at a steady speed.

Peeling energy (N/mm) is the force applied to the width of the specimen's bonding surface during steady-speed peeling. It is the force the bio-adhesive material can withstand as the two substrates are pulled away from the bond line. It is derived by dividing the average force measured during the test at constant speed, divided by the specimen's unit width.

Through these stages, the sample is pulled to its breaking point to determine the material's ultimate peel force. Measurements are continuously made of the load (F) applied to the sample and of its displacement change (ΔL).

The software used on the U-Stretch Mechanical Test System does not calculate the stresses (σ). Therefore, in this work, a basic approach was used, in which stress was calculated as the load (F) divided by the specimen's area (A). The results were in N/m^2, which is also expressed in Pascals (Pa). The strain (ε) was calculated (referring to equation 3.6) by measuring the length (L) of the specimen tested and dividing it by the change in length (ΔL).

The energy input formula for calculating G (J/m2) is shown below in equation 3.8, where G is the adhesive energy input, F (N) is the peeling load, and b (mm) is the width of the specimen. The focus of this experimental work is to demonstrate the properties of the bio-adhesive material experimentally. Hence, any effects of specimen geometrical details will not be investigated further in this paper. This means that when only elastic deformation occurs in the peel arm, there will be no energy dissipation.

$G = G_C$ (G_C is the plastic work done in bending the peeling arm).

$$G = \frac{F(1\ Cos\ \theta)}{b} \qquad 3.6$$

For the T-Peel test, two samples are arranged back-to-back.

$$\theta = \frac{\pi}{2} \qquad 3.7$$

Therefore:

$$G = \frac{2F}{b} \qquad 3.8$$

3.7.4 T-Peel testing Procedure

For this experimental approach, the procedure consists of five experimental runs conducted for each temperature parameter. The approach and assumptions were that, from the five experimental runs, an average of 3 runs per temperature parameter would yield positive results, as elaborated in Table 3.8. In this case, an application of a Taguchi experimental matrix L18 of 6 levels with 18 experimental runs was used to influence the strength and confidence of the results. The data collected were to be analyzed using a statistical test of the normal distribution curve, as this is mostly applicable in the science field for most variables with numerical data.

Table 3. 8 Experimental design – Taguchi's method (self-developed)

Sample Number	Number of experimental runs	Temperature (^{0}C)	Adhesive Weight (g)
1	3	100	0,25
2	3	110	0,25
3	3	120	0,25
4	3	130	0,25
5	3	140	0,25
6	3	150	0,25

The flow diagram in Figure 3.25 demonstrates the key processes followed to conduct a T-Peel

test. These stages start with the development of paper substrates 1 and 2, using a bio-adhesive material in a hot liquid state to join them. The specimen is mounted and clamped on the T-Peel test machine, and the T-Peel tester operating parameters are set. The T-Peel test machine is operated to start the mechanical analysis testing process, and T-Peel test results and data recordings are made available for analysis.

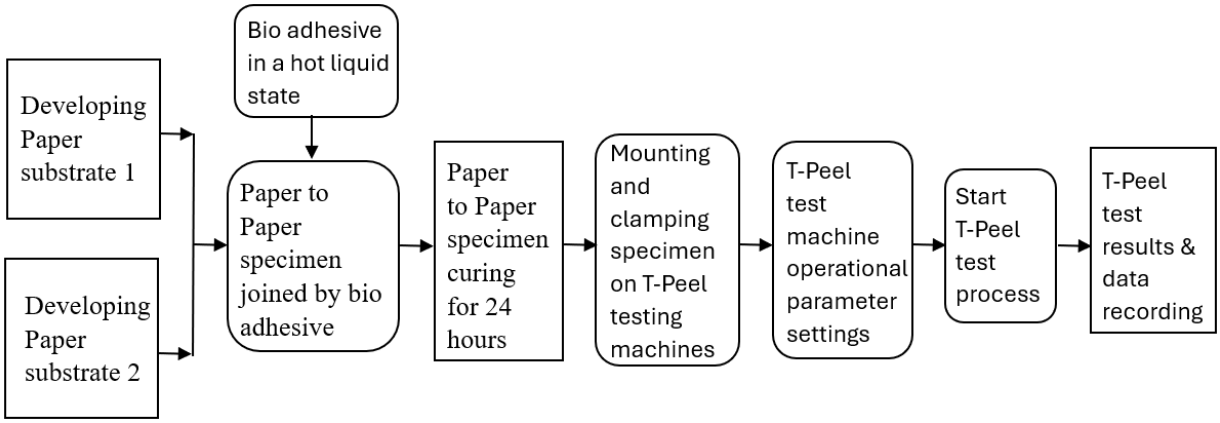


Figure 3. 25 Flow diagram and steps followed to execute T-Peel testing methods (self-developed)

The T-peel test was conducted by ensuring that the specimen parameters were measured to comply with ASTM 1876 – 08 (Peel Resistance of Adhesive). The experimental approach for the T-peel test was carried out using a U-Stretch Mechanical Test System that was calibrated in accordance with the Original Equipment Manufacturer (OEM) specifications and requirements.

Two test sets are included in that sequence. The first set preconditions the specimen, while the second set performs the actual test. To achieve a satisfactory state, two identical test cycles were implemented in the first preconditioning set. Finally, the second set (testing) consists of three cycles. During each cycle, five phases occur, including preloading, stretching, holding, recovering, and resting.

A preload is applied to define the starting point of a test. To compensate for changes in specimen geometry caused by a loading cycle, preload adjustment is used. In the stretch phase, the specimen undergoes deformation by applying force or measuring displacement. The holding phase is the process of maintaining deformation over a given period. The duration depends on the nature of the test.

The recovery phase is when the specimen is free of the applied force. The duration of the recovery time can be configured based on the nature of the test as well as the duration of the test. Finally, the rest phase occurs between one cycle and the next. In some tests, the recovery time may be specified as a short time, while in others, it may be specified as a longer time, depending on the nature of the test. Data obtained from the T-Peel test is critical and will be examined to determine bio-adhesive mechanical properties.

3.8 Summary

In Chapter 3, the discussion was on the extraction of latex from the candelabra tree and the processing methods undertaken to transform latex into bio-adhesive material. The focus was on

understanding the bio-adhesive material's behavior and performance under varying processing temperatures from 100^0C to 150^0C. Thermal testing procedures, namely TGA, DSC, and rheological testing, were undertaken to analyze weight loss, thermal transitions, and the performance of the bio-adhesive material. Mechanical properties were assessed by conducting both T-Peel and single-lap shear experimental tests. Both thermal and mechanical testing procedures were undertaken to understand the bio-adhesive transition behavior and mechanical strength. In Chapter 4, data obtained from this testing procedure can now be analyzed and interpreted.

CHAPTER FOUR

4. RESULTS AND DISCUSSIONS

4.1 Overview

In this section, the results are presented and discussed in relation to the methodology used in Chapter 3. The findings are presented in a structured manner, highlighting key trends, patterns, and anomalies observed during the analysis. This discussion aims to connect the results with the research objectives, providing an overview of how the data supports or challenges the initial objectives. Thermal and mechanical testing approaches were used to investigate the impact of temperature on bio-adhesives. This chapter includes experimental and characterization results that state the findings of the research as well as the validation of the results.

4.2 Thermal analysis results

The thermal testing method was executed on unprocessed latex and bio-adhesive processed at 100^0C, 110^0C, 120^0C, 130^0C, 140^0C and 150^0C. This testing method commenced with differential scanning calorimetry (DSC), thermogravimetric analysis (TGA), and rheology. The data retrieved from this thermal testing method are discussed, explained, elaborated, and analyzed in this section.

4.3 Thermogravimetric analysis (TGA)

TGA determines, observes, and records sample weight changes over time within a fixed temperature span. This procedure involves heating under controlled inert conditions at a constant temperature. The specimen is placed inside a furnace, which is then sealed to maintain controlled conditions. Gas is delivered through the specimen at a specified flow rate, time, and temperature to enable the measurement of bio-adhesives. The measurement phase is undertaken through a temperature program, a precision balance scale joined to the specimen pan inside the furnace, and a thermocouple. The balance scale measures the sample mass inside the furnace, and a thermocouple observes specimen temperature. This method of measurement enables the collection of accurate material data that can be logged as decomposition, dryness, and oxidation of a specimen. Data collected during this process is important because it provides more understanding of the bio-adhesive material's decomposition properties. The results, which are the characteristic thermogravimetric curves derived from percentage mass loss versus temperature change, are discussed in detail below.

4.3.1 Temperature against TGA mass percentage of bio-adhesive at varying temperatures limitations

Below is a brief representation of the curve showing mass percentages versus temperature for bio-adhesive materials prepared at 100^0C, 110^0C, 120^0C, 130^0C, 140^0C, 150^0C, and for unprocessed latex. By analyzing the curve in Figure 4.1, it is possible to determine the

remaining weight value for this bio-adhesive material. This is done by comparing the change in weight at varying stages and determining temperature limitations.

As illustrated in Figure 4.1, for the processed bio-adhesive materials (processed at 100^0C, 110^0C, 120^0C, 130^0C, 140^0C, and 150^0C), the curve at a furnace temperature of 350^0C shows that most of the bio-adhesive carbon-based material has disintegrated. This occurs at a weight percentage of about 15%, which indicates the remaining value of these bio-adhesive materials. The remaining mass is mainly due to non-reactive compound material, which will most likely end up as ash after the characterization process is completed. Still focusing on these processed bio-adhesive materials, the major percentage weight loss occurs, as shown in Figure 4.1 (A & B), at temperatures from approximately 260^0C to 350^0C, when these five bio-adhesive materials are reactive, with a major loss of volatile chemical compounds.

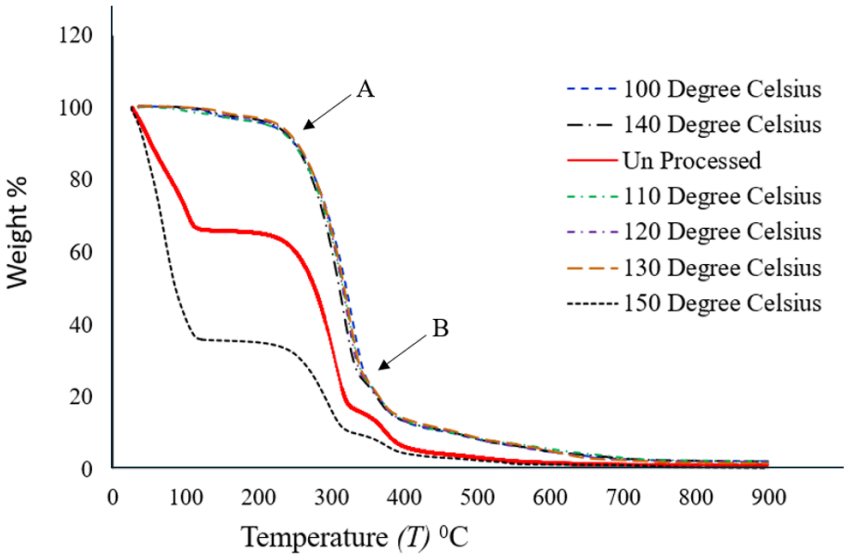


Figure 4. 1 TGA Percentage weight against temperature curve indicating varying processing temperatures of bio-adhesive materials

In Figure 4.1 (A), the minimum percentage weight loss can be due to the loss of moisture that remains in the bio-adhesive materials, and the only difference between points A and B is the processing temperature. Figure 4.2 shows that materials processed at 100^0C, 130^0C, and 110^0C have much higher values than those processed at 140^0C and 120^0C. This is due to differences in reaction temperatures, as bio-adhesives processed at lower temperatures tend to require more heat to complete their reaction process. Compared with the bio-adhesive processed at 100^0C to 140^0C in Figure 4.1, the unprocessed latex specimens initially exhibit a higher material weight loss beginning at 30%.

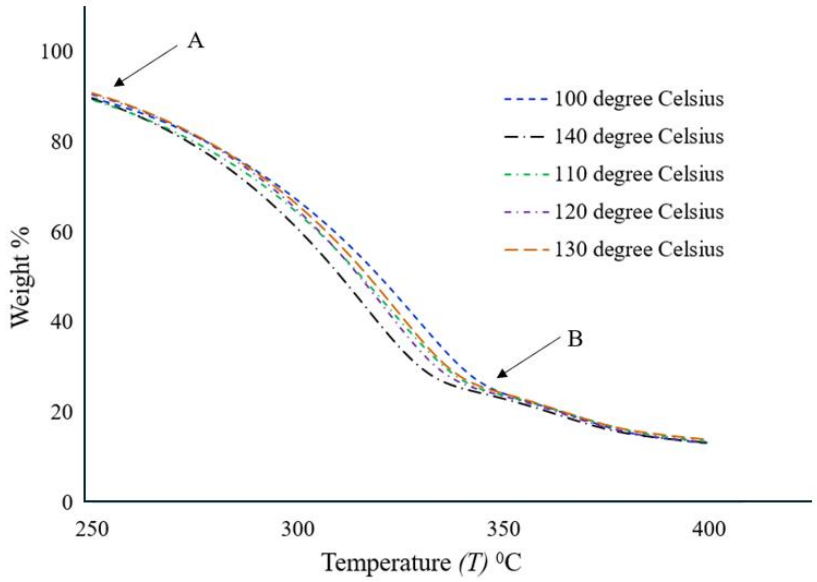


Figure 4. 2 TGA Percentage weight against temperature curve showing points A & B of five bio-adhesive materials prepared at varying temperatures (100^0C, 110^0C, 120^0C, 130^0C & 140^0C)

Figure 4.3 illustrates that as the thermal experiment progressed, the weight loss gradually decreased from 100% to 70%, possibly due to the higher moisture content in unprocessed latex. It should be noted that the furnace temperature was initially set to room temperature and gradually increased to 100^0C during this process.

Following that, there was an immutable reaction state inside the furnace ranging from 100^0C to about 260^0C, with minimal to no degradation occurring at 70%. After this point, the degradation rate increased significantly at furnace temperatures exceeding 260^0C to 310^0C, with the weight percentage dropping sharply from 70% to 20%. This is when unprocessed bio-adhesive is most reactive. This is due to the presence of active chemical compounds that promote molecular interactions, which in turn result in the release of reactive byproducts.

This highlights the critical temperature range at which unprocessed latex degrades more rapidly, losing 50% of its weight, as shown in Figure 4.3. It must be noted that at temperatures of 310^0C to 400^0C, a slight reaction occurs, and at this point the unprocessed latex degrades with a weight loss of 20% to 10%. This could be due to a small percentage of reactive compounds still contained in the unprocessed latex. At this stage, most of the chemical compounds have reacted, and the remainder is ash that cannot react further.

Figure 4.3 elaborates that the final reaction stage is from 400^0C to 900^0C, with minimal weight loss, and that the weight stabilizes at less than 10%, indicating complete thermal decomposition. At this stage, most chemical compounds have reacted, and the remainder consists of ash compounds that cannot react further. Notably, both processed bio-adhesive material and unprocessed latex begin reacting at approximately 260^0C. This reaction is critical for both materials, as it determines their bio-adhesive properties and overall performance.

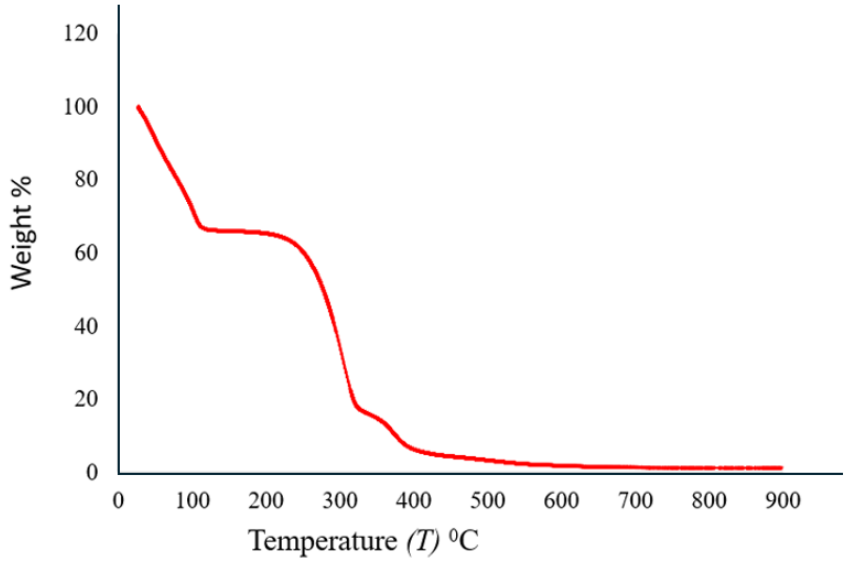


Figure 4. 3 TGA Percentage weight against temperature curve for unprocessed latex

Figure 4.4 illustrates that during the thermal experiment, there is a significant percentage weight loss from 100% to 40%. This is when the bio-adhesive that is processed at 150^0C is most reactive. This could be because, at the highest temperature, some chemical compounds have already reacted during processing.

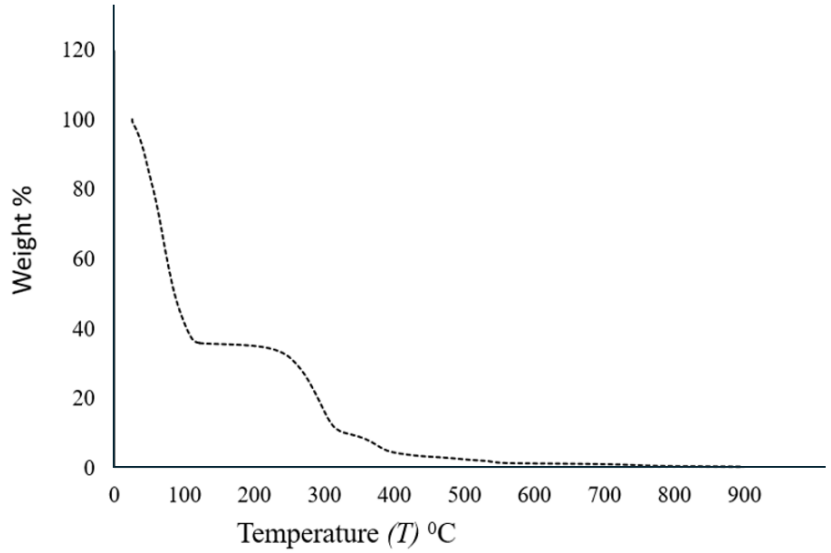


Figure 4. 4 TGA Percentage weight versus temperature curve of bio-adhesive prepared at 150^0C

Figure 4.4 shows a constant reaction inside the furnace ranging from 100^0C to about 260^0C, with minimal to no degradation occurring at 40%. After this point, the degradation rate slightly increases from 260^0C to 310^0C, with the weight percentage dropping from 40% to 15%. Notably, at temperatures of 310^0C to 400^0C, a slight reaction occurs, and at this point the bio-adhesive degrades with a weight loss of 15% to 10%. This is due to a small percentage of reactive compounds still left in the bio-adhesive material. The last reaction stage is from 400^0C to 900^0C, with minimal weight loss, and the weight stabilizes at less than 10%, indicating complete thermal decomposition.

In this study, TGA analysis revealed a three-stage process, with stage 1 involving the decomposition of moisture and easily volatile compounds. In stage 2, extracted components were removed from the bio-adhesive sample at temperatures ranging from 260°C to 350°C. During this stage, 75% of the decomposition occurred, breaking down compound particles. By this point, most of the cellulose and hemicellulose had been cracked, allowing maximum bioenergy conversion. In the third stage, complex compounds decomposed slowly and steadily, losing 15% of their mass. The analysis is comparable to [140], where assessment of mass loss over the three stages of TGA analysis is consistent with previous studies [141], where major decomposition takes place at stage 2. The results contradict [142], however, only in the temperature range and mass percentage loss where these three stages occur. Stage 2 findings occur between 192°C and 441°C, resulting in 59,61% decomposition, which may be due to variability in material structural composition.

4.3.2 TGA derivative weight percent against temperature curve of bio-adhesive processed at different temperature parameters

Figure 4.5 elaborates the derivative weight curve as a function of temperature. The plotted data can be used to determine the bio-adhesive material's oxidation temperature and to describe occasional weight loss through processes such as single-, shoulder-, or double-peak events. The material temperature measured at the highest point on the curve, as indicated in Figure 4.5 (E), can be used to identify the bio-adhesive material's thermal stability, also referred to as the primary oxidation temperature.

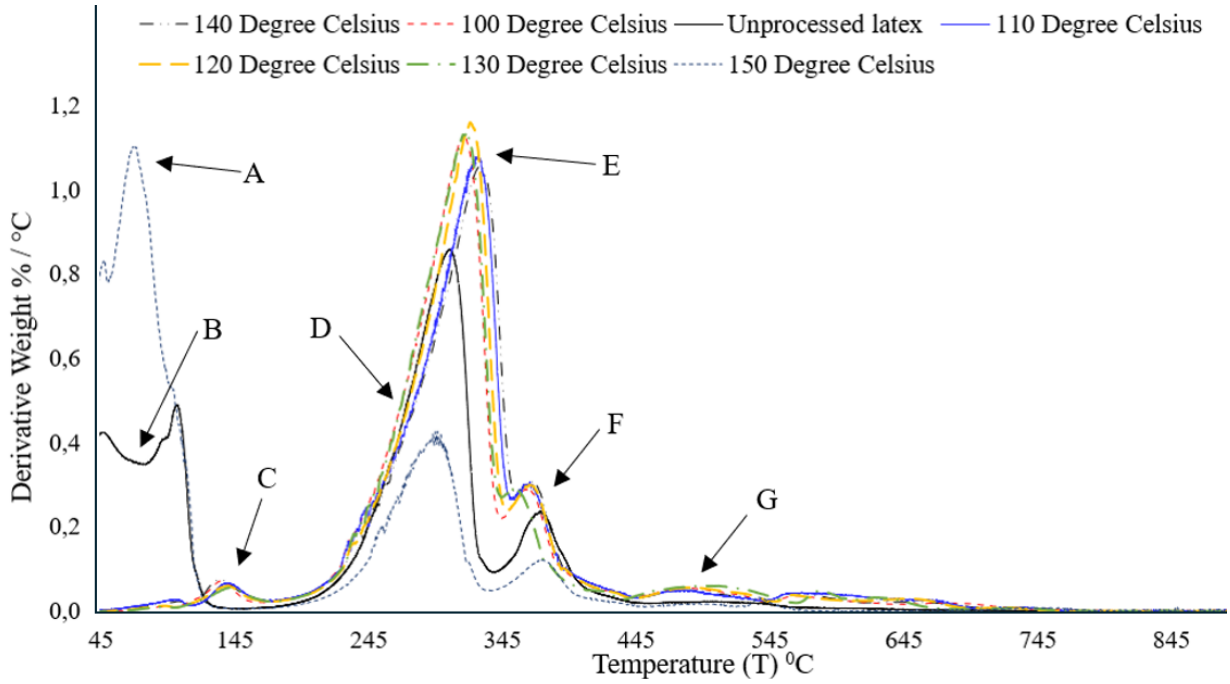


Figure 4. 5 TGA Derivative weight against temperature curve indicating varying processing temperatures of bio-adhesive materials

The peak temperature of unprocessed latex material is approximately 310^0C, which corresponds to the oxidation temperature, as shown in Figure 4.5 (4). At this temperature, the material begins to break down and release volatile compounds, leading to potential degradation. Maintaining

temperatures below this threshold is crucial to preserve the integrity and quality of the latex during processing and storage. As shown in Figure 4.5 (points B, C, F & G), this material also undergoes multiple degradation processes.

These processes include oxidation, thermal degradation, and chemical reactions. As shown in Figure 4.5 (point B), this could be due to the presence of other compounds that oxidize at low temperatures. Another possibility is the presence of other compounds that require high oxidation temperatures, as shown in Figure 4.5 (points F & G). For unprocessed latex material, decomposition starts at Figure 4.5 (point B) at a temperature of approximately 70^0C, which is much lower than that of other processed bio-adhesive materials. Figure 4.5 further illustrates that bio-adhesive processed at 150^0C shows a low derivative of less than 0,1% at 345^0C.

The five processed bio-adhesives (processed at 100^0C, 1100C, 120^0C, 130^0C, 140^0C, and 150^0C), as illustrated in Figure 4.6, appear to exhibit similar reactive behavior, with all samples showing similar thermal stability patterns. The first lower-temperature reactive peak in Figure 4.6 (point C) occurs at about 145^0C, and this extends to point D. However, slight performance variations were observed. All processed bio-adhesives reacted at lower temperatures, whereas unprocessed latex reacted at a slightly higher furnace temperature.

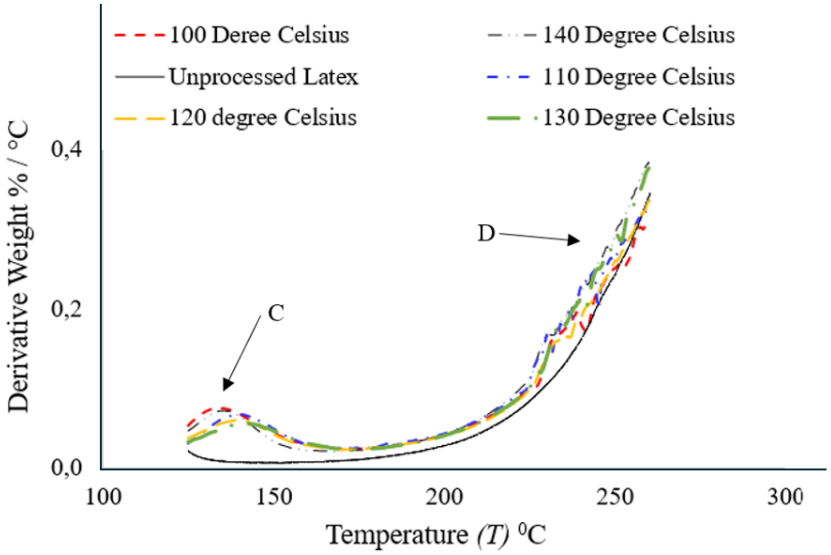


Figure 4. 6 TGA Derivative weight percent against temperature curve showing a detailed section between points C & D for processed & unprocessed bio-adhesive material

The third high-temperature reactive peak is shown in Figure 4.7 at point F at a temperature of 365^0C, with almost identical behavior for the five-bio-adhesive material from point F to the end of the thermal experimental process at 440^0C.

However, as illustrated in Figure 4.7, the bio-adhesive processed at 130^0C appears to react first at this stage, requiring less heat than the rest of the processed bio-adhesive material. This could be due to a lower concentration of the chemical compound involved in the reaction at this temperature. This could also suggest that the bio-adhesive material processed at 130^0C undergoes a more efficient thermal reaction, potentially due to changes in its molecular structure or composition during processing.

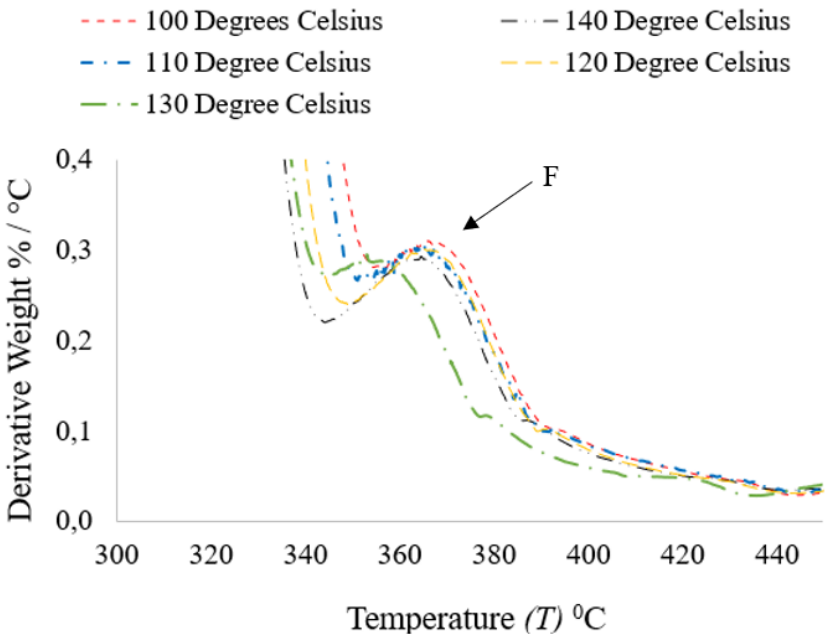


Figure 4. 7 TGA derivative weight percent against temperature curve showing a detailed section between point F for bio-adhesive material

Following this, an unprocessed latex material reacts at 345^{0}C with a 0,08% weight derivative. This indicates that the unprocessed latex and the bio-adhesive processed at 150^{0}C have significantly lower thermal reactivity than other processed bio-adhesive materials. The difference in derivative percentage indicates that processing temperature impacts the material's chemical stability and reaction rate. This makes the unprocessed latex and the bio-adhesive processed at 150^{0}C more suitable for applications requiring lower thermal reactivity, while the other five processed bio-adhesives will be used in applications requiring higher thermal reactivity.

Figure 4.8 shows the highest peak for processed bio-adhesive material (processed at 100^{0}C, 110^{0}C, 120^{0}C, 130^{0}C, and 140^{0}C). This peak corresponds to the oxidation temperature, the temperature at which a material or substance reacts with oxygen to form oxides. It is a critical parameter in materials characterization, as it determines the material's resistance to deformation at higher temperatures.

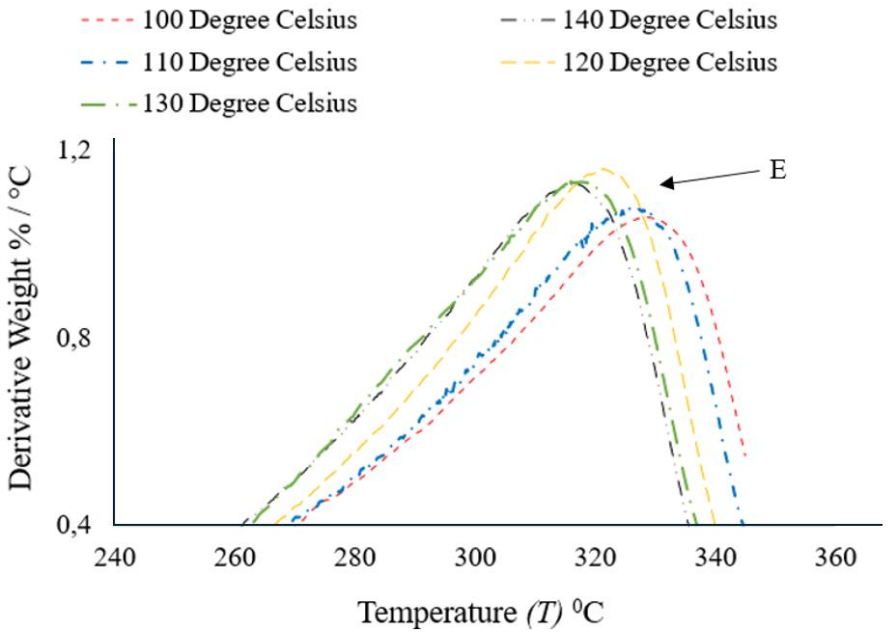


Figure 4. 8 TGA derivative weight percent against temperature curve showing a detailed section between point E for the bio-adhesive material

Table 4.1 details the TGA thermal stages that both processed bio-adhesives and unprocessed latex material undergo. It further indicates that the bio-adhesive's initial degradation temperature shifts to a lower value of 145^{0}C at 0,07% weight derivatives. The analysis and results are comparable to those of previous studies in [143], which clearly demonstrate the initial degradation temperature over a wider temperature range between 200^{0}C and 300^{0}C. According to the results of thermogravimetric analysis, bio-adhesive samples processed at 120^{0}C degraded between 200^{0}C and 500^{0}C in two stages.

Table 4. 1 TGA thermal stages for both processed bio-adhesives and unprocessed latex material

	Initial Stage (Point A & B)		**First Peak (Point C)**		**Second Peak (Point F)**		**Oxidation (Point E)**	
	Temperature (T) (^{0}C)	**% Weight Derivative (%WD)**	**T (^{0}C)**	**% WD**	**T (^{0}C)**	**% WD**	**T (^{0}C)**	**% WD**
Un Processed	70^{0}C	0,35	145^{0}C	0,01	345^{0}C	0,08	310^{0}C	0,82
100^{0}C	70^{0}C	0,01	145^{0}C	0,08	358^{0}C	0,26	332^{0}C	0,95
110^{0}C	70^{0}C	0,01	145^{0}C	0,08	355^{0}C	0,25	328^{0}C	0,93
120^{0}C	70^{0}C	0,01	145^{0}C	0,07	350^{0}C	0,23	320^{0}C	1,12
130^{0}C	70^{0}C	0,01	145^{0}C	0,06	340^{0}C	0,26	315^{0}C	1,1
140^{0}C	70^{0}C	0,01	145^{0}C	0,07	340^{0}C	0,2	315^{0}C	1,08
150^{0}C	70^{0}C	1,5	145^{0}C	0,01	345^{0}C	0,06	310^{0}C	0,4

The peak oxidation temperature and deformation resistance of the material are determined at 320^{0}C, with a 1,12% weight derivative. This is a two-stage process. The first stage, between 260^{0}C and 330^{0}C, involves the breakdown of smaller or unreacted molecules. The second stage, between 340^{0}C and 440^{0}C, involves the dissociation of larger molecules. As the char layer

formed in the previous phase dissociates at temperatures above 440^0C, thermal degradation occurs.

The results are contradictory [144], to the oxidation peak temperature occurring between 350^0C and 500^0C. The difference in oxidation temperature could be due to oxidation being a kinetic process. Changing these experimental variables will shift the peak temperature, breaking direct comparability [145]. Thermogravimetric analysis identifies the inflection point where oxidation or decomposition rates are at their maximum. Furthermore, the kinetic parameters suggest that sample porosity and heating rate significantly influence the rate constants, complicating direct cross-study comparisons. Additional isothermal studies could help isolate the contributions of moisture, ash content, and catalysis, clarifying the observed discrepancies and refining the thermal model.

4.4 Differential scanning calorimetry (DSC)

DSC is a widely used method for investigating and analyzing the key properties of materials. It also provides development information for untried materials, including bio-adhesive materials. DSC is a thermal analysis technique in which the temperatures of the sample and reference specimen are maintained and measured at nearly the same rate, and the results reflect the quantity of heat required to increase the temperatures of both the sample and reference specimen. DSC results were obtained from thermal tests as raw data, covering both unprocessed latex materials and processed bio-adhesive material at 100^0C, 110^0C, 120^0C, 130^0C, 140^0C, and 150^0C. Two tests were conducted for each unprocessed latex and processed bio-adhesive. The data were recorded in an Excel spreadsheet, which was used to develop the heat flow versus temperature curve.

4.4.1 Heat Flow (normalized) (W/g) verses Temperature (^{0}C) curve (first stage at Ramp 10^0C /min to 200^0C

There are three stages in the DSC thermal analysis process. The first heating phase is a ramp from 10^0C to 200^0C, which is exothermic. The cooling phase is a ramp from 10^0C to $–65^0$C, which is endothermic. Lastly, the second heating phase is a ramp from 10^0C to 200^0C.

Figure 4.9 illustrates the first exothermic heating phase, ranging from -55^0C to 200^0C, with a heat flow range of –0,001 W/g to 0,07 W/g. Based on the curve, it can be observed that the 110^0C bio-adhesive material reaches a maximum heat flow of 0,064 W/g at a transitional temperature from negative to positive. This peak value indicates the material's capability to absorb and release energy during its heating process. This is a significant attribute of its thermal performance. The observed heat flow range and transitional behavior indicate that the bio-adhesive material processed at 110^0C exhibits favorable exothermic properties.

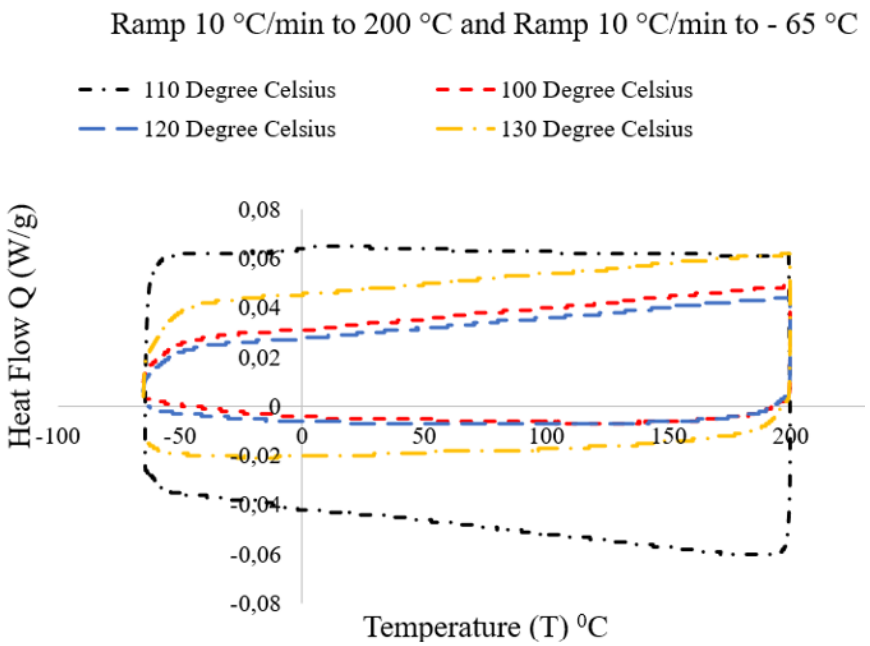


Figure 4. 9 DSC heat flow (normalized) (W/g) versus temperature (^{0}C) curve for bio-adhesive processed at 100^{0}C, 110^{0}C, 120^{0}C and 130^{0}C

This material reaches a heat-flow energy of 0,062 W/g at a maximum temperature of 200^{0}C. Bio-adhesive processed at 130^{0}C displays similar behavior, reaching a slightly lower transitioning heat flow energy of 0,043 W/g, then increasing to 0,062 W/g at 200^{0}C. Similarly, bio-adhesive materials processed at 100^{0}C and 120^{0}C achieve higher energy values of 0,04 and 0,038 W/g, making them the least exothermic materials.

The exothermic behavior in this paper is comparable to that reported in [146], where partially bio-sourced glycerol glycidyl ether (GDE) was used to improve the bonding strength of the resin formed, and the material was characterized by DSC. The results revealed that these modified bio-sourced adhesives exhibited typical exothermic behavior, as is the case with most thermoset resins. The study further indicated a slightly higher curing temperature of 162^{0}C, which was concluded to be acceptable, particularly considering the improved bonding performance resulting from the addition of bio-sourced GDE. The study further justified that the delayed exothermic peak is likely to be due to additional crosslinking reactions involving GDE with hydroxyl groups of starch and lignin, as well as with secondary amino groups of urea.

As illustrated in Figure 4.9, the cooling endothermic phase spans from -60^{0}C to 200^{0}C with a heat flow range of –0,062 W/g to -0,062 W/g. The curve illustrates similar behavior across all four bio-adhesive materials, with the 110^{0}C bio-adhesive material reaching a maximum heat flow of -0,062 W/g, while the remaining three bio-adhesives (100^{0}C, 120^{0}C & 130^{0}C) reach an overlapping higher heat flow of 0,001W/g. The 110^{0}C bio-adhesive material reaches a transitional heat flow of -0,04 W/g, while the 130^{0}C, 120^{0}C, and 100^{0}C achieve heat flows of -0,02 W/g, 0,003 and 0,002 respectively.

The final re-heating phase is also an exothermic process, as illustrated in Figure 4.10, ranging from 10^{0}C to 200^{0}C and spanning from -0,03 W/g to 0,07 W/g. This curve illustrates similar

behavior across all four bio-adhesive materials, with the 110^{0}C bio-adhesive material reaching a maximum heat flow of 0,06 W/g, while the remaining three bio-adhesive materials (100^{0}C, 120^{0}C & 130^{0}C) reach heat flows of 0,04 W/g, 0,04 W/g and 0,06 W/g, respectively. The bio-adhesive material processed at 110^{0}C reaches a transitional heat flow of 0,062 W/g, while the 130^{0}C, 100^{0}C and 120^{0}C achieve heat flows of 0,042 W/g, 0,025 W/g, and 0,022 W/g, respectively.

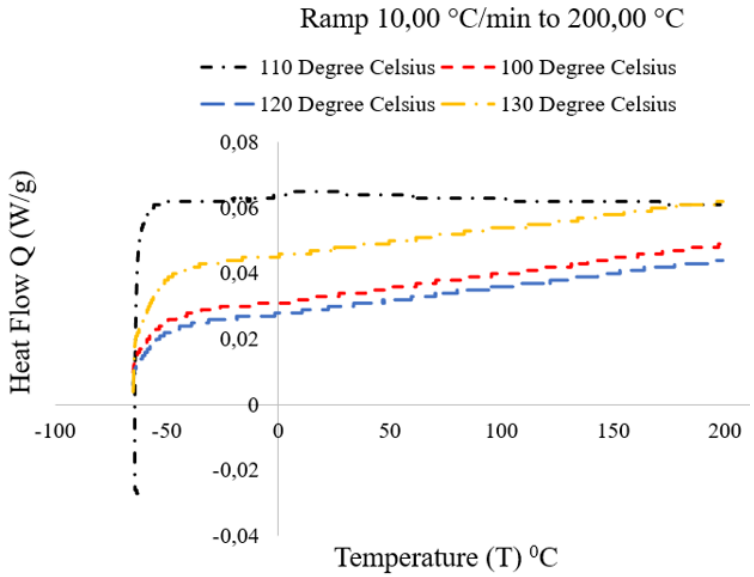


Figure 4. 10 DSC heat flow (normalized) (W/g) versus temperature (0C) curve for bio-adhesive processed at 100^{0}C, 110^{0}C, 120^{0}C and 130^{0}C (ramp 10^{0}C /min to 200^{0}C)

The thermal analysis results at 140^{0}C and 150^{0}C are much higher and out of range compared with those at 100^{0}C, 110^{0}C, 120^{0}C, and 130^{0}C. Therefore, 150^{0}C and 140^{0}C will be analyzed separately. In Figure 4.11, the first exothermic, endothermic, and second exothermic stages are illustrated for 140^{0}C bio-adhesive. In the first heating phase of this bio-adhesive, the maximum heat flow value is 1,2 W/g at 200^{0}C, and the transitional heat flow energy is 0,9 W/g. Endothermic heat flow begins at -0,75 W/g and, at 200^{0}C, it reaches -0,8 W/g, gradually overlapping with 1.2 W/g, and the transitional heat flow is -0,9 W/g. At -60^{0}C and at -0,25 W/g, the second exothermic phase began.

A temperature range of 50^{0}C to 165^{0}C shows small transformation changes, but 175^{0}C shows the biggest change, with the heat flow increasing from -0,27 to 2 W/g. This indicates an exothermic material, reflecting the material's ability to release energy during the exothermic phase. This implies that the bio-adhesive undergoes significant structural changes at higher temperatures, which contribute to its bio-adhesive properties. The observed heat flow variations highlight the material's thermal behavior and its suitability for applications requiring heat-resistant bonding.

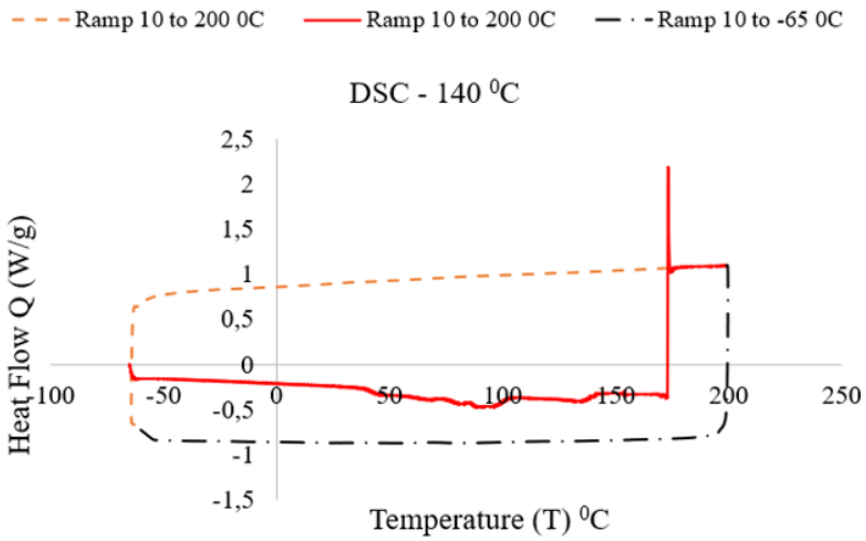


Figure 4. 11 DSC heat flow (normalized) (W/g) versus temperature (0C) curve for bio-adhesive processed at 140^{0}C

In Figure 4.12, the first exothermic, endothermic, and second exothermic stages are illustrated for the 150^{0}C bio-adhesive. The first heating phase has a maximum heat flow of 0,7 W/g at 200^{0}C, and the transitional heat flow is 0,55 W/g. Endothermic heat flow begins at -0,5 W/g and, at 200^{0}C, reaches -0,5 W/g, gradually overlapping to 0,7 W/g, while the transitional heat flow is -0,6 W/g. The second exothermic phase began at a temperature of -60^{0}C with a heat flow of 0,2. A temperature range of 45^{0}C to 110^{0}C shows small transformation changes, but 160^{0}C shows the biggest change, with the heat flow energy increasing from 0,4 to -2,2 W/g. This indicates an endothermic material, meaning it absorbs energy during the endothermic phase.

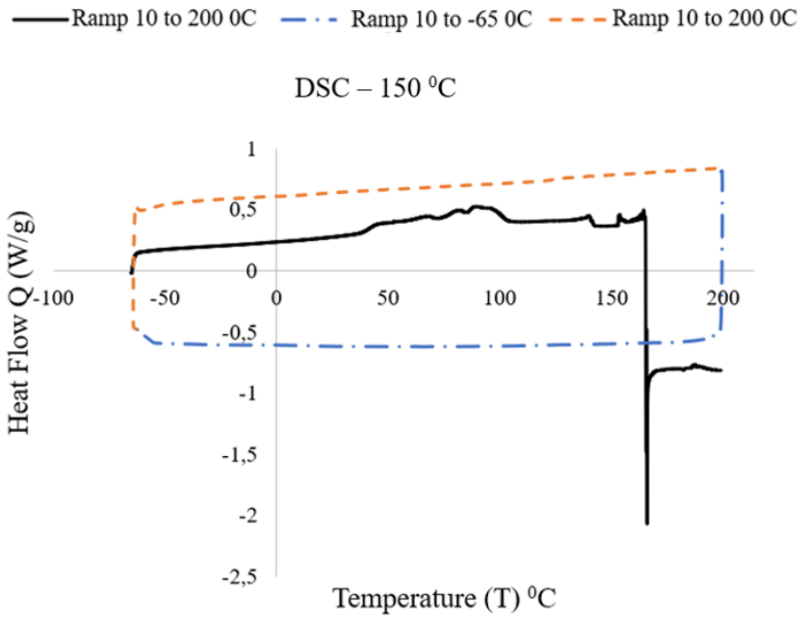


Figure 4. 12 DSC heat flow (normalized) (W/g) versus temperature (^{0}C) curve for bio-adhesive processed at 150^{0}C

Figure 4.13 illustrates the thermal behavior of an unprocessed latex material. Observations from this curve indicate linear behavior in the second heating phase at zero heat flow. This indicates that the material neither absorbs nor releases heat significantly during this phase. This behavior suggests that the material does not store or release heat significantly during the heating phase. This is evidence of its thermal stability and non-reactive nature under these conditions. The cooling phase also shows linear behavior, with slight exothermic behavior from 180^0C to 200^0C. The first heating phase is the only graph with endothermic properties at heat flows of -5 W/g, -10 W/g, and -17 W/g. The first heating phase exhibits endothermic behavior due to the absorption of heat required for physical or chemical changes, such as melting or decomposition. This contrasts with the cooling phase, where exothermic behavior indicates the release of heat as the material transitions to a more stable state.

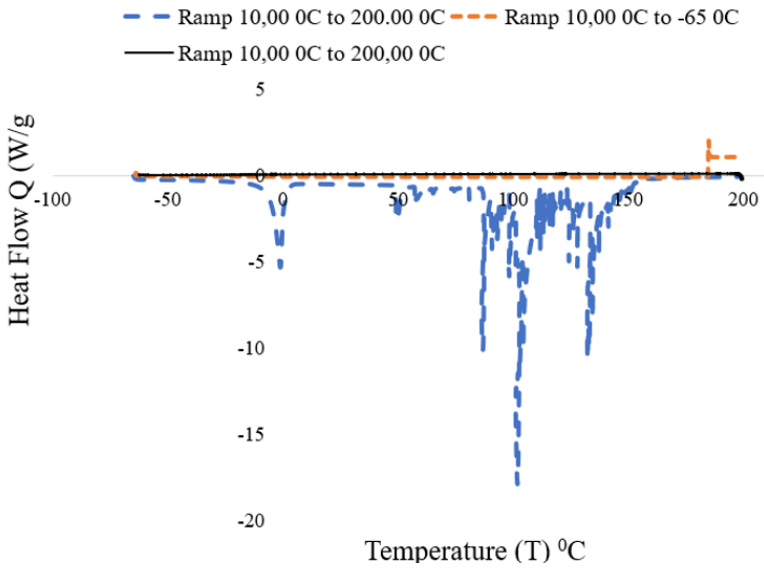


Figure 4. 13 DSC heat flow (normalized) (W/g) versus temperature (^{0}C) curve for unprocessed latex

Table 4.2 elaborates on the different DSC thermal stages that both processed bio-adhesives and unprocessed latex material undergo.

Various DSC partial contributions arising from desorption are primarily endothermic [147]. From the three-stage results of the DSC testing process, three endothermic partial contributions can be observed (sensible heat for solids, sensible heat for vapor, and heat of desorption). The endothermic "melting" peak of various polymers is characterized by a decrease in heat capacity at the end of the peak [147]. From Table 4.2, the unprocessed bio-adhesive also exhibits an endothermic low peak of -100 W/g at 90^0C and 140^0C, whereas the 150^0C processed bio-adhesive exhibits an endothermic peak of -2 W/g at 160^0C. The endothermic behavior of the other bio-adhesive materials in this paper was much more gradual and stable. However, on the contrary, the exothermic contribution of this other bio-adhesive material is not at all counterbalanced, as can be observed in this paper by the different maximum values of their heat values (W/g) [148].

Table 4. 2 DSC thermal stages for processed bio-adhesives

		Heat Flow Q (W/g)				Temperature (T) ^{0}C			
		Q1	Q2	Q3	Q4	T1	T2	T3	T4
First Heating Phase (Exothermic)	100^{0}C	0,001	0,02	0,03	0,04	-55	-50	0	200
	110^{0}C	0,001	0,06	0,064	0,062	-60	-55	0	200
	120^{0}C	0,001	0,018	0,028	0,038	-60	-55	0	200
	130^{0}C	-0,02	0,04	0,042	0,06	-60	-50	0	200
	140^{0}C	-0,6	0,8	0,9	1,2	-60	-55	0	200
	150^{0}C	-0,4	0,5	0,55	0,7	-60	-60	0	200
Cooling Phase (Endothermic)	100^{0}C	0,001	-0,001	0,002	0,001	-60	40	0	200
	110^{0}C	0,001	-0,038	-0,04	-0,062	-60	-50	0	200
	120^{0}C	-0,001	-0,002	-0,0033	0,001	-60	-55	0	200
	130^{0}C	-0,001	-0,02	-0,02	0,001	-60	-55	0	200
	140^{0}C	0,75	-0,8	-0,8	-0,8 and 1,2	-60	-56	0	200
	150^{0}C	-0,5	-0,6	-0,6	-0,6 and 0,7	-60	-50	0	200
	Unprocessed Latex	0	0	0	0,15 and 0,1	0	0	0	180 200
Second Heating Phase	100^{0}C	0,18	0,22	0,25	0,045	-60	-50	0	200
	110^{0}C	-0,03	0,06	0,62	0,06	-60	-55	0	200
	120^{0}C	0,16	0,018	0,022	0,04	-60	-50	0	200
	130^{0}C	0,006	0,04	0,042	0,06	-60	-58	0	200
	140^{0}C	0	-0,25	-0,25	-0,3 and 2,0	-60	-60	0	175
	150^{0}C	0	0,2	0,3	0,4 and -2,2	-60	-60	0	160
	Unprocessed Latex	0	0	0	0	-60	-55	0	200

4.5 Rheological analysis

Performing a rheological assessment of bio-adhesives primarily aims to determine the relationship between complex viscosity, measured in Pascal-seconds (Pa. s), and angular frequency, determined in radians per second (rad. s^{-1}). The study seeks to deepen understanding of how applied shear stress influences loss modulus (G") and storage modulus (G') and to classify this bio-adhesive material based on its loss and storage moduli, as well as its thermal properties. The rheometer used was an Anton Paar CTD 450 Modular compact MCR302 model.

The technique used in the Rheological testing method is thermal analysis, whereby a controlled shear force is applied to the bio-adhesive material and measured under specific operating conditions as defined in section 3.4.3. Rheological outcomes were obtained from Rheometer thermal tests as raw data. These were for processed bio-adhesive material at 100^{0}C, 110^{0}C, 120^{0}C, 130^{0}C,140^{0}C and 150^{0}C. Two tests were done for each processed bio-adhesive. The data obtained were in Excel spreadsheet format and were used to develop the Complex viscosity versus Angular viscosity curve, Loss Modulus versus shear stress in percentage curve, and Storage Modulus versus shear stress in percentage curve. The rheological thermal testing method, data analysis, and results were executed in accordance with the guidelines of ASTM D7175 and DIN 51810-2 standards.

4.5.1 Rheology, complex viscosity versus angular viscosity curve for bio-adhesive at different temperature parameters

Figure 4.14 shows sample data from a rheometer used to plot the complex viscosity, defined as the ratio of shear stress to shear rate obtained from a dynamic test, versus angular frequency at temperatures of 100^0C, 110^0C, 120^0C, 130^0C, 140^0C and 150^0C. The plotted data indicate that the initial stage is less dependent on angular frequency for bio-adhesives processed at 100^0C, 110^0C, 120^0C, 130^0C and 140^0C. This is due to higher complex viscosities of 150 Pa/s, 96 Pa/s, 125 Pa/s, 103 Pa/s and 70 Pa/s, respectively. This occurs at a very low angular frequency of 0,1 rad/s. However, the bio-adhesive processed at 140^0C is more dependent on angular frequency, as its initial stage records a low complex viscosity of 10 rad/s.

As shown in Figure 4.14, the complex viscosity decreases with increasing angular frequency, indicating a transition from elastic to viscous behavior. This trend is more pronounced at higher angular frequencies, where the material exhibits greater fluid-like characteristics. The data highlight the temperature-dependent nature of the material's viscoelastic properties. A breaking point is at an angular frequency of 0,6 rad/s. This is due to the gap between all bio-adhesive materials. This gap gradually closes once all the curves reach 10 rad/s. This will also indicate a reduction in chemical reactions due to insufficient compounds in the bio-adhesive material.

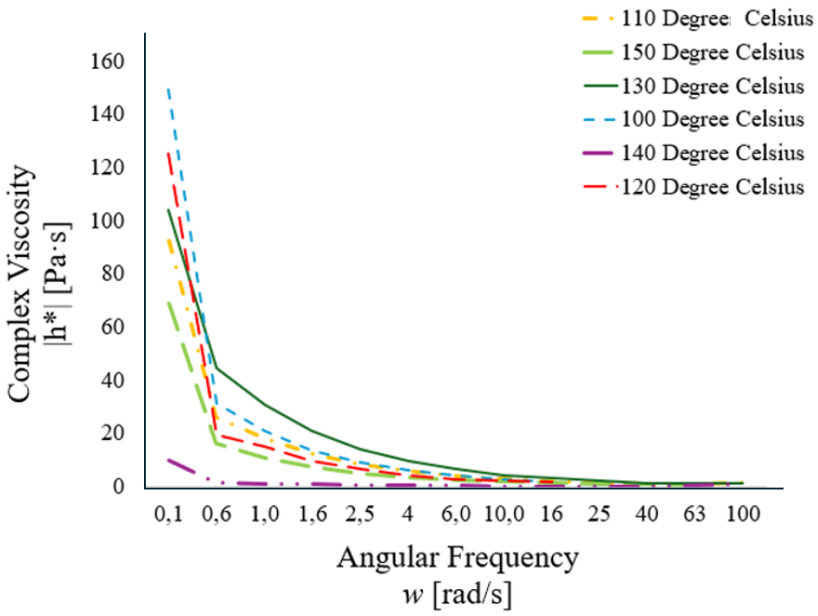


Figure 4. 14 Rheology: complex viscosity versus angular viscosity curve for bio-adhesive at different temperature parameters

From Table 4.3 the processed bio-adhesive processed at 100^0C, 120^0C, 130^0C and 150^0C have higher initial complex viscosity of 150 Pa/s, 125 Pa/s, 103 Pa/s and 70 Pa/s respectively.

Table 4. 3 Rheology: complex viscosity versus angular viscosity performance parameters

Temperature T (^{0}C)	Complex Viscosity (η*) (Pa/s)			Angular Frequency ω (Rad/s)		
	η*(1)	η*(2)	η*(3)	ω (1)	ω (2)	ω (2)
100	150	32	18	0,1	0,6	1,6
110	96	30	18	0,1	0,6	1,6
120	125	20	15	0,1	0,6	1,6
130	103	45	20	0,1	0,6	1,6
140	10	0	0	0,1	0,6	1,6
150	70	18	10	0,1	0,6	1,6

In summary, at low angular frequencies, the bio-adhesive behaves more like a viscous liquid under slow deformation. This behavior indicates strong molecular entanglements or networks that resist flow due to strong molecular interactions. At high frequencies, however, these structures cannot fully rearrange, making the material more elastic and less viscous. This behavior is attributed to the material's resistance to distortion when exposed to rapid oscillatory forces generated by parallel plates during testing [149].

Because of this, this bio-adhesive material has the potential to adapt to environments that also require mechanical stability and adaptability. The viscoelastic properties of bio-adhesives, as gels and pastes, are evident in this way. The graph indicates long-term stability and resistance, shear-thinning behavior, and a rapid drop in viscosity during fast movements. This combination of properties makes the bio-adhesive material versatile and adaptable for various environmental applications, such as biomedical devices and industrial settings, where both durability and adaptability are essential. The material's ability to transition between solid-like and fluid-like states ensures it can perform effectively under different mechanical stresses [150]. In contrast, the 140^{0}C-processed bio-adhesive materials exhibit lower complex viscosity at similar frequencies, show less resistance under similar conditions, and flow more easily.

4.5.2 Rheology, loss modulus versus shear stress in percentage curve for bio-adhesive at different temperature parameters

Figure 4.15 shows data from a rheometer, plotted as loss modulus versus percentage shear stress. A thermal test is performed on bio-adhesive materials processed at 100^{0}C, 110^{0}C, 120^{0}C, 130^{0}C, 140^{0}C, and 150^{0}C. Figure 4.15 shows that at the beginning of the rheometer testing phase, the loss modulus starts at a low value and gradually increases with increasing percentage shear stress. This pattern holds for bio-adhesive materials processed at 1100C, 130^{0}C, 140^{0}C, and 150^{0}C, with initial loss moduli of 10 Pa, 15 Pa, 0 Pa, and 8 Pa, respectively. This is at an initial percentage shear stress of 7 Pa. Figure 4.15 shows that the 140^{0}C-processed bio-adhesive material remained at zero percentage shear stress from 7 to 15,5 Pa.

The loss modulus rapidly increases from 16 Pa to a maximum of 75 Pa at a percentage shear strain of 41 Pa. As the percentage shear stress increases from 7 Pa to 16 Pa, the 110^{0}C-, 130^{0}C, and 150^{0}C processed bio-adhesives show a small increase in loss modulus. At a percentage shear stress of 16 Pa, the loss modulus rapidly increases until it reaches a maximum of 130 Pa at a percentage shear strain of 41 Pa for the 130^{0}C-processed bio-adhesive. A shear stress of 31

Pa produced a maximum loss modulus of 60 Pa and 35 Pa for bio-adhesives processed at 110^0C and 150^0C, respectively.

Both the 120^0C and 100^0C bio-adhesive materials begin at much higher loss modulus, 120 Pa and 48 Pa, respectively. The bio-adhesive processed at 100^0C shows a slight increase in loss modulus from 48 Pa to 65 Pa as the percentage shear stress increases from 7 Pa to 15,5 Pa, respectively. This bio-adhesive gradually increases until reaching a maximum loss modulus of 180 Pa.

A bio-adhesive processed at 120^0C exhibits a completely different response, starting with a loss modulus of 120 Pa, dropping to 50 Pa at a percentage shear stress of 11 Pa, then gradually increasing to a maximum loss modulus of 180 Pa at 41 Pa percentage shear stress.

For all processed bio-adhesive materials, the loss modulus increases sharply at a percentage shear stress of 19 Pa, 20 Pa, and 31 Pa. This could be due to increased stress, which shifts the molecular structure of the bio-adhesive. This could lead to higher deformation resistance. This sharp increase in loss modulus suggests that the material at these different points is experiencing a similar proportion of shear stress. This behavior indicates a transition in the material's structural properties, potentially enhancing its ability to withstand mechanical stress.

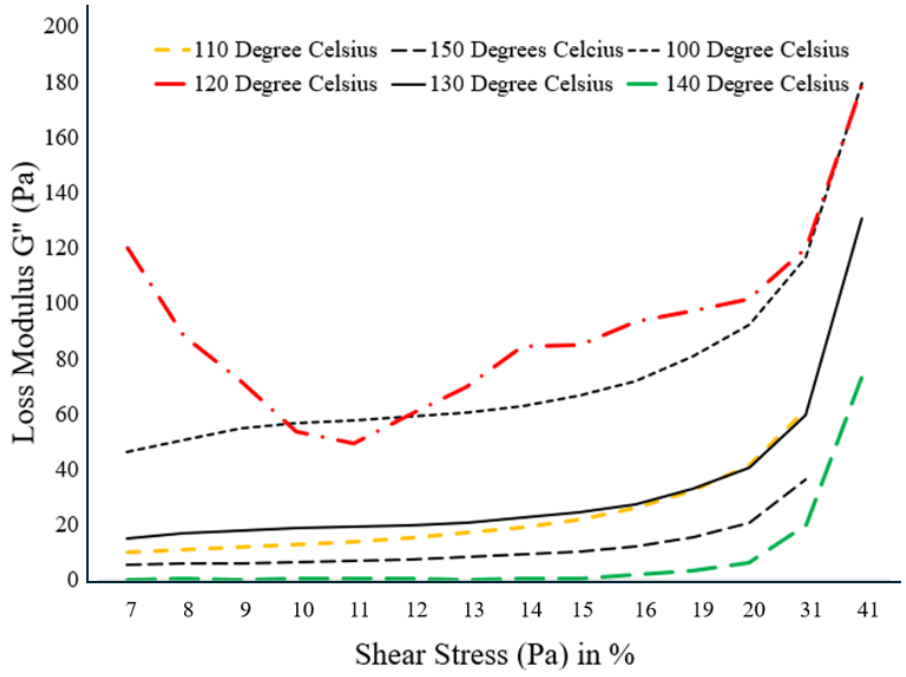


Figure 4. 15 Rheology: loss modulus versus shear stress in percentage curve for bio-adhesive at different temperature parameters

According to Table 4.4, the 120^0C bio-adhesive material initially exhibits a high loss modulus during deformation. In this situation, a large amount of energy is dissipated as heat, indicating that the material has a greater degree of viscosity. Under initial furnace conditions of low temperature, this indicates the presence of a bio-adhesive material with a strong internal structure.

Table 4. 4 Rheology: loss modulus versus % shear stress performance parameters

T (^{0}C)	Loss Modulus (G") (Pa)						Shear stress (τ) (Pa) %					
	(G") 1	(G") 2	(G") 3	(G") 4	(G") 5	(G") 6	τ (1)	τ (2)	τ (3)	τ (4)	τ (5)	τ (6)
100	48	60	60	95	119	180	7	11	13	20	31	41
110	10	16	19	40	60	-	7	11	13	20	31	41
120	120	50	72	100	120	180	7	11	13	20	31	41
130	15	20	21	40	60	130	7	11	13	20	31	41
140	0	0	0	8	20	92	7	11	13	20	31	41
150	9	9	10	20	38	-	7	11	13	20	31	41

This bio-adhesive material stores and releases energy because of its highly entangled structure. This behavior is characteristic of bio-adhesive materials with complex molecular structures. As the material is deformed, these entanglements resist applied shear stress, leading to significant energy dissipation [151]. At 120^{0}C, the bio-adhesive material undergoes a transition phase as the furnace temperature rises. This occurs when molecular chains become more mobile and flow more easily, reducing internal friction and dissipating energy for a short period of time. A new mechanism for dissipating energy emerges because of the subsequent rapid increase. In most cases, this happens when the material enters a phase above its glass-transition temperature. Because the bio-adhesive structural state is more flexible, more energy can be dissipated through viscous flow.

Initially, the remaining processed bio-adhesives (100^{0}C, 130^{0}C, 140^{0}C, and 150^{0}C) show a low loss modulus that gradually increases, indicating that they behave more like an elastic solid with minor energy dissipation. This behavior indicates that bio-adhesives retain their structural integrity under varying temperature conditions, with only minor energy losses. Once external conditions, such as temperature, change, the bio-adhesive material transitions into a state of increased fluidity, resulting in greater energy loss [152]. This transition phase is maintained until the maximum loss modulus is reached.

4.5.3 Rheology, storage modulus versus shear stress in percentage curve for bio-adhesive at different temperature parameters

Figure 4.16 shows data from a rheometer, plotted as storage modulus versus percentage shear stress. Thermal tests were performed on bio-adhesive materials processed at 100^{0}C, 110^{0}C, 120^{0}C, 130^{0}C, 140^{0}C, and 150^{0}C.

As illustrated in Figure 4.16, both 120^{0}C and 100^{0}C bio-adhesive materials begin with much higher storage modulus, 60 Pa and 39 Pa, respectively. A bio-adhesive processed at 100^{0}C has a gradually increasing storage modulus, from 39 Pa to 124 Pa, as the percentage shear stress increases from 6 Pa to 19 Pa. Then, a slight decrease in storage modulus from 19 Pa to 20 Pa percentage of shear strain. This is followed by a rapid decrease in storage modulus from 20 Pa to 41 Pa percentage of shear strain. In comparison to other processed bio-adhesives, 100^{0}C bio-adhesives have a maximum storage modulus of 124 Pa. A bio-adhesive processed at 120^{0}C has a completely different reaction, starting at a storage modulus of 60 Pa. It drops to 35 Pa and 30

Pa at a percentage shear stress of 7 Pa and 10,5 Pa, respectively. Then gradually increases until it reaches a maximum storage modulus of 52 Pa at 25 percentage shear stress.

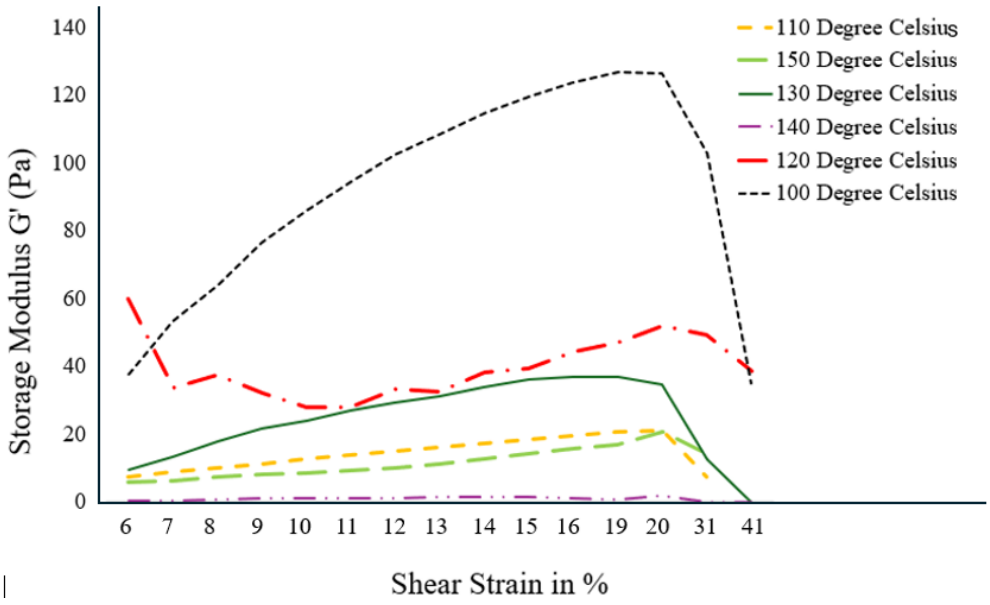


Figure 4. 16 Rheology: storage modulus versus shear stress in percentage curve for bio-adhesive at different temperature parameters

Figure 4.17 shows that at the beginning of the rheometer testing phase, the relative storage modulus starts at a low value and gradually increases as the shear stress percentage increases. This pattern holds for bio-adhesive materials processed at temperatures of 100^0C, 110^0C, 130^0C, 140^0C and 150^0C, with initial storage moduli of 39 Pa, 7,5 Pa, 9 Pa, 0 Pa, and 6 Pa, respectively. This is at an initial percentage shear stress of 6 Pa.

As illustrated in Figure 4.17, the storage modulus of these 110^0C and 150^0C processed bio-adhesives increases as the percentage shear stress increases from 6 Pa to 20 Pa. The maximum storage modulus was achieved at 22 Pa and 20 Pa, respectively. At a percentage shear stress of 20 Pa, the storage modulus rapidly decreases to 7 Pa and 15 Pa, respectively. The storage modulus of these 110^0C and 150^0C processed bio-adhesives increases as the percentage shear stress increases from 6 Pa to 20 Pa.

The maximum storage modulus was achieved at 22 Pa and 20 Pa, respectively. At a percentage shear stress of 20 Pa, the storage modulus rapidly decreased to 7 Pa and 15 Pa, respectively. In the 130^0C-processed bio-adhesive, the storage modulus increases as percentage shear stress increases from 6 Pa to 16 Pa, reaching a maximum of 35 Pa that remains constant up to 19 Pa. A slight decrease in storage modulus occurs between 19 and 20 Pa, followed by a sharp decrease thereafter. In Figure 4.17 above, the 140^0C-processed bio-adhesive material maintained zero at percentage shear stresses of 6 Pa, 19 Pa, and 31 to 41 Pa. The peak storage modulus of this bio-adhesive was 2 Pa at a percentage shear stress of 20 Pa. Throughout the testing process, it maintained a 1 Pa storage modulus.

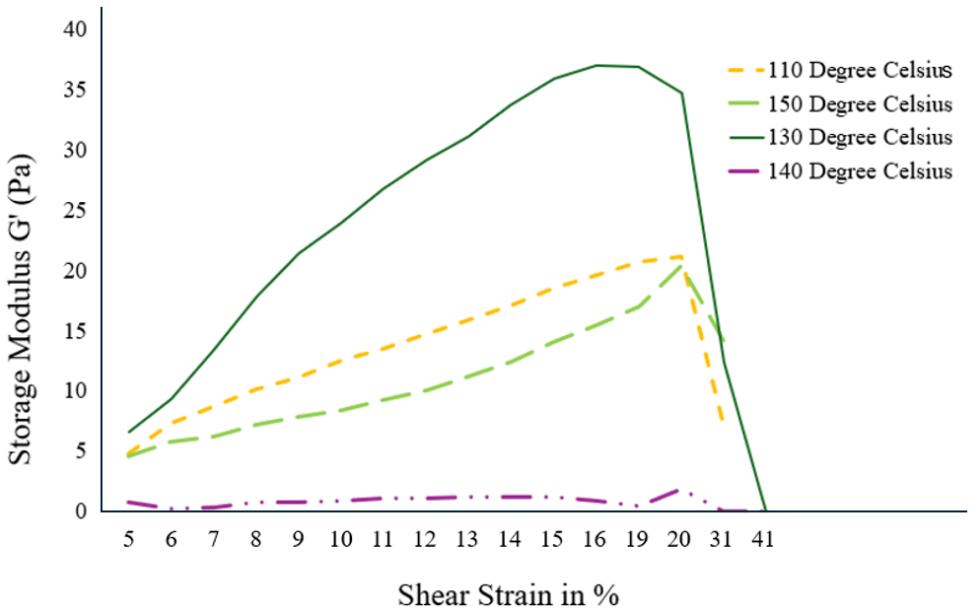


Figure 4. 17 Rheology analysis: storage modulus versus shear stress in percentage curve for bio-adhesive at different temperature parameters (110^0C, 130^0C, 140^0C and 150^0C)

Table 4.5 presents the initial and maximum storage moduli for all processed bio-adhesive materials. According to Table 4.5, the 100^0C bio-adhesive is the only material to reach a maximum storage modulus of 120 PA, compared with the other processed bio-adhesive materials. Its high maximum storage modulus indicates resistance to deformation and enhanced structural integrity under applied stress [153]. These properties make this bio-adhesive material suitable for applications subjected to significant mechanical stress.

Table 4. 5 Rheology: loss modulus versus % shear stress performance parameters

T (^{0}C)	Storage Modulus (G') (Pa)						Shear stress (τ) (Pa) %					
	(G') 1	(G') 2	(G') 3	(G') 4	(G') 5	(G') 6	τ (1)	τ (2)	τ (3)	τ (4)	τ (5)	τ (6)
100	39	84	122	124	100	40	6	10	16	20	31	41
110	7,5	12,5	19	22	7	-	6	10	16	20	31	41
120	60	30	42	52	50	40	6	10	16	20	31	41
130	9	24	37	35	13	0	6	10	16	20	31	41
140	0	1	1	2	0	-	6	10	16	20	31	41
150	6	8	15	20	15	-	6	10	16	20	31	41

From Table 4.5, the other bio-adhesive materials (110^0C, 130^0C, and 140^0C) exhibited a medium-to-low storage modulus of between 20 Pa and 35 Pa, so that these can be classified as flexible with low energy storage capacity. This bio-adhesive material is ideal for applications requiring a greater degree of flexibility and less resistance to deformation. The 120^0C and 140^0C indicate a nearly linear graph, which indicates that the material state remains constant throughout the testing process. Other changing factors, like furnace temperature, have little effect on these bio-adhesives. Compared to the 140^0C bio-adhesive's energy storage capabilities, the 120^0C material is more flexible, with medium-to-low energy storage capability.

The 140^0C material exhibits the lowest reactivity during testing. This material did not change much, as it remained at a zero-storage modulus most of the time.

4.6 Experimental results

The specimens were prepared under similar processing conditions, which are the processing temperature and curing conditions of the bio-adhesive material. The curing process was carried out at a specific temperature to ensure uniformity in material properties. The experimental testing procedures were conducted using a tensile testing machine for T-Peel and a single-lap shear test performed with a U-Stretch Mechanical Test System. The specimens for both single-lap shear and T-Peel tests were paper-to-paper substrates joined with a processed bio-adhesive, and, for uniformity, all paper-to-paper specimen sizes were held constant. Data received from mechanical testing approaches were used to investigate the impact of temperature on bio-adhesives. This section includes the analysis and discussion of experimental results.

4.7 Single-lap-shear tests

Raw data were obtained from single-lap shear tests executed on the tensile test machine. Each bio-adhesive processing temperature parameter, $1,00^0$C, 110^0C, 120^0C, 130^0C, 140^0C and 150^0C, three tests were conducted. The results in this section are based on only three samples per bio-adhesive processing temperature and use the Taguchi analytical method.

Based on the raw experimental data, tensile stress, tensile displacement, and ultimate force were obtained. Based on these data, the stress-strain graph was presented, the average ultimate tensile and elastic modulus stresses were calculated, the maximum tensile force was determined, and the Taguchi analytical method was used to assess the impact of bio-adhesive processing. This section analyzes and discusses the experimental results of single-lap shear tests.

Figure 4.18 indicates that the stress-strain curves of all six processed bio-adhesive materials go through a phase of elastic deformation, a phase of plastic deformation, and finally a failure fracture stage. This progression indicates the material's ability to withstand applied stress before failure and helps in providing an understanding of the bio-adhesive material’s key mechanical property. The elastic phase represents reversible deformation, while plastic deformation marks permanent changes. Finally, the ultimate fracture stage marks the point at which the material can no longer withstand the applied load, resulting in complete failure. As a result of this stress-strain curve, the ultimate tensile stress can be extracted, as well as the elastic modulus, and these outcomes are shown in Table 4.6.

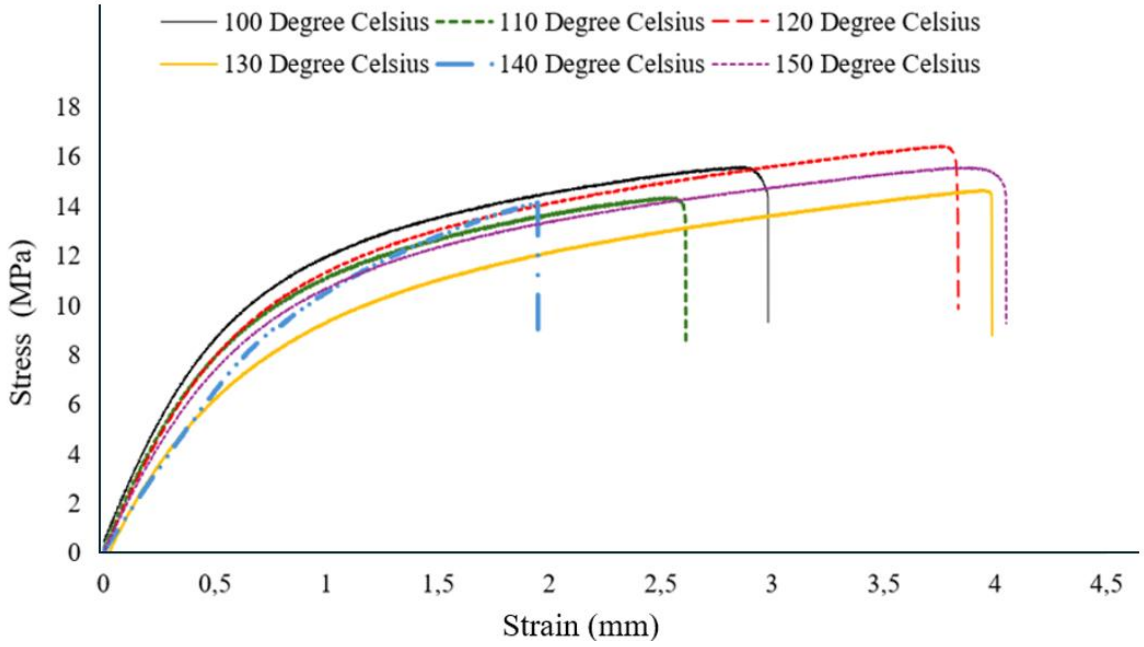


Figure 4. 18 Stress-strain curve for paper-to-paper specimens joined by process bio-adhesive (Test 1)

Table 4.6 shows the Elastic Modulus of the six processed bio-adhesives for single-lap shear tests 1, 2, and 3. At the maximum point in the elastic phase, the stress-strain curve was utilized to find the elastic modulus. The method is elaborated in Appendix A. Three examinations per phase were used to calculate the average elastic modulus. Based on Table 4.6, the 110^0C processed bio-adhesive has the highest average elastic modulus, 17,333 MPa, followed by the 100^0C and 120^0C processed bio-adhesives. This observation further indicates that the bio-adhesive material processed at low temperatures has a higher average elastic modulus.

Table 4. 6 Single-lap shear test elastic modulus and ultimate tensile strength for Test 1, Test 2 & Test 3

Sample Number	Bio Adhesive Processing Temperature (^{0}C)	Elastic Modulus E (MPa)			Elastic Modulus Average MPa	Ultimate Tensile Strength (UTS)			UTS Average MPa
		Sample Test 1	Sample Test 2	Sample Test 3		Sample Test 1	Sample Test 2	Sample Test 3	
1	100	20,535	16,734	12,821	16,697	15,47	14,895	14,788	15,051
2	110	18,939	15,559	17,502	17,333	14,169	15,163	15,652	14,995
3	120	17,491	14,187	16,994	16,224	16,322	13,745	15,672	15,246
4	130	12,494	14,153	14,676	13,774	14,525	14,202	16,444	15,057
5	140	13,038	13,951	14,766	13,918	14,082	17,816	17,505	16,468
6	150	18,874	12,606	9,423	13,634	15,241	14,069	14,322	14,544

Compared to the previous study [154], which tested bio-adhesive through an experimental approach, using single-lap shear to evaluate adhesion performance. The shear strength produced in the study [154] was 0,5 MPa, which was less than the highest average elastic modulus of 17,333 MPa achieved in this paper. The adhesive performs well compared to many commercial bio-adhesives.

This means that bio-adhesives processed within this temperature range tend to be rigid and have a greater capacity to withstand high mechanical loads. However, rigid materials range from 1

MPa to above 10 MPa, and flexible materials range from 0,1 to 1 MPa [155]. This implies that even the 150^0C bio-adhesive material possesses some element of rigid properties.

From Table 4.6, the ultimate tensile strength was determined from the stress-strain curve at the maximum point for all six processed bio-adhesives, representing the maximum stress they can withstand before the fracture stage began. This was also determined for three tests per temperature parameter, and the average ultimate tensile strength was then calculated. The results show that the 150^0C processed bio-adhesive still had the lowest UTS of 14,544 MPa, which is comparable to the average Elastic Modulus.

As shown in Figure 4.19, the average UTS and Elastic Modulus of bio-adhesives vary with processing temperature. The average UTS of bio-adhesives processed at lower temperatures (100^0C, 110^0C, 120^0C, and 130^0C) is nearly the same, forming an almost straight line that reaches about 15 MPa. In contrast, the Elastic Modulus is highest at 100^0C, 110^0C, and 120^0C for the first three processing temperatures. These lower-temperature-processed bio-adhesives have a high elastic modulus and a low UTS, making them stiff but weak. Although they can withstand small loads before breaking due to their high stiffness, they are not robust enough to handle larger loads. They are less effective in applications requiring significant mechanical strength. However, their high stiffness can be advantageous in scenarios where maintaining structural integrity under low stress is required [156].

The last three processing temperatures (130^0C, 140^0C, and 150^0C) are the opposite, with the highest being UTS and the lowest being Elastic Modulus. This combination of properties describes a bio-adhesive that is both highly durable and flexible. This makes it ideal for applications where the bio-adhesive must withstand significant stress or strain without breaking or losing its bond. This is because it has a low modulus and high stretchability, and it can stretch considerably and absorb significant energy without permanently breaking because of its high UTS capabilities. With bio-adhesive UTS and Elastic Modulus results analyzed and discussed, the next step is to understand the impact of applied force on the paper-to-paper specimen bonded with bio-adhesive material.

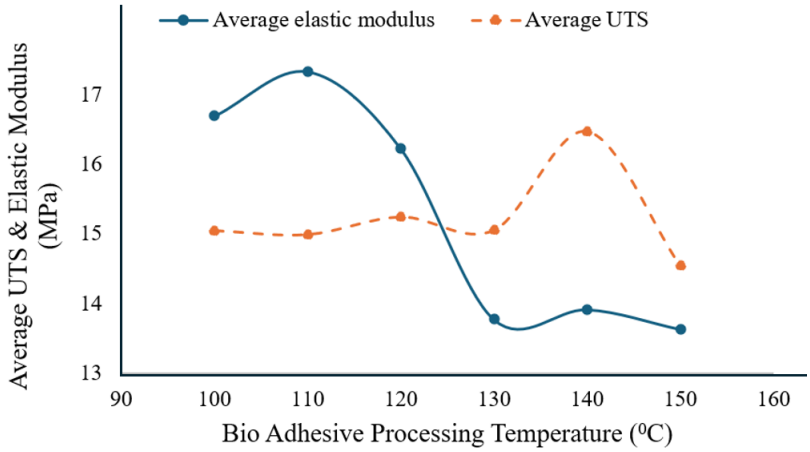


Figure 4. 19 UTS and varying elastic modulus of processed bio-adhesive materials processed at 100^0C, 110^0C, 120^0C, 130^0C, 140^0C & 150^0C

Figure 4.20 was developed using data obtained from a tensile test as shown in Table 4.7. These data were for six processed bio-adhesives for single-lap shear tests 1, 2, and 3. From these data, the force-versus-strain curve was produced and is shown in Appendix B. From this curve, the maximum Tensile Force was determined. Table 4.7 shows that the average Maximum Tensile Force was calculated from the three tests per phase per temperature parameter.

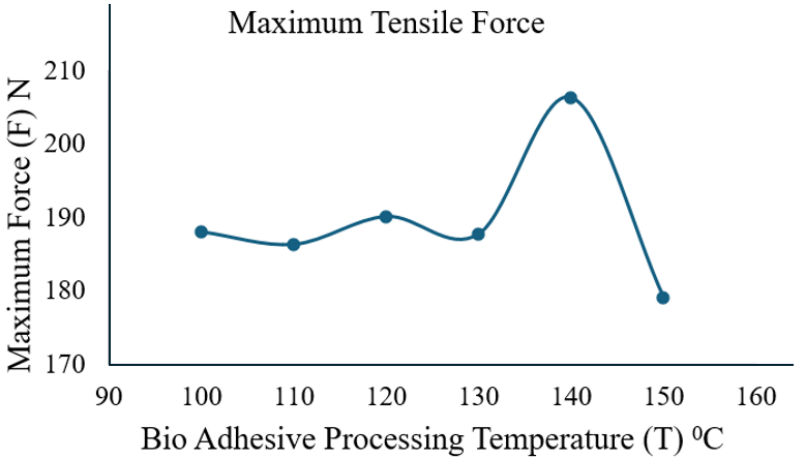


Figure 4. 20 UTS and modulus of elasticity of processed bio-adhesive materials processed at 100^0C, 110^0C, 120^0C, 130^0C, 140^0C & 150^0C

Referring to Table 4.7 and Figure 4.20, the 140^0C-processed bio-adhesive has the highest average maximum tensile force of 206,33 N, while the lowest is the bio-adhesive material processed at 110^0C, achieving 186,33 N. This provides further validation that higher-temperature-processed bio-adhesive material with higher UTS and lower Elastic Modulus can endure significant stress, strain, and applied Force without breaking or losing its bond [157].

The impact fatigue life and load-level analyses, along with their S-N data and results, show that four joint configurations exhibit different fatigue behavior under impact fatigue conditions [158]. The results reveal distinct trends in fatigue life as a function of applied load levels. Fatigue life was reported on a logarithmic scale to better capture the data distribution. The reference substrate, when joined with bio-adhesive materials, showed the lowest load level. This was followed by a rapid decline in performance as the load increased.

This steep slope indicates a pronounced sensitivity to load variations, emphasizing weak structural resistance of adhesive joints under cyclic loading. This behavior contrasts with the study in this paper, which presented steady linear adhesive behavior at an average force of 185 N, as shown in Figure 4.20, and a sudden maximum peak force of 206,33 N. This indicated relatively steady adhesive life at higher average load levels, suggesting consistent and improved load resistance.

Table 4. 7 Single-lap shear: average maximum force (F) and strain (mm)

Sample Number	Bio Adhesive Processing Temperature (^{0}C)	Maximum Force (N)			Max Force Average N	Strain at Max Force (mm/mm)			Strain at Max F Average (mm/mm)
		Sample Test 1	Sample Test 2	Sample Test 3		Sample Test 1	Sample Test 2	Sample Test 3	
1	100	193,3	185,4	185,4	188,03	2,895	3,564	4,167	3,54
2	110	177,4	189,7	191,9	186,33	2,556	3,518	3,494	3,19
3	120	202,8	170,1	197,5	190,13	3,807	2,786	4,244	3,61
4	130	180,7	178,4	204,2	187,77	3,984	3,769	5,197	4,32
5	140	175,8	222,7	220,5	206,33	1,933	3,831	4,685	3,48
6	150	190,4	170	177	179,13	4,008	3,903	4,199	4,04

As the investigated parameters are the processing temperatures of bio-adhesive materials, the signal-to-noise ratio was used to determine which processing temperature influences the improvement in the elastic modulus of bio-adhesive materials. Taguchi's method was used with Equation 4.1, which introduces a processing loss function in the experimental design.

$$\eta = -10ln_{10}\frac{1}{n}\sum_{i=1}^{n}\frac{1}{y_1^2} \qquad 4.\ 1$$

Where:
S/N is the signal-to-noise ratio,

n is the number of observations on the product

y is the respective character in the elastic modulus

E is the elastic modulus

The average elastic modulus per test and temperature parameter, as shown in Table 4.6, was used to generate the signal-to-noise ratio as in Table 4.8. At levels 1, 2, 3, 4, 5, and 6, the average elastic modulus of processed bio-adhesive material at different temperature parameters (100^{0}C, 110^{0}C, 120^{0}C, 130^{0}C, 140^{0}C and 150^{0}C) is presented as a signal-to-noise ratio. Equation 4.1 calculates the noise-to-signal ratio for each temperature parameter. Appendix C provides further details on how these calculations were undertaken and shows the resulting results of the signal-to-noise ratio values. Looking at Table 4.8, the highest and lowest average elastic modulus are 17,333 MPa and 13,634 MPa. This also corresponds to signal-to-noise ratios of 24,69 and 21,66, respectively. In each parameter, the difference between high and low signal-to-noise ratios represents the ranking of that parameter's impact.

(Emax-Emin/Emin) X 100% = Percentage impact (S/N) 4. 2

(17,333 - 13,634 / 13,634) X 100% = 27,13%

Using Equation 4.2, the percentage impact of bio-adhesive processing temperature on the elastic modulus can be calculated. By substituting the maximum (E_{max}) and minimum (E_{min}) average elastic modulus into Equation 4.2, 27,13% is calculated as the percentage impact. According to the Taguchi method, the bio-adhesive material processed at 110^{0}C is the highest-performing because it has the highest signal-to-noise ratio. As a result, bio-adhesive materials processed at 110^{0}C perform 27,13% better than those processed at 150^{0}C. In this Taguchi method approach,

the ranking will be 1, as processing temperature is the only parameter that influences the average bio-adhesive elastic modulus.

Table 4. 8 Single-lap shear test: signal-to-noise ratio (S/N)

Level	Bio Adhesive Processing Temperature (^{0}C)	Elastic Modulus E (MPa)			Elastic Modulus Average MPa	$S/N = -10Log_{10}\frac{1}{3}\sum_{i=1}^{3}\frac{1}{E_1^2}$
		Sample Test 1	Sample Test 2	Sample Test 3		
1	100	20,535	16,734	12,821	16,697	23,97
2	110	18,939	15,559	17,502	17,333	24,69
3	120	17,491	14,187	16,994	16,224	24,09
4	130	12,494	14,153	14,676	13,774	22,72
5	140	13,038	13,951	14,766	13,918	22,84
6	150	18,874	12,606	9,423	13,634	21,68
					Difference	24,69 - 21,68 = 3,01
					Rank	1 (non-comparable)

In summary, the single-lap shear test approach provided sufficient data to demonstrate that bio-adhesives prepared at low temperatures tend to have a higher overall elastic modulus. This illustrates a potential for rigid mechanical properties. It was further proven that high-temperature-processed bio-adhesive materials, in contrast, have a lower average elastic modulus, indicating more flexible mechanical properties. This was demonstrated using stress-strain curves and the Taguchi analytical method for all three tests per temperature parameter. As a result, bio-adhesive material processed at higher temperatures (140^{0}C) has a higher UTS and force, and a lower average elastic modulus. This bio-adhesive has both high durability and flexible mechanical properties.

4.8 T-Peel test

U-Stretch Mechanical Test System was used to perform T-Peel tests. The test was conducted on a paper-to-paper specimen bonded with a bio-adhesive processed at 100^{0}C, 110^{0}C, 120^{0}C, 130^{0}C, 140^{0}C, and 150^{0}C. This section's results are based on three samples per bio-adhesive processing temperature, as well as the Taguchi analytical method, showing the results of the T-Peel test, from which the peeling force (F) in Newtons (N), the rate of time in seconds (s), and the peeling displacement in millimeters (mm) are obtained.

Based on these results, the average peeling force and maximum peeling strength could be calculated. Peel strength is calculated by dividing peeling load by peeling displacement, and Newtons per meter (N/m) is the unit of peel strength. The average peel force is calculated by adding the peel forces of tests 1, 2, and 3 and dividing the total by 3. Test 1, 2, and 3 results are shown as force-versus-time curves in Figure 4.21 (test 1) and shown in Appendix D. The Taguchi analytical method was used to determine the impact of bio-adhesive processing. This section analyses and discusses the experimental results of the T-Peel test.

Figure 4.21 shows that the maximum T-Peel force achieved in test 1 was 10,88 N at a recorded time of 17.31 s on the first circle, which is for the 140^{0}C-processed bio-adhesives. The

maximum T-Peel force for subsequent circles showed slight variations, with an average force of 6,5 N across all five test cycles. The recorded peak force times also remained within a narrow range, confirming the testing procedure's repeatability.

In this paper, the maximum peel force is similar to the average maximum peel force of 11,8 N. In a similar study using a different setup, such as the Y-peel test, an adhesion strength increase of 23,8 N [5]. As a result, the setup, strains, and angles used on adhesive materials can cause differences in the maximum values achieved during the experimental process. The Y-peel value gives higher results because the tails of the samples are already under mechanical stress due to their fixation method [5]. However, in this study, the T-peel test was considered primarily because it is the most accurate and realistic way to isolate the bond strength between two flexible materials. Unlike other configurations, it prevents rigid substrate biases and measures pure progressive tensile separation along a changing, symmetrical plane [159].

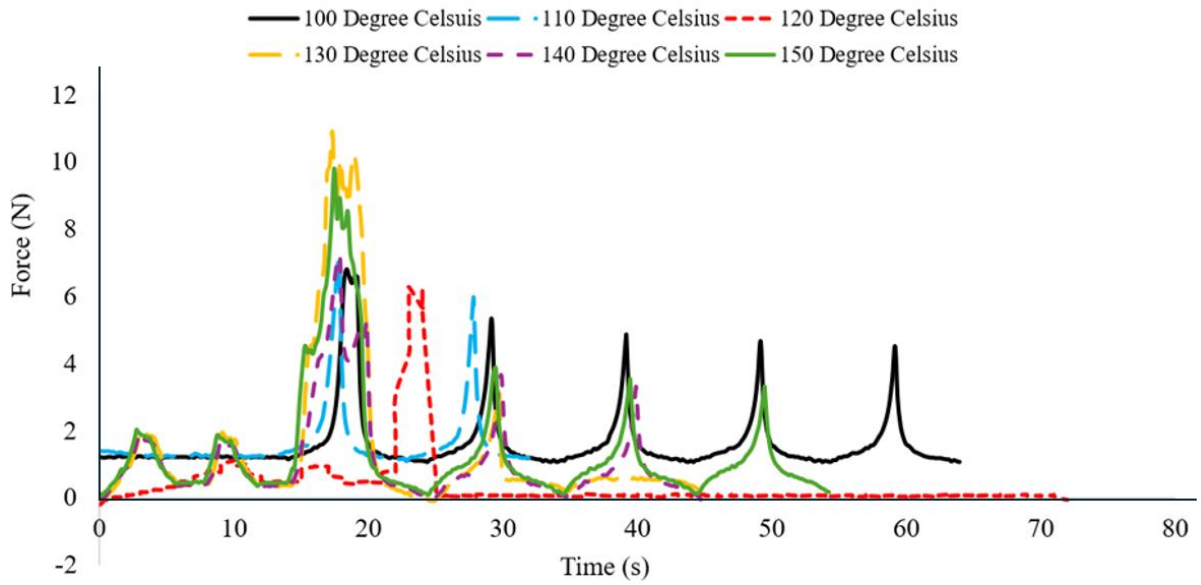


Figure 4. 21 T-Peel test force versus time curve (Test 1 at 100^0C, 110^0C, 120^0C, 130^0C, 140^0C and 150^0C)

Figure 4.22 shows the peel arm displacement-time curve. As with the force-versus-time curve discussed, these results are based on the same number of phases and circles. As shown in Figure 4.22, the maximum displacement occurs in the 120^0C-processed bio-adhesive material, reaching 22 mm at 27 s. The displacements at 100^0C, 130^0C, 140^0C and 150^0C follow similar patterns, with maximum displacements of 17,999 mm. By comparison, 110^0C reaches the lowest peak of 13,999 mm.

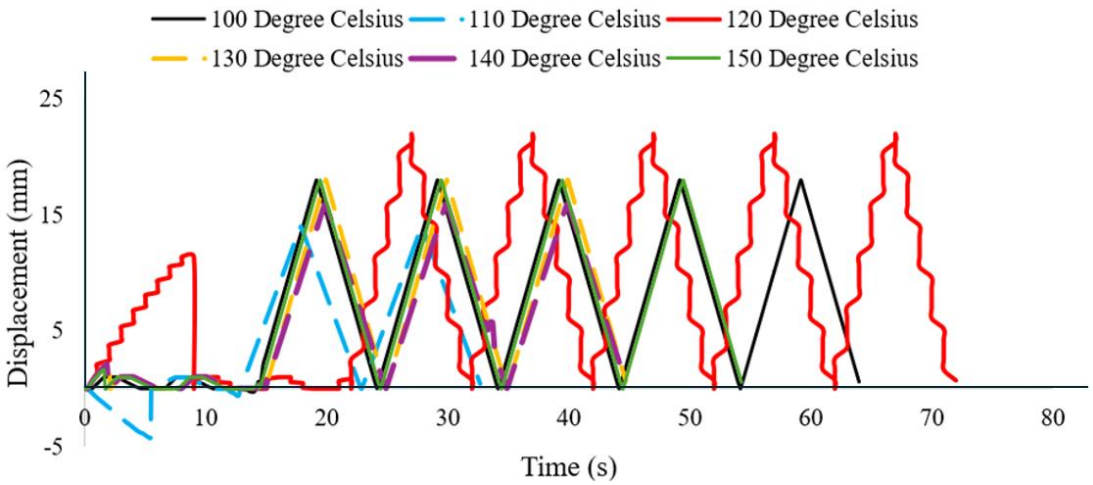


Figure 4. 22 T-Peel test peel displacement versus time curve (Test 1 at 100^{0}C, 110^{0}C, 120^{0}C, 130^{0}C, 140^{0}C and 150^{0}C)

Table 4.9 indicates the average peeling forces and peel displacement for tests 1, 2, and 3, across all the bio-adhesive processing temperature parameters. The average maximum peeling force is at a processing temperature of 130^{0}C, with 140^{0}C being slightly the second- highest. It can further be observed that the average displacement is at 130^{0}C and 150^{0}C, but the 140^{0}C-processed bio-adhesive is still the second greatest. As elaborated in Table 4.9, average peeling forces and peel displacements are calculated for all bio-adhesive processing temperatures. The average maximum peeling force is at 130^{0}C, with 140^{0}C coming in second.

This suggests that bio-adhesive properties are influenced by processing temperature, with 130^{0}C showing superior performance in terms of both force and displacement. To understand the impact of temperature on the processed bio-adhesive material, the Taguchi analytical method is used.

Table 4. 9 T-Peel test: average peel force and peel displacement for Test 1, Test 2 & Test 3

Sample Number	Bio Adhesive Processing Temperature (^{0}C)	Maximum Peeling Force (N)			Peeling Force Average (N)	Maximum Peel Displacement (L) (mm)			Average L (mm)
		Sample Test 1	Sample Test 2	Sample Test 3		Sample Test 1	Sample Test 2	Sample Test 3	
1	100	6,59	10,69	11,68	9,66	17,998	19,228	21,99	19,74
2	110	7,19	8,66	11,31	9,05	13,999	19,998	21,153	18,38
3	120	6,22	10,36	9,335	8,64	22,000	20,22	13,2	18,47
4	130	10,79	10,322	11,422	10,84	17,999	22,00	21,998	20,67
5	140	10,88	9,762	9,912	10,19	17,999	21,999	21,163	20,39
6	150	9,81	8,14	9,022	8,99	17,998	21,999	21,999	20,67

Using Taguchi's method with Equation 4.1 from Section 4.3.1. Where n is the number of observations on the products, S/N is the signal-to-noise ratio, y is the respective characteristic of peel strength, and P is peel strength. Bio-adhesive material processing temperatures were investigated to determine which temperature improved peel strength. In this case, peel strength was derived from the peel force divided by displacement. This was done at each level and temperature parameter, and for each test. These calculations are shown in Appendix F. For example, at 100^{0}C the peel force at level 1 was 6,596 N divided by the peel displacement of

0,018 m, resulting in 366,43 N/m of peel strength. Equation 4.1 calculates the noise-to-signal ratio for each temperature parameter. A detailed explanation of how these calculations were carried out can be found in Appendix G, along with the results of the signal-to-noise ratio measurements.

Table 4.10 indicates that the highest average peel strength is 529,22 N/m and the lowest is 441,71 N/m. Furthermore, these correspond to 54,34 and 52,56, respectively, for the signal-to-noise ratio. The difference between a high and low signal-to-noise ratio represents the impact of each parameter.

The influence of bio-adhesive processing temperature on peel strength can be calculated using Equation 4.2 from section 4.3.1. Substituting the maximum (*P*max) and minimum (*P*min) average Peel Strengths into Equation 4.2 results in 19,81%, which is calculated as the impact percentage.

529,22 – 441,71 / 441,71) X 100% = 19,81%

A bio-adhesive prepared at 130^0C using the Taguchi method exhibits the highest performance. This is because it has the highest signal-to-noise ratio. A bio-adhesive material processed at 130^0C performs 19,81% better than one processed at 150^0C. Based on the Taguchi method, the ranking will be 1 in this case since processing temperature is the only factor influencing the average peel strength of bio-adhesives.

Table 4. 10 T-Peel test: signal-to-noise ratio (S/N)

Level	Bio Adhesive Processing Temperature (^{0}C)	(*P*) Peel Strength (N/m)			Peel Strength Average (N/m)	$S/N = -10Log_{10}\frac{1}{3}\sum_{i=1}^{3}\frac{1}{P_1^2}$
		Sample Test 1	Sample Test 2	Sample Test 3		
1	100	366,43	555,96	531,15	484,51	53,24
2	110	513,75	433,04	534,68	493,82	53,76
3	120	282,82	512,36	707,20	500,79	52,14
4	130	599,26	469,18	519,23	529,22	54,34
5	140	604,70	443,75	468,36	505,60	53,85
6	150	545,01	370,02	410,11	441,71	52,56
					Difference	55,2 – 52,14 = 2,64
					Rank	(non-comparable)

In summary, Figure 4.23 shows that bio-adhesives processed at lower temperatures possess a minimum average peel force, while higher processing temperatures show a much lower average peeling force. As previously stated, the 130^0C material has a much higher average peeling strength. These findings suggest that processing temperature significantly influences the mechanical properties of the bio-adhesive, with higher temperatures generally improving displacement characteristics. However, additional examinations are needed to determine the underlying components contributing to these differences and their implications for practical applications.

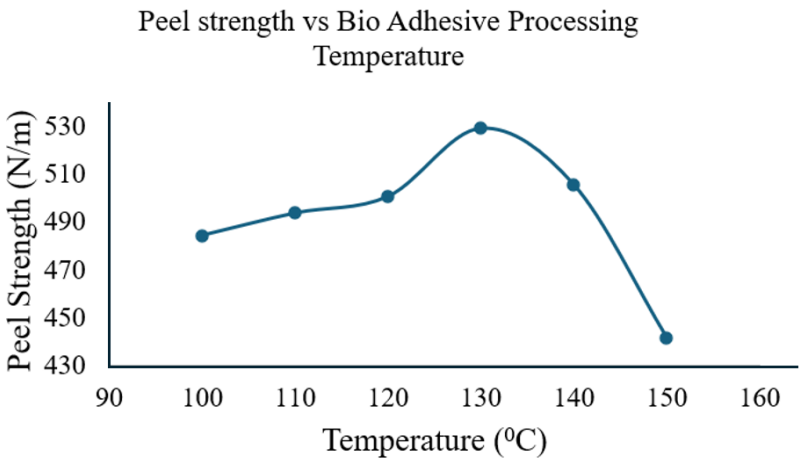


Figure 4. 23 T-Peel test: average peel strength versus bio-adhesive processing temperature

Furthermore, an increase in force and greater displacement generally indicate a stronger and tougher adhesive bond. Higher performance forces indicate higher debonding resistance properties, and greater displacement indicates the bond's ability to stretch without breaking. This means that the bio-adhesive can withstand greater stress before failure, and the ability to stretch indicates the material's flexibility and the bio-adhesive's ability to deform and absorb energy during peeling.

CHAPTER FIVE

5. CONCLUSION AND RECOMMENDATIONS

In this paper, a novel initiative was undertaken to establish and quantify the effect of temperature on latex processing, with the intention of producing naturally sourced bio-adhesive materials.

This study mainly focused on the development and evaluation of a thermal, experimentally based approach, and the results were presented and discussed in Chapter 4. The experimental approach was conducted through a single-lap shear test via tensile testing equipment. This was done to investigate bio-adhesive mechanical properties, namely elastic modulus, UTS, and the signal-to-noise ratio. The second experimental approach was carried out using the T-Peel test, and the results were determined by identifying the maximum peeling force and peeling strength.

Thermal examination was used to understand the mass percentage loss through TGA, the heat flow energy via DSC analysis, and the relation among shear rate and shear stress via rheological analysis.

This chapter summarizes the conclusions regarding the temperature parameters that affect the processing of latex into bio-adhesive materials.

5.1 Experimental study

The parameters investigated in the experimental approach were bio-adhesive materials processed at temperatures of 100^0C, 110^0C, 120^0C, 130^0C, 140^0C, and 150^0C. Two experimental approaches were conducted, namely the T-Peel test and a single-lap shear test. For both approaches, the specimens were paper-to-paper bonded using the processed bio-adhesive material. The single-lap shear test and the T-Peel test were executed using tensile testing equipment and a U-Stretch Mechanical Test System, respectively.

The results observed under the experimental approach were analyzed and discussed in detail in Chapter 4. Hence, in Chapter 5, the conclusions drawn from the results are discussed in detail.

5.1.1 The effect of processing temperature on elastic modulus investigated via single-lap shear test

The Taguchi method results indicate that the bio-adhesive material processed at lower temperatures performs 27,13% better than those processed at higher temperatures. The single-lap shear test showed that processing temperature clearly influences the elastic modulus and overall mechanical behavior of the bio-adhesive. The material processed at 110°C produced the highest signal-to-noise ratio of 24,69 and the highest average elastic modulus of 17,333 MPa, indicating superior stiffness, strength, and rigidity. In comparison, the material processed at 150°C had the lowest signal-to-noise ratio of 21,68 and a lower elastic modulus of 13,634 MPa, although it demonstrated greater flexibility and a higher tensile response.

In conclusion, these results indicate enhanced mechanical strength and rigidity at lower bio-adhesive processing temperatures, whereas higher-temperature-processed bio-adhesives exhibit greater mechanical flexibility. Furthermore, the higher-temperature-processed bio-adhesive material, with a lower Elastic Modulus and higher UTS, can withstand significant stress, strain, and applied forces without breaking.

5.1.2 The effect of processing temperature on peeling strength is investigated through T-Peel test results

The T-Peel test confirmed that temperature also strongly affects peeling resistance and bond toughness. The best performance was obtained at 130°C, where the bio-adhesive achieved the highest signal-to-noise ratio of 54,234, the highest average peeling strength of 529,22 N/m, and the highest peeling load of 10,84 N. Although the 150°C material showed a comparable displacement of 20,67 mm, its lower peeling strength of 441,71 N/m and a lower signal-to-noise ratio of 52,36 indicate reduced resistance to debonding compared with the 130°C sample.

These findings indicate that bio-adhesive materials treated at lower to moderate temperatures tend to have a higher average peel force. Conversely, higher processing temperatures result in a lower average peel force. Notably, bio-adhesive processed at 130^0C exhibits a significantly higher average peel strength.

5.2 Summary of mechanical investigations findings

Overall, the results demonstrate that processing temperature is a critical factor governing the mechanical performance of the bio-adhesive. Lower-to-moderate processing temperatures produced the most favorable bonding properties. 110°C was optimal for elastic modulus and rigidity in the single-lap shear test, while 130°C was optimal for peel strength and debonding resistance in the T-peel test. Higher processing temperatures, particularly 150°C, improved flexibility and displacement behavior but reduced stiffness and peel strength. Therefore, the most suitable processing temperature depends on the application. 110°C is preferred when stiffness and shear resistance are important, whereas 130°C is recommended where peel strength and bond toughness are the main requirements.

5.3 Thermal analysis investigations

Three thermal analysis approaches were employed, including TGA, DSC, and rheology. For all thermal approaches, the specimens were raw latex and processed bio-adhesive material. The sample specimens weighed 9 mg, 0,5 mg, and 6 g for TGA, DSC, and rheology, respectively. In addition, for all three thermal analysis approaches, two specimens were prepared and tested for each processing temperature: 100^0C, 110^0C, 120^0C, 130^0C, 140^0C, 150^0C, and unprocessed latex.

5.3.1 The effect of processing temperature on percentage weight loss and percentage weight derivative of processed bio-adhesive material investigated through TGA

Bio-adhesive material processed at 100^0C, 110^0C, 120^0C, 130^0C, and 140^0C. These materials exhibit high thermal stability, with most of the carbon-based decomposition occurring only at furnace temperatures of 350^0C. The peak reactivity, with 75% weight loss, occurs between 260^0C and 350^0C, marking the release of volatile compounds.

Compared with bio-adhesives processed between 100^0C and 140^0C, unprocessed latex shows lower stability, gradually losing weight from the start due to its high moisture content. It reaches its peak reactivity earlier (260^0C–310^0C). Unprocessed latex is most reactive. Upon reaching 260^0C, degradation rates increase significantly up to 310^0C, with a weight percentage loss of 50%. The percentage weight loss results indicate that bio-adhesives processed between 100^0C, and 140^0C required more heat to reach their peak reactive region than unprocessed latex material. Bio-adhesive material is processed at 150^0C. This material is most reactive at very low furnace temperatures (0^0C–100^0C), likely because many chemical reactions were already completed during the high-heat processing stage. This bio-adhesive is the lowest-performing, with an oxidation peak of 0,4 at a furnace temperature of 310^0C.

Bio-adhesive processed at 130^0C is the top performer, with the highest oxidation peak of 1,12 %WD at 320^0C, indicating superior resistance to thermal deformation. The high-peak oxidation temperature is a critical parameter for characterizing bio-adhesive materials, as it determines resistance to deformation under high-temperature conditions.

Thermal analysis of latex-based bio-adhesives shows a strong correlation between processing temperature and thermal stability. Processing temperatures between 100^0C and 140^0C enhance the thermal properties of bio-adhesives by promoting molecular cross-linking and structural stability. The 130^0C parameter represents the ideal balance for creating a heat-resistant bond that withstands extreme furnace conditions. Conversely, processing at 150^0C leads to premature degradation, while unprocessed latex lacks the structural maturity to resist high-temperature environments.

5.3.2 The effect of processing temperature on bio-adhesive's percentage weight loss and percentage weight derivative of processed bio-adhesive material investigated through DSC

The three bio-adhesives 100^0C, 120^0C, and 130^0C exhibited overlapping high heat flows of 0,001 W/g during the cooling endothermic stage. At 120^0C, the second heat stage reached a heat flow of 0,022 W/g. Under DSC thermal analysis, these bio-adhesives showed the lowest thermal performance. These results suggest that they are less thermally active, or "reactive", in terms of energy transitions compared to the 140^0C variant. Hence, they are low-performance: bio-adhesives processed

The 140^0C bio-adhesive exhibits three exothermic stages. The endothermic heat flow begins at -0,75 W/g, continues to -0,8 W/g at 200^0C, gradually overlaps with 1,2 W/g, and reaches -0,9 W/g at transitional temperatures. At -60^0C, the heat flow is -0,25 W/g. The 140^0C processed bio-adhesive demonstrated the highest thermal performance, reaching a maximum exothermic heat flow of 1.2 W/g at 200^0C. It shows significant structural changes and energy release capabilities.

The processing temperature is the primary driver of thermal reactivity in these bio-adhesives. While lower temperatures from 100^0C to 130^0C yield thermally dormant materials, a processing temperature of 140^0C significantly activates the adhesive, delivering the high energy release and structural dynamism required for heat-resistant, high-performance bonding applications.

5.3.3 The effects of processing temperature on viscosity investigated through rheological analysis

Rheology data are provided to clarify how processing temperature affects the material's viscosity and molecular structure.

Complex viscosity and frequency dependence of bio-adhesives processed at 100^0C to 130^0C exhibit high initial complex viscosities ranging from 103 to 150 Pa/s at low angular frequencies of 0.1 rad/s. These materials initially show minimal frequency dependence, suggesting stable molecular networks. In contrast, the 140^0C material is highly frequency-sensitive, showing a rapid drop in viscosity at higher rad/s.

A breaking point occurs at 0.6 rad/s, where the performance gap across processing temperatures begins to close. By 10 rad/s, the curves converge, indicating a depletion of reactive compounds and reduced chemical interaction within the material.

The viscoelastic transition shows that at low frequencies, the adhesive behaves like a viscous liquid, relying on strong molecular entanglements to resist flow. At high frequencies, the material transitions to a more elastic state because the molecular structures cannot rearrange quickly enough to accommodate rapid oscillatory forces.

5.3.4 The effects of processing temperature on loss modulus investigated through rheological analysis

The rheological analysis of the loss modulus across the different processing temperatures reveals distinct patterns in energy dissipation and structural integrity. Bio-adhesives processed at temperatures of 110^0C, 130^0C, 140^0C, and 150^0C generally exhibit low loss moduli of 0 to 15 Pa at the onset of shear stress at 7 Pa. Notably, the 140^0C variant exhibited minimal initial response, maintaining a zero-loss modulus until the shear stress reached 15.5 Pa.

Bio-adhesives processed at temperatures of 100^0C and 120^0C, unlike the others, begin with significantly higher loss modulus values of 48 Pa and 120 Pa, respectively. The 100^0C material shows a steady increase, eventually peaking at 180 Pa.

The 120^0C bio-adhesive exhibits a unique "V-shaped" response. It begins with high energy dissipation, indicating high viscosity and a strong internal structure. It then shows a sharp drop in modulus as molecular chains become mobile, before finally rising to a maximum of 180 Pa as shear stress increases.

This performance indicates that high loss modulus values at lower processing temperatures suggest materials with greater internal friction and resistance to viscous flow. The transition observed at 120^0C highlights a critical phase in which the material shifts from a stable, resistant state to a more mobile fluid state under increasing thermal and mechanical loads.

5.3.5 The effects of processing temperature on storage modulus investigated through rheological analysis

The rheological thermal results for storage modulus reveal a clear hierarchy in the mechanical resistance and internal structure of the bio-adhesives as a function of processing temperature. The 100^0C-processed material is the most robust, with a high storage modulus of 39 Pa and a peak of 124 Pa. This high maximum value indicates optimal rigidity, superior resistance to deformation, and enhanced adhesion properties compared with all other processed bio-adhesives.

The 130^0C processed bio-adhesive variant shows a steady increase in stiffness with increasing shear stress, reaching a plateau of 35 Pa. It maintains this moderate stability until a sharp drop at a shear stress of 20 Pa, marking the limit of elastic recovery. The 140^0C material exhibits the lowest performance, remaining at or near zero storage modulus for most of the test. Its negligible peak of only 2 Pa indicates the least reactive behavior and minimal internal elastic structure in rheological analysis.

Overall, lower processing temperatures, specifically 100^0C, appear to preserve or enhance the elastic networks within the latex-based adhesive, whereas extreme temperatures like 140^0C lead to a near-total loss of storage capacity.

5.4 Summary of thermal investigation findings

Thermal analysis revealed that as the bio-adhesive processing temperature increases, the materials require more energy to react and release chemical compounds. The three thermal analyses showed that increasing the processing temperature enhances the thermal properties of bio-adhesives. The results showed that bio-adhesive processed at 130^0C is the optimal "all-rounder" for thermal stability and heat resistance, whereas 140^0C is required for maximum reactive energy release and chemical dynamism. Bio-adhesive processed at 100^0C is ideal only if maximum mechanical strength and rigidity are priorities. By contrast, material processed above 140^0C, specifically at 150^0C, and unprocessed latex lead to premature degradation, poor mechanical resistance, and inferior materials that lack the necessary resistance to thermal and mechanical stress.

Because of different bio-adhesive processing temperatures, thermal properties may change over time, improving the bio-adhesive capabilities and resistance to mechanical stress. The material's thermal behavior and potential for heat-resistant bonding are demonstrated by variations in heat flow.

6. RECOMMENDATIONS FOR UPCOMING RESEARCH WORK

In conjunction with this study, the following recommendations are made for future research. They are:

- Studying the effects of biodegradable additives that can improve the performance properties of this bio-adhesive material.
- Biodegradable additives influencing the application of the bio-adhesive. In a Hot-melt, gel, or liquid state.
- Investigate the performance of this bio-adhesive material when it is applied fully submerged in water.
- Study the toxicity rating levels and develop methods for identifying and extracting toxic compounds from raw latex.

7. REFERENCES

[1] M. J. T. Niekus, P. R. Kozowyk, G. H. Langejans, D. Ngan-Tillard, H. van Keulen, J. van der Plicht, K. M. Cohen, W. van Wingerden, B. van Os, B. I. Smit and L. W. Amkreutz, "Middle Paleolithic complex technology and a Neandertal tar-backed tool from the Dutch North Sea," *Proceedings of the National Academy of Sciences,* vol. 116, no. 44, pp. 22081-22087, 2019.

[2] R. D. Adams, "Science, technology and applications," in *Adhesive bonding*, Bristol, Woodhead Publishing, 2021, pp. 4-10.

[3] P. P. A. Mazza, F. Martini, B. Sala, M. Magi, M. P. Colombini, G. Giachi, F. Landucci, C. Lemorini, F. Modugno and E. Ribechini, "A new Palaeolithic discovery: tar-hafted stone tools in a European Mid-Pleistocene bone-bearing bed," *Journal of Archaeological Science,* vol. 33, no. 9, pp. 1310-1318, 2006.

[4] T. J. Koch and P. Schmidt, "The formation conditions of birch tar in oxygen-depleted environments," *Archaeological and Anthropological Sciences,* vol. 13, no. 6, pp. 1-5, 2021.

[5] G. Xu, H. Tian, X. Xi, J. Song, H. Lei and G. Du, "Preparation and characterization of urea–formaldehyde adhesives modified with glyoxalated tannin," *European Journal of Wood and Wood Products,* vol. 80, no. 5, pp. 1215-1223, 2022.

[6] A. Arias, E. Entrena-Barbero, G. Feijoo and M. T. Moreira, "Sustainable non-isocyanate polyurethanes bio-adhesives for engineered," *Journal of Environmental Chemical Engineering,* vol. 10, no. 1, pp. 1-12, 2022.

[7] A. Bharadwaj, D. Yadav and S. Varshney, "Non-biodegradable waste–its impact & safe disposal," *International Journal of Advanced Technology in Engineering and Science,* vol. 3, no. 1, pp. 184-191, 2015.

[8] M. Viljanmaa, A. Södergård and P. Törmälä, "Adhesion properties of lactic acid-based hot melt adhesives and their storage stability in different packaging applications," *International Journal of Adhesion and Adhesives,* vol. 22, no. 6, pp. 447-457, 2002.

[9] I. Calvez, R. Garcia, A. Koubaa, V. Landry and A. Cloutier, "Recent advances in bio-based adhesives and formaldehyde-free technologies for wood-based panel manufacturing," *Current Forestry Reports,* vol. 10, no. 5, pp. 386-400, 2024.

[10] X. Shi, S. Gao, C. Jin, D. Zhang, C. Lai, C. Wang, F. Chu, A. Ragauskas and M. Li, "A facile strategy to fabricate a lignin-based thermoset alternative to formaldehyde-based wood adhesives," *Green Chemistry,* vol. 25, no. 15, pp. 5907-5915, 2023.

[11] J. Ahire, S. Mousavi-Avval, N. Rajendran, R. Bergman, T. Runge, C. Jiang and J. Hu, "Techno-economic and life cycle analyses of bio-adhesives production from isolated soy protein and kraft lignin," *Journal of Cleaner Production,* no. 447, pp. 1-10, 2024.

[12] L. Liu, Y. Jia, L. Zheng, R. Luo, H. Essawy, H. Huang, Y. Wang, S. Deng and J. Zhang, "Development and characterization of bio-based formaldehyde-free sucrose-based adhesive for fabrication of plywood," *Polymers,* vol. 16, no. 5, pp. 2-13, 2024.

[13] J. Janesch, A. Solt-Rindler, L. Dumschat, O. Vay, A. Mija, W. Gindl-Altmutter, T. Rosenau, W. Raffeiner and C. Hansmann, "Flexible Biobased Thermosets from Epoxidized Plant Oils: A Study of Aliphatic Cross-Linking Agents," *ACS Applied Polymer Materials,* vol. 7, no. 6, pp. 3686-3697, 2025.

[14] C. Mpala, P. Sibanda, M. Dlamini and B. Sibanda, "Are quelea birds really a menace? Innovative use of indigenous knowledge systems in the harvesting and utilization of quelea, Quelea quelea lathamii," *Hwange District of Matabeleland North Province, International Journal of Agricultural Sciences,* vol. 2, no. 2, pp. 71-82, 2015.

[15] A. Eisen, M. Bussa and H. Röder, "A review of environmental assessments of biobased against petrochemical adhesives," *Journal of Cleaner Production,* vol. 277, pp. 1-12, 2020.

[16] M. L. Łebkowska, M. Załęska-Radziwiłł and A. Tabernacka, "Adhesives based on formaldehyde–environmental problems," *BioTechnologia Journal of Biotechnology, Computational Biology and Bionanotechnology,* vol. 98, no. 1, pp. 53-65, 2017.

[17] Y. Xiong, K. Du and Y. Huang, "One-third of global population at cancer risk due to elevated volatile organic compounds levels," *npj Climate and Atmospheric Science,* vol. 7, no. 1, pp. 1-11, 2024.

[18] M. Strum and R. Scheffe, "National review of ambient air toxics observations," *Journal of the Air & Waste Management Association,* vol. 66, no. 2, pp. 120-133, 2016.

[19] S. Omura, Y. Kawazoe and D. Uemura, "Development of a novel adhesive composed of all-natural components," *International Journal of Adhesion and Adhesives,* vol. 74, pp. 35-39, 2017.

[20] A. Arias, S. González-Rodríguez, M. V. Barros, R. Salvador, A. C. de Francisco, C. M. Piekarski and M. T. Moreira, "Recent developments in bio-based adhesives from renewable natural resources," *Journal of Cleaner Production,* vol. 314, pp. 2-11, 2021.

[21] L. Yu, K. Dean and L. Li, "Polymer blends and composites from renewable resources," *Progress in Polymer Science,* vol. 31, no. 6, pp. 576-602, 2006.

[22] S. S. Samaila Saleh, M. Y. Nor Zurairahetty, K. A. Kamarudin Ahmad and N. A. Nazri Ali, "Improving the strength of weak soil using polyurethane grouts: a review," *Construction and Building Materials,* vol. 202, pp. 738-752, 2019.

[23] A. Gandini and M. N. Belgacem, "Recent contributions to the preparation of polymers derived from renewable resources," *Journal of Polymers and the Environment,* vol. 10, no. 3, pp. 105-114, 2002.

[24] D. E. Packham, "Adhesive technology and sustainability," *International Journal of Adhesion and Adhesives,* vol. 29, no. 3, pp. 248-252, 2009.

[25] S. K. Vineeth and R. V. Gadhave, "Sustainable raw materials in hot melt adhesives: A review," *Open Journal of Polymer Chemistry,* vol. 10, no. 3, p. 49 to 65, 2020.

[26] J. P. Kalish, S. Ramalingam, H. Bao, D. Hall, O. Wamuo, S. L. Hsu, C. W. Paul, A. Eodice and Y. G. Low, "An analysis of the role of wax in hot melt adhesives," *International Journal of Adhesion and Adhesives,* vol. 60, pp. 63-68, 2015.

[27] L. Tous, R. A. Ruseckaite and E. M. Ciannamea, "Sustainable hot-melt adhesives based on soybean protein isolate and polycaprolactone," *Industrial Crops and Products,* vol. 135, pp. 153-15, 2019.

[28] E. M. Ciannamea, P. M. Stefani and R. A. Ruseckaite, "Physical and mechanical properties of compression molded and solution casting soybean protein concentrate based films," *Food Hydrocolloids,* vol. 38, pp. 193-204, 2014.

[29] H. Liu, C. Li and X. S. Sun, "Improved water resistance in undecylenic acid (UA)-modified soy protein isolate (SPI)-based adhesives," *Industrial Crops and Products,* vol. 74, pp. 577-584, 2015.

[30] S. I. Hong, W. Y. Choi, S. Y. Cho, S. H. Jung, B. Y. Shin and H. J. Park, "Mechanical properties and biodegradability of poly-ε-caprolactone/soy protein isolate blends compatibilized by coconut oil," *Polymer Degradation and Stability,* vol. 94, no. 10, pp. 1876-1881, 2009.

[31] A. Pizzi and K. L. Mittal, "Handbook of adhesive technology, Third Edition," in *Theories and Mechanisms of Adhesion*, Amsterdam, CRC Press, Taylor and Francis Group, 2018, pp. 3-15.

[32] F. G. Calvo-Flores, M. Monteagudo-Arrebola, J. A. Dobado and J. Isac-García, "Green and bio-based solvents," *Topics in Current Chemistry,* vol. 376, no. 3, pp. 1-18, 2018.

[33] T. B. L. Melo, R. S. A. de Batista, J. V. C. Júnior, F. H. D. de Andrade, F. S. de Souza and R. O. de Macêdo, "Recrystallization of ferulic acid using the anti-solvent and sonocrystallisation processes," *Journal of Thermal Analysis and Calorimetry,* vol. 138, no. 5, pp. 3758-3764, 2019.

[34] P. Sriamornsak and K. Burapapadh, "Characterization of recrystallized itraconazole prepared by cooling and anti-solvent crystallization," *Asian Journal of Pharmaceutical Sciences,* vol. 10, no. 3, pp. 230-238, 2015.

[35] W. El Bazi, M. T. M. Abou Jaoude, C. Porte, I. Mabille and J. L. Havet, "Isothermal crystallization of glycine in semi-continuous mode by anti-solvent addition," *Journal of Crystal Growth,* vol. 498, pp. 202-208, 2018.

[36] Y. Cai, Y. E. Cai, Y. Shi, J. Liu, S. Mou and Y. Lu, "A liquid–liquid extraction technique for phthalate esters with water-soluble organic solvents by adding inorganic salts," *Microchimica Acta,* vol. 157, no. 1, pp. 73-79, 2007.

[37] R. D. Rogers and C. B. Bauer, "Partitioning behavior of group 1 and 2 cations in poly (ethylene glycol)-based aqueous biphasic systems," *Journal of Chromatography B: Biomedical Sciences and Applications,* vol. 680, no. 2, pp. 237-241, 1996.

[38] K. H. Schumacher, "New water-based adhesives for flexible food packaging: chemical design, performance and toxicological safety," *Journal of Applied Packaging Research,* vol. 8, no. 1, pp. 38-42, 2016.

[39] B. Ramezanzadeh, E. Ghasemi, M. Mahdavian, E. Changizi and M. M. Moghadam, "Covalently-grafted graphene oxide nanosheets to improve barrier and corrosion protection properties of polyurethane coatings," *Carbon,* vol. 93, pp. 555-573, 2015.

[40] C. S. Chern, "Emulsion polymerization mechanisms and kinetics," *Progress in Polymer Science,* vol. 31, no. 5, pp. 443-486, 2006.

[41] H. A. Schuyten, J. W. Weaver, J. D. Reid and J. F. Jurgens, "Trimethylsilylcellulose," *Journal of the American Chemical Society,* vol. 70, no. 5, pp. 1919-1920, 1948.

[42] H. Zhang, P. Liu, S. M. Musa, C. Mai and K. Zhang, "Dialdehyde cellulose as a bio-based robust adhesive for wood bonding," *ACS Sustainable Chemistry & Engineering,* vol. 7, no. 12, pp. 10452-10459, 2019.

[43] S. Magalhães, L. Alves, B. Medronho, A. C. Fonseca, A. Romano, J. F. Coelho and M. Norgren, "Brief overview on bio-based adhesives and sealants, *Polymers,* vol. 11, no. 10, pp. 1-20, 2019.

[44] Z. Wang, Z. Gu, Y. Hong, L. Cheng and Z. Li, "Bonding strength and water resistance of starch-based wood adhesive improved by silica nanoparticles," *Carbohydrate Polymers,* vol. 86, no. 1, pp. 72-76, 2011.

[45] Z. Li, J. Wang, L. Cheng, Z. Gu, Y. Hong and A. Kowalczyk, "Improving the performance of starch-based wood adhesive by using sodium dodecyl sulfate," *Carbohydrate Polymers,* vol. 99, pp. 579-583, 2014.

[46] Y. Gu, L. Cheng, Z. Gu, Y. Hong, Z. Li and C. Li, "Preparation, characterization and properties of starch-based adhesive for wood-based panels," *International Journal of Biological Macromolecules,* vol. 134, pp. 247-254, 2019.

[47] T. A. Khan, J. H. Lee and H. J. Kim, "Lignin-based adhesives and coatings," *In Lignocellulose for future bioeconomy*, Elsevier, 2019, pp. 153-206.

[48] X. Gong, T. Liu, S. Yu, Y. Meng, J. Lu, Y. Cheng and H. Wang, "The preparation and performance of a novel lignin-based adhesive without formaldehyde," *Industrial Crops and Products,* vol. 153, pp. 1-4, 2020.

[49] H. Younesi-Kordkheili and A. Pizzi, "A comparison among lignin modification methods on the properties of lignin–phenol–formaldehyde resin as wood adhesive," *Polymers,* vol. 13, no. 20, pp. 1-11, 2021.

[50] M. N. Islam, F. Rahman, A. K. Das and S. Hiziroglu, "An overview of different types and potential of bio-based adhesives used for wood products," *International Journal of Adhesion and Adhesives,* vol. 112, pp. 1-12, 2022.

[51] G. Yang, Z. Gong, B. Zhou, X. Luo, J. Liu, G. Du, C. Zhao and L. Shuai, "Hydrodeoxygenation of condensed lignins followed by acid-mediated methylolation enables preparation of lignin-based wood adhesives," *Green Chemistry,* vol. 26, no. 2, pp. 753-759, 2024.

[52] W. Huang and X. Sun, "Adhesive properties of soy proteins modified by sodium dodecyl sulfate and sodium dodecylbenzene sulfonate," *Journal of the American Oil Chemists' Society,* vol. 77, no. 7, pp. 705-708, 2000.

[53] Y. Liu and K. Li, "Development and characterization of adhesives from soy protein for bonding wood," *International Journal of Adhesion and Adhesives,* vol. 27, no. 1, pp. 59-67, 2007.

[54] P. Nordqvist, N. Nordgren, F. Khabbaz and E. Malmström, "Plant proteins as wood adhesives: Bonding performance at the macro-and nanoscale," *Industrial Crops and Products,* vol. 44, pp. 246-252, 2013.

[55] Y. Zhou, G. Zeng, F. Zhang, K. Li, X. Li, J. Luo, J. Li and J. Li, "Design of tough, strong and recyclable plant protein-based adhesive via dynamic covalent crosslinking chemistry," *Chemical Engineering Journal,* vol. 460, pp. 1-12, 2023.

[56] Y. Xu, Y. Han, J. Li, J. Luo, S. Shi, J. Li, Q. Gao and A. Mao, "Research progress of soybean protein adhesive: a review," *Journal of Renewable Materials,* vol. 10, no. 10, pp. 2520-2540, 2022.

[57] Z. Hao, X. Xi, D. Hou, H. Lei, C. Li, G. Xu and G. Du, "A fully bio-based soy protein wood adhesive modified by citric acid with high water tolerance," *International Journal of Biological Macromolecules,* vol. 253, p. 127135, 2023.

[58] H. Lin, X. Chen, H. Lei, X. Zhou, G. Du, H. Essawy, X. Xi, D. Hou, J. Song and M. Cao, "Synthesis and characterization of a bio-aldehyde-based lignin adhesive with desirable water resistance," *International Journal of Biological Macromolecules,* vol. 264, p. 130020, 2024.

[59] Z. Lv, X. Yan, S. Jia, J. Pan, X. Hao, G. Chen, B. Lü, J. Rao and F. Peng, "Bio-based hot-melt adhesive from xylan," *Nature Sustainability,* vol. 8, no. 7, pp. 827-836, 2025.

[60] N. Mati-Baouche, P. H. Elchinger, H. de Baynast, G. Pierre, C. Delattre and P. Michaud, "Chitosan as an adhesive," *European Polymer Journal,* vol. 60, pp. 198-212, 2014.

[61] Wikipedia, "Biodegradation," Wikipedia, [Online]. Available: https://en.wikipedia.org/wiki/Biodegradation. [Accessed 01 July 2025].

[62] D. Watts, B. Ratner, A. Hoffman, F. Schoen and J. Lemons, "Adhesives and sealants. In Biomaterials Science," in *Bioadhesives*, Manchester, Elsevier BV, 2013, pp. 889-904.

[63] A. Tenorio-Alfonso, M. Sánchez and J. Franco, "Preparation, characterization and mechanical properties of bio-based polyurethane adhesives from isocyanate-functionalized cellulose acetate and castor oil for bonding wood," *Polymers,* vol. 9, no. 14, pp. 1-14, 2017.

[64] A. Arias, S. González-García, G. Feijoo and M. Moreira, "Tannin-based bio-adhesives for the wood panel industry as sustainable alternatives to petrochemical resins," *Journal of Industrial Ecology,* vol. 26, no. 2, pp. 627-642, 2022.

[65] A. Tzagiollari, H. McCarthy, T. Levingstone and N. Dunne, "Biodegradable and biocompatible adhesives for the effective stabilization, repair and regeneration of bone," *Bioengineering,* vol. 9, no. 6, pp. 1-31, 2022.

[66] Wikipedia, "Cyanoacrylate," Wikipedia, [Online]. Available: https://en.wikipedia.org/wiki/Cyanoacrylate#Safety_issues. [Accessed 06 June 2024].

[67] PLANT-RESOURCES-OF-TROPICAL-AFRICA, "Euphorbia Ingens," PROTA, [Online]. Available: https://uses.plantnet-project.org/en/Euphorbia_candelabrum_(PROTA). [Accessed 10 September 2021].

[68] Wikipedia, "Nanoparticle," Wikipedia, [Online]. Available: https://en.wikipedia.org/wiki/Nanoparticle#Mechanical. [Accessed 22 January 2024].

[69] A. Dhawan and V. Sharma, "Toxicity assessment of nanomaterials: methods and challenges," *Analytical and Bioanalytical Chemistry,* vol. 398, no. 2, pp. 589-605, 2010.

[70] S. Rajabi, A. Ramazani, M. Hamidi and T. Naji, "Artemia salina as a model organism in toxicity assessment of nanoparticles," *DARU Journal of Pharmaceutical Sciences,* vol. 23, no. 1, pp. 1-6, 2015.

[71] D. Drobne, "Nanotoxicology for safe and sustainable nanotechnology," *Arhiv za higijenu rada i toksikologiju,* vol. 58, no. 4, pp. 471-478, 2007.

[72] A. Ikramullah, D. Salve, G. Pai, M. Rathore and D. Joshi, "In vitro cytotoxicity testing of silver nanoparticals in lymphocyte and sperm cells," *Ind J Fund Appl Life Sci,* vol. 3, pp. 44-47, 2013.

[73] SAHPRA, "Quality and bioequivalence guidelines - Version 7," SAHPRA, SOUTH AFRICA, 2019.

[74] W. H. Suh, K. S. Suslick, G. D. Stucky and Y. H. Suh, "Nanotechnology, nanotoxicology, and neuroscience," *Progress in neurobiology,* vol. 87, no. 3, pp. 133-170, 2009.

[75] S. Ebnesajjad and A. H. Landrock, Adhesives technology handbook, Norwich, NY: William Andrew, 2014.

[76] G. Barin, R. S. Forgan and J. F. Stoddart, "Mechanostereochemistry and the mechanical bond," *Proceedings of the Royal Society A: Mathematical, Physical and Engineering Sciences,* vol. 468, no. 2146, pp. 2849-2880, 2012.

[77] C. J. Bruns and J. F. Stoddart, The nature of the mechanical bond, Tokyo: From molecules to machines, 2016.

[78] S. J. Marshall, S. C. Bayne, R. Baier, A. P. Tomsia and G. W. Marshall, "A review of adhesion science," *Dental Materials,* vol. 26, no. 2, pp. 11-16, 2010.

[79] Wikipedia, "Valence electron," Wikipedia, [Online]. Available: https://en.wikipedia.org/wiki/Valence_electron. [Accessed 22 March 2025].

[80] L. O. Nilsson, "Durability concept, pore structure and transport processes," in *Advanced Concrete Technology*, Jordan Hill, Oxford, An Imprint of Elsevier, 2003, pp. 4-8.

[81] Wikipedia, "Mechanically interlocked molecular architectures," Wikipedia, [Online]. Available: https://en.wikipedia.org/wiki/Mechanically_interlocked_molecular_architectures#Mechanical_bonding_and_chemical_reactivity. [Accessed 01 November 2024].

[82] T. Geminger and S. Jarka, "Injection molding of multimaterial systems," in *Specialized injection molding techniques*, William Andrew Publishing, 2016, pp. 165-210.

[83] B. A. Morris, "Science and Technology of Flexible Packaging," in *Multilayer Films from Resin and Process to End Use*, PDL Handbook Series, 2017, pp. 365-368.

[84] Wikipedia, "Chemical Bonding," [Online]. Available: https://en.wikipedia.org/wiki/Chemical_bond. [Accessed 04 November 2025].

[85] F. Lapique and K. Redford, "Curing effects on viscosity and mechanical properties of a commercial epoxy resin adhesive," *International Journal of Adhesion and Adhesives,* vol. 22, no. 4, pp. 337-346, 2002.

[86] M. A. Winnik, "Latex film formation," *Current Opinion in Colloid & Interface Science,* vol. 2, no. 2, pp. 192-199, 1997.

[87] S. Ebnesajjad, "Introduction and adhesion theories," in *Handbook of Adhesives and Surface Preparation*, Kidlington, William Andrew Publishing, 2011, pp. 3-13.

[88] H. Rajabi, M. H. Mosleh, P. Mandal, A. Lea-Langton and M. Sedighi, "Emissions of volatile organic compounds from crude oil processing–Global emission inventory and environmental release," *Science of the Total Environment,* vol. 727, pp. 1-15, 2020.

[89] C. A. Mahieux, "Mechanical Properties of Polymer Solids and Liquids," in *Environmental Degradation of Industrial Composites*, Amsterdam, The Netherlands, Elsevier, 2006, pp. 149-154.

[90] C. P. Maladeniya and R. C. Smith, "Influence of Component Ratio on Thermal and Mechanical Properties of Terpenoid-Sulfur Composites," *Journal of Composites Science,* vol. 5, no. 10, pp. 2-11, 2021.

[91] J. Richard, "Dynamic micromechanical properties of styrene-butadiene copolymer latex films," *Polymer,* vol. 33, no. 3, pp. 562-571, 1992.

[92] M. B. Zellner, W. Vogan McNeil, G. T. Gray III, D. C. Huerta, N. S. P. King, G. E. Neal, S. J. Valentine, J. R. Payton, J. Rubin, G. D. Stevens and W. D. Turley, "Surface preparation methods to enhance dynamic surface property measurements of shocked metal surfaces," *Journal of Applied Physics,* vol. 103, no. 8, pp. 1-10, 2008.

[93] S. Cao, J. Wang, H. Chen and D. Chen, "Progress of marine biofouling and antifouling technologies," *Chinese Science Bulletin,* vol. 56, no. 7, pp. 598-612, 2011.

[94] A. Oláh and G. J. Vancso, "Characterization of adhesion at solid surfaces: Development of an adhesion-testing device," *European Polymer Journal,* vol. 41, no. 12, pp. 2803-2823, 2005.

[95] F. Awaja, M. Gilbert, G. Kelly, B. Fox and P. J. Pigram, "Adhesion of polymers," *Progress in Polymer Science,* vol. 34, no. 9, pp. 948-968, 2009.

[96] D. J. Yarusso, D. A. Dillard and A. V. Pocius, "Chapter 6 - Mechanical Testing of Adhesive Joints," in *Adhesion Science and Engineering-The Mechanics of Adhesion*, Salt Lake City, Utah, Elsevier Science B.V, 2002, pp. 193-234.

[97] R. Singh, "Applied welding engineering: processes, codes, and standards," in *Butterworth-Heinemann*, Kindlington, Matthew Deans, 2020, pp. 87-94.

[98] C. A. Mahieux, "Effect of temperature on polymer matrix composites," in *Environmental Degradation of Industrial Composites*, Amsterdam, The Netherlands, Elsevier, 2006, pp. 17-83.

[99] G. T. Gray, P. J. Maudlin, L. M. Hull, Q. K. Zuo and S. R. Chen, "Predicting material strength, damage, and fracture: the synergy between experiment and modeling," *Journal of Failure Analysis and Prevention,* vol. 5, no. 3, pp. 7-17, 2005.

[100] J. K. Lim, "Tensile, bending and shear strength distributions of adhesive-bonded butt joint specimens," *Composites Science and Technology,* vol. 65, no. 9, pp. 1421-1427, 2005.

[101] T. E. Experts, "General Bonding Design And Guideline," [Online]. Available: https://theepoxyexperts.com/general-bonding-design-guideline/. [Accessed 12 August 2024].

[102] K. L. DeVries and D. O. Adams, "Mechanical testing of adhesive joints," in *Handbook of Adhesive Surface and Preparation*, Salt Lake City, Adhesion Science and Engineering, 2002, pp. 193-234.

[103] D. R. Moore, J. G. Williams and A. Pavan, Fracture mechanics testing methods for polymers, adhesives and composites, Kindlington: Elsevier, ESIS Publication 28, 2001.

[104] E. M. Petrie, Handbook of adhesives and sealants, McGraw-Hill Education, 2007.

[105] L. F. Kawashita, "The peeling of adhesive joints," Imperial College London (University of London), London, 2006.

[106] M. Götz, F. Kayatz and M. Hauptmann, "Numerical Investigations of the Seam Opening Behavior of Peelable Seal Seams as a Function of the Seal Seam Formation," *Polymers,* vol. 17, no. 7, pp. 1-20, 2025.

[107] L. F. Kawashita, D. R. Moore and J. G. Williams, "Protocols for the measurement of adhesive fracture toughness by peel tests," *The Journal of Adhesion,* vol. 82, no. 10, pp. 973-995, 2006.

[108] R. D. Adams and R. G. H. Davies, "Strength of lap shear joints. In Adhesive Science and Engineering-1" in *The Mechanics of Adhesion*, Bristol, Elsevier Science, 2002, pp. 111-144.

[109] B. C. Duncan and W. R. Broughton, Characterizing strength of adhesion, Teddington : National Physical Laboratory, 2004.

[110] J. S. Bergstrom, "Theory and computational modeling," in *Mechanics of solid polymers*, San Diego, William Andrew, an imprint of Elsevier, 2015, pp. 1-10.

[111] L. J. Hart-Smith, "Design of adhesively bonded joints," in *Adhesion Science and Engineering*, Huntington Beach, Elsevier Applied Science Publishers Ltd, Joining Fibre-Reinforced Plastics, 1987, pp. 271-311.

[112] ADMET, "Tensile Testing," ADMET Material Testing System manufacturer, [Online]. Available: https://www.admet.com/testing-applications/test-types/tension-testing/#core-concepts. [Accessed 10 1 2024].

[113] K. Pamlényi, K. Kristó, T. Sovány and G. Regdon Jr, "Development and evaluation of bioadhesive buccal films based on sodium alginate for allergy therapy," *Heliyon,* vol. 8, no. 8, pp. 1-10, 2022.

[114] WIKIPEDIA, "Thermogravimetric analysis," WIKIPEDIA, [Online]. Available: https://en.wikipedia.org/wiki/Thermogravimetric_analysis. [Accessed 15 April 2024].

[115] D. M. Price, D. J. Hourston and F. Dumont, "Thermogravimetry of polymers," *Encyclopedia of analytical chemistry,* vol. 105, pp. 1-10, 2000.

[116] T. A. Instruments, "High Performance TGA systems," [Online]. Available: https://www.tainstruments.com/pdf/brochure/BROCH-DTGA-HP750.pdf. [Accessed 15 April 2024].

[117] N. Saadatkhah, A. Carillo Garcia, S. Ackermann, P. Leclerc, M. Latifi, S. Samih, G. S. Patience and J. Chaouki, "Experimental methods in chemical engineering: Thermogravimetric analysis (TGA)," *The Canadian Journal of Chemical Engineering,* vol. 98, no. 1, pp. 34-43, 2020.

[118] S. K. Z. Industrial, "Key Differences Between DSC and TGA," 2015. [Online]. Available: https://www.skztester.com/blog/DSC-vs-TGA-Whats-the-Difference-in-Thermal-Analysis#:~:text=Measurement%20Focus:%20Energy%20vs.&text=Differential%20Scanning%20Calorimetry%20(DSC)%20and,lose%20mass%20under%20thermal%20stress.. [Accessed 2024 October 12].

[119] Torontech, "DSC vs TGA A component guide to the difference," Torontech, [Online]. Available: https://www.torontech.com/articles/dsc-and-tga/#:~:text=The%20main%20difference%20between%20TGA%20and%20DSC%20is%20that%20TGA,in%20heat%20flow%20or%20energy.. [Accessed 23 August 2025].

[120] Q. Zheng, Y. Zhang, M. Montazerian, O. Gulbiten, J. C. Mauro and E. D. A. Y. Y. Zanotto, "Understanding glass through differential scanning calorimetry," *Chemical Reviews,* vol. 119, no. 13, pp. 7839-7949, 2019.

[121] Wikipedia, "Differential scanning calorimetry," [Online]. Available: https://en.wikipedia.org/wiki/Differential_scanning_calorimetry. [Accessed 12 September 2024].

[122] A. Bashirgonbadi, Y. Ureel, L. Delva, R. Fiorio, K. M. Van Geem and K. Ragaert, "Accurate determination of polyethylene (PE) and polypropylene (PP) content in polyolefin blends using machine learning-assisted differential scanning calorimetry (DSC) analysis," *Polymer Testing,* vol. 131, pp. 1-10, 2024.

[123] T. A. Instruments, "Interpreting Unexpected Events," 2024. [Online]. Available: https://cms9-prod.rdg.ac.uk/caf/-/media/project/functions/research/chemical-analysis-facility/documents/dscq2000-caf-interpreting-unexpected-events-and-transitions.pdf?la=en&hash=885EC482FFEC6673D89A0DAFFC3F7D55#:~:text=SOLUTIONS:%20Weigh%20the%20sample%2. [Accessed 12 April 2024].

[124] B. A. Ibrahim and K. M. Kadum, "Influence of polymer blending on mechanical and thermal properties," *Modern Applied Science,* vol. 4, no. 9, pp. 157-161, 2010.

[125] Y. Xu, X. Ren and M. A. Hanna, "Chitosan/clay nanocomposite film preparation and characterization," *Journal of Applied Polymer Science,* vol. 99, no. 4, pp. 1684-1691, 2006.

[126] T. A. Instruments, "DSC Manual," [Online]. Available: https://www.tainstruments.com/pdf/brochure/Discovery-DSC-Brochure.pdf. [Accessed 11 April 2024].

[127] M. M. H. Al Omari, I. S. Rashid, N. A. Qinna, A. M. Jaber and A. A. Badwan, "Profiles of drug substances, excipients and related methodology," in *Chapter Two - Calcium Carbonate*, Philadelphia, The Jordanian Pharmaceutical Manufacturing Co., Amman, Jordan, 2016, pp. 31-132.

[128] H. Ramli, N. F. A. Zainal, M. Hess and C. H. Chan, "Basic principles and good practices of rheology for polymers for teachers and beginners," *Chemistry Teacher International,* vol. 4, no. 4, pp. 307-326, 2022.

[129] H. U. Bahia, "Modeling of Asphalt Binder Rheology and Its Application to Modified Binders," in *Modeling of Asphalt Concrete, 1st Edition*, New York, The American Society of Civil Engineers, 2004, pp. 11-64.

[130] A. Gurt and M. Khonsari, "A Review of the Rheological Consistency of Materials," *Lubricants,* vol. 12, no. 7, pp. 1-26, 2024.

[131] A. Paar, "Basics of rheology," Anto Paar, [Online]. Available: https://wiki.anton-paar.com/za-en/basics-of-rheology/. [Accessed 10 September 2024].

[132] A. Paar, "Rheological measurements," Anton Paar, [Online]. Available: https://wiki.anton-paar.com/za-en/basics-of-rheology/rheological-measurements/#:~:text=In%20an%20oscillatory%20test%20the,%E2%80%9Coscillates%E2%80%9D%20around%20the%20axis.&text=When%20measuring%20ketchup%20for%20instance,determines%20the%20required%20sh. [Accessed 10 Spetember 2024].

[133] NETZSCH, "NETZSCH Rotational Rheology," [Online]. Available: file:///H:/MASTERS%202023%20NOV/MASTERS/MASTERS%20WORK%202024/RHEOLOGY/NETZSCH_Rotational_Rheology_web%20OPERARION.pdf. [Accessed 12 September 2024].

[134] T. A. Instruments, "Rheology and dynamic mechanical analysis," 21 May 2019. [Online]. Available: file:///H:/MASTERS%202023%20NOV/MASTERS/MASTERS%20WORK%202024/RHEOLOGY/IMPORTANT/TA-Instruments-UW-Facilities-Day-2015-05-21%20IMPORTANT.pdf. [Accessed 16 September 2024].

[135] R. Joseph, Practical guide to latex technology, Shropshire: A Smith Group Company, 2013.

[136] A. B. Othman and C. B. Lye, "Effect of pH Coagulation and Sulphuric Acid as a Coagulant on Natural Rubber Properties," *Journal of the Rubber Research Institute of Malaysia,* vol. 28, no. 3, pp. 109-117, 1980.

[137] Z. Wang, J. Xu, X. Wu, M. Han, R. Peng, R. Zhao, M. Qin, T. Li, J. Yin, l. Yu and Y. Li, "A Sprayable Janus Hydrogel as an Effective Bioadhesive for Gastrointestinal Perforation Repair," *RESEARCH ARTICLE,* vol. 34, no. 48, pp. 1-18, 2024.

[138] F. Zhang, M. Chien, Q. Fan and D. Jiang, "Advances in bioadhesive hydrogels for musculoskeletal tissue application," *Advanced Functional Materials,* vol. 34, no. 32, pp. 1-25, 2024.

[139] P. Bioscience, "Prime Bioscience," USTRETCH, Mechanical testing systems, [Online]. Available: https://primebioscience.com/pb-applications/ustretch-a-versatile-uniaxial-benchtop-mechanical-tester-for-biomaterials/. [Accessed 29 January 2024].

[140] E. Apaydın Varol and Ü. Mutlu, "TGA-FTIR analysis of biomass samples based on the thermal decomposition behavior of hemicellulose, cellulose, and lignin," *Energies,* vol. 16, no. 9, pp. 2-19, 2023.

[141] J. Liu, X. Jiang, H. Cai and F. Gao, "Study of combustion characteristics and kinetics of agricultural briquettes using thermogravimetric analysis," *ACS Omega,* vol. 6, no. 24, pp. 15827-15833, 2021.

[142] M. Reza, S. Islam, S. Afroze, M. Bakar, R. Sukri, S. Rahman and A. Azad, "Evaluation of the bioenergy potential of invasive Pennisetum purpureum through pyrolysis and thermogravimetric analysis," *Energy, Ecology & Environment,* vol. 5, no. 2, pp. 118-133, 2020.

[143] S. Parekh, M. Chaudhary, R. Patel, P. Patel and R. Gupta, "Analyzing the influence of diols' chain length on the properties of bio-based wood adhesive," *Polymer Engineering & Science,* vol. 64, no. 9, pp. 4234-4245, 2024.

[144] R. Pereira, L. da Silva, B. Carvalho, A. Mattos, S. Mazzetto and D. Lomonaco, "Development of bio-based polyurethane wood adhesives from agroindustrial waste," *Journal of Polymers and the Environment,* vol. 30, no. 5, pp. 1959-1972, 2022.

[145] A. Boussetta, A. Benhamou, H. Charii, E. Ablouh, M. Mennani, M. Kasbaji, N. Boussetta, N. Grimi and A. Moubarik, "Formulation and characterization of chitin-starch bio-based wood adhesive for the manufacturing of formaldehyde-free composite particleboards," *Waste and Biomass Valorization,* vol. 14, no. 11, pp. 3671-3687, 2023.

[146] X. Chen, A. Pizzi, B. Zhang, X. Zhou, E. Fredon, C. Gerardin and G. Du, "Particleboard bio-adhesive by glyoxalated lignin and oxidized dialdehyde starch crosslinked by urea," *Wood Science and Technology,* vol. 56, no. 1, pp. 63-85, 2022.

[147] C. Tsioptsias, "Exothermic contributions in the DSC signal of endothermic effects," *Journal of Thermal Analysis and Calorimetry,* vol. 150, no. 7, pp. 5239-5248, 2025.

[148] M. Hussin, A. Aziz, A. Iqbal, M. Ibrahim and N. Abd Latif, "Development and characterization novel bio-adhesive for wood using kenaf core (Hibiscus cannabinus) lignin and glyoxal," *International Journal of Biological Macromolecules,* vol. 122, pp. 713-722, 2019.

[149] D. Macocinschi, D. Filip, B. Ciubotaru, R. Dumitriu, C. Varganici and M. Zaltariov, "Blends of sodium deoxycholate-based poly (ester ether) urethane ionomer and hydroxypropylcellulose with mucosal adhesiveness." *International Journal of Biological Macromolecules,* vol. 162, pp. 1262-1275, 2020.

[150] A. Arunachalam, E. Le Cornec, J. Es Sayed and M. Kamperman, "Bioinspired Pressure Sensitive Adhesives Based on Natural Deep Eutectic Solvents," *Macromolecules,* vol. 58, no. 16, pp. 8786-8797, 2025.

[151] A. Borrero-López, C. Valencia, G. Domínguez, M. Eugenio and J. Franco, "Rheology and adhesion performance of adhesives formulated with lignins from agricultural waste straws subjected to solid-state fermentation." *Industrial Crops and Products,* vol. 177, pp. 1-8, 2021.

[152] A. Tenorio-Alfonso, M. Sánchez and J. Franco, "Impact of moisture curing conditions on the chemical structure and rheological and ultimate adhesion properties of polyurethane adhesives based on castor oil and cellulose acetate," P*rogress in Organic Coatings,* vol. 161, pp. 1-11, 2021.

[153] F. Ullah, M. Khan, A. Shahzad, L. Shah, R. Ullah, M. Ibrahim and H. Yoo, "Fabrication of xanthan gum-based polymeric hydrogels: Rheological investigation, toughness, and adhesion optimization." *International Journal of Adhesion and Adhesives,* vol. 138, pp. 1-11, 2025.

[154] Z. Bashir, W. Yu, Z. Xu, Y. Li, J. Lai, Y. Li, Y. Cao and B. Xue, "Engineering bio-adhesives based on protein–polysaccharide phase separation." *International Journal of Molecular Sciences,* vol. 23, no. 17, pp. 3-12, 2022.

[155] A. Aman, K. Yeneneh, A. Shemsedin, B. Zegale and E. Wakshume, "Development and Optimization of a Bio-Based Adhesive from Euphorbia trigon Latex Reinforced with Alumina for Sustainable Wood Bonding Applications," *Results in Engineering,* vol. 1, no. 1, pp. 1-14, 2025.

[156] J. G. V. Villanueva, P. A. S. Huertas, F. S. Galan, R. J. E. Rueda, J. C. B. Triana and J. C. Rodriguez, "Bio-adhesion evaluation of a chitosan-based bone bio-adhesive," *International Journal of Adhesion and Adhesives,* vol. 92, pp. 80-88, 2019.

[157] P. Patel, R. Patel, J. Chaudhari and R. Gupta, "Role of crosslinkers on the properties of bio-based wood adhesives," *Polymer Engineering & Science,* vol. 64, no. 6, pp. 2841-2853, 2024.

[158] S. Jalali, R. Carbas, E. Marques and L. da Silva, "Advancing impact and fatigue resistance in bio-adhesive joints: the combined effect of adhesive penetration and tough-layer techniques." *Composite Structures,* pp. 1-12, 2025.

[159] I. Georgiou, A. Ivankovic, A. Kinloch and V. Tropsa, "Rate-dependent fracture behavior of adhesively bonded joints," *European Structural Integrity Society,* vol. 32, pp. 317-328, 2003.

8. APPENDICES

8.1 Appendix A: Determining Elastic Modulus using Stress-Strain Curve

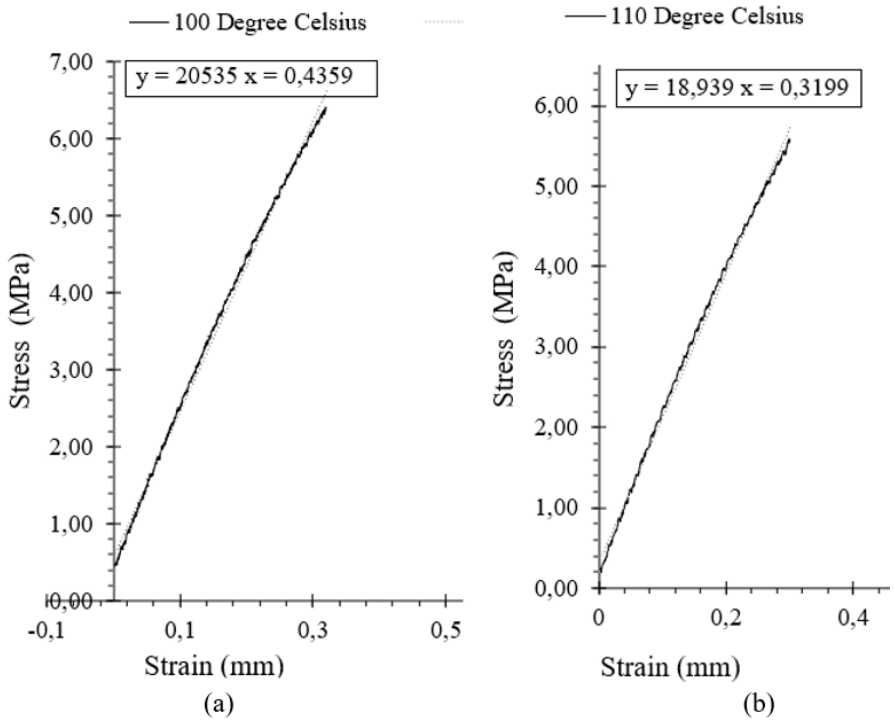


Figure 7. 1 Test 1: Finding the elastic modulus using the stress-strain curve (a) 100^0C (b) 110^0C

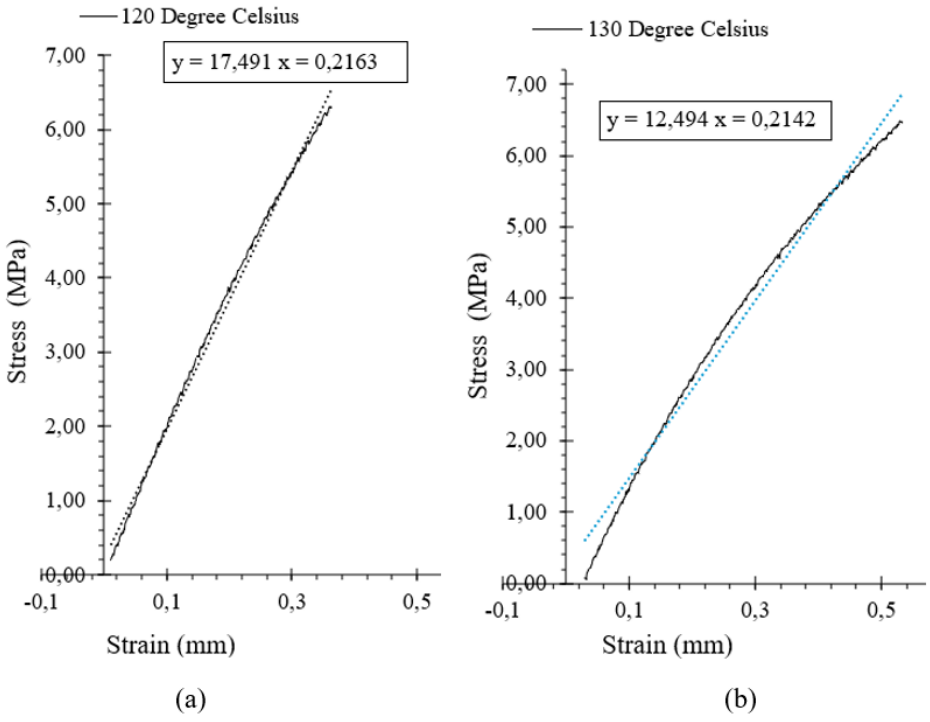


Figure 7. 2 Test 1: Finding the elastic modulus using the stress-strain curve (a) 120^0C (b) 130^0C

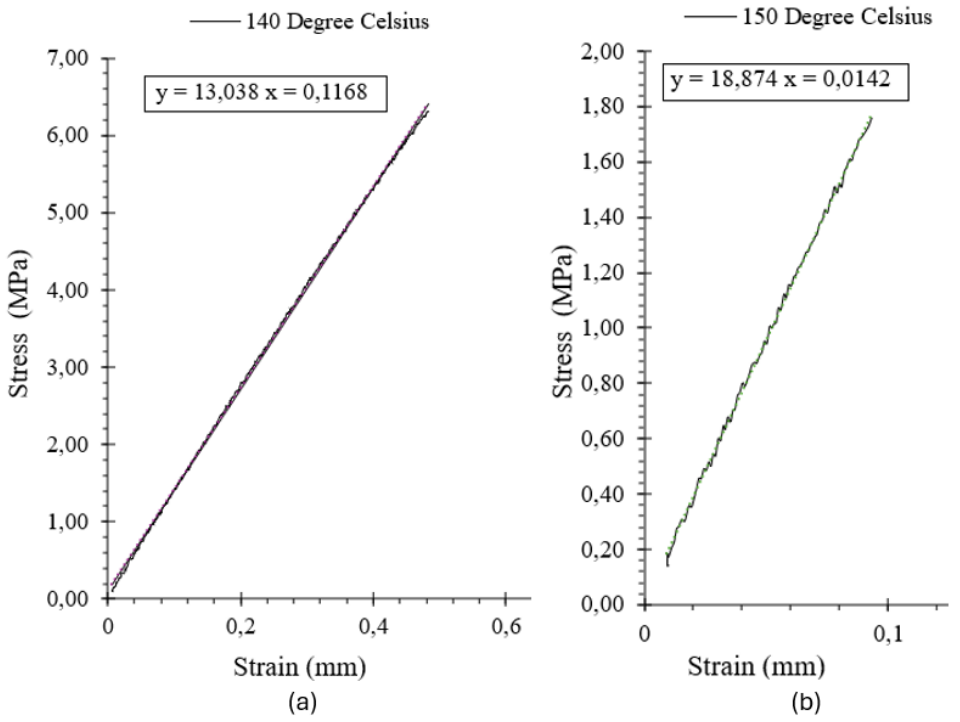


Figure 7. 3 Test 1: Finding the elastic modulus using the stress-strain curve (a) 140^0C (b) 150^0C

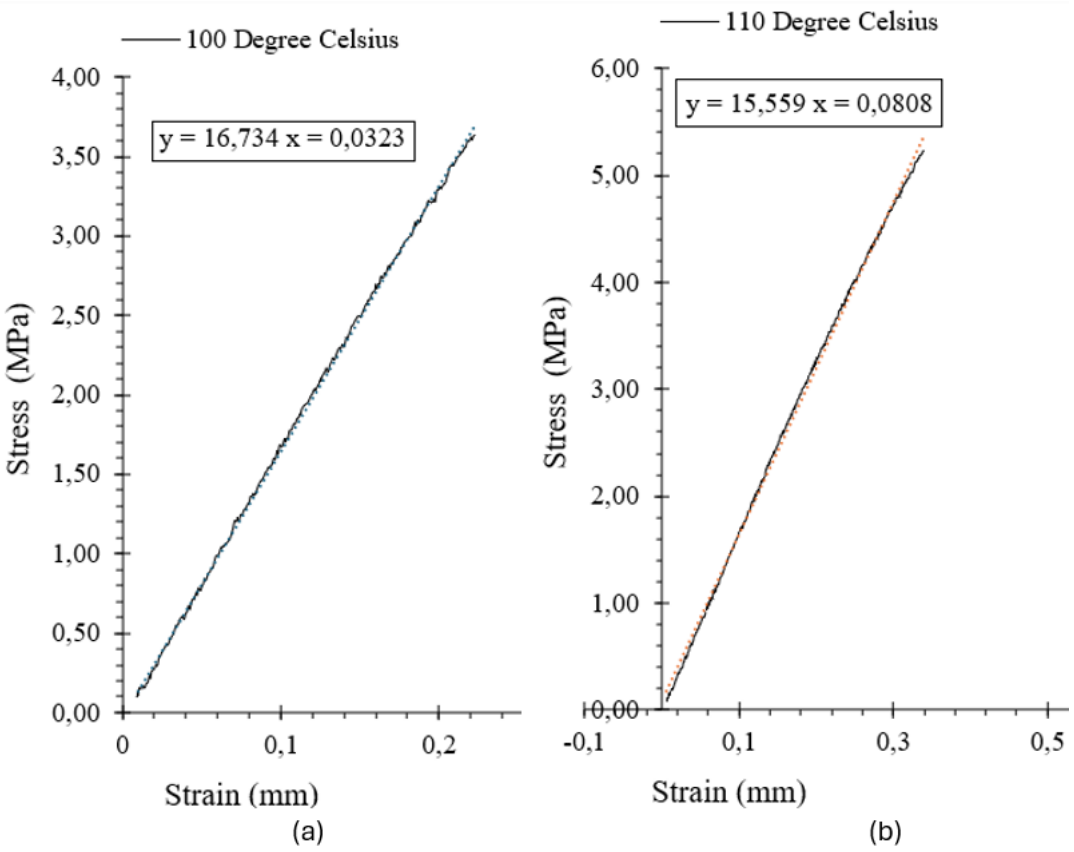


Figure 7. 4 Test 2: Finding the elastic modulus using the stress-strain curve (a) 100^0C (b) 110^0C

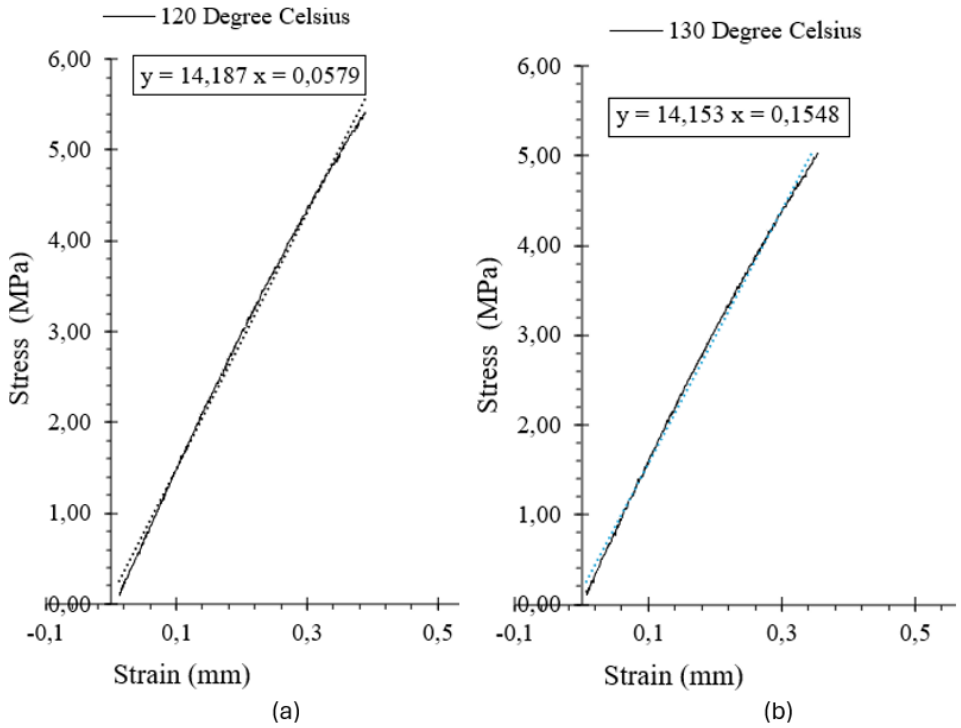


Figure 7. 5 Test 2: Finding the elastic Modulus using the stress-strain curve (a) 120^0C (b) 130^0C

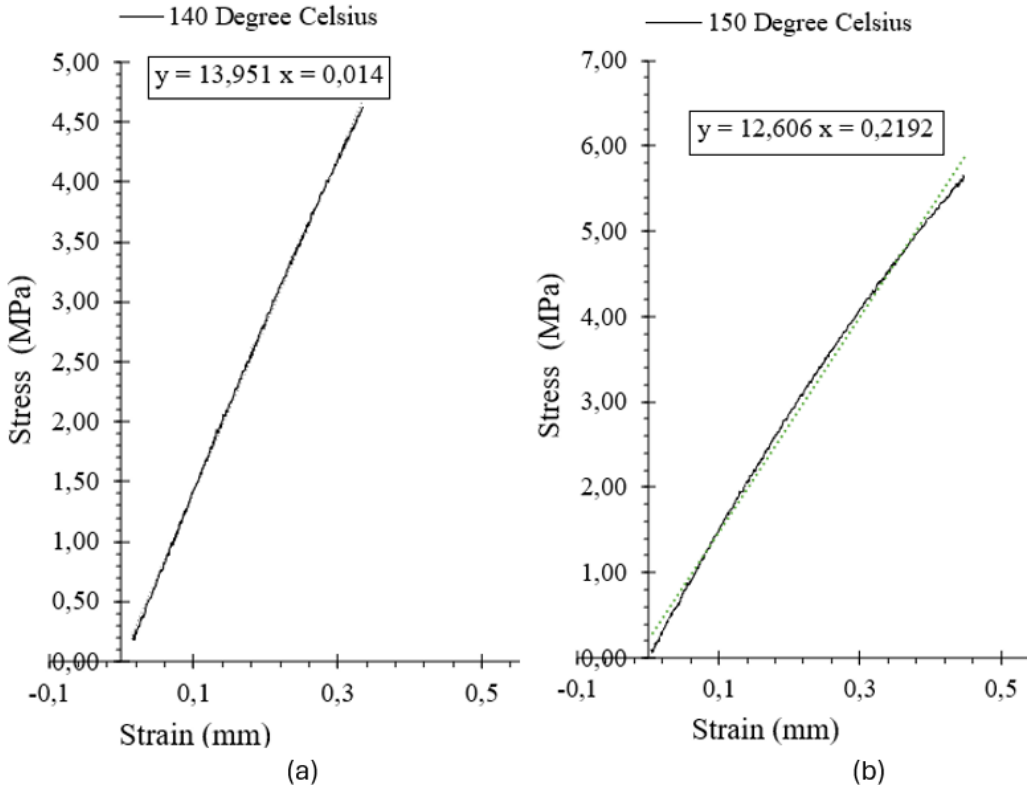


Figure 7. 6 Test 2: Finding the elastic Modulus using the stress-strain curve (a) 140^0C (b) 150^0C

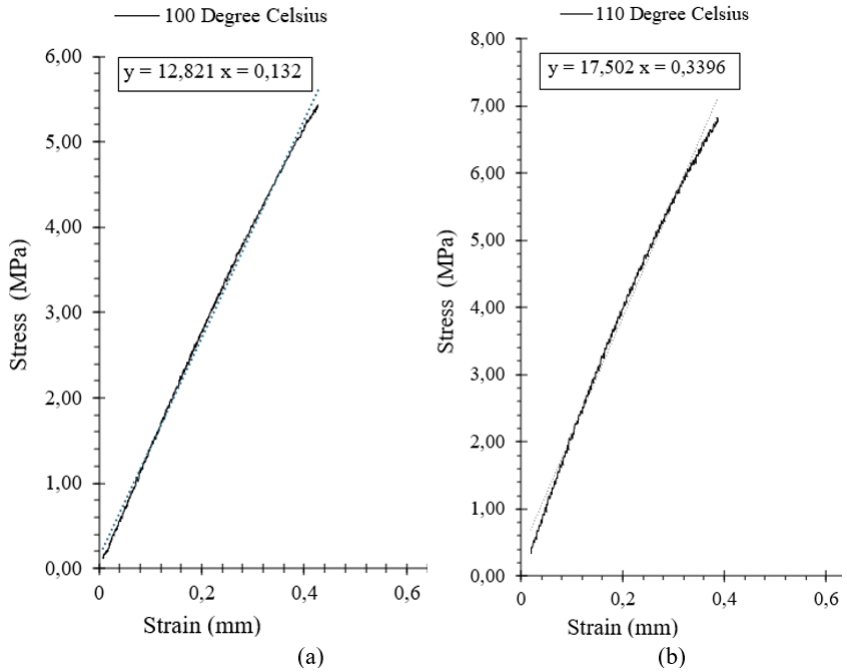


Figure 7. 7 Test 3: Finding the elastic modulus using the stress-strain curve (a) 100^0C (b) 110^0C

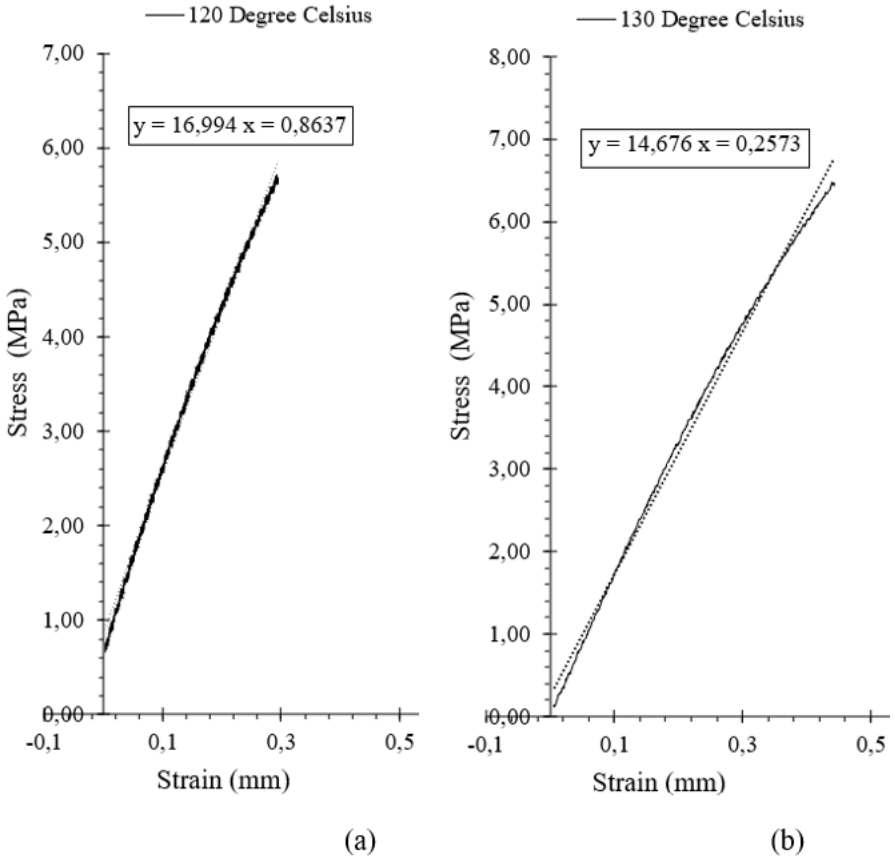


Figure 7. 8 Test 3: Finding the elastic Modulus using the stress-strain curve (a) 120^0C (b) 130^0C

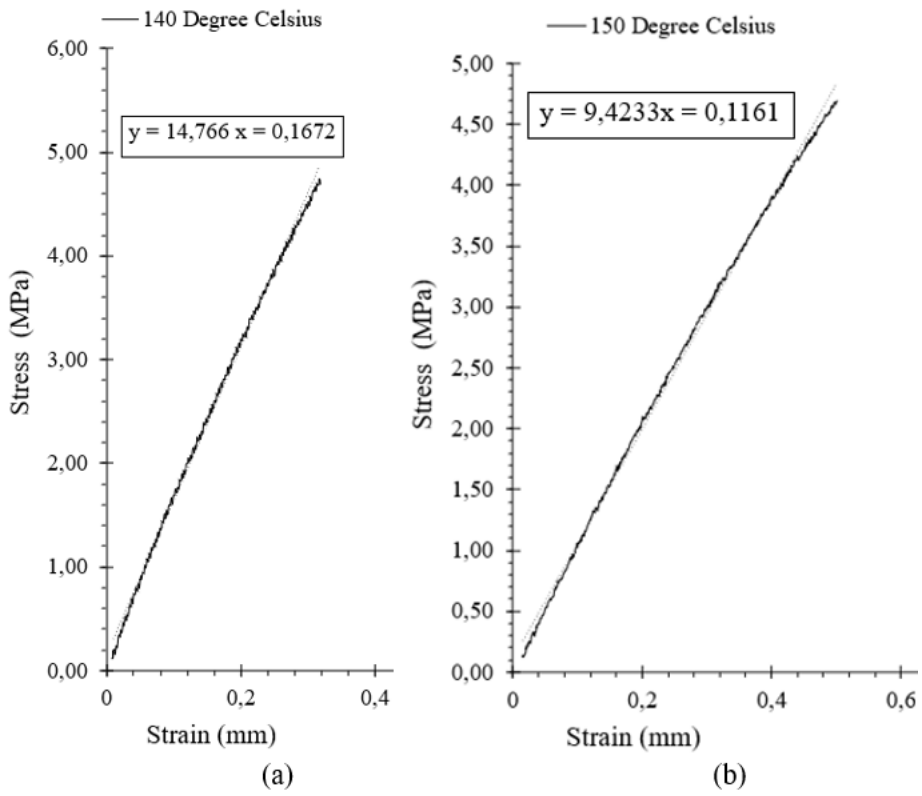


Figure 7. 9 Test 3: Finding the elastic Modulus using the stress-strain curve (a) 140^0C (b) 150^0C

8.2 Appendix B: Single-lap shear test force versus strain curve

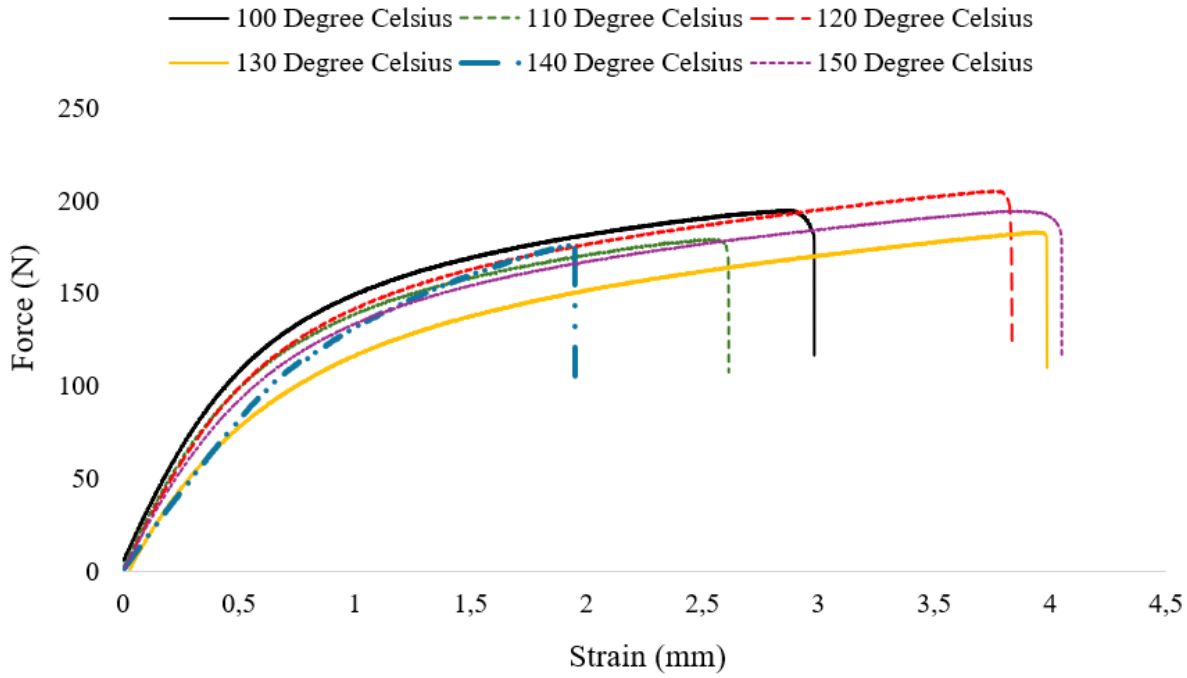


Figure 7. 10 Force versus strain curve for paper-to-paper specimens joined by process bio-adhesive (Test 1)

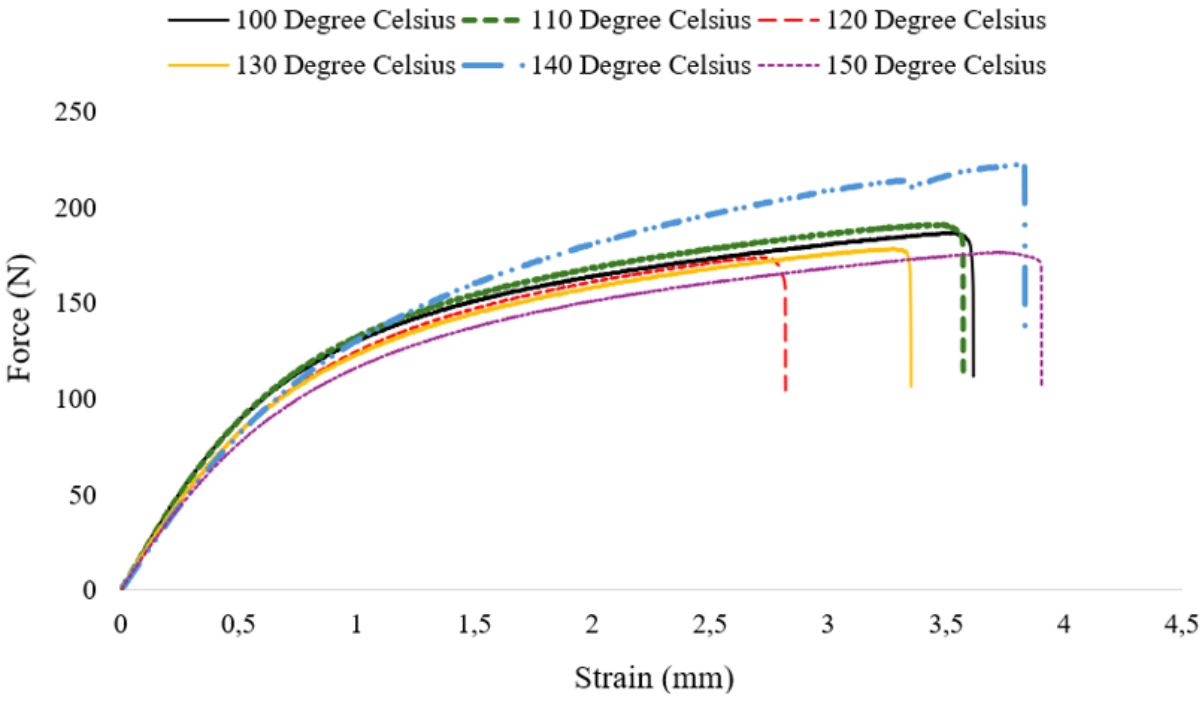


Figure 7. 11 Force versus strain curve for paper-to-paper specimens joined by process bio-adhesive (Test 2)

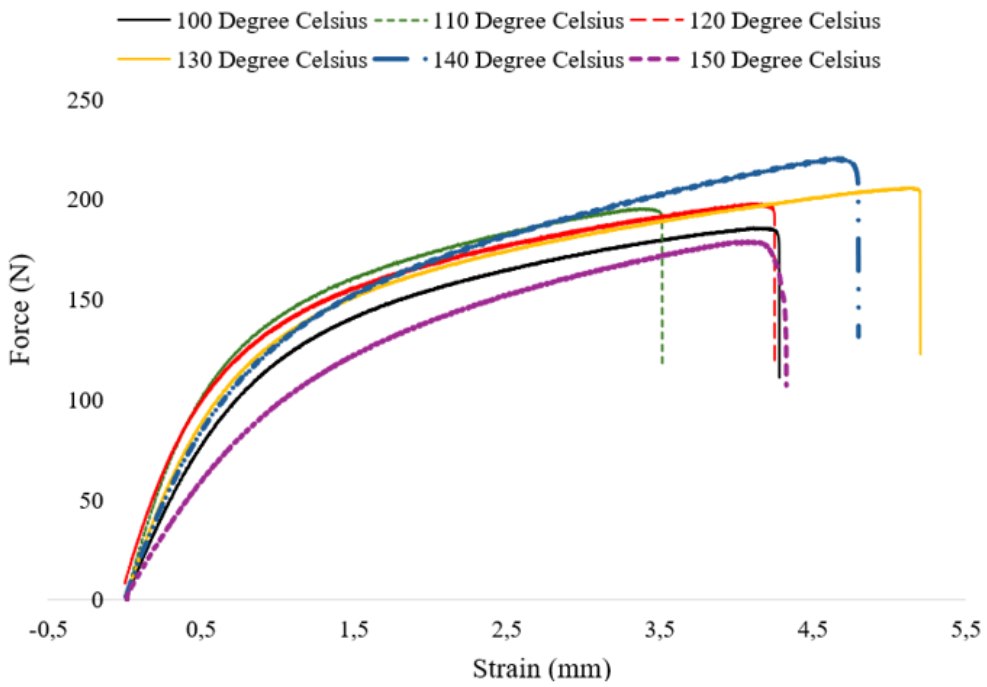


Figure 7. 12 Force versus strain curve for paper-to-paper specimens joined by process bio-adhesive (Test 3)

8.3 Appendix C: Single-Lap Shear Test: Signal-to-Noise Ratio calculations for Level 1 to Level 6

(100^0C) S/N = (-10Log) (1/3) $(1/20{,}535^2 + 1/16{,}734^2 + 1/12{,}821^2) = 23{,}97$
(110^0C) S/N = (-10Log) (1/3) $(1/18{,}939^2 + 1/15{,}559^2 + 1/17{,}502^2) = 24{,}69$
(120^0C) S/N = (-10Log) (1/3) $(1/17{,}491^2 + 1/14{,}187^2 + 1/16{,}994^2) = 24{,}09$
(130^0C) S/N = (-10Log) (1/3) $(1/12{,}494^2 + 1/14{,}153^2 + 1/14{,}676^2) = 22{,}72$
(140^0C) S/N = (-10Log) (1/3) $(1/13{,}038^2 + 1/13{,}951^2 + 1/14{,}766^2) = 22{,}84$
(140^0C) S/N = (-10Log) (1/3) $(1/18{,}874^2 + 1/12{,}606^2 + 1/9{,}423^2) = 21{,}68$

8.4 Appendix D: T-Peel Test Force versus Time curve (Test 1, 100^0C to 150^0C)

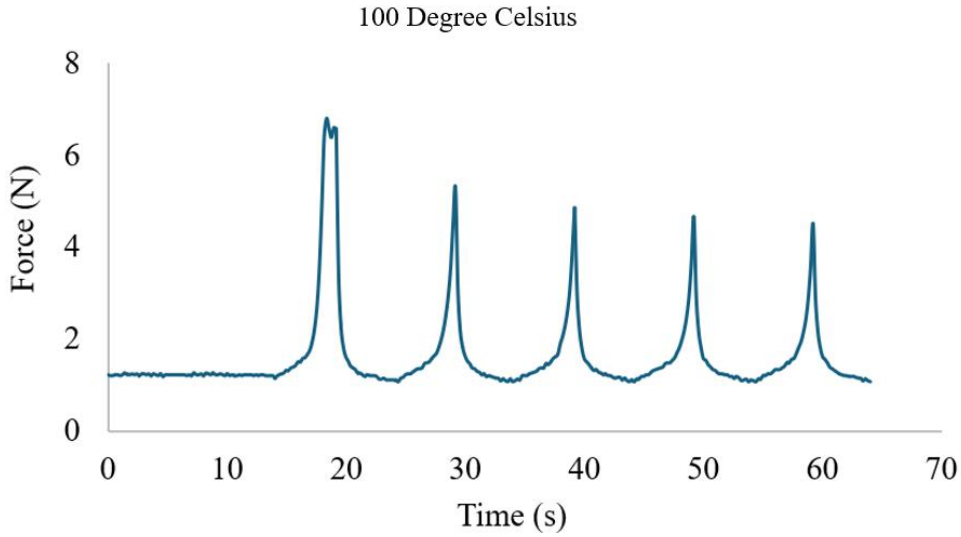


Figure 7. 13 T-Peel test force versus time curve (Test 1 at 100^0C)

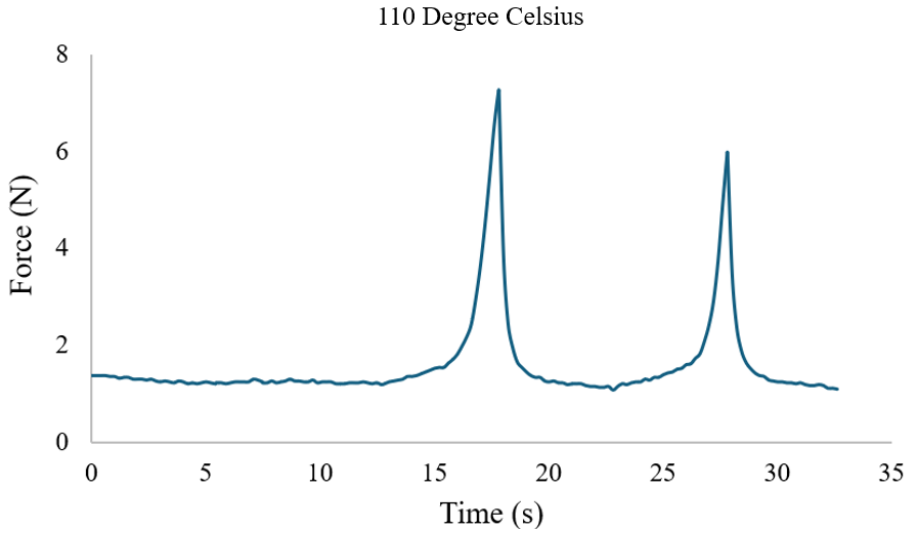


Figure 7. 14 T-Peel test force versus time curve (Test 1 at 110^0C)

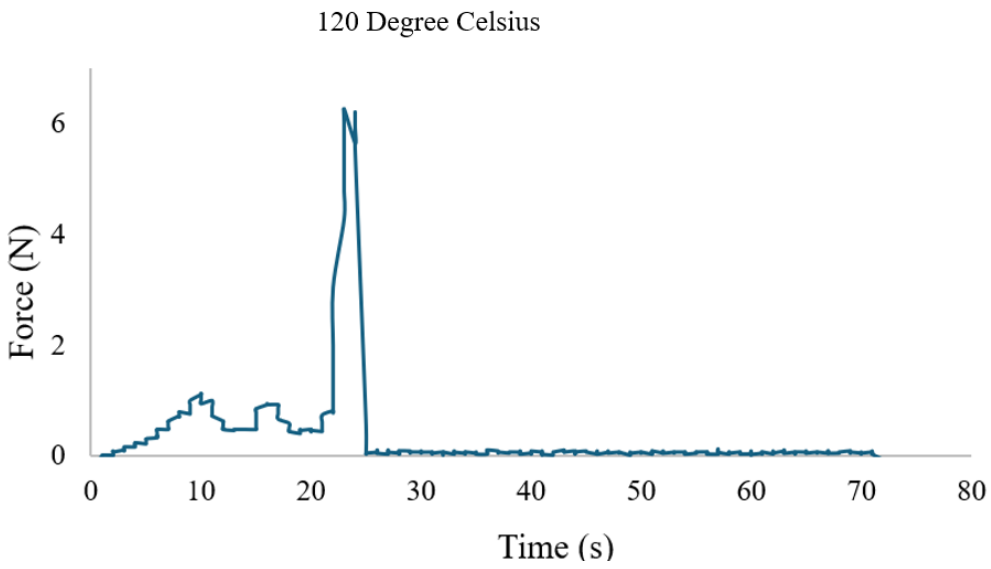


Figure 7. 15 T-Peel test force versus time curve (Test 1 at 120^0C)

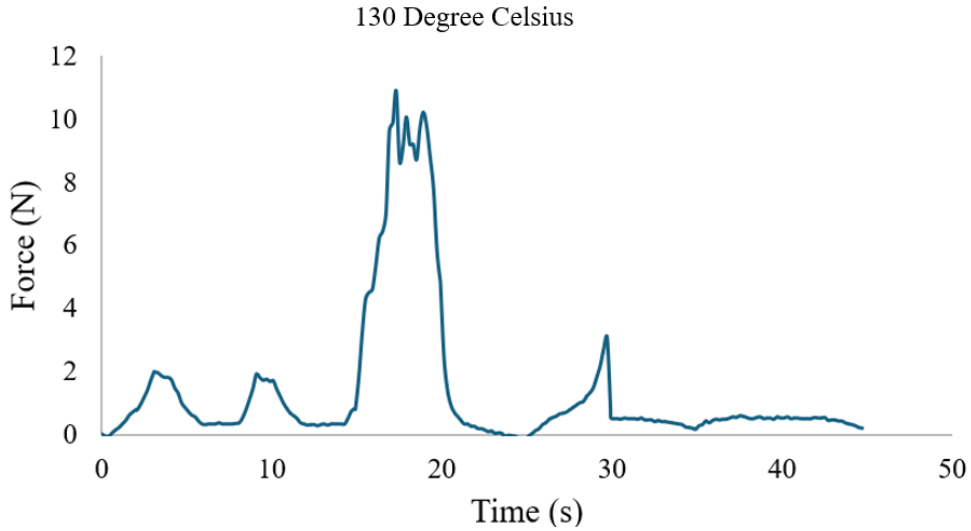


Figure 7. 16 T-Peel test force versus time curve (Test 1 at 130^0C)

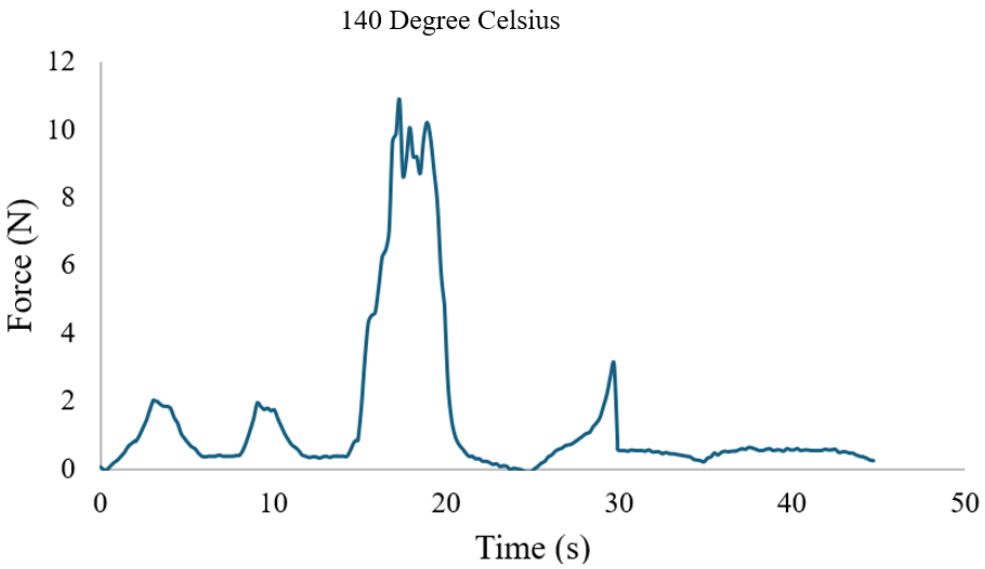


Figure 7. 17 T-Peel test force versus time curve (Test 1 at 140^0C)

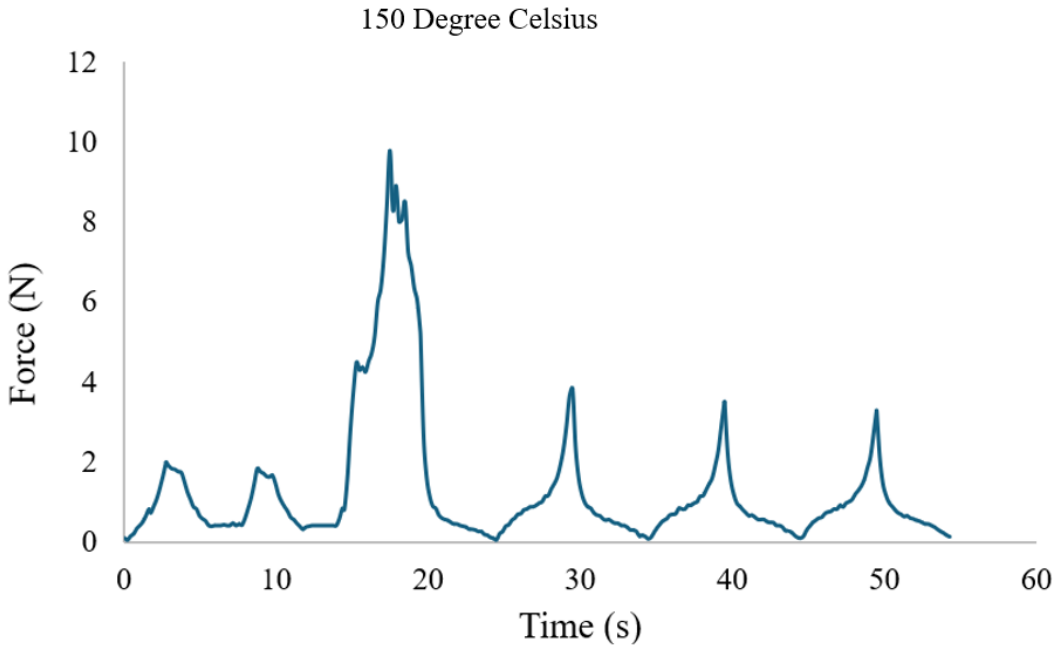


Figure 7. 18 T-Peel test force versus time curve (Test 1 at 150^0C)

8.5 Appendix E: T-Peel Test Displacement Versus Time curve (Test 1, 100^0C to 150^0C)

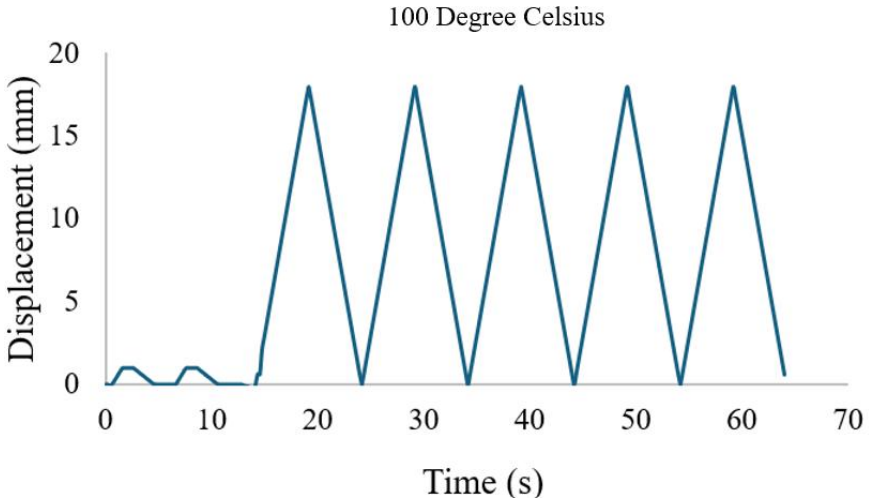


Figure 7. 19 T-Peel test peel displacement versus time curve (Test 1 at 100^0C)

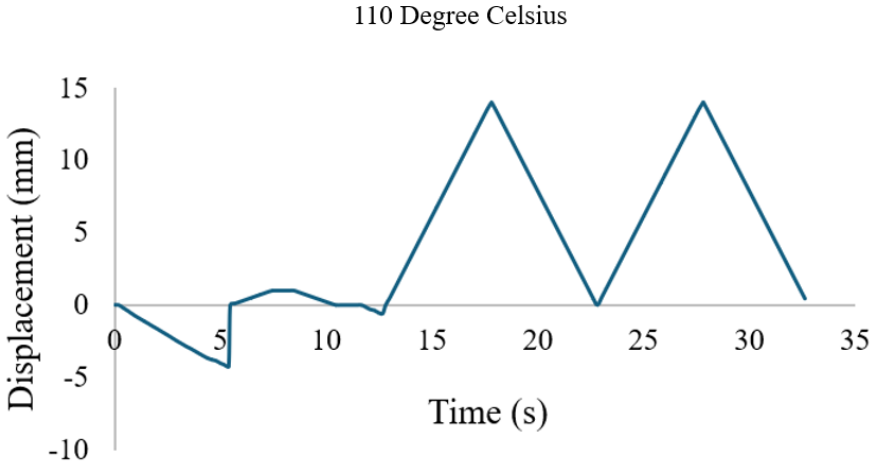


Figure 7. 20 T-Peel test peel displacement versus time curve (Test 1 at 110^0C)

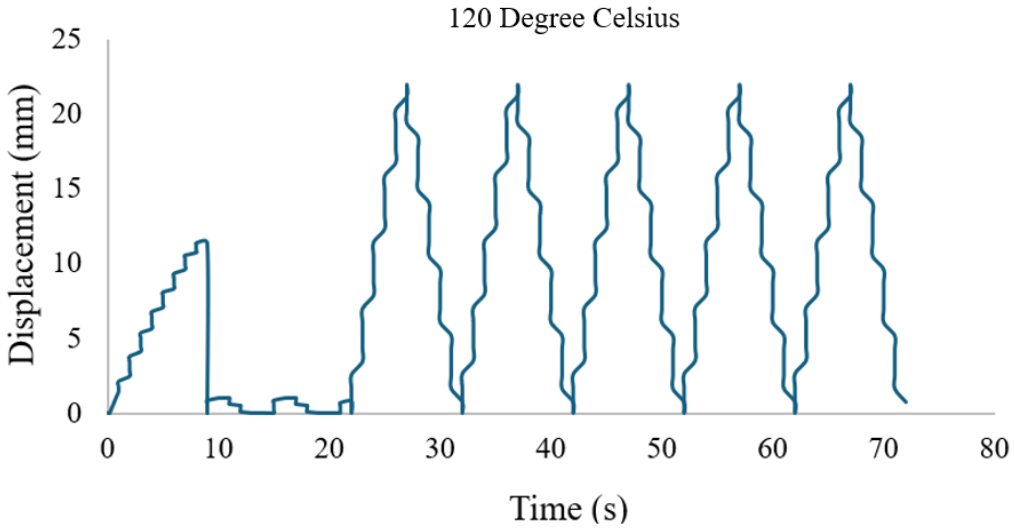


Figure 7. 21 T-Peel test peel displacement versus time curve (Test 1 at 120^0C)

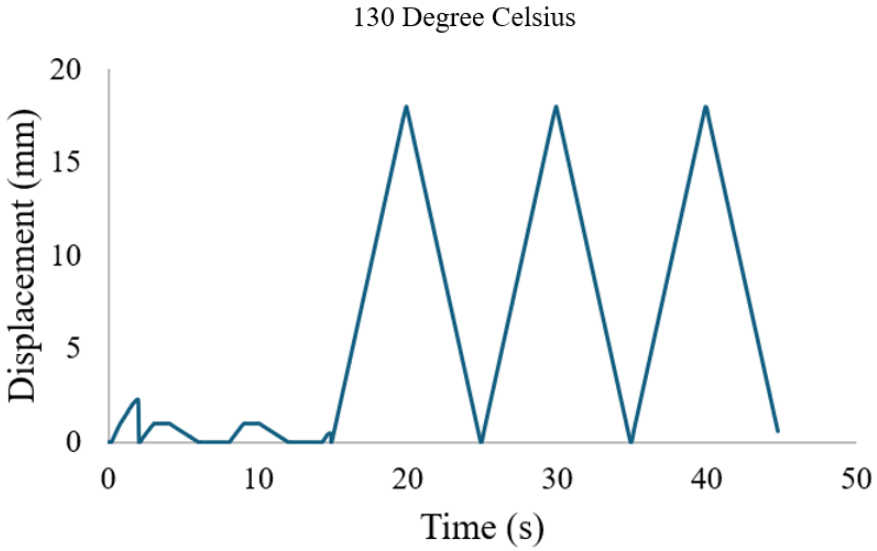


Figure 7. 22 T-Peel test peel displacement versus time curve (Test 1 at 130^0C)

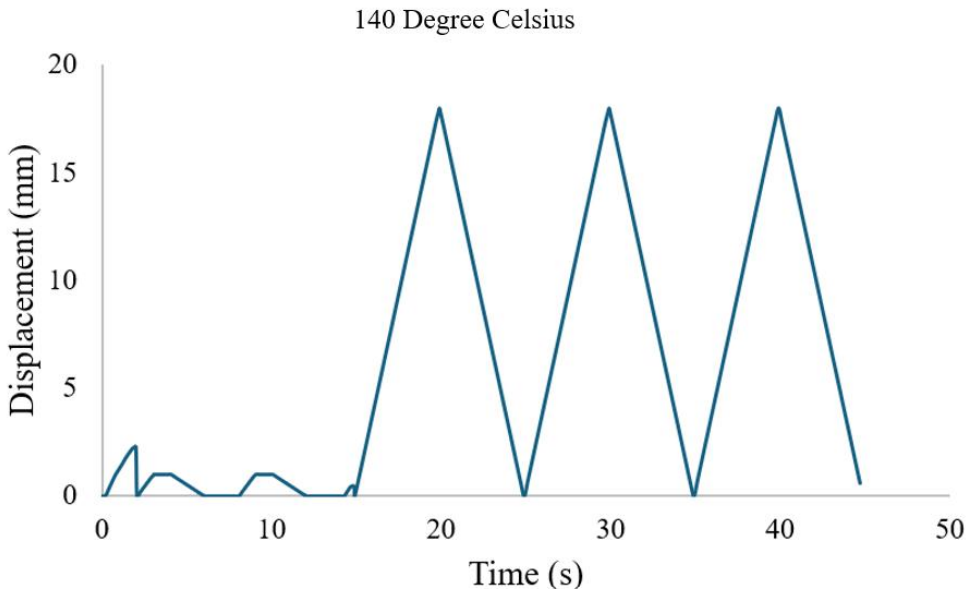


Figure 7. 23 T-Peel test peel displacement versus time curve (Test 1 at 140^0C).

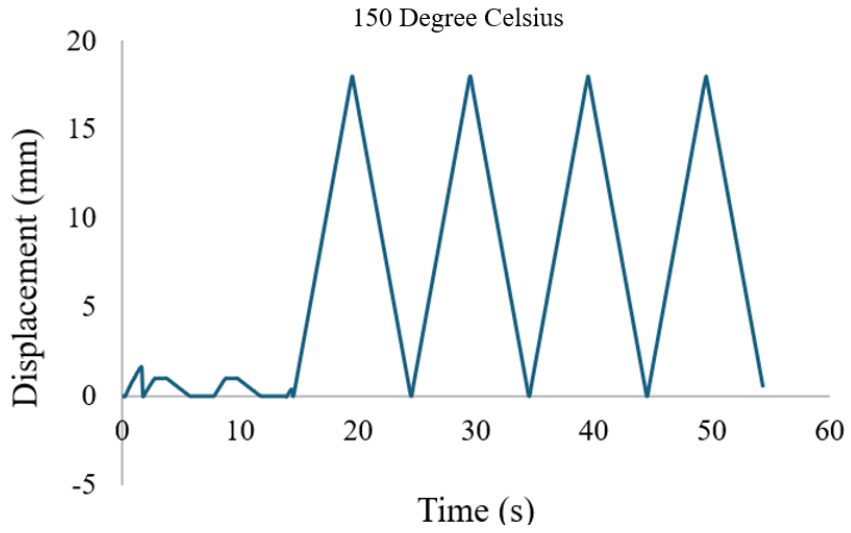


Figure 7. 24 T-Peel test peel displacement versus time curve (Test 1 at 150^0C)

8.6 Appendix F: T-Peel Test, Maximum Peel Strength for test 1, test 2, and test 3

Table 7. 1 T-Peel test: maximum peel force and maximum peel displacement for Test 1, Test 2 & Test 3

Sample Number	Bio-Adhesive Processing Temperature (^{0}C)	Maximum Peeling Force (N)			Maximum Peel Displacement (L) (m)		
		Sample Test 1	Sample Test 2	Sample Test 3	Sample Test 1	Sample Test 2	Sample Test 3
1	100	6,59	10,69	11,68	0,018	0,019	0,022
2	110	7,19	8,66	11,31	0,014	0,02	0,021
3	120	6,22	10,36	9,335	0,022	0,02	0,013
4	130	10,79	10,322	11,422	0,018	0,022	0,022
5	140	10,88	9,762	9,912	0,018	0,022	0,021
6	150	9,81	8,14	9,022	0,018	0,022	0,022

Table 7. 2 T-Peel test: maximum peel strength for Test 1, Test 2, and Test 3

Sample Number	Bio-Adhesive Processing Temperature (0C)	Peel Strength (F x L) (N/m)		
		Sample Test 1	Sample Test 2	Sample Test 3
1	100	6,59 x 0,018 = **366,43**	10,69 x 0,019 = **555,96**	11,68 x 0,022 = **531,15**
2	110	7,19 x 0,014 = **513,75**	8,66 x 0,02 = **433,04**	11,31 x 0,021 = **534,68**
3	120	6,22 x 0,022 = **282,82**	10,36 x 0,02 = **512,36**	9,335 x 0,013 = **707,2**
4	130	10,79 x 0,018 = **599,26**	10,32 x 0,022 = **469,18**	11,42 x 0,022 = **519,23**
5	140	10,88 x 0,018 = **604,7**	9,762 x 0,022 = **443,75**	9,912 x 0,021 = **468,36**
6	150	9,81 x 0,018 = **545,01**	8,14 x 0,022 = **370,02**	9,02 x 0,022 = **410,11**

8.7 Appendix G: T-Peel Test: Signal-to-Noise Ratio calculations for Level 1 to Level 6

(100^0C) S/N = (-10Log) (1/3) ($1/366{,}43^2 + 1/555{,}96^2 + 1/531{,}15^2$) = -53,24
(110^0C) S/N = (-10Log) (1/3) ($1/513{,}75^2 + 1/433{,}04^2 + 1/534{,}68^2$) = 53,76
(120^0C) S/N = (-10Log) (1/3) ($1/282{,}82^2 + 1/512{,}36^2 + 1/707{,}20^2$) = 52,144
(130^0C) S/N = (-10Log) (1/3) ($1/599{,}26^2 + 1/469{,}18^2 + 1/519{,}23^2$) = 54,34
(140^0C) S/N = (-10Log) (1/3) ($1/604{,}7^2 + 1/443{,}75^2 + 1/468{,}36^2$) = 53,85
(140^0C) S/N = (-10Log) (1/3) ($1/545{,}01^2 + 1/370{,}02^2 + 1/410{,}11^2$) = 52,56

8.8 Appendix H: Conference Paper Submitted & Presented



Figure 7. 25 Conference paper certificate. Presented at ICMIMT and to be published by Springer Nature

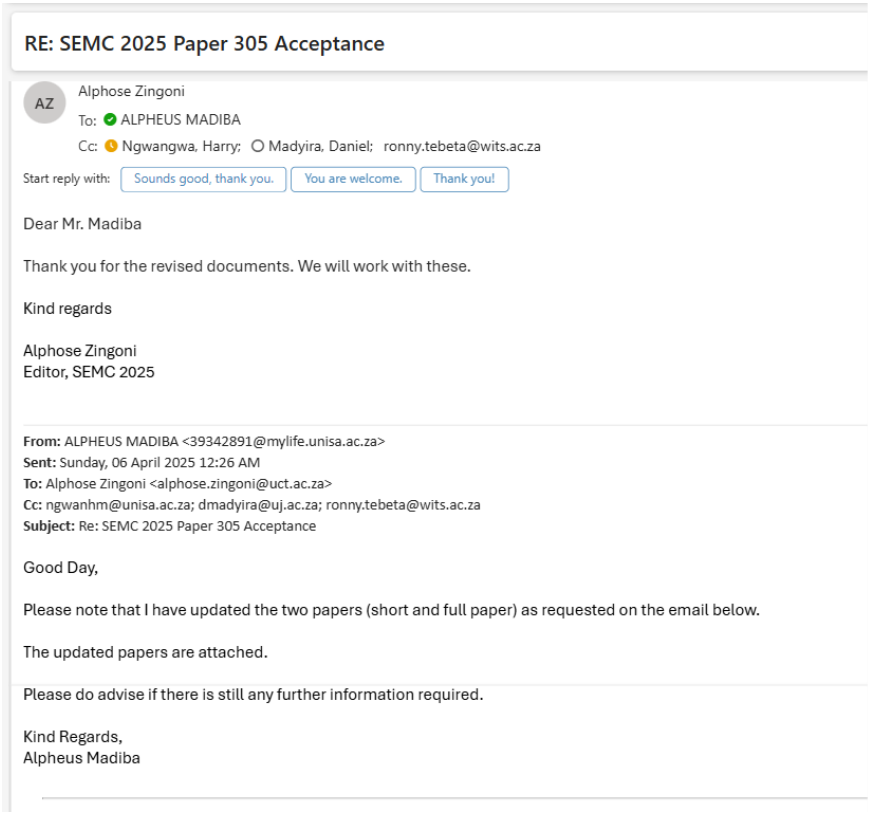


Figure 7. 26 Proof of conference paper submission. Presented at Structural Engineering Mechanical and Computation (SEMC)

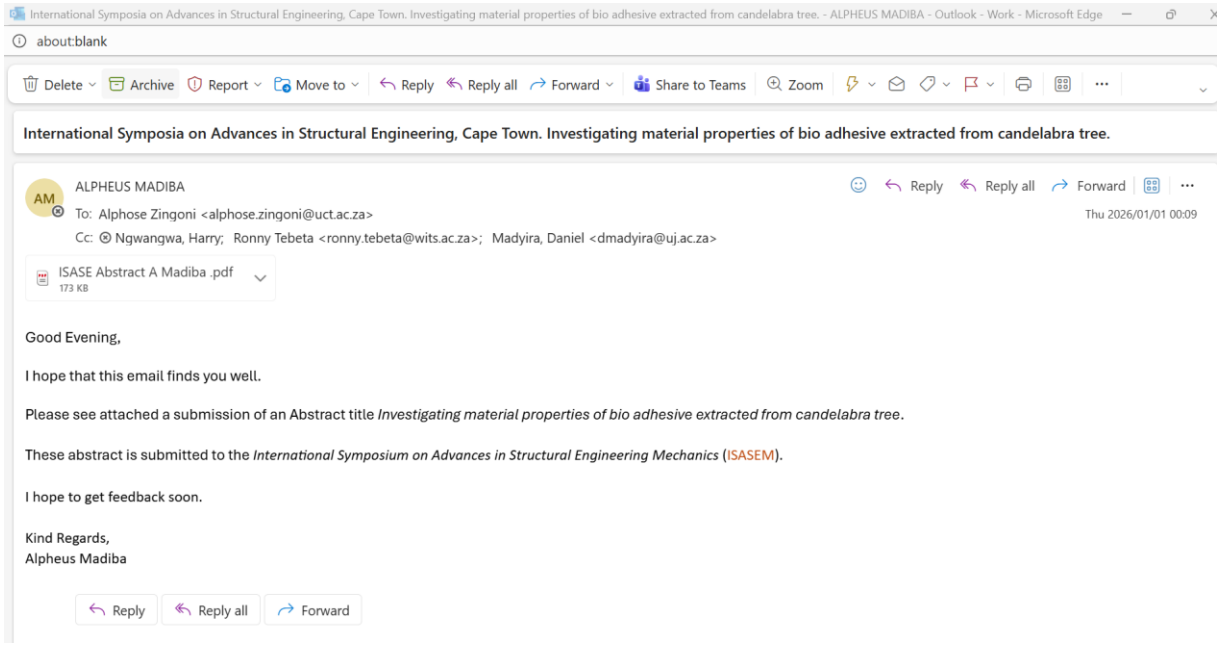


Figure 7. 27 Proof of conference paper submission. Submitted to the International Symposium on Advances in Structural Engineering Mechanics (ISASEM)